RENAL CELL REGULATION AND CANCER

# Tumor Suppressor Networks and the Primary Cilium

Timothy Klasson

Renal Cell Regulation and Cancer:
Tumor Suppressor Networks and the Primary Cilium



ISBN: 978-90-393-6734-6
Cover and lay-out: Wendy Schoneveld || wenz iD
Printed by: Proefschriftmaken.nl

The research described in this thesis was financially supported by the European Community's Seventh Framework Programme under grant agreements no: 241955 Syscilia and 305608 EURenOmics.

Renal Cell Regulation and Cancer:
Tumor Suppressor Networks and the Primary Cilium

Regulatie van de Niercellen en Kanker:
Tumorsuppressor Netwerken en de Primary Cilium

*(met een samenvatting in het Nederlands)*

Proefschrift

ter verkrijging van de graad van doctor aan de Universiteit Utrecht
op gezag van de rector magnificus, prof. dr. G.J. van der Zwaan, ingevolge het besluit
van het college voor promoties in het openbaar te verdedigen op
dinsdag 7 maart 2017 des middags te 2.30 uur

door

Timothy Daniel Klasson

geboren op 28 juni 1989 te New York City, Verenigde Staten van Amerika

**Promotoren:**
Prof. dr. M.C. Verhaar
Prof. dr. V.V.A.M. Knoers

**Copromoter:**
Dr. R.H. Giles

# TABLE OF CONTENTS

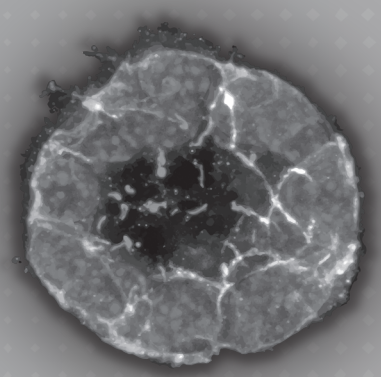

# CHAPTER 1

# Introduction

Adapted and published as "Molecular Genetics of Renal Cancer".
**Klasson TD** and Giles RH. In: eLS. John Wiley & Sons Ltd, Chichester. September 2016.
Available at http://www.els.net [doi: 10.1002/9780470015902.a0024468]

The primary non-motile cilium is an antenna-like protrusion which projects outwards from the cell body and can be found connected to the membrane of almost all human cells. This organelle was long considered a vestigial and unimportant version of its motile cousin (e.g. sperm tails), but it has now been shown that primary cilia are vital players in a number of cellular processes. Primary cilia are especially vital for regulating critical signal transduction pathways which control the activity of the cell in response to physical and chemical signals in its environment and based on the activities of its neighboring cells. Thus, the cilium plays an important part in the health of the cell and in the growth and development of tissues and organisms [1-3]. Improper function of the cilium can be a symptom of, or cause, pathophysiological changes in the cell or tissue. Indeed, a class of diseases called ciliopathies has now been shown to be associated with mutations which cause improper ciliogenesis, maintenance of the cilium, disassembly of the cilium, or other ciliary malfunctions. Because of its wide array of functions, a disease resulting from dysregulation or dysfunction of the cilium can vary wildly in symptoms and severity. A number of these diseases that are caused primarily by problems with the cilia or ciliary proteins, collectively termed ciliopathies, have now been identified, such as Meckel–Gruber Syndrome (MKS), Bardet-Biedl (BBS), and Jeune asphyxiating thoracic dystrophy. Other conditions which are not directly caused by ciliary malfunctions have also been shown to be associated with reduced ciliary number or function, including many cancers and developmental disorders [4-6].

The primary cilium (**Figure 1.a**) is produced by the cell when it enters a quiescent state during G1 phase and does not take part in the normal cell cycle, a state known as G zero (G0)**(Figure 1.b)**. As the cell exits the cell cycle, the mother centriole differentiates into the basal body which will form the foundation of the cilium. First, it docks with a Golgi-derived vesicle via its distal appendages (also known as transition fibers) and migrates to the plasma membrane near the nucleus [7, 8]. Here, the ciliary vesicle becomes contiguous with the plasma membrane of the cell. The area of the membrane to which the transition fibers attach is known as the periciliary membrane and it is in this area where regulation, recycling and endocytosis of ciliary membrane components and membrane-bound proteins occurs. In some cells, the periciliary membrane invaginates forming a ciliary pocket which controls the composition of the ciliary membrane through a method which is not completely understood [9, 10]. Although the ciliary membrane is continuous with the cell membrane, it has a significantly different composition of membrane components and membrane bound proteins thanks to this regulation mechanism. The basal body also attaches to the microtubule cytoskeleton of the cell via the sub-distal appendages. These appendages, along with the ciliary rootlets and basal feet, stabilize and orient the basal body. Once the basal body is attached to the cell surface, the backbone of the cilium, termed the ciliary axoneme, is built as microtubules extend from the ciliary rootlet of the basal body, pushing outwards

against the plasma membrane. The area above the transition fibers where the basal body transitions into the axoneme is known as the transition zone. The transition zone is characterized by rings of y-links, forming the characteristic "ciliary necklace", which act as a barrier between the interior of the cilium and the cytoplasm of the cell. The transition zone controls the passage of proteins and other molecules into and out of the ciliary space, making the interior of the cilium a closed environment [2, 7, 9].

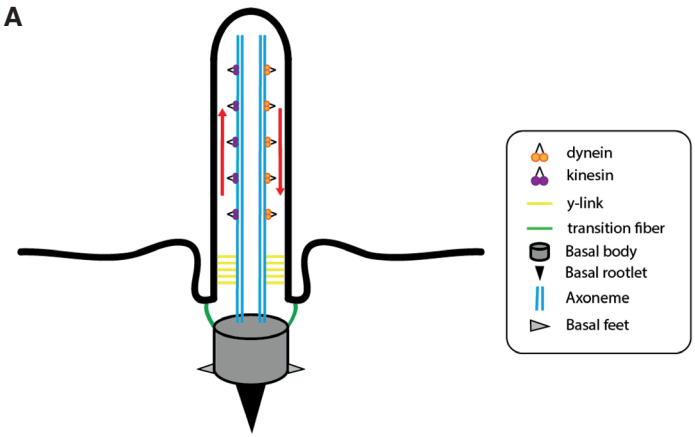


**Figure 1a.** A schematic representation of the primary non-motile cilium. Red arrows represent the direction of intraflagellar transport (IFT).

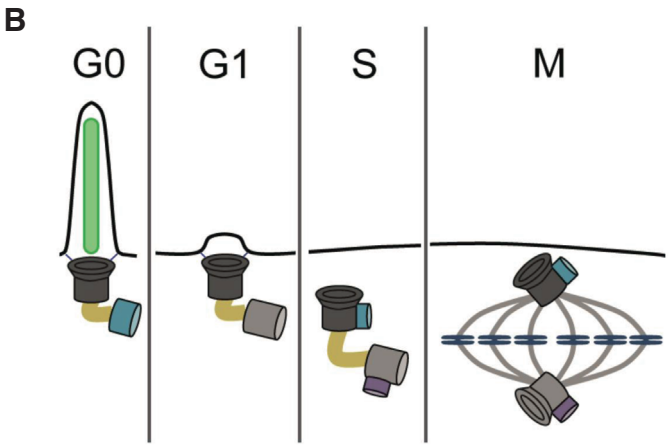


**Figure 1b.** Schematic showing the relationship of presence of the primary cilium and the position of the basal body with the cell cycle (Figure reproduced from chapter 2).

The axoneme of the primary non-motile cilium is formed of 9 doublets of microtubules in a ring which is patterned on the shape of the basal body which is comprised of, like the centrioles, nine triplets of microtubules. The 9 doublet pattern is sometimes referred to as the 9+0 pattern, to contrast it with the 9+2 pattern found in motile cilia and flagella, which have a central pair of microtubule doublets (**Figure 1.c**). In the motile forms of cilia, each microtubule doublet in the outer ring produces projections inwards called the radial spokes which connect to a protein web which surrounds the central pair. Each doublet is connected to its neighbors with a strand of the protein nexin. Outer and inner dynein arms project from the microtubule doublets in the outer ring. The motor action of the dynein arms causes the microtubule doublets to move past each other. This motion is resisted by the nexin links and the connection to the central pair, which causes the cilium to bend instead [11]. This bending action is used to produce a directional beating motion which is used, for example, by motile cilia to produce fluid flow across the surface of the cell or by flagella to produce forward motion of the sperm. Motile cilia are particularly characteristic of multi-ciliated cells, such as mucosal cells lining the airway, although some cells have only a single motile cilium (e.g. sperm or cells of the developmental node).

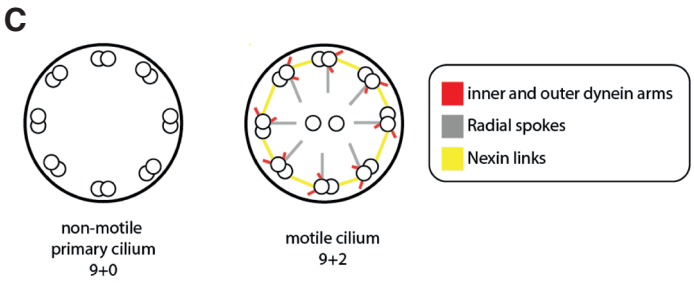


**Figure 1c.** Schematic comparison of the orientation of microtubule doublets in the two types of primary cilia. Additional components of the motile cilium are also shown.

The mechanism by which the axoneme is built, maintained, and eventually disassembled is known as intraflagellar transport (IFT). Microtubule components are moved to and from the tip of the cilium by two specialized complexes of IFT proteins attached to the molecular motor proteins kinesin-2 and dynein-2. IFT-A components connect to dynein and participate in tip-to-base (retrograde) transport, while IFT-B components proceed in the opposite (anterograde) direction with kinesin-2. These two components also cooperate: once an IFT complex has moved cargo to the end in one direction, it is returned to its starting point by the other IFT complex. IFT also traffics other proteins along the ciliary axoneme [12]. Recent results indicate that distinct sub-complexes within the IFT-B complex are responsible for

exocyst function or trafficking [Boldt *et al.* Nature Communications, in press].
The primary cilium is a vital signal transduction organelle that plays a role in a wide array of important cellular pathways because of its function in the sensing of the extracellular environment. This includes not only physical and chemical signals in the extracellular environment like fluid flow past the cell surface [13] and ion levels [14], but also cell-to-cell signals released by nearby cells such as morphogens, growth factors and developmental signals. The primary cilium transduces these signals into a diverse range of cellular responses that lead to downstream effects including proliferation, differentiation, polarity, cell survival, migration and apoptosis [2, 15, 16]. For example, the Wingless-int (wnt) signaling pathway, a promoter of many downstream effects including cellular proliferation, passes through the cilium. The Wnt receptor, Frizzled, is found on the ciliary membrane and its signaling proteins, such as Disheveled, pass through or associate with the cilium. Without proper ciliation, these signals cannot localize correctly and effective signaling is lost, which can lead to disease [17-19]. Other important signaling pathways which pass through the cilium include the Hippo, Hedgehog, and Notch signaling pathways, all of which are important during development [20-25].
With such a wide array of functions associated with the primary cilium, it is no surprise that ciliopathies also show considerable complexity. These diseases, although individually rare, are common as a group, with an incidence of 1 in every 300-400 individuals. Although there is phenotypic overlap, ciliopathies display significant heterogeneity in both their underlying genetics and their phenotypes and symptoms **(Figure 2.a)**. Similar phenotypes can arise from mutations in distinct genes, while other times a mutation in a single gene can be associated with varied phenotypes in different ciliopathies **(Figure 2.b)**. In addition to these canonical ciliopathies, other diseases have been associated with changes in ciliary number and function, including various cancer subtypes and inherited tumor syndromes [6, 26-32].

**A**

| | | selected phenotypes | | | |
|---|---|---|---|---|---|
| | abbreviation | renal cysts | situs inversus | polydactyly | bone malformation |
| Nephronophthisis | NPHP | x | | | |
| Bardet-Biedl syndrome | BBS | x | x | x | |
| Meckel-Gruber Syndrome | MKS | x | x | x | |
| Jeune Asphyxiating Thoracic Dystrophy | JATD | x | | x | x |

**Figure 2a.** table showing selected ciliopathies and a selection of their associated phenotypes. Note that some phenotypes overlap, but not all.

**B**

| | associated with mutations in | | | | |
|---|---|---|---|---|---|
| | TTC21B | IFT80 | IFT144 | TMEM67 | NPHP3 |
| NPHP | x | | x | x | x |
| BBS | x | | | x | |
| MKS | x | | | x | x |
| JATD | x | x | x | | |

**Figure 2b.** Table showing the same ciliopathies and a selection of some of the genes which have been found mutated in those diseases. Note the overlap in genes despite different phenotypes.

The von Hippel-Lindau protein (pVHL) is an E3 ubiquitin ligase encoded by the von-Hippel-Lindau Gene (*VHL*). The *VHL* gene encodes two isoforms of pVHL, one which is 30 kDa and one which is 19 kDa. Although there is differential expression of these isoforms in some tissues and the 19 kDa form lacks an acidic domain of unclear function, studies have shown that both isoforms have comparable activity both in assays and *in vivo* [33] although other studies suggest distinct functional roles for the two isoforms [34, 35]. The most well-studied function of pVHL is to regulate the cells' oxygen sensing (see Figure 2). In the presence of oxygen, prolyl-hydroxylase (PHD) proteins target and hydroxylate hypoxia inducible transcription-factor alpha-subunits (HIFα), a class of transcription factors responsible for promoting a wide variety of more than 800 downstream genes that help the cell and tissue respond to a lack of oxygen: "hypoxia" **(figure 3)**. HIFα gene targets include erythropoietin (*EPO*), which promotes erythrocyte differentiation, vascular endothelial growth factor (*VEGF*) a growth factor which promotes angiogenesis, and glucose transporter 1 (*GLUT1*) which transports glucose into the cell. When HIFα subunits are hydroxylated, they can be targeted by an ubiquitin ligase complex containing pVHL, elongin B, elongin C, Cullin 2 and ring-box protein 1. This complex then catalyzes the addition of ubiquitin to HIFα factors, marking them for degradation in the proteasome. Oxygen is a biochemical requirement for PHD proteins to hydroxylate HIFα. Thus, in low oxygen conditions, HIFα is stabilized and forms heterodimers with HIF1β subunits. These HIF heterodimers bind to hypoxia response elements (HREs) on the DNA and proceed to promote the expression of their target genes. This pathway allows the cell and the body to adapt to lower oxygen environments, including chronic and acute hypoxia. Some examples of the results of HIF activity include increased angiogenesis and vasculogenesis, metabolic changes, and increased cell survival [36-39]. There are three different paralogs of HIFα: HIF1α, HIF2α and HIF3α. HIF1α is ubiquitously expressed, whereas HIF2α is cell-type specific and is found enriched mostly in the endothelium and in lung, renal and hepatic cells. These two forms are both stabilized during hypoxia and bind many of the same HREs, but they do not perform

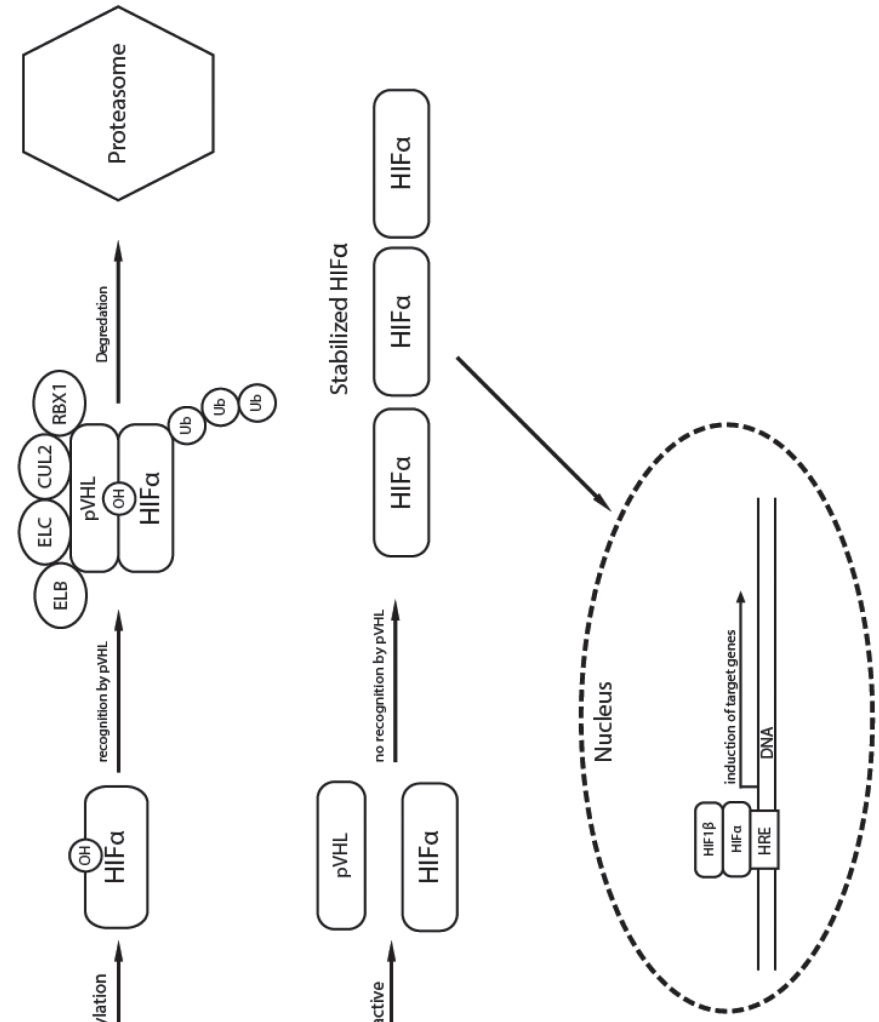


**Figure 3.** Schematic overview of the molecular mechanism of pVHL action

identical functions and appear to contribute to hypoxia response differently in different contexts [40, 41]. HIF3α lacks the transactivation domain present in the other two types and may be a negative regulator of the activity of HIF1α and HIF2α [42].

Another consequence of HIF activity is the expression of micro RNAs (miRNA). miRNA regulation is a highly evolutionarily conserved form of post-translational regulation of genes. miRNA activity is an integral part of gene regulation networks in the body, including pVHL/HIF dependent signaling [43, 44]. miRNA are non-coding RNA that function in the post-translational regulation of genes **(Figure 4)**. miRNA are transcribed from their own genes or from sequences in the introns of other genes. Active mature miRNA are derived from longer (around 80 nucleotide) pre-miRNA transcripts which are transcribed into folded hairpin shapes. Pre-miRNA hairpins are then converted into active miRNA by the enzyme Dicer. Mature miRNA are small (around 22 nucleotides in length) pieces of RNA which are complementary to sequences on the mRNA of target genes. miRNA control the translation of their target mRNA through the action of a protein complex for which the miRNA acts as a target selector. These RNA-induced silencing complexes (RISCs) include the RNAse III enzyme Dicer and a number of other proteins, of which Argonaut (Ago) proteins play a vital role. Ago proteins bind the mature miRNA and hold onto it so that it can interact with target mRNA. After the miRNA binds to its target, the Ago protein directs the activity of the RISC to repress the translation of the targeted mRNA in different ways depending on the exact Ago protein involved. There are four members of the mammalian Ago family; Ago2 directly cleaves the target transcript, while other Ago family

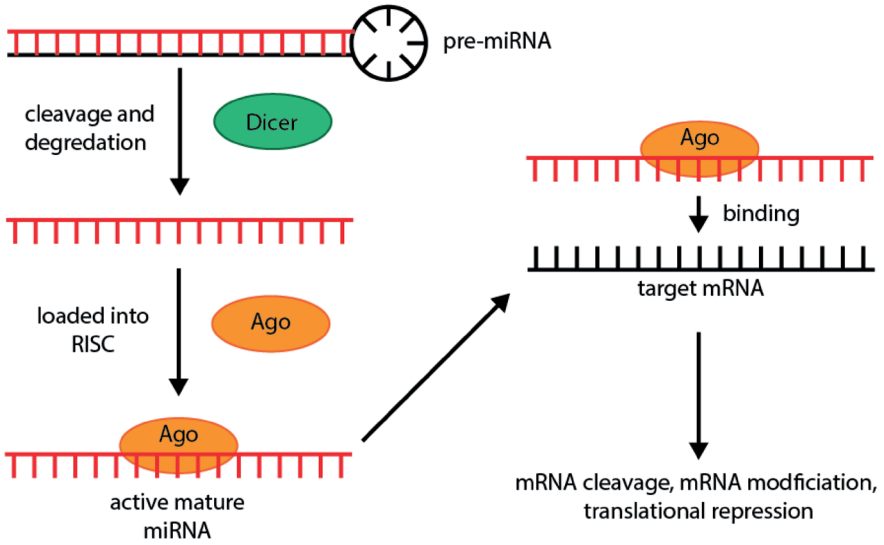


**Figure 4.** Schematic representation of miRNA processing and mechanism of action.

members recruit other proteins to assist them in translational repression through other means. There is also a family of proteins called the PIWI proteins which perform the same role as the Ago proteins but in germ cells and in certain stem cell populations (25027649). MiRNA may play a role in the pathology of many diseases, including ciliopathies and cilia related disorders. For example, in testicular germ cell tumors associated with mutations in cilia regulator *DNAAF1*, PIWI accumulates [45]. Likewise, in *VHL*-deficient cells, miRNA are expressed which contribute to adaptation to hypoxia (see **Chapter 5**).

The responses promoted by HIFα activity, such as increased angiogenesis, cell survival, an elevated rate of proliferation and switching from an oxygen based metabolism to a glucose based (glycolytic) metabolism are all also all associated with the growth of tumors [36, 46, 47]. The vital role that pVHL plays in oxygen-sensing and modulating the strength of downstream signals control by HIFs makes pVHL an important tumor suppressor protein. Indeed, patients born with von Hippel-Lindau (VHL) syndrome, who possess an inactivating mutation in one allele of the *VHL* gene, have a predisposition to develop cysts as well as cancerous and benign tumors in many different tissues over the course of their lives, including kidney, pancreas, eye and brain tumors. Although these patients still have a single functional copy of the *VHL* gene, the healthy allele is frequently mutated or lost, eventually leading to the development of neoplasms, although the exact mechanisms through which this occurs are still under investigation and discussion [6, 38, 48]. In addition, sporadic clear cell renal cell carcinoma (ccRCC), the most common form of sporadic kidney cancer, almost always displays the mutation or inactivation of the *VHL* gene. Among these, the vast majority, up to 92% in some studies, display complete biallelic inactivation of *VHL* [49-52]. Interestingly, despite this fact, humans born with an inactivating mutation in *VHL* do not develop tumors until relatively late in life, usually after 20 years of age, although they do develop ccRCC earlier than patients with sporadic ccRCC [6, 38, 48]. Additionally, mouse models of VHL deficiency alone do not develop any renal tumors. Therefore it is believed that another mutation which promotes tumorigenesis must occur before tumors can develop, although loss of *VHL* seems to produce a "pre-cancerous" phenotype that promotes the occurrence of the secondary mutation and then contributes to tumor growth [6, 47, 53, 54].

In recent years, sequencing of ccRCC tumors to try and find other mutations which contribute to ccRCC tumor growth has shown that these tumors display considerable intra-tumor genetic heterogeneity and that many different genetic events, in addition to loss of pVHL function, can drive tumorigenesis **(Figure 5)**. Loss of, or aberrations in, chromosome 3p which includes *VHL* (located at 3p25.3), are the most frequently observed chromosomal aberrations in ccRCC [52, 55-57]. Other chromosomal alterations are observed as well,

selected genes found disrupted in ccRCC in addition to VHL

| gene symbol | modification in ccRCC | gene function and important interactions |
|---|---|---|
| BAP1 | mutated | regulation of tumor suppressor BRCA1, protein deubiquitinylation, chromatin remodeling |
| JARID1C | mutated | chromatin remodeling |
| PBRM1 | mutated | chromatin remodeling |
| SETD2 | mutated | histone methyltransferase, chromatin remodeling |
| TCEB1 | mutated | adaptor protein for E3 ubiquitin ligase complex, interacts with VHL, transcription elongation factor |
| KEAP1 | mutated | adaptor protein for E3 ubiquitin ligase complex, regulates the antioxidant NFE2L2 pathway |
| TET2 | mutated | demethylation of DNA |
| TSC1 | mutated | part of a tumor suppressor complex |
| UTX | mutated | histone methyltransferase, chromatin remodeling |
| DUSP9 | downregulated | cell proliferation and differentiation |
| NOTCH1 | overexpressed | part of the notch developmental signaling pathway, cell differentiation |
| AQP1 | overexpressed | water transport membrane protein, important in renal tubular epithelium |
| BIRC5 | overexpressed | cell survival, anti-apoptosis |
| ET2 | overexpressed | angiogenesis, vasoconstriction, inflamation, cell growth and differentation |
| DKK2 | methylated | regulator of the wnt pathway: important for development, differentiation, proliferation, migration, tissue patterning |
| APAF1 | methylated | pro-apoptotic protein |
| KILLIN | methylated | p53 regulated pro-apoptotic protein, cell cycle arrest |

**Figure 5.** Table of selected genes which have been found disrupted in patient ccRCC in addition to VHL.

including duplication of chromosome 5q, which is the second most common chromosomal aberration observed. A number of genes mapped to this region have been shown to be amplified in certain subtypes of ccRCC including *TGFB1* which encodes an important growth factor that promotes growth, proliferation and differentiation [55, 57, 58]. Interestingly, ccRCC does not frequently display somatic mutations in tumor suppressor genes (TSGs) such as *TP53*, *PTEN*, *RB1* or *BRAF* which are frequently seen to be mutated in many other tumor types which arise from epithelial cell lineages. However, mutations and other disruptions in many other genes in addition to *VHL* have been reported in ccRCC. Genes found mutated in ccRCC include 3 TSGs which are found, like VHL, on chromosome 3p: BRCA associated protein 1 (*BAP1:* mutated in up to 11% of ccRCC tumors), SET domain containing 2 (*SETD2*, mutated in up to 12% of ccRCC tumors) and Polybromo 1 (*PBRM1*, mutated in up to 41% of ccRCC tumors), all of which are involved in the regulation and remodeling of chromatin [49, 52, 59, 60]. The mechanisms by which mutations in these genes contribute to tumorigenesis are still being studied but they do seem to play a part in the development of ccRCC. For example, in many ccRCC tumors, a single mutant allele of *VHL* is present and the other is lost through deletion leading to loss of heterozygosity. Because these three genes are found on chromosome 3p around *VHL*, they are also sometimes lost in the same deletion event. As mentioned above, mouse models of *VHL* deficiency do not develop ccRCC tumors. However, interestingly, a mouse model which combines conditional biallelic deletion of *Vhlh*, the mouse ortholog of *VHL,* with the conditional deletion of a single allele of *Bap1,* the mouse ortholog of *BAP1*, in nephron progenitor cells did develop small solid renal tumors which resemble human ccRCC. This indicates that *BAP1* can play the role of the second gene, along with *VHL*, in which mutations lead to ccRCC [61]. In human patients, *BAP1* mutations define a subclass of ccRCC tumors with poor outcomes [62]. However, tumor sequencing shows that *BAP1* is just one of many genes which is mutated in ccRCC and can possibly contribute to tumorigenesis [52, 63, 64]. Indeed, different secondary mutations can lead to the development of different tumor sub-clones within the same single ccRCC tumor [64]. Although the genetics of ccRCC is far from well understood, developments in next-generation sequencing will improve our ability to diagnose patient mutations and examine the complex genetic events underlying the growth of ccRCC tumors.

pVHL has a number of other non-canonical targets in addition to HIF. pVHL usually catalyzes the addition of ubiquitin to these interactors, as it does with HIF, but not always, such as in the case of KIF3A [65]. Another example of a non-canonical target is the apoptosis-related protein programmed cell-death 5 (PDCD5) which is involved in cell-cycle arrest and the induction of apoptosis in response to certain types of DNA damage. The localization of PDCD5 is regulated in part by its interaction with pVHL [66, 67](**Chapter 6**). pVHL also binds to and ubiquitinylates microtubules to modulate their stability,

including within the cilium. Without this function, the cilium cannot remain stable enough and cells ciliate less frequently [68-70]. ccRCC displays reduced ciliary frequency compared to the surrounding healthy tissues [71, 72] and VHL disease can be considered a ciliopathy [73]. Interestingly, there are a number of tumor suppressor proteins which, like pVHL, are tumor suppressors that possess a distinct ciliary function and are necessary for proper ciliation in cells. Although these two functions seem very disparate, they are actually more related than they may at first appear. The cilium is inextricably linked with the processes that control cell division because of the presence of the basal body at the root of the cilium. The basal body is derived from the mother centriole that has an important role during cell duplication. Therefore, the cilium must be disassembled before the cell can re-enter the cell cycle. Thus, ciliation and cell division are mutually exclusive events but share an important common piece that ties them together. Because of this connection, many proteins which are present in the cilium during G1 phase of the cell cycle have separate functions during cell division. For example, many proteins found at or around the cilium are also involved in the replication and division of DNA in the nucleus during mitosis. For example, polo-like kinase 4 (PLK4) is a protein which is recruited to the basal body when the cilium is being resorbed.

PLK4 is required for the duplication of the mother centriole. If PLK4 malfunctions during division, a dividing cell can end up with an inadequate number or supernumerary centrosomes and uneven or improper division of DNA can occur, leading to cyst formation, aneuploidy and genetic instability which can lead to a malfunctioning cellular environment and a predisposition to further mutation (For more, see **Chapter 2)** [6, 74-77]. Another example is NimA-Related Kinase 8 (NEK8), a protein found in the primary cilium at the Inversin compartment just distal of the transition zone, an area of the cilium with a poorly understood function to which several proteins specifically localize. NEK8 is required for proper ciliogenesis and *NEK8* mutations are associated with nephronophthisis, a renal ciliopathy, and cause 3D cell-structure defects *in vitro*. NEK8 is also a negative regulator of the Hippo pathway, a signaling pathway which is important during organ development, the signals of which are transduced through the primary cilium. When the cell is not ciliated, NEK8 also functions in the replication fork during DNA duplication and is important for modulating the cellular response to DNA damage. The same *NEK8* mutations which cause nephronophthisis and renal cystic dysplasia also lead to replication stress and an accumulation of DNA damage [78, 79].

However, despite the connection between de-ciliation and cell cycle progression, as well as the presence of tumor suppressors at the cilium, the link between ciliary function and tumorigenesis remains unclear. Cilia loss does not always correlate with tumor formation,

and cilia loss alone is not sufficient to drive a cell into excessive proliferation. In some cases, the loss of cilia through disruption of a ciliary protein can cause the cell to re-enter the cell cycle more frequently, but neoplasm formation is not observed. For example, Centrosomal Protein 164 (CEP164) is required for ciliation and knockdown of *CEP164* causes both a reduction in cilia formation and a significant reduction in the amount of time required to enter S-phase, although S-phase itself is significantly longer than control cells. However, although cells depleted for *CEP164* proliferate more often than control cells, the amount of viable cells actually decreases due to a corresponding increase stress and apoptosis [80]. Alternatively, loss of a ciliary protein may not always cause loss of cilia, but does cause excessive proliferation. For example, Polycystin-1 (PC1) is a protein encoded by the *PKD1* gene that localizes to the primary cilium where it dimerizes with Polycystin-2 in order to regulate intracellular calcium levels in kidney tubular epithelial cells. This regulation was believed to be based on the fluid flow across the surface of the cell which can be sensed by the polycystin proteins through the bending of the primary cilium [13], although recent results show that this may not actually be the case [81]. However, ciliary localization of polycystin 1 and 2 are still required for calcium signaling [82]. Knockdown of *PKD1* leads to centrosomal and chromosomal abnormalities [83] as well as faster cell cycle progression [84] but not a reduction in ciliogenesis [85]. Cilia can sometimes act as both promoters of tumorigenesis as well as tumor suppressors, sometimes even within the same tissue or even in the same tumor subtype. For example, in medulloblastoma, the most common form of malignant pediatric brain tumor, the primary cilium may or may not be lost depending on the molecular basis of tumorigenesis [86]. This sort of contrast typifies the complexity and context-specificity of the biological processes at play. Thus, the need for more information about the interplay between ciliary biology and tumorigenesis is clear.

To model the activity of these proteins *in vitro* we use a 3D cell culture system: spheroids grown in matrigel **(Figure 6)**. To produce these spheroids we use mouse kidney tubular cells from the collecting duct (mIMCD3) which form small spheres inside the matrigel. As these spheroids grow, they develop a cleared lumen into which the cilia protrude. These spheroids more accurately model the *in vivo* condition of the kidney, because they are polarized and have more physiological interactions between cells. These spheroids can also be imaged in 3D making them convenient for studying the organization and orientation of cells. Because many ciliary proteins are involved in the cytoskeleton, IFT and other directional functions, these 3D polarized spheroids can give us an excellent model of their activity [87, 88].

Until recently, a mammalian model that fully recapitulated the phenotypes of human VHL deficiency did not exist. Mouse models with germ-line inactivating mutations in *Vhlh,* the

murine ortholog of *VHL,* do not survive [89] and conditional knockouts of only *Vhlh* do not develop phenotypes resembling human patients [90], although in one mouse model, targeted deletion of Vhlh in the kidney leads to cysts at a low incidence (20%)[91]. Generating conditional double-mutant *Vhlh* mice that have additional mutations or deletions in other tumor suppressor genes, such as *Trp53* (*TP53* ortholog), can produce a mouse with kidney cysts and tumors that resemble ccRCC in some ways [92], but no completely satisfactory model existed for many years. Mouse models which combine conditional *Vhlh* deletion with another genetic insult, such as the above mentioned *Vhlh*-negative *Bap1*-heterozygote kidney mouse [61], have now been developed that more accurately replicate VHL-related disease in a mammalian model organism, many limitations of these models still exist [93]. This is especially true when it comes to studying development. Thus, for modeling VHL deficiency and to study the early cellular changes in renal cells that lead to ccRCC development, we use a *vhl* mutant zebrafish line **(Figure 7)**. Zebrafish possess their own ortholog to the *VHL* gene and their kidneys are similar to human kidneys but significantly simpler. Zebrafish are an excellent model for modeling development because the embryos develop outside the body and are transparent, allowing us to observe their phenotypes at an early stage of development without sacrificing the parent animals [94, 95]. Heterozygous *vhl* mutant zebrafish are easy to maintain without discomfort and produce a large amount of offspring quickly, especially relative to mammalian models. By in-crossing this heterozygous stock of *vhl* mutant zebrafish, we produce a population of

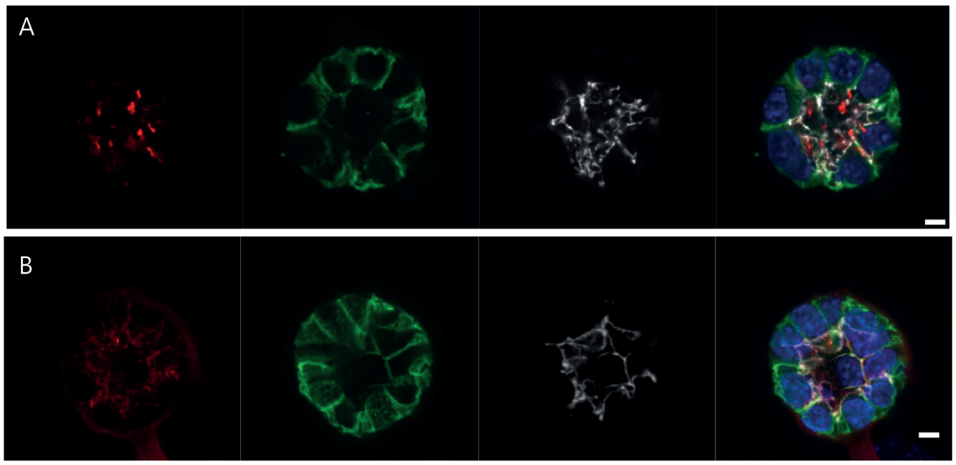


**Figure 6.** Example of an IMCD3 spheroid assay used to assess the function of a ciliary gene. Red channel (acetylated tubulin) shows the primary cilia. Green channel (betacatenin) shows the basal side of the cell while the white channel (Z-01) shows the apical side, allowing us to see the polar organization of these cells in a 3D structure. (A) spheroid grown from cells transfected with a control scrambled siRNA. (B) cells grown from cells transfected with siRNA against a gene required for ciliation, note the lack of primary cilia. Adapted with permission from Schueler *et al.*[104]

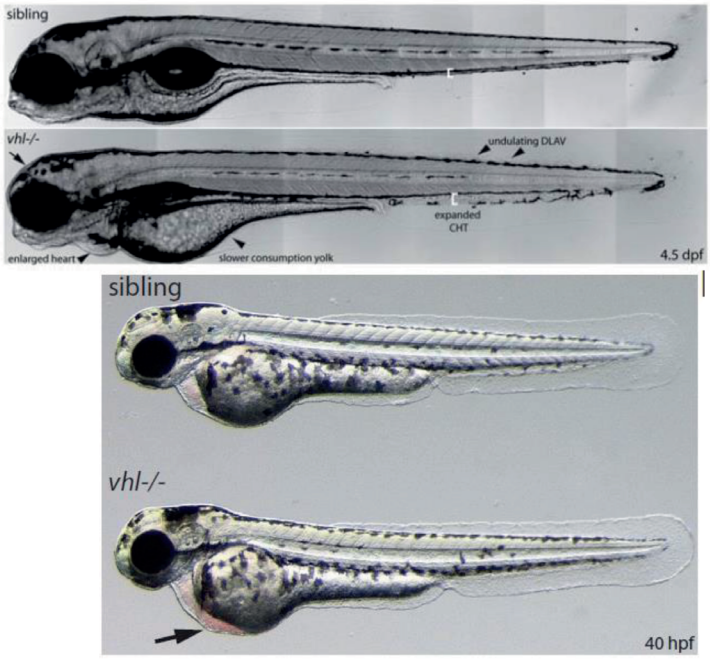


**Figure 7.** Characterization of VHL mutant zebrafish phenotypes. (A) Mutant zebrafish display cranial edema, heart compartment edema and heart enlargement, slower consumption of the yolk, and blood-vessel defects (arrows). Note also the absence of a swim bladder and reduction in melanosome density. (B) Even at an earlier stage of development, VHL mutant embryos display visibly enlarged hearts and polycythemia. Figures used with permission from Van Rooijen *et al.* [96, 97]

embryos which includes double-mutants without pVHL function that do not survive very long (usually less than a week) but which we can observe developing in real time during the first five days of life, unlike mouse embryos. These *vhl*-null embryos display symptoms remarkably similar to human patients, including polycythemia (excess red blood cells), excessive angiogenesis and neoplasm formation including alveolar dysplastic lesions in the kidney which resemble human ccRCC histologically [96-99]. This fish model is also appropriate for drug discovery [100]. Because miRNA expression is highly evolutionarily conserved, we can also use zebrafish to examine the role of miRNA in the pathology of VHL deficient phenotypes, in particular excessive angiogenesis. This zebrafish model provides a flexible and powerful tool to study VHL function and deficiency and also provides us with the opportunity to effectively test treatments in a high-throughput manner.

For the same reasons, zebrafish are useful for studying ciliopathies *in vivo*. In response to the deletion of a ciliopathy gene, zebrafish display a profile of symptoms that can be

identified during early development, much like *vhl* mutant zebrafish. Common phenotypes indicating a ciliopathy include bent body axis, left-right asymmetry of the heart, hydrocephalus, edema (especially around the heart), kidney cysts, agenesis of the swim bladder, eye defects and melanosome deficiency [101-108]. In zebrafish models of VHL disease and other ciliopathies, these phenotypes are present in embryos during early development, allowing phenotyping at less than 5 days after fertilization. Zebrafish are also easy to genetically manipulate, especially in comparison with mammalian models. In addition, by injecting mutant fish with human DNA we can easily perform rescue experiments to examine the effect of mutations taken from human patients.

In this thesis I investigate the connection between tumor suppressor pathways, particularly the VHL pathway, and the function and components of the primary cilium. In **Chapter 2** we examine in depth the connection between the cilium and neoplasm formation. We review work that regards the role that dysfunction of the primary cilium and ciliary proteins play in the pathophysiology of hereditary tumor predisposition syndromes, including von Hippel-Lindau disease, adenomatous polyposis coli, tuberous sclerosis, and Birt-Hogg-Dubé syndrome. In **Chapter 3** we review the etiology of von Hippel-Lindau disease in depth, including symptoms, inheritance patterns, and discussion of treatment options including ones currently under development. In **Chapter 4** we use the previously discussed zebrafish model of VHL disease and an established *in vitro* co-culture model of angiogenic activity to test the effectiveness of a specific drug regimen in reducing the angiogenic burden of *VHL* deficiency while managing toxicities at lower drug doses. Specifically, we show that a combination of two drugs works better to reduce the angiogenic phenotype induced by the lack of pVHL activity than either drug individually. These drugs are cibotentan, which targets the powerfully angiogenic Vascular Endothelial Growth Factor (VEGF) pathway, a downstream target of HIF signaling, and zibotentan which antagonizes the activity of the ET-A pathway, another important angiogenic signaling vector. In **Chapter 5** we again examine the molecular mechanisms of *VHL* deficiency and how the lack of functional pVHL promotes tumor growth, in this case, by promoting the transcription of the 212/132 miRNA family. These miRNA, important regulators of mRNA, cooperate with other HIF targets to promote angiogenesis by reducing levels of anti-proliferation proteins. One of these proteins is the anti-tumor protein Phosphatase and Tensin Homologue (PTEN) which we show is reduced in our VHL-null models. This reduction of PTEN activity may contribute to neoplasm formation. **Chapter 6**, we show that VHL interacts with the p53 pathway, one of the most important tumor suppressor pathways, through a non-canonical interaction with Programmed Cell Death 5 (PDCD5), which in turn regulates mouse double minute 2 homolog (MDM2) one of the most important regulators of p53 activity. We show that loss of pVHL causes PDCD5 to translocate to the nucleus and degrade MDM2, leading to an accumulation of p53. However, despite the induction of pro-apoptotic p53, we show

that the lack of pVHL leads to an induction of anti-apoptotic signaling capable of causing the cells to survive, which may explain why p53 is rarely mutated in VHL-related cancer and why these cancers are difficult to treat with traditional chemotherapy. Finally, in **Chapter 7**, we examine another tumor suppressor protein, HUWE1. Like pVHL, this protein is also an E3 ubiquitin ligase with a large variety of targets that has anti-tumor activity. Here we identify HUWE1 as a novel promoter of the cilium and show that loss of HUWE1 leads to pathology with ciliopathy-like features in a zebrafish model. A general discussion of the findings of all the work in this thesis is presented in **Chapter 8**.

# REFERENCES


1. Gerdes, J.M., E.E. Davis, and N. Katsanis, *The vertebrate primary cilium in development, homeostasis, and disease.* Cell, 2009. **137**(1): p. 32-45.
2. Fry, A.M., M.J. Leaper, and R. Bayliss, *The primary cilium: guardian of organ development and homeostasis.* Organogenesis, 2014. **10**(1): p. 62-8.
3. Oh, E.C. and N. Katsanis, *Cilia in vertebrate development and disease.* Development, 2012.**139**(3): p. 443-8.
4. Badano, J.L., et al., *The ciliopathies: an emerging class of human genetic disorders.* Annu Rev Genomics Hum Genet, 2006. **7**: p. 125-48.
5. Marshall, W.F., *The cell biological basis of ciliary disease.* J Cell Biol, 2008. **180**(1): p. 17-21.
6. Klasson, T.D. and R.H. Giles, *The role of the cilium in hereditary tumor predisposition syndromes.* Journal of Pediatric Genetics, 2014. **3**(2): p. 129-140.
7. Kim, S. and B.D. Dynlacht, *Assembling a primary cilium.* Curr Opin Cell Biol, 2013. **25**(4): p. 506-11.
8. Lu, Q., et al., *Early steps in primary cilium assembly require EHD1/EHD3-dependent ciliary vesicle formation.* Nat Cell Biol, 2015. **17**(3): p. 228-40.
9. Blacque, O.E. and A.A. Sanders, *Compartments within a compartment: what C. elegans can tell us about ciliary subdomain composition, biogenesis, function, and disease.* Organogenesis, 2014. **10**(1): p. 126-37.
10. Nachury, M.V., E.S. Seeley, and H. Jin, *Trafficking to the ciliary membrane: how to get across the periciliary diffusion barrier?* Annu Rev Cell Dev Biol, 2010. **26**: p. 59-87.
11. Lindemann, C.B. and K.A. Lesich, *Flagellar and ciliary beating: the proven and the possible.* J Cell Sci, 2010. **123**(Pt 4): p. 519-28.
12. Lechtreck, K.F., *IFT-Cargo Interactions and Protein Transport in Cilia.* Trends Biochem Sci, 2015. **40**(12): p. 765-78.
13. Mangolini, A., L. de Stephanis, and G. Aguiari, *Role of calcium in polycystic kidney disease: From signaling to pathology.* World J Nephrol, 2016. **5**(1): p. 76-83.
14. Slaats, G.G., et al., *Screen-based identification and validation of four new ion channels as regulators of renal ciliogenesis.* J Cell Sci, 2015. **128**(24): p. 4550-9.
15. Goetz, S.C. and K.V. Anderson, *The primary cilium: a signalling centre during vertebrate development.* Nat Rev Genet, 2010. **11**(5): p. 331-44.
16. Berbari, N.F., et al., *The primary cilium as a complex signaling center.* Curr Biol, 2009. **19**(13): p. R526-35.
17. Park, T.J., et al., *Dishevelled controls apical docking and planar polarization of basal bodies in ciliated epithelial cells.* Nat Genet, 2008. **40**(7): p. 871-9.
18. Wallingford, J.B. and B. Mitchell, *Strange as it may seem: the many links between Wnt signaling, planar cell polarity, and cilia.* Genes Dev, 2011. **25**(3): p. 201-13.
19. Goggolidou, P., *Wnt and planar cell polarity signaling in cystic renal disease.* Organogenesis, 2014. **10**(1): p. 86-95.
20. Briscoe, J. and P.P. Therond, *The mechanisms of Hedgehog signalling and its roles in development and disease.* Nat Rev Mol Cell Biol, 2013. **14**(7): p. 416-29.
21. Wong, S.Y. and J.F. Reiter, *The primary cilium at the crossroads of mammalian hedgehog signaling.* Curr Top Dev Biol, 2008. **85**: p. 225-60.
22. Ezratty, E.J., et al., *A role for the primary cilium in Notch signaling and epidermal differentiation during skin development.* Cell, 2011. **145**(7): p. 1129-41.
23. Kim, M., et al., *The MST1/2-SAV1 complex of the Hippo pathway promotes ciliogenesis.* Nat Commun, 2014. **5**: p. 5370.
24. Hansen, C.G., T. Moroishi, and K.L. Guan, *YAP and TAZ: a nexus for Hippo signaling and beyond.* Trends Cell Biol, 2015. **25**(9): p. 499-513.
25. van Reeuwijk, J., H.H. Arts, and R. Roepman, *Scrutinizing ciliopathies by unraveling ciliary interaction networks.* Hum Mol Genet, 2011. **20**(R2): p. R149-57.
26. Waters, A.M. and P.L. Beales, *Ciliopathies: an expanding disease spectrum.* Pediatr Nephrol, 2011. **26**(7): p. 1039-56.
27. Ferkol, T.W. and M.W. Leigh, *Ciliopathies: the central role of cilia in a spectrum of pediatric disorders.* J Pediatr, 2012. **160**(3): p. 366-71.
28. Arts, H.H. and N.V. Knoers, *Current insights into renal ciliopathies: what can genetics teach us?* Pediatr Nephrol, 2013. **28**(6): p. 863-74.
29. Praveen, K., E.E. Davis, and N. Katsanis, *Unique among ciliopathies: primary ciliary dyskinesia, a motile cilia disorder.* F1000Prime Rep, 2015. **7**: p. 36.
30. Tobin, J.L. and P.L. Beales, *The nonmotile ciliopathies.* Genet Med, 2009. **11**(6): p. 386-402.
31. Fliegauf, M., T. Benzing, and H. Omran, *When cilia go bad: cilia defects and ciliopathies.* Nat Rev Mol Cell Biol, 2007. **8**(11): p. 880-93.
32. Han, Y.G. and A. Alvarez-Buylla, *Role of primary cilia in brain development and cancer.* Curr Opin Neurobiol, 2010. **20**(1): p. 58-67.
33. Blankenship, C., et al., *Alternate choice of initiation codon produces a biologically active product of the von Hippel Lindau gene with tumor suppressor activity.* Oncogene, 1999. **18**(8): p. 1529-35.
34. Bartels, M., et al., *Novel Homozygous Mutation of the Internal Translation Initiation Start Site of VHL is Exclusively Associated with Erythrocytosis: Indications for Distinct Functional Roles of von Hippel-Lindau Tumor Suppressor Isoforms.* Hum Mutat, 2015. **36**(11): p. 1039-42.
35. Lolkema, M.P., et al., *Tumor suppression by the von Hippel-Lindau protein requires phosphorylation of the acidic domain.* J Biol Chem, 2005. **280**(23): p. 22205-11.
36. Gossage, L., T. Eisen, and E.R. Maher, *VHL, the story of a tumour suppressor gene.* Nat Rev Cancer, 2015. **15**(1): p. 55-64.
37. Li, M. and W.Y. Kim, *Two sides to every story: the HIF-dependent and HIF-independent functions of pVHL.* J Cell Mol Med, 2011. **15**(2): p. 187-95.
38. Frantzen, C., et al., *Von Hippel-Lindau Syndrome.* GeneReviews. Seattle, WA: University of Washington, 2015.
39. Hsu, T., *Complex cellular functions of the von Hippel-Lindau tumor suppressor gene: insights from model organisms.* Oncogene, 2012. **31**(18): p. 2247-57.

40. Semenza, G.L., *Hypoxia-inducible factors: mediators of cancer progression and targets for cancer therapy.* Trends Pharmacol Sci, 2012. **33**(4): p. 207-14.
41. Carroll, V.A. and M. Ashcroft, *Role of hypoxia-inducible factor (HIF)-1alpha versus HIF-2alpha in the regulation of HIF target genes in response to hypoxia, insulin-like growth factor-I, or loss of von Hippel-Lindau function: implications for targeting the HIF pathway.* Cancer Res, 2006. **66**(12): p. 6264-70.
42. Hara, S., et al., *Expression and characterization of hypoxia-inducible factor (HIF)-3alpha in human kidney: suppression of HIF-mediated gene expression by HIF-3alpha.* Biochem Biophys Res Commun, 2001. **287**(4): p. 808-13.
43. Nallamshetty, S., S.Y. Chan, and J. Loscalzo, *Hypoxia: a master regulator of microRNA biogenesis and activity.* Free Radic Biol Med, 2013. **64**: p. 20-30.
44. Azzouzi, H.E., et al., *HypoxamiRs: regulators of cardiac hypoxia and energy metabolism.* Trends Endocrinol Metab, 2015. **26**(9): p. 502-8.
45. Basten, S.G., et al., *Mutations in LRRC50 predispose zebrafish and humans to seminomas.* PLoS Genet, 2013. **9**(4): p. e1003384.
46. Shen, C. and W.G. Kaelin, Jr., *The VHL/HIF axis in clear cell renal carcinoma.* Semin Cancer Biol, 2013. **23**(1): p. 18-25.
47. Baldewijns, M.M., et al., *VHL and HIF signalling in renal cell carcinogenesis.* J Pathol, 2010. **221**(2): p. 125-38.
48. Maher, E.R., H.P. Neumann, and S. Richard, *von Hippel-Lindau disease: a clinical and scientific review.* Eur J Hum Genet, 2011. **19**(6): p. 617-23.
49. Linehan, W.M., *Genetic basis of kidney cancer: role of genomics for the development of disease-based therapeutics.* Genome Res, 2012. **22**(11): p. 2089-100.
50. Moore, L.E., et al., *Von Hippel-Lindau (VHL) inactivation in sporadic clear cell renal cancer: associations with germline VHL polymorphisms and etiologic risk factors.* PLoS Genet, 2011. **7**(10): p. e1002312.
51. Nickerson, M.L., et al., *Improved identification of von Hippel-Lindau gene alterations in clear cell renal tumors.* Clin Cancer Res, 2008. **14**(15): p. 4726-34.
52. Sato, Y., et al., *Integrated molecular analysis of clear-cell renal cell carcinoma.* Nat Genet, 2013. **45**(8): p. 860-7.
53. Mandriota, S.J., et al., *HIF activation identifies early lesions in VHL kidneys: evidence for site-specific tumor suppressor function in the nephron.* Cancer Cell, 2002. **1**(5): p. 459-68.
54. Montani, M., et al., *VHL-gene deletion in single renal tubular epithelial cells and renal tubular cysts: further evidence for a cyst-dependent progression pathway of clear cell renal carcinoma in von Hippel-Lindau disease.* Am J Surg Pathol, 2010. **34**(6): p. 806-15.
55. Rydzanicz, M., et al., *Genomics and epigenomics of clear cell renal cell carcinoma: recent developments and potential applications.* Cancer Lett, 2013. **341**(2): p. 111-26.
56. Moore, L.E., et al., *Genomic copy number alterations in clear cell renal carcinoma: associations with case characteristics and mechanisms of VHL gene inactivation.* Oncogenesis, 2012. **1**: p. e14.
57. Beroukhim, R., et al., *Patterns of gene expression and copy-number alterations in von-hippel lindau disease-associated and sporadic clear cell carcinoma of the kidney.* Cancer Res, 2009. **69**(11): p. 4674-81.
58. Matsuda, D., et al., *Identification of copy number alterations and its association with pathological features in clear cell and papillary RCC.* Cancer Lett, 2008. **272**(2): p. 260-7.
59. Dalgliesh, G.L., et al., *Systematic sequencing of renal carcinoma reveals inactivation of histone modifying genes.* Nature, 2010. **463**(7279): p. 360-3.
60. Liao, L., J.R. Testa, and H. Yang, *The roles of chromatin-remodelers and epigenetic modifiers in kidney cancer.* Cancer Genet, 2015. **208**(5): p. 206-14.
61. Wang, S.S., et al., *Bap1 is essential for kidney function and cooperates with Vhl in renal tumorigenesis.* Proc Natl Acad Sci U S A, 2014. **111**(46): p. 16538-43.
62. Pena-Llopis, S., et al., *BAP1 loss defines a new class of renal cell carcinoma.* Nat Genet, 2012. **44**(7): p. 751-9.
63. *Comprehensive molecular characterization of clear cell renal cell carcinoma.* Nature, 2013. **499**(7456): p. 43-9.
64. Gerlinger, M., et al., *Genomic architecture and evolution of clear cell renal cell carcinomas defined by multiregion sequencing.* Nat Genet, 2014. **46**(3): p. 225-33.
65. Mans, D.A., et al., *Mobility of the von Hippel-Lindau tumour suppressor protein is regulated by kinesin-2.* Exp Cell Res, 2008. **314**(6): p. 1229-36.
66. Essers, P.B., et al., *The von Hippel-Lindau tumor suppressor regulates programmed cell death 5-mediated degradation of Mdm2.* Oncogene, 2015. **34**(6): p. 771-9.
67. Li, G., D. Ma, and Y. Chen, *Cellular functions of programmed cell death 5.* Biochim Biophys Acta, 2016. **1863**(4): p. 572-80.
68. Esteban, M.A., et al., *Formation of primary cilia in the renal epithelium is regulated by the von Hippel-Lindau tumor suppressor protein.* J Am Soc Nephrol, 2006. **17**(7): p. 1801-6.
69. Frew, I.J., et al., *Genetic deletion of the long isoform of the von Hippel-Lindau tumour suppressor gene product alters microtubule dynamics.* Eur J Cancer, 2013. **49**(10): p. 2433-40.
70. Thoma, C.R., et al., *Quantitative image analysis identifies pVHL as a key regulator of microtubule dynamic instability.* J Cell Biol, 2010. **190**(6): p. 991-1003.
71. Schraml, P., et al., *Sporadic clear cell renal cell carcinoma but not the papillary type is characterized by severely reduced frequency of primary cilia.* Mod Pathol, 2009. **22**(1): p. 31-6.
72. Basten, S.G., et al., *Reduced cilia frequencies in human renal cell carcinomas versus neighboring parenchymal tissue.* Cilia, 2013. **2**(1): p. 2.
73. Hildebrandt, F., T. Benzing, and N. Katsanis, *Ciliopathies.* N Engl J Med, 2011. **364**(16): p. 1533-43.
74. Holland, A.J., et al., *Polo-like kinase 4 controls centriole duplication but does not directly regulate cytokinesis.* Mol Biol Cell, 2012. **23**(10): p. 1838-45.
75. Holland, A.J., W. Lan, and D.W. Cleveland, *Centriole duplication: A lesson in self-control.* Cell Cycle, 2010. **9**(14): p. 2731-6.
76. Sonnen, K.F., et al., *Human Cep192 and Cep152 cooperate in Plk4 recruitment and centriole duplication.* J Cell Sci, 2013. **126**(Pt 14): p. 3223-33.

77. Holland, A.J. and D.W. Cleveland, *Losing balance: the origin and impact of aneuploidy in cancer.* EMBO Rep, 2012. **13**(6): p. 501-14.
78. Choi, H.J., et al., *NEK8 links the ATR-regulated replication stress response and S phase CDK activity to renal ciliopathies.* Mol Cell, 2013. **51**(4): p. 423-39.
79. Grampa, V., et al., *Novel NEK8 Mutations Cause Severe Syndromic Renal Cystic Dysplasia through YAP Dysregulation.* PLoS Genet, 2016. **12**(3): p. e1005894.
80. Slaats, G.G., et al., *Nephronophthisis-associated CEP164 regulates cell cycle progression, apoptosis and epithelial-to-mesenchymal transition.* PLoS Genet, 2014. **10**(10): p. e1004594.
81. Delling, M., et al., *Primary cilia are not calcium-responsive mechanosensors.* Nature, 2016. **531**(7596): p. 656-60.
82. Xu, C., et al., *Human ADPKD primary cyst epithelial cells with a novel, single codon deletion in the PKD1 gene exhibit defective ciliary polycystin localization and loss of flow-induced Ca2+ signaling.* Am J Physiol Renal Physiol, 2007. **292**(3): p. F930-45.
83. AbouAlaiwi, W.A., et al., *Endothelial cells from humans and mice with polycystic kidney disease are characterized by polyploidy and chromosome segregation defects through survivin down-regulation.* Hum Mol Genet, 2011. **20**(2): p. 354-67.
84. Aguiari, G., et al., *Novel role for polycystin-1 in modulating cell proliferation through calcium oscillations in kidney cells.* Cell Prolif, 2008. **41**(3): p. 554-73.
85. Nauli, S.M., et al., *Polycystins 1 and 2 mediate mechanosensation in the primary cilium of kidney cells.* Nat Genet, 2003. **33**(2): p. 129-37.
86. Han, Y.G., et al., *Dual and opposing roles of primary cilia in medulloblastoma development.* Nat Med, 2009. **15**(9): p. 1062-5.
87. Giles, R.H., H. Ajzenberg, and P.K. Jackson, *3D spheroid model of mIMCD3 cells for studying ciliopathies and renal epithelial disorders.* Nat Protoc, 2014. **9**(12): p. 2725-31.
88. Ajzenberg, H., et al., *Non-invasive sources of cells with primary cilia from pediatric and adult patients.* Cilia, 2015. **4**: p. 8.
89. Gnarra, J.R., et al., *Defective placental vasculogenesis causes embryonic lethality in VHL-deficient mice.* Proc Natl Acad Sci U S A, 1997. **94**(17): p. 9102-7.
90. Kleymenova, E., et al., *Susceptibility to vascular neoplasms but no increased susceptibility to renal carcinogenesis in Vhl knockout mice.* Carcinogenesis, 2004. **25**(3): p. 309-15.
91. Rankin, E.B., J.E. Tomaszewski, and V.H. Haase, *Renal cyst development in mice with conditional inactivation of the von Hippel-Lindau tumor suppressor.* Cancer Res, 2006. **66**(5): p. 2576-83.
92. Albers, J., et al., *Combined mutation of Vhl and Trp53 causes renal cysts and tumours in mice.* EMBO Mol Med, 2013. **5**(6): p. 949-64.
93. Kapitsinou, P.P. and V.H. Haase, *The VHL tumor suppressor and HIF: insights from genetic studies in mice.* Cell Death Differ, 2008. **15**(4): p. 650-9.
94. Cheng, C.N., V.A. Verdun, and R.A. Wingert, *Recent advances in elucidating the genetic mechanisms of nephrogenesis using zebrafish.* Cells, 2015. **4**(2): p. 218-33.
95. Pickart, M.A. and E.W. Klee, *Zebrafish approaches enhance the translational research tackle box.* Transl Res, 2014. **163**(2): p. 65-78.
96. van Rooijen, E., et al., *A zebrafish model for VHL and hypoxia signaling.* Methods Cell Biol, 2011. **105**: p. 163-90.
97. van Rooijen, E., et al., *Zebrafish mutants in the von Hippel-Lindau tumor suppressor display a hypoxic response and recapitulate key aspects of Chuvash polycythemia.* Blood, 2009. **113**(25): p. 6449-60.
98. Santhakumar, K., et al., *A zebrafish model to study and therapeutically manipulate hypoxia signaling in tumorigenesis.* Cancer Res, 2012. **72**(16): p. 4017-27.
99. van Rooijen, E., et al., *von Hippel-Lindau tumor suppressor mutants faithfully model pathological hypoxia-driven angiogenesis and vascular retinopathies in zebrafish.* Dis Model Mech, 2010. **3**(5-6): p. 343-53.
100. Metelo, A.M., et al., *Pharmacological HIF2alpha inhibition improves VHL disease-associated phenotypes in zebrafish model.* J Clin Invest, 2015. **125**(5): p. 1987-97.
101. Hildebrandt, F. and W. Zhou, *Nephronophthisis-associated ciliopathies.* J Am Soc Nephrol, 2007. **18**(6): p. 1855-71.
102. Estrada-Cuzcano, A., et al., *Non-syndromic retinal ciliopathies: translating gene discovery into therapy.* Hum Mol Genet, 2012. **21**(R1): p. R111-24.
103. Slaats, G.G., et al., *DNA replication stress underlies renal phenotypes in CEP290-associated Joubert syndrome.* J Clin Invest, 2015. **125**(9): p. 3657-66.
104. Schueler, M., et al., *DCDC2 mutations cause a renal-hepatic ciliopathy by disrupting Wnt signaling.* Am J Hum Genet, 2015. **96**(1): p. 81-92.
105. Otto, E.A., et al., *Candidate exome capture identifies mutation of SDCCAG8 as the cause of a retinal-renal ciliopathy.* Nat Genet, 2010. **42**(10): p. 840-50.
106. Jaffe, K.M., et al., *c21orf59/kurly Controls Both Cilia Motility and Polarization.* Cell Rep, 2016. **14**(8): p. 1841-9.
107. Ramachandran, H., et al., *Interaction with the Bardet-Biedl gene product TRIM32/BBS11 modifies the half-life and localization of Glis2/NPHP7.* J Biol Chem, 2014. **289**(12): p. 8390-401.
108. Coon, B.G., et al., *The Lowe syndrome protein OCRL1 is involved in primary cilia assembly.* Hum Mol Genet, 2012. **21**(8): p. 1835-47.

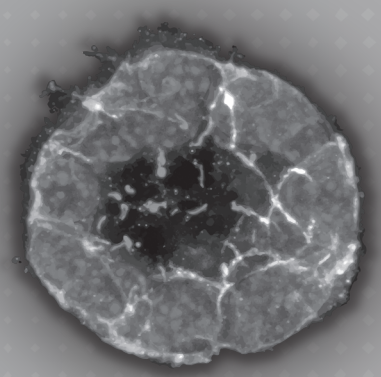

## CHAPTER 2

# The role of the cilium in hereditary tumor predisposition syndromes

J Pediatr Genet. 2014 Jun; 3(2): 129–140. doi: 10.3233/PGE-14091

**Klasson TD** and Giles RH

## ABSTRACT

The primary cilium is a highly conserved cell organelle that is closely connected to processes involved in cell patterning and replication. Amongst their many functions, cilia act as "signal towers" through which cell-cell signaling cascades pass. Dysfunction of cilia or the myriad processes that are connected with cilium function can lead to disease. Due to the sheer number of cellular processes that at some point involve the primary cilium, the effects of misregulation are highly heterogeneous between different cell populations. However, because of the importance of primary cilia in the development, growth, patterning and orientation of cells and tissues, a common thread has emerged in which defective cilia can lead to disorganization, which can contribute to the growth of neoplasms, including cancer and pre-cancerous phenotypes. Because cilia are so vital for signaling during cell replication and the cell fate decisions that are important in childhood growth, symptoms often arise early in life. Here we review recent work connecting misregulation of the primary cilium with tumor formation in a variety of tissues in the developing body, with a particular focus on the syndromes in which classic tumor genes are mutated, including von Hippel-Lindau disease (OMIM 193300), adenomatous polyposis coli (OMIM 175100), tuberous sclerosis (OMIM 191100) and Birt-Hogg-Dub´e syndrome (OMIM 135150). Timely diagnosis of these syndromes is essential for entry into appropriate screening protocols,which have been shown to effectively prolong life expectancy in these cohorts of patients.

## INTRODUCTION

The primary cilium, an antenna-like structure found on almost all mammalian cells, was once considered to be a mostly unimportant vestigial organelle but has now emerged as a vital player in a number of cellular processes. Cilia respond to physical and chemical signals to regulate critical signal transduction pathways; for example, cilia are both negative and positive regulators of the hedgehog pathway [1]. Many of these signaling pathways are crucial in proliferation and patterning of developing tissue. Because of their importance in growth and development at all levels, from single cells to tissue organization to the positioning of entire organs, misregulation of primary cilia is now widely acknowledged to be an important mechanism in the biology of developmental and degenerative disorders. Emerging data likewise indicates that cilia participate in tumorigenesis as well. Here we will focus on tumor types affecting children and the pathophysiology of inherited tumor syndromes implicated with cilia dysfunction.

The primary cilium is central to pleiotropic effects in growth and patterning of cells, tissues and organ-isms both through its involvement in a wide variety of cellular signaling and sensory pathways and by its direct involvement in cell division. In order to have proper ciliary function, a cell must be able to assemble, maintain, and then disassemble its primary cilium. Cells with malfunctioning cilia display varied phenotypes including the disruption of many signaling pathways, aberrations in the cell cycle and intracellular trafficking defects. A mutation which affects the structure or function of cilia can therefore lead to down-stream changes in the phenotype of the cell population and even the tissue, including anomalies in cell polarization, cell fate determination, cell metabolism and cell division as well as an inability to properly respond to extracellular signals and changes in the internal environment such as DNA damage [2–4]. Because of this wide array of functions, many outcomes of ciliary dys-function are possible including the development of pathogenic phenotypes in humans as well as model organisms [5–7]. Diseases arising from misregulation of cilia formation, maintenance or disassembly, known collectively as ciliopathies, can be pathologically mild or so severe that they cause neonatal death. The ciliopathies include a number of inherited developmental disorders that are directly caused by, or involve, misregulation of cilia, as well as different tumor types, cancerous diseases and syndromes. In this context, some pediatric tumors, such as Wilms' tumor of the kidney, can be viewed as a developmental disorder as it arises from mutations in survival and developmental pathways that cause these processes to be co-opted to provide survival strategies for tumor cells [8, 9]. Currently, the role of primary cilia in tumorigenesis and cancer-related processes is not well understood, but recent data indicate that cell cycle misregulation caused by defective cilia as well as associated signal-ing irregularities contributes to tumor formation [10, 11].

## THE PRIMARY CILIUM AND CELL CYCLE REGULATION

The essential biology of the primary cilium (which will not be covered by this review as it has already been well-reviewed elsewhere [1, 12–14]) links it inextricably to the cell cycle through the basal body. The cilium is formed during the stationary G0-phase of the cell cycle. Prior to cell division, the ciliary axoneme must be disassembled. The basal body then decouples from the plasma membrane to function as the centrosome anchoring the mitotic spindle. The centriole also forms the microtubule organizing center which nucleates the microtubule skeleton. Thus, proliferation and ciliation are mutually exclusive; a cell cannot divide and remain ciliated. This makes the disassembly of cilia a crucial checkpoint in the cell cycle (Figure 1). One might expect that in the absence of cilia, this checkpoint is abolished and a cell would divide at a higher rate. Indeed, loss of cilia increases tumor incidence in murine models of basal cell carcinoma and medulloblastoma, both of which will be discussed in greater detail below [15–18]. A number of efforts have been made to catalogue cilia presence in human cancers: pancreatic cancer, renal cell carcinoma (RCC), cholangiocarcinoma, melanoma, ovarian cancer, prostate cancer, and breast cancer. All of these neoplasms feature significantly fewer cilia [19–27]. In addition, a number of proteins that are closely related to ciliogenesis and ciliary function are also known to have direct roles in cell cycle control. For example, reduction of cellular levels of Ift88, an intraflagellar

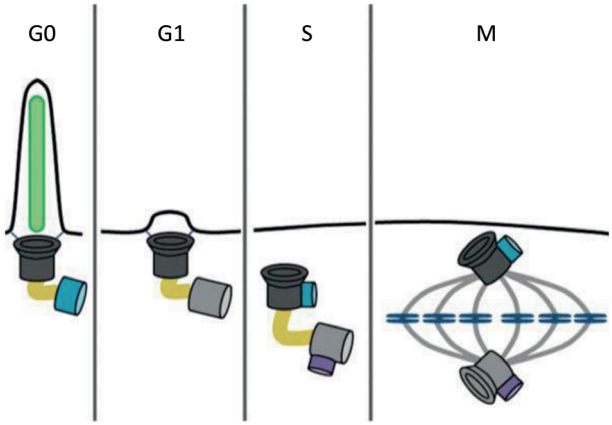


**Figure 1.** The presence of the primary cilium and cell replication are mutually exclusive. In G0-phase of the cell cycle, a fully formed cilium is present. As the cell progresses into G1-phase, the ciliary axoneme must be disassembled. The centrosome can then decouple from the plasma membrane allowing it to migrate into the cell where it will be replicated during S-phase. This process is required for normal mitotic spindle formation during mitosis. Mutations, which inhibit the construction of the ciliary axoneme or the coupling of the centrosome to the cell membrane may hypothetically promote replication by removing the need for deconstruction of the cilium before replication. Mutations affecting the centrosome itself may also interfere with proper mitotic spindle organization.

transport protein required for the formation of the primary cilium, induces cell cycle progression *in vitro*. *IFT88* mutations have been found in human postnatal lethal Meckel-Gruber syndrome (OMIM 249000) patients. Hypomorphic mutations in have also been shown to cause a ciliopathy in mice [28]; *orpk/Ift88* mutant mice also display epithelial cell hyperproliferation [21, 29, 30]. Interestingly, recent data suggest that modulation of retinoblastoma signaling, (responsible for entry into the S-phase of the cell cycle), by the von Hippel-Lindau tumor suppressor protein (pVHL) is related to overall survival in both sporadic and hereditary RCC [31]. Collectively, these data support the hypothesis that loss of cilia may promote cancer development in certain tissues. In particular, the localization of classic tumor suppressor proteins, typically mutated in familial tumor predisposition syndromes, to the cilium raises interesting questions concerning the relation between cilia and tumor development. For example, canonical tumor suppressor proteins such as pVHL, liver kinase B (LKB) 1, tuberous sclerosis (TSC) 1, TSC2 and adenomatous polyposis coli (APC) have been shown to localize to ciliary axonemes and/or basal bodies in ciliated cells [32]. Many of these proteins bind microtubules and thus have overlapping roles during interphase and mitosis. However, although many ciliopathies involve cell cycle defects, not all ciliopathies involve hyperplasia. Therefore, while the disassembly of cilia is required for cell proliferation, it will not always suffice to cause an increased rate of cell division on its own. While tumor formation frequently results from multiple germline and somatic mutations acquired over the course of many years, many ciliopathies are diagnosed in childhood. This may attribute to the absence of tumor prevalence in ciliopathy patients when diagnosed. Thus, while not all genetic mutations that cause a loss of ciliation will lead to cancer, many of them have the potential to cause, or at least contribute to, a proliferative phenotype, including cyst formation.

## CILIOPATHY-RELATED RENAL CYSTS

Data collected on ciliopathies support the hypothesis that misregulation of cilia can be a cause of neoplasm formation. A common feature of kidney diseases associated with the loss of function of cilia-associated proteins is the development of multiple fluid-filled cysts along the renal nephron. These cysts develop in part due to misaligned centrosomes that cause misoriented cell division (Figure 2). Many ciliopathies share this feature, including autosomal dominant (AD) (OMIM#173900) or recessive polycystic kidney disease (OMIM#263200), Bardet-Biedl syndrome (OMIM#209900) and Joubert syndrome (OMIM#213300). These cysts progressively impair renal function leading to the development of end-stage renal disease [14, 33]. They stain positive for markers characteristic of altered proliferation, wingless-related integration site (Wnt) signaling or proliferation (e.g. nuclear b-catenin [34])

but only rarely progress into renal tumors. Intriguingly, disorganization and improper regulation of the centrosome is also considered a hallmark of multiple cancer types [35], many of which also display neoplasm formation of this kind. Because the centrosome also functions as the basal body, many proteins that localize to the basal body and other parts of the cilium while the cell is ciliated in the G0-phase of the cell cycle contribute to the function and regulation of the centrosome during mitosis. For example, before cell division can occur, the mother centriole must duplicate itself to form the daughter centriole. This pair of centrioles is then used to form the spindle poles during mitosis (see previous section). The process of centriole duplication is controlled by the protein polo-like kinase 4 (PLK4) which localizes to the centrosome. Abnormal expression of PLK4 in some cancer types has been implicated in genomic instability that might contribute to tumor formation. Overexpression of PLK4 can cause extra centrioles to be produced, leading to malformed mitotic spindles and aneuploidy of daughter cells after division [36, 37]. The incidence of renal cysts in many syndromic ciliopathies and the incrimination of certain proteins which normally localize to the cilium and regulate or participate in cell division as assisting tumor growth when malfunctioning has led to the hypothesis that renal cysts found in ciliopathy patients are a pre-malignant stage and that renal cancers might develop from such cysts [38]. In some cases, such as in the case of the *VHL* gene, which is itself an oncogene due to its vital role in regulating hypoxia signaling, a mutation that causes cysts might also directly contribute to the development of cancer. In other cases, a second (or more) somatic mutations may be required in order to fully transform cells.

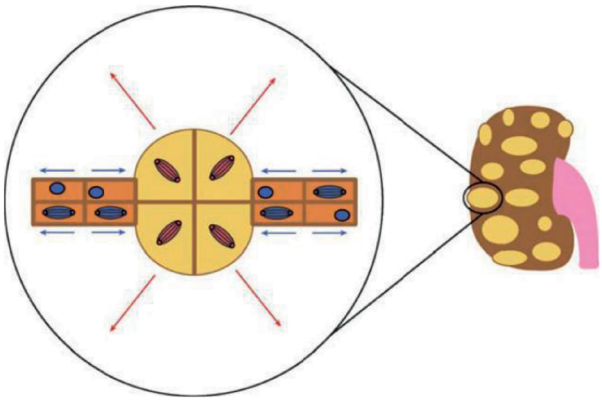

**Figure 2.** Cells dividing out of phase with the rest of the tissue can produce cysts. In this example, most of the renal cells are dividing in a similar direction (horizontal arrows). A mutation causes division to proceed out of the plane of the tissue, leading to a bulge. This bulge eventually becomes a renal cyst and widespread expression of this phenotype leads to a polycystic kidney. Cysts in other tissues can develop in a similar way.

## CILIA MISREGULATION AND TUMORIGENESIS

The natural course of any inherited tumor syndrome varies from individual to individual, with symptoms ranging from very mild to quite severe, occurring only when an independent somatic mutation inactivates the wild-type allele producing a cell with biallelic inactivation of the tumor suppressor in question [39]. At this point, the direct contribution of mutations which cause cilia dysfunction to tumorigenesis is incompletely understood and remains highly contentious. The connection between the primary cilium and the cell cycle, on the other hand, is both fundamental and undebatable. As mentioned above, cystic growths are a common symptom of ciliopathies and cyst development often occurs in hereditary cancer syndromes. In addition, some tumor types, a selection of which will be covered below, have also been shown to have reduced ciliary frequency, cilium function or signaling. However, cilia loss does not always correlate with tumorigenesis. Importantly, several studies on other tumor types, such as subsets of basal cell carcinoma and medulloblastoma, have indicated that in these tumors cilia are actually retained. As we dis-cuss in greater detail below, the oncogenic mutations in these tumors are driven by members of the hedge-hog signaling network, which is dependent on normal ciliary function to successfully generate downstream transcriptional activators and repressors [15, 16]. How-ever, as we have previously mentioned, in other subsets of these same tumor types with different genetic back-grounds, cilia act as tumor suppressors. The ability of the cilium to act as both a tumor suppressor and an oncogenic force in the same tissues and even among the same tumor types shows the context-specificity of the cellular response to the loss of proper ciliary functions. Given the heterogeneity of the proteins involved in ciliation, the true extent of the role of misregulation of cilia in tumorigenesis remains to be completely elucidated. Below we review some of the cancer syndromes and tumor types in which there is any data with regard to the role of the primary cilium and discuss the emerging importance of ciliary malfunction in hereditary cancer syndromes and precursor cell populations (Table 1).

**VHL**

VHL disease is a rare (1:36,000 incidence) genetic condition that predisposes patients to tumor formation in a variety of tissues. Typically, the first tumors observed in children or young adults are retinal hemangioblastomas, although cerebellar hemangioblastomas and pheochrocytomas have also been frequently reported in childhood and adolescence. RCCs occur in 70% of patients and represent the most common cause of mortality. Primary care physicians should refer any pediatric patient with a typical VHL tumor for genetic testing. RCCs occurring in individuals under the age of 45 yr are increasingly being referred for genetic testing as well because about 10% of them will carry germline *VHL* mutations and

require additional screening for other tumors. Clinical diagnosis can be made following standardized guidelines and involves the presence of two tumors in an affected individual or one tumor and a family history of VHL. VHL disease is caused by mutations in the *VHL* gene that encodes the pVHL tumor suppressor protein. VHL disease is inherited in an AD manner and the majority of patients (80%) have an affected parent. Molecular diagnosis via sequencing of the *VHL* gene is the preferred method as this will detect the disease causing mutation in >90% of patients [40].

Table 1.

| Disease/ syndrome | Frequency | Type of inheritance | Earliest manifestations | Clinical features |
|---|---|---|---|---|
| von Hippel-Lindau disease | 1:36,000 | Autosomal dominant | Retinal hemangioblastomas | Hemangioblastomas of the brain, spinal cord and retina, renal cell carcinomas, pheochromocytomas, neuroendocrine tumors, endolymphatic sac tumors, pancreatic, epididymal, broad ligament and renal cysts |
| Adenomatous polyposis coli- related disease | 1:7,000–1:22,000 | Autosomal dominant | Colonic polyps | Colonic polyps, polyps in stomach and intestines, osteomas and dental anomalies, congenital hypertrophy of the retinal pigment epithelium, soft tissue tumors, desmoid tumors |
| Tuberous sclerosis | 1:6,000 | Autosomal dominant | Highly variable, skin lesions are the most common symptom | Hypomelanotic macules, facial angiofibromas, shagreen patches, fibrous facial plaques, ungual fibromas, angiomyolipomas, kidney cysts, renal cell carcinomas, rhabdomyomas, heart arrhythmias, lymphangioleiomyomatosis |
| Birt-Hogg-Dubé syndrome | 1:200,000 | Autosomal dominant | Fibrofolliculomas | Fibrofolliculomas, trichodiscomas/angiofibromas, perifollicular fibromas and acrochordons, pulmonary cysts, pneumothorax, renal tumors |

Under physiological circumstances, pVHL is an E3 ubiquitin ligase, responsible for the regulation of HIF-alpha transcription factors that modulate the cell's response to low oxygen levels in the body (hypoxia). In the absence of functional pVHL, pseudo-hypoxia signaling stabilizes HIF-alpha and causes aberrant induction of a wide variety of target genes, including pro-survival and vasoproliferative genes that contribute to tumor formation. In addition, the most common form of renal cancer, clear cell RCC (ccRCC), is always associated with mutations or loss of the *VHL* gene in humans [41]. For an in depth review of pVHL and HIF signaling in renal cancer, please see [42]. Both pVHL and HIF1-alpha have been shown to be required for the maintenance of ciliation *in vitro* [43–48]. In addition, RCC tumors lacking functional pVHL display reduced ciliary frequency compared with neighboring tissues [20, 22]. pVHL localizes to cilia and interacts with the ciliary motor kinesin-2 [49, 50]. Although the loss of pVHL function is not sufficient to inhibit ciliogenesis, it does interfere with normal cilia dynamics and (mechano)-sensory roles [48, 51–53]. *In vivo* studies using inducible Cre-Lox deletion of *Vhl, Gsk3β, Pten* and *Tp53* in renal tubules in mice furthermore indicate that the combined loss of *Vhl* and *Gsk3β*

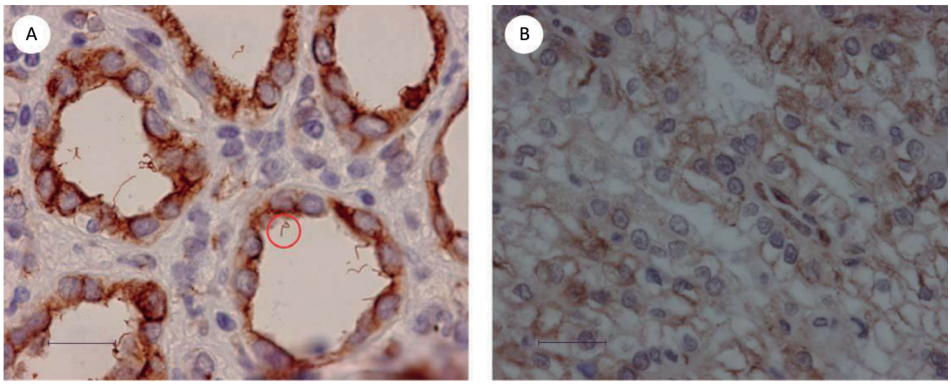


**Figure 3.** Acetylated alpha-tubulin stained renal tissue sections. This staining highlights the cells in the walls of the renal tubules and their cilia. (A) Normal parenchyma. Note the organized tubules, regular presence of cilia and the expected lack of staining in the supportive tissue cells between tubules. A primary cilium is encircled. (B) Renal cell cancer parenchyma. Organized tubular structures are lost, staining is diffuse and randomized and noticeable cilia are not present. Note the enlarged alveolar-like appearance of the cells.

or *Pten* or *Tp53* (second site modifiers), but not any of these genetic lesions alone, results in a reduction of renal tubule ciliogenesis and facilitates kidney cyst development in the same manner as described above for ciliopathies [54–57] (Figure 3). However, mice with loss of *Vhl* and/or *Gsk3β* in their kidney epithelium do not develop renal tumors, indicating that, at least in mice, additional somatic mutations are necessary for tumor formation. In humans how-ever, deep sequencing of tumors has shown that *VHL* mutations or deletions are ubiquitous events in all surveyed incidences of ccRCC implying that, in contrast to mouse models, the loss of pVHL function in humans is a required event in the development of these renal tumors [41]. Another function of the pVHL protein is the regulation of microtubule stability, and the loss of *VHL* has been linked to chromosome segregation errors [53]. Thus, tumor formation could be induced by aneuploidy events independently of cyst formation. These results present the question of whether cilia loss is critical for renal tumorigenesis or if it is just one part of a larger process. Although there is a well-documented proliferation burst in the kidney upon loss of renal cilia, this localized proliferation is not necessarily associated with tumor formation. Polycystic kidney disease has been shown to be caused by ciliary defects but is not associated with tumor formation [58]. Additional signaling pathways are therefore likely to play a role in the transformation of a kidney cyst into a tumor. In the case of RCC, the absence of functional pVHL, the over-expression of survival and proliferative genes as well as the destabilization of microtubules and cilia, com-bine to contribute to tumor formation. Thus, ccRCC is a good example of the heterogeneity inherent in the function of many ciliary proteins and how the multiple roles of these proteins have complex implications on human diseases.

**APC**

*APC* is a gene mutated in disease spectrum that share similar diagnoses and manifestations, including familial adenomatous polyposis, attenuated familial adenomatous polyposis, Gardner syndrome, and Turcot syndrome (OMIM 175100 for all). These conditions are characterized by the development of thousands of precancerous colonic polyps which can develop in patients as young as seven with an aver-age age of incidence at 16 yr. In addition, patients may develop osteomas and soft-tissue tumors (Gardner syn-drome) or tumors of the central nervous system (Turcot syndrome). For all *APC*-associated conditions, colon cancer is a certainty later in life without colectomy. All of these syndromes are caused by mutations in the *APC* gene and the differences in their symptoms are believed to be modulated by the particular pathogenic variant of mutation. Much like VHL syndrome, *APC* mutations are inherited in an AD manner and 80% of patients also have an affected parent. Molecular diagnosis can establish the basis of disease in upwards of 90% of cases by identifying the causal mutation. Clinical diagnosis is based on the presence of many (100+) colonic adenomatous polyps [59].

The APC protein is also the tumor suppressor protein most frequently mutated in sporadic colorectal cancer [57]. It acts upstream of pVHL [60] and, like pVHL, binds kinesin-2 and regulates microtubule [61–63] and chromosomal stability [64, 65]. Furthermore, inactivation of *Apc* in mouse kidneys results in renal cysts [66], suggesting a role for cilia regulation in neoplastic lesions occurring upon loss of *APC*. While the mechanisms leading to colorectal cancer are unlikely to be cilia-driven, particularly because under physiological conditions enterocytes continuously progress through the cell cycle and refrain from ciliogenesis, some of the syndromic extra-intestinal manifestations of *APC* inactivation can be attributed to ciliary malfunction, such as skin cysts, and congenital hypertrophy of the retinal pigmented epithelium observed in Gardner syndrome patients, which are clinically similar to symptoms occurring in classic ciliopathies [67].

**TSC**

TSC is a genetic disease associated with benign tumors in the brain, kidneys, heart, eyes, lungs, and skin with an incidence of 1:6,000. TSC usually affects the central nervous system and results in a combination of symptoms including seizures, developmental delay, behavioral problems, skin abnormalities, and kidney disease. Most tumors in TSC patients are not malignant; however, those that are malignant primarily affect the kidneys. Renal cysts and angiomyolipomas occur in >70% of TSC patients between the age of 15 and 30 yr. Prenatal fetus ultrasounds can identify cardiac rhabdomyoma in the hearts of infants but these can also develop in young children with TSC as well. Beyond tumors, TSC patients can manifest seizures, mental retardation, behavior problems, and skin abnormalities. Many TSC patients are diagnosed in the first year of life, and infants with TSC may manifest

cardiac rhabdomyomas or seizures at birth. However, clinical features can be subtle initially, or take years to develop. Consequently, TSC can be unrecognized or misdiagnosed for years. Further complicating diagnosis, patients are typically the first in their family and bear de novo heterozygous germline mutations in either *TSC1* or *TSC2* genes, encoding harmarin and tuberin, respectively [68].

In contrast to *VHL*, loss of *TSC1* or *TSC2* in TSC patients increases cilia length in fibroblasts and the renal tubule [69–71]. Low nutrient levels are thought to increase cilia length to potentiate a delay in cell cycle progression and protect the cell from stress. Because TSC1 and TSC2 are major regulators of energy sensing through the mammalian target of rapamycin/ribosomal protein S6 kinase (mTOR/S6) pathway, failure to activate this pathway in TSC could explain the increased cilia length [72]. Recent data also from leptin-deficient mice show that nutrient-sensing also regulates cilia length through Pten and Gsk3b [73]. In addition to cilia length, changes in mTOR signaling might contribute to tumorigenesis. The mTOR pathway is normally responsible for modulating the cellular response to stress. Activation of mTOR signaling leads to down-stream activation of genes that lead to cell survival, growth and a change in cellular metabolism so that the cell can survive in a low oxygen and low nutrient environment. Consequently, aberrant mTOR signaling has been implicated in tumorigenesis and research into mTOR inhibitors as therapeutic agents for the treatment of cancer is a crowded field [74]. Germline mutations in *PTEN* also contribute to increased pre-disposition of RCC in Cowden syndrome (OMIM # 158350) [75], although the cilia have not been examined in these patients. TSC patients are predisposed to develop benign renal angiomyolipoma but only demonstrate a slightly elevated lifetime risk for RCC; however, in cases where RCC does develop in TSC patients, the age of onset is 25 yr earlier in TSC patients as compared to the general population, at an average age of 28 yr [76, 77].

**Birt-Hogg-Dubé syndrome (BHD)**

BHD syndrome is an AD disease caused by mutations in the *FLCN* gene on chromosome 17. BHD (incidence 1:200,000) predisposes individuals to RCC (characteristically chromophobe-oncocytoma hybrid tumors, although other subtypes can also occur), cystic disease of the kidney and lung, as well as benign tumors of the hair follicles in the skin, called fibro-folliculomas [78, 79]. Any combination of these three symptoms can occur, although fibrofolliculomas are the most common manifestation, found on the face and upper trunk in over 80% of people with BHD over the age of 40 yr, and can be very similar in appearance to skin tags. Most patients with BHD are not diagnosed until the second or third decade of life. Pulmonary cysts are also common and can contribute to collapsed lung/ pneumothorax. Molecular diagnosis by sequencing the *FLCN* gene detects mutation in 88% of the patients.

The FLCN protein localizes to the centrosome during interphase and the mitotic spindle during mitosis and *FLCN* knockdown in healthy cells has been shown to delay ciliogenesis [80]. BHD patients as well as *Flcn* heterozygous mice develop renal cysts and neoplasms as well as aberrant activation of mTOR signaling associated with loss-of-heterozygosity [81]. As mentioned above, mTOR activation is believed to contribute to tumor growth, suggesting a classic tumor suppressor function for FLCN. In addition, *FLCN* mutations have been shown to lead to activation of the canonical Wnt signaling pathway [80]. The Wnt family of proteins comprise another fundamental signaling pathway which directs cell polarity and cell fate decisions [82]. Aberrant Wnt signaling has also been linked to cancer [83]. Collectively, these data suggest that FLCN has a role in the nutrient/energy-sensing pathway, similar to tumor suppressors TSC1, TSC2, PTEN and LKB1, and that mutations in *FLCN* probably cause tumorigenesis through the activation of pro-survival pathways.

**Hedgehog signaling and medulloblastoma**

The hedgehog signaling pathway is a particularly good example of the importance of the primary cilium in cell communication. The *hedgehog* gene was originally found in genetic experiments in *Drosophila melanogaster* where it was shown to have an effect on body patterning. The gene was eventually shown to code for a secreted protein that, once released by a cell, can control the patterning of neighboring cells. Over time, homologs in many other species were discovered, including the mammalian homologs Indian hedgehog, Desert hedgehog and Sonic hedge-hog (Shh). It is now known that the members of the hedgehog family of proteins are responsible for cell-cell communication in a diverse, but evolutionarily conserved, family of signaling cascades that control many types of tissue patterning, e.g. limb formation and midline structures in the brain, spinal cord and the thalamus. As an adjunct to their morphogenic function in development, hedgehog family proteins are also responsible for the maintenance of progenitor and stem cell populations in many adult tissues. For example, during brain development, Shh secreted by Purkinje cells in the cerebellum promotes the proliferation of granule cell precursors through the activation of proliferative genes like *v-myc avian myelocytomatosis viral oncogene homolog (MYC)*. In the adult organ, hedge-hog signaling is required to maintain homeostasis of the local neural stem cell population. Its function as a regulator of proliferation has led to hedgehog signaling being implicated in a number of cancers including basal cell carcinomas as previously mentioned as well as rhabdomyosarcomas [84].

Both the developmental function and the homeostasis function of hedgehog signaling require the primary cilium. Hedgehog receptors are enriched in the ciliary membrane and proteins involved in the signaling cascade are found in or around the primary cilium. Secreted proteins must travel to the cilium in order to be modified before being released [85]. This means that mutations, which affect cilia function can affect hedgehog signaling without

directly interacting with the pathway. This fact has implications in both the mechanisms of diseases involving hedgehog, and possible treatments for these diseases.

One of the cell types whose homeostasis is con-trolled through the cilia and hedgehog signaling are the granule neuron precursor (GNP) cells, a cell population which can give rise to medulloblastoma. Although rare in adults, medulloblastoma is the most common type of malignant pediatric brain tumor, accounting for 12–25% of all childhood central nervous system tumors [86]. As mentioned above, Shh signaling controls the expansion of the GNP population. Shh signaling elements concentrate in the primary cilium and the cilium is required for proper Shh signaling. Mice that have had the cilia removed from their GNP population via conditional inactivation of the *Kif3a* gene, which encodes for a kinesin-2 subunit necessary for ciliation, show a drastic decrease in Shh signaling and a corresponding decrease in the proliferation of their GNPs, leading to improper brain development. Removing *Smoothened (Smo)*, a gene encoding for an essential transducer of Shh, lead to the same mouse phenotypes [87]. Conversely, constitutive activation of the Shh pathway in these cells can lead to excessive proliferation and the formation of medulloblastoma. Mice with constitutively active Smo developed medulloblastoma by postnatal day 10 and Smo was found enriched in the primary cilium in these tumors. Intriguingly, by removing *Kif3a* or *Ift88* and therefore blocking ciliogenesis, tumor formation due to excessive Smo signaling was completely blocked. On the other hand, overexpression of Gli2, a transcriptional activator downstream of Smo, did not predispose to medulloblastoma. In fact, tumors were not formed in this experiment until cilia were ablated [15]. Thus, cilia act as both promoters and repressors of tumorigenesis in the same signaling cascade. Although human medulloblastoma caused by activating mutations in *SMO* are rare and no tumors caused by activating *GLI2* mutations along with another mutation leading to a loss of ciliation have ever been found, mutations in many genes that encode for proteins in the Shh signaling cascade and the related Wnt signaling pathways have been seen in tumors taken from patients with primary medulloblastomas [88]. Medulloblastomas taken from sporadic patients have also been observed to have patterns in their ciliation depending on their genetic background [15]. An examination of tumor cilia might therefore be a useful diagnostic tool used to determine the molecular basis of tumorigenesis in patients.

**Tumors from undifferentiated embryonic tissue**

An interesting pattern that has emerged in the study of hereditary cancer syndromes involving the primary cilia is the recurrence in many of these syndromes of tumors developing from undifferentiated embryonic tissue as well as precursor cell populations in early life. In addition to RCC, VHL patients develop characteristic tumors in two tissue types derived from embryonic mesonephric tissue: the broad ligament and epididymis [89].

The angiomyolipomas that develop in the kidneys of TSC patients are partially derived from immature smooth muscle cells and the tumors in medulloblastoma are derived from a precursor cell population as mentioned above. In addition to syndromes already discussed, patients with mutations in the dynein arm assembly factor *DNAAF1* develop tumors in the seminiferous vesicle early in life culminating in the accumulation of the testicular germ cell tumor subtype seminoma. DNAAF1 is found in the primary cilium of early germ cells and tumor sections taken from these patients show reduced ciliary frequency, implying a hypothetical role for DNAAF1 and the primary cilium in the normal growth and maintenance of the germ cell population [90]. In a study of 23 Wilms' tumors, another type of pediatric kidney tumor that is partially derived from immature cells, only eight were found to be ciliated when examined with electron microscopy [91]. The fact that many tumors that are characterized by low cilia counts arise from undifferentiated or immature cell populations might imply that these cells are somehow more sensitive to tumorigenesis caused by misregulation of the primary cilium. Perhaps the tendency towards tumors in these cell types can be accounted for by their reliance on growth and tissue patterning pathways that require the presence of the cilium such as the Shh and Wnt signaling pathways.

## CONCLUSIONS AND FUTURE PERSPECTIVES

Although the role of ciliary dysfunction in tumorigenesis is far from clear at the moment, certain patterns in the data imply a common set of mechanisms by which tumors arise. It is still unclear if misregulation of cilia causes cell cycle progression or if cell cycle progression and the loss of cilia are related processes controlled by a common upstream factor. However, from the currently available data, we propose a hypothetical model of cilia-related tumorigenesis as follows: a mutation arises or is inherited which affects cilia directly or affects a pathway associated with cilium function. The loss of proper ciliary function contributes to increased proliferation based on both the direct relationship of the cilium with cell division and the absence of proper signaling that requires functional cilia. In some cases, this increase in proliferation may lead immediately to tumor formation depending on the sensitivity of the cell type to ciliary signaling, whether it is embryonic tissue, and the exact function of the mutated gene. In other cases, increased proliferation may lead only to benign growths, which may constitute an unstable pre-cancerous environment that predisposes the cells to further mutations that will result in tumor formation.

A significant amount of further research is needed before this hypothetical model can be validated. The study of cilia is still relatively young, and much more data remains to be gathered. In particular, examination of the primary cilium (% cells that are ciliated, ciliary length, structure) in many well-studied tumor types is still needed. Integrating our understanding of the primary cilium into our understanding of these diseases and *vice versa* will provide a much deeper understanding of the biology of both cancer and the cilium. Nevertheless, these results show the complexity and importance of the primary cilium as an organelle. To what extent cancer can be considered a ciliopathy remains to be seen but therapeutics which target the cilium have the potential to treat many different types of patients. Because of the intersection between cancer and ciliopathies, treatment modifications from both fields have the potential to effectively treat both types of patients. In addition, rare inherited tumor syndromes have a relatively large window for therapeutic intervention, although such treatment might have to be lifelong. Treatments which involve the cilium or ciliary signaling pathways are already being researched, including PTC124 (ataluren) which can allow transcription of proteins despite premature stop codon mutations for the treatment of multiple diseases including Duchenne muscular dystrophy [92, 93]. There are also new possibilities for immunotherapy such as anti-PD-L1 therapy, which activates the immune system to more aggressively seek out cancer cells [94]. How-ever, immunotherapy may not be the best choice for the treatment of hereditary genetic syndromes such as the ones outlined above, given that this may cause a widespread immune response due to the potentially thousands of PD-L1-positive lesions in a single individual.

Nevertheless, treatments like these show the exciting potential of the primary cilium as an avenue of future study into the treatment and mechanisms of cancer and other diseases.

**Acknowledgments**
The authors wish to acknowledge EU FP7 programme numbers 241955 "SYSCILIA" and 305608 "EURenOmics".

## REFERENCES


1. Goetz SC, Anderson KV. The primary cilium: A signalling centre during vertebrate development. Nat Rev Genet 2010;11(5):331-44.
2. Chaki M, Airik R, Ghosh AK, Giles RH, Chen R, Slaats GG, et al. Exome capture reveals ZNF423 and CEP164 mutations, linking renal ciliopathies to DNA damage response signaling. Cell 2012;150(3):533-48.
3. Choi HJ, Lin JR, Vannier JB, Slaats GG, Kile AC, Paulsen RD, et al. NEK8 links the ATR-regulated replication stress response and S phase CDK activity to renal ciliopathies. Mol Cell 2013;51(4):423-39.
4. Airik R, Slaats GG, Guo Z, Weiss AC, Khan N, Ghosh A, et al. Renal-retinal ciliopathy gene sdccag8 regulates dna damage response signaling. J Am Soc Nephrol 2014 (in press).
5. Barker AR, Thomas R, Dawe HR. Meckel-Gruber syndrome and the role of primary cilia in kidney, skeleton, and cen-tral nervous system development. Organogenesis 2014;10(1): 6-107.
6. Reiter JF, Blacque OE, Leroux MR. The base of the cilium: Roles for transition fibres and the transition zone in ciliary for-mation, maintenance and compartmentalization. EMBO Rep 2012;13(7):608-18.
7. Waters AM, Beales PL. Ciliopathies: An expanding disease spectrum. Pediatr Nephrol 2011;26(7):1039-56.
8. Ellisen LW. Regulation of gene expression by WT1 in devel-opment and tumorigenesis. Int J Hematol 2002;76(2):110-6.
9. Niaudet P, Gubler MC. WT1 and glomerular diseases. Pediatr Nephrol 2006;21(11):1653-60.
10. Basten SG, Giles RH. Functional aspects of primary cilia in signaling, cell cycle and tumorigenesis. Cilia 2013;2(1):6.
11. Hassounah NB, Bunch TA, McDermott KM. Molecular path-ways: The role of primary cilia in cancer progression and therapeutics with a focus on hedgehog signaling. Clin Cancer Res 2012;18(9):2429-35.
12. Kim S, Dynlacht BD. Assembling a primary cilium. Curr Opin Cell Biol 2013;25(4):506-11.
13. Fry AM, Leaper MJ, Bayliss R. The primary cilium: Guardian of organ development and homeostasis. Organo-genesis 2014;10(1):62-8.
14. Yuan S, Sun Z. Expanding horizons: Ciliary proteins reach beyond cilia. Annu Rev Genet 2013;47(1):353-76.
15. Han YG, Kim HJ, Dlugosz AA, Ellison DW, Gilbertson RJ, Alvarez-Buylla A. Dual and opposing roles of primary cilia in medulloblastoma development. Nat Med 2009;15(9): 1062-5.
16. Wong SY, Seol AD, So PL, Ermilov AN, Bichakjian CK, Epstein EH, et al. Primary cilia can both mediate and suppress Hedgehog pathway-dependent tumorigenesis. Nat Med 2009;15(9):1055-61.
17. Barakat MT, Humke EW, Scott MP. Kif3a is necessary for ini-tiation and maintenance of medulloblastoma. Carcinogenesis 2013;34(6):1382-92.
18. Han YG, Alvarez-Buylla A. Role of primary cilia in brain development and cancer. Curr Opin Neurobiol 2010;20(1): 8-67.
19. Kim J, Dabiri S, Seeley ES. Primary cilium depletion typifies cutaneous melanoma *in situ* and malignant melanoma PLoS One 2011;6(11):e27410.
20. Basten SG, Willekers S, Vermaat JS, Slaats GG, Voest EE, van Diest PJ, et al. Reduced cilia frequencies in human renal cell carcinomas versus neighboring parenchymal tissue. Cilia 2013;2(1):2.
21. Seeley ES, Carriere C, Goetze T, Longnecker DS, Korc M. Pancreatic cancer and precursor pancreatic intraepithelial neoplasia lesions are devoid of primary cilia. Cancer Res 2009;69(2):422-30.
22. Schraml P, Frew IJ, Thoma CR, Boysen G, Struckmann K, Krek W, et al. Sporadic clear cell renal cell carcinoma but not the papillary type is characterized by severely reduced frequency of primary cilia. Mod Pathol 2008;22(1):31-6.
23. Gradilone SA, Radtke BN, Bogert PS, Huang BQ, Gajdos GB, LaRusso NF. HDAC6 inhibition restores ciliary expres-sion and decreases tumor growth. Cancer Res 2013;73(7): 259-70.
24. Egeberg DL, Lethan M, Manguso R, Schneider L, Awan A, Jorgensen TS, et al. Primary cilia and aberrant cell signaling in epithelial ovarian cancer. Cilia 2012;1(1):15.
25. Hassounah NB, Nagle R, Saboda K, Roe DJ, Dalkin BL, McDermott KM. Primary cilia are lost in preinvasive and invasive prostate cancer. PLoS One 2013;8(7):e68521.
26. Yuan K, Frolova N, Xie Y, Wang D, Cook L, Kwon YJ, et al. Primary cilia are decreased in breast cancer: Analysis of a collection of human breast cancer cell lines and tissues. J Histochem Cytochem 2010;58(10):857-70.
27. Nobutani K, Shimono Y, Yoshida M, Mizutani K, Minami A, Kono S, et al. Absence of primary cilia in cell cycle-arrested human breast cancer cells. Genes Cells 2014;19(2):141-52.
28. McIntyre JC, Davis EE, Joiner A, Williams CL, Tsai IC, Jenk-ins PM, et al. Gene therapy rescues cilia defects and restores olfactory function in a mammalian ciliopathy model. Nat Med 2012;18(9):1423-8.
29. Zhang Q, Davenport JR, Croyle MJ, Haycraft CJ, Yoder BK. Disruption of IFT results in both exocrine and endocrine abnormalities in the pancreas of Tg737orpk mutant mice. Lab Invest 2004;85(1):45-64.
30. Robert A, Margall-Ducos G, Guidotti JE, Bregerie O, Celati C, Brechot C, et al. The intraflagellar transport compo-nent IFT88/polaris is a centrosomal protein regulating G1-S transition in non-ciliated cells. J Cell Sci 2007;120(Pt 4): 628-37.
31. Mans DA, Vermaat JS, Weijts BG, van Rooijen E, van Reeuwijk J, Boldt K, et al. Regulation of E2F1 by the von Hippel-Lindau tumour suppressor protein predicts survival in renal cell cancer patients. J Pathol 2013;231(1):117-29.
32. van Dam TJ, Wheway G, Slaats GG, Group SS, Huynen MA, Giles RH. The SYSCILIA gold standard (SCGSv1) of known ciliary components and its applications within a systems biol-ogy consortium. Cilia 2013;2(1):7.

33. Gascue C, Katsanis N, Badano JL. Cystic diseases of the kid-ney: Ciliary dysfunction and cystogenic mechanisms. Pediatr Nephrol 2011;26(8):1181-95.
34. Foy RL, Chitalia VC, Panchenko MV, Zeng L, Lopez D, Lee JW, et al. Polycystin-1 regulates the stability and ubiq-uitination of transcription factor Jade-1. Hum Mol Genet 2012;21(26):5456-71.
35. Holland AJ, Cleveland DW. Losing balance: The origin and impact of aneuploidy in cancer. EMBO Rep 2012;13(6): 501-14.
36. Holland AJ, Lan W, Cleveland DW. Centriole duplication: A lesson in self-control. Cell Cycle 2010;9(14):2731-6.
37. Habedanck R, Stierhof YD, Wilkinson CJ, Nigg EA. The Polo kinase Plk4 functions in centriole duplication. Nat Cell Biol 2005;7(11):1140-6.
38. Maher ER. Genetics of familial renal cancers. Nephron Exp Nephrol 2011;118(1):e21-6.
39. Berger AH, Knudson AG, Pandolfi PP. A continuum model for tumour suppression. Nature 2011;476(7359):163-9.
40. Frantzen C, Links TP, Giles RH. Von Hippel-Lindau disease. In: Pagon RA, Adam MP, Ardinger HH, Bird TD, Dolan CR, Fong CT, Smith RJH, Stephens K, editors. GeneReviews. Seattle (WA), 1993-2014. Available at: http:// www.ncbi.nlm.nih.gov/books/NBK1463/. Accessed 20th June 2014.
41. Gerlinger M, Horswell S, Larkin J, Rowan AJ, Salm MP, Varela I, et al. Genomic architecture and evolution of clear cell renal cell carcinomas defined by multiregion sequencing. Nat Genet 2014;46(3):225-33.
42. Baldewijns MM, van Vlodrop IJ, Vermeulen PB, Soetekouw PM, van Engeland M, de Bruine AP. VHL and HIF signalling in renal cell carcinogenesis. J Pathol 2010;221(2):125-38.
43. Lolkema MP, Mans DA, Ulfman LH, Volpi S, Voest EE, Giles RH. Allele-specific regulation of primary cilia function by the von Hippel-Lindau tumor suppressor. Eur J Hum Genet 2008;16(1):73-8.
44. Thoma CR, Frew IJ, Hoerner CR, Montani M, Moch H, Krek W. pVHL and GSK3 beta are components of a primary cilium-maintenance signalling network. Nat Cell Biol 2007;9(5):588-95.
45. Schermer B, Ghenoiu C, Bartram M, Muller RU, Kotsis F, Hohne M, et al. The von Hippel-Lindau tumor suppressor protein controls ciliogenesis by orienting microtubule growth. J Cell Biol 2006;175(4):547-54.
46. Lutz MS, Burk RD. Primary cilium formation requires von hippel-lindau gene function in renal-derived cells. Cancer Res 2006;66(14):6903-7.
47. Esteban MA, Harten SK, Tran MG, Maxwell PH. Formation of primary cilia in the renal epithelium is regulated by the von Hippel-Lindau tumor suppressor protein. J Am Soc Nephrol 2006;17(7):1801-6.
48. Troilo A, Alexander I, Muehl S, Jaramillo D, Knobeloch KP, Krek W. HIF1a deubiquitination by USP8 is essen-tial for ciliogenesis in normoxia. EMBO Rep 2013;15(1): 77-85.
49. Mans DA, Lolkema MP, van Beest M, Daenen LG, Voest EE, Giles RH. Mobility of the von Hippel-Lindau tumour suppressor protein is regulated by kinesin-2. Exp Cell Res 2008;314(6):1229-36.
50. Lolkema MP, Mans DA, Snijckers CM, van Noort M, van Beest M, Voest EE, et al. The von Hippel-Lindau tumour sup-pressor interacts with microtubules through kinesin-2. FEBS Lett 2007;581(24):4571-6.
51. Frew IJ, Smole Z, Thoma CR, Krek W. Genetic deletion of the long isoform of the von Hippel-Lindau tumour suppres-sor gene product alters microtubule dynamics. Eur J Cancer 2013;49(10):2433-40.
52. Thoma CR, Matov A, Gutbrodt KL, Hoerner CR, Smole Z, Krek W, et al. Quantitative image analysis identifies pVHL as a key regulator of microtubule dynamic instability. J Cell Biol 2010;190(6):991-1003.
53. Hergovich A, Lisztwan J, Barry R, Ballschmieter P, Krek W. Regulation of microtubule stability by the von Hippel-Lindau tumour suppressor protein pVHL. Nat Cell Biol 2003;5(1): 4-70.
54. Hergovich A, Lisztwan J, Thoma CR, Wirbelauer C, Barry RE, Krek W. Priming-dependent phosphorylation and regu-lation of the tumor suppressor pVHL by glycogen synthase kinase 3. Mol Cell Biol 2006;26(15):5784-96.
55. Albers J, Rajski M, Schonenberger D, Harlander S, Schraml P, von Teichman A, et al. Combined mutation of Vhl and Trp53 causes renal cysts and tumours in mice. EMBO Mol Med 2013;5(6):949-64.
56. Frew IJ, Thoma CR, Georgiev S, Minola A, Hitz M, Mon-tani M, et al. pVHL and PTEN tumour suppressor proteins cooperatively suppress kidney cyst formation. EMBO J 2008;27(12):1747-57.
57. Giles RH, van Es JH, Clevers H. Caught up in a Wnt storm: Wnt signaling in cancer. Biochim Biophys Acta 2003;1653(1):1-24.
58. Deane JA, Ricardo SD. Polycystic kidney disease and the renal cilium. Nephrology (Carlton) 2007;12(6):559-64.
59. Jasperson KW, Burt RW. APC-associated polyposis con-ditions. In: Pagon RA, Adam MP, Ardinger HH, Bird TD, Dolan CR, Fong CT, Smith RJH, Stephens K, edi-tors. GeneReviews. Seattle (WA), 1993-2014. Available at:http://www.ncbi.nlm.nih.gov/books/NBK1345/. Accessed 20th June 2014.
60. Giles RH, Lolkema MP, Snijckers CM, Belderbos M, van der Groep P, Mans DA, et al. Interplay between VHL/HIF1 alpha and Wnt/beta-catenin pathways during colorectal tumorigen-esis. Oncogene 2006;25(21):3065-70.
61. Jimbo T, Kawasaki Y, Koyama R, Sato R, Takada S, Haraguchi K, et al. Identification of a link between the tumour sup-pressor APC and the kinesin superfamily. Nat Cell Biol 2002;4(4):323-7.
62. Kroboth K, Newton IP, Kita K, Dikovskaya D, Zumbrunn J, Waterman-Storer CM, et al. Lack of adenomatous polypo-sis coli protein correlates with a decrease in cell migration and overall changes in microtubule stability. Mol Biol Cell 2007;18(3):910-8.
63. Mogensen MM, Tucker JB, Mackie JB, Prescott AR, Nathke IS. The adenomatous polyposis coli protein unambigu-ously localizes to microtubule plus ends and is involved in establishing parallel arrays of microtubule bundles in highly polarized epithelial cells. J Cell Biol 2002;157(6): 1041-8.
64. Fodde R, Kuipers J, Rosenberg C, Smits R, Kielman M, Gaspar C, et al. Mutations in the APC tumour suppressor

gene cause chromosomal instability. Nat Cell Biol 2001;3(4): 433-8.
65. Giles RH, Voest EE. Tumor suppressors APC and VHL: Gate-keepers of the intestine and kidney. In: Macieira-Coelho A, editor. Developmental biology of neoplastic growth. Berlin Heidelberg: Springer, 2005; p. 151-181.
66. Qian CN, Knol J, Igarashi P, Lin F, Zylstra U, Teh BT, et al. Cystic renal neoplasia following conditional inactivation of apc in mouse renal tubular epithelium. J Biol Chem 2005;280(5):3938-45.
67. Gomez Garcia EB, Knoers NV. Gardner's syndrome (famil-ial adenomatous polyposis): A cilia-related disorder. Lancet Oncol 2009;10(7):727-35.
68. Northrup H, Koenig MK, Au KS. Tuberous sclerosis complex. In: Pagon RA, Adam MP, Ardinger HH, Bird TD, Dolan CR, Fong CT, Smith RJH, Stephens K, editors. GeneReviews. Seattle (WA), 1993-2014. Available at: http://www.ncbi.nlm.nih.gov/books/NBK1220/. Accessed 20th June 2014.
69. Armour EA, Carson RP, Ess KC. Cystogenesis and elongated primary cilia in Tsc1-deficient distal convoluted tubules. Am J Physiol Renal Physiol 2012;303(4):F584-92.
70. DiBella LM, Park A, Sun Z. Zebrafish Tsc1 reveals functional interactions between the cilium and the TOR pathway. Hum Mol Genet 2009;18(4):595-606.
71. Hartman TR, Liu D, Zilfou JT, Robb V, Morrison T, Watnick T, et al. The tuberous sclerosis proteins regulate formation of the primary cilium via a rapamycin-insensitive and poly-cystin 1-independent pathway. Hum Mol Genet 2009;18(1): 151-63.
72. Yuan S, Li J, Diener DR, Choma MA, Rosenbaum JL, Sun Z. Target-of-rapamycin complex 1 (Torc1) signaling modulates cilia size and function through protein synthesis regulation. Proc Natl Acad Sci U S A 2012;109(6):2021-6.
73. Han YM, Kang GM, Byun K, Ko HW, Kim J, Shin MS, et al. Leptin-promoted cilia assembly is critical for normal energy balance. J Clin Invest 2014;124(5):2193-7.
74. Porta C, Paglino C, Mosca A. Targeting PI3K/Akt/mTOR signaling in cancer. Front Oncol 2014;4:64.
75. Shuch B, Ricketts CJ, Vocke CD, Komiya T, Middelton LA, Kauffman EC, et al. Germline PTEN mutation Cowden syndrome: An underappreciated form of hereditary kidney cancer. J Urol 2013;190(6):1990-8.
76. Crino PB, Nathanson KL, Henske EP. The tuberous sclerosis complex. N Engl J Med 2006;355(13):1345-56.
77. Henske EP. Tuberous sclerosis and the kidney: From mesenchyme to epithelium, and beyond. Pediatr Nephrol 2005;20(7):854-7.
78. Toro JR. Birt-Hogg-Dube syndrome. In: Pagon RA, Adam MP, Ardinger HH, Bird TD, Dolan CR, Fong CT, Smith RJH, Stephens K, editors. GeneReviews. Seattle (WA), 1993-2014. Available at: http://www.ncbi.nlm.nih.gov/books/NBK1522/. Accessed 20th June 2014.
79. Menko FH, van Steensel MA, Giraud S, Friis-Hansen L, Richard S, Ungari S, et al. Birt-Hogg-Dube syndrome: Diag-nosis and management. Lancet Oncol 2009;10(12):1199-206.
80. Luijten MN, Basten SG, Claessens T, Vernooij M, Scott CL, Janssen R, et al. Birt-Hogg-Dube syndrome is a novel ciliopa-thy. Hum Mol Genet 2013;22(21):4383-97.
81. Hasumi Y, Baba M, Ajima R, Hasumi H, Valera VA, Klein ME, et al. Homozygous loss of BHD causes early embryonic lethality and kidney tumor development with activation of mTORC1 and mTORC2. Proc Natl Acad Sci U S A 2009;106(44):18722-7.
82. MacDonald BT, Tamai K, He X. Wnt/beta-catenin signaling: Components, mechanisms, and diseases. Dev Cell 2009;17(1):9-26.
83. Clevers H. Wnt/beta-catenin signaling in development and disease. Cell 2006;127(3):469-80.
84. Briscoe J, Therond PP. The mechanisms of Hedgehog signalling and its roles in development and disease. Nat Rev Mol Cell Biol 2013;14(7):416-29.
85. Nozawa YI, Lin C, Chuang PT. Hedgehog signaling from the primary cilium to the nucleus: An emerging picture of ciliary localization, trafficking and transduction. Curr Opin Genet Dev 2013;23(4):429-37.
86. Bartlett F, Kortmann R, Saran F. Medulloblastoma. Clin Oncol (R Coll Radiol) 2013;25(1):36-45.
87. Spassky N, Han YG, Aguilar A, Strehl L, Besse L, Laclef C, et al. Primary cilia are required for cerebellar development and Shh-dependent expansion of progenitor pool. Dev Biol 2008;317(1):246-59.
88. Thompson MC, Fuller C, Hogg TL, Dalton J, Finkelstein D, Lau CC, et al. Genomics identifies medulloblastoma sub-groups that are enriched for specific genetic alterations. J Clin Oncol 2006;24(12):1924-31.
89. Mehta GU, Shively SB, Duong H, Tran M, Moncrief TJ, Smith JH, et al. Progression of epididymal maldevelopment into hamartoma-like neoplasia in VHL disease. Neoplasia 2008;10(10):1146-53.
90. Basten SG, Davis EE, Gillis AJ, van Rooijen E, Stoop H, Babala N, et al. Mutations in LRRC50 predispose zebrafish and humans to seminomas. PLoS Genet 2013;9(4): e1003384.
91. Ito J, Johnson WW. Ultrastructure of Wilms' tumor. I. Epithe-lial cell. J Natl Cancer Inst 1969;42(1):77-99.
92. Karijolich J, Yu YT. Therapeutic suppression of premature termination codons: Mechanisms and clinical considerations (review). Int J Mol Cell Med 2014;34(2):355-62.
93. Li M, Andersson-Lendahl M, Sejersen T, Arner A. Muscle dysfunction and structural defects of dystrophin-null sapje mutant zebrafish larvae are rescued by ataluren treatment. FASEB J 2014;28(4):1593-9.
94. Lines JL, Sempere LF, Broughton T, Wang L, Noelle R. VISTA Is a novel broad-spectrum negative checkpoint reg-ulator for cancer immunotherapy. Cancer Immunol Res 2014;2(6):510-7.

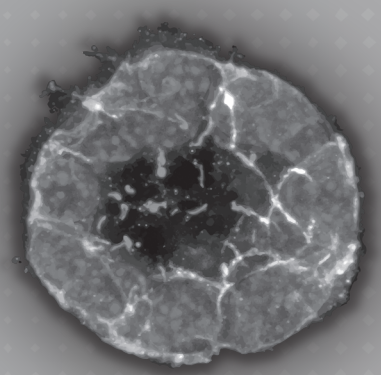

## CHAPTER 3

# Von Hippel-Lindau Syndrome

available at NCBI Bookshelf. A service of the National Library of Medicine, National Institutes of Health. Bookshelf ID: NBK1463PMID: 20301636

Pagon RA, Adam MP, Ardinger HH, et al., editors. GeneReviews® [Internet]. Seattle (WA): University of Washington, Seattle; 1993-2016.

Frantzen C, **Klasson TD**, Links TP, Giles RH

## SUMMARY

**Clinical Characteristics**

Von Hippel-Lindau (VHL) syndrome is characterized by hemangioblastomas of the brain, spinal cord, and retina; renal cysts and clear cell renal cell carcinoma; pheochromocytoma, pancreatic cysts, and neuroendocrine tumors; endolymphatic sac tumors; and epididymal and broad ligament cysts. Cerebellar hemangioblastomas may be associated with headache, vomiting, gait disturbances, or ataxia. Spinal hemangioblastomas and related syrinx usually present with pain. Sensory and motor loss may develop with cord compression. Retinal hemangioblastomas may be the initial manifestation of VHL syndrome and can cause vision loss. Renal cell carcinoma occurs in about 70% of individuals with VHL and is the leading cause of mortality. Pheochromocytomas can be asymptomatic but may cause sustained or episodic hypertension. Pancreatic lesions often remain asymptomatic and rarely cause endocrine or exocrine insufficiency. Endolymphatic sac tumors can cause hearing loss of varying severity, which can be a presenting symptom. Cystadenomas of the epididymis are relatively common. They rarely cause problems, unless bilateral, in which case they may result in infertility.

**Diagnosis/testing**

The diagnosis of VHL is established in a proband who fulfills existing diagnostic clinical criteria. Identification of a heterozygous germline *VHL* pathogenic variant on molecular genetic testing establishes the diagnosis if clinical features are inconclusive.

**Management**

*Treatment of manifestations:* Intervention for most CNS lesions (remove brain and spinal lesions completely when large and/or symptomatic); treat retinal (but not optic nerve) angiomas prospectively; early surgery (nephron-sparing or partial nephrectomy when possible) for renal cell carcinoma; renal transplantation following bilateral nephrectomy; remove pheochromocytomas (partial adrenalectomy when possible); monitor pancreatic cysts and neuroendocrine tumors and consider removal of neuroendocrine tumors; consider surgical removal of endolymphatic sac tumors (particularly small tumors in order to preserve hearing and vestibular function); cystadenomas of the epididymis or broad ligament need treatment when symptomatic or threatening fertility.

*Prevention of secondary complications:* Early detection and removal of tumors to prevent/minimize secondary deficits such as hearing loss, vision loss, neurologic symptoms, and the need for renal replacement therapy.

*Surveillance:* For individuals with VHL syndrome, those with a *VHL* pathogenic variant, and at-risk relatives of unknown genetic status:

- Starting at age one year: Annual evaluation for neurologic symptoms, vision problems, and hearing disturbance; annual blood pressure monitoring; annual ophthalmology evaluation.
- Starting at age five years: Annual blood or urinary fractionated metanephrines; audiology assessment every two to three years; thin-slice MRI with contrast of the internal auditory canal in those with repeated ear infections.
- Starting at age 16 years: Annual abdominal ultrasound; MRI scan of the abdomen and MRI of the brain and total spine every two years.

*Agents/circumstances to avoid*: Tobacco products should be avoided since they are considered a risk factor for kidney cancer; chemicals and industrial toxins known to affect VHL-involved organs should be avoided; contact sports should be avoided if adrenal or pancreatic lesions are present.

*Evaluation of relatives at risk:* If the pathogenic variant in a family is known, molecular genetic testing can be used to clarify the genetic status of at-risk family members to eliminate the need for surveillance of family members who have not inherited the pathogenic variant.

*Pregnancy management*: Intensified surveillance for cerebellar hemangioblastoma and pheochromocytoma during preconception and pregnancy; MRI without contrast of the cerebellum at four months' gestation.

**Genetic counseling**

VHL syndrome is inherited in an autosomal dominant manner. Approximately 80% of individuals with VHL syndrome have an affected parent and about 20% have VHL syndrome as the result of a *de novo* pathogenic variant. Parental mosaicism has been described; the incidence is not known. The offspring of an individual with VHL syndrome are at a 50% risk of inheriting the *VHL* pathogenic variant. Prenatal testing for pregnancies at risk is possible if the pathogenic variant has been identified in a family member.

# DIAGNOSIS

## Suggestive Findings

Von Hippel-Lindau syndrome **should be suspected** in individuals with or without a family history of VHL and:

- Retinal angioma, especially in a young patient
- Spinal or cerebellar hemangioblastoma
- Adrenal or extra-adrenal pheochromocytoma
- Renal cell carcinoma, if the patient is under age 47 years or has a personal or family history of any other tumor typical of VHL
- Multiple renal and pancreatic cysts
- Neuroendocrine tumors of the pancreas
- Endolymphatic sac tumors
- Less commonly, multiple papillary cystadenomas of the epididymis or broad ligament

## Establishing the Diagnosis

The diagnosis of von Hippel-Lindau (VHL) syndrome **is established** in a proband with the following clinical features [Lonser et al 2003, Butman et al 2008, Maher et al 2011] and/or after the identification of a heterozygous germline *VHL* pathogenic variant on molecular genetic testing. Identification of a heterozygous germline *VHL* pathogenic variant on molecular genetic testing (Table 1) establishes the diagnosis and supports periodic follow up even if clinical and radiographic features are inconclusive.

Various tests can be used to establish the diagnosis and determine the extent of the clinical manifestations (MRI of the brain and spinal cord, fundoscopy, ultrasound examination/MRI of the abdomen, and blood/urinary catecholamine metabolites can be used to establish the clinical diagnosis). See Surveillance.

**A simplex case** (i.e., an individual with no known family history of VHL syndrome) presenting with **two or more** characteristic lesions:

- Two or more hemangioblastomas of the retina, spine, or brain or a single hemangioblastoma in association with a visceral manifestation (e.g., multiple kidney or pancreatic cysts)
- Renal cell carcinoma
- Adrenal or extra-adrenal pheochromocytomas
- Less commonly, endolymphatic sac tumors, papillary cystadenomas of the epididymis or broad ligament, or neuroendocrine tumors of the pancreas

An individual with a positive family history of VHL syndrome in whom one or more of the following syndrome manifestations is present:

- Retinal angioma
- Spinal or cerebellar hemangioblastoma
- Adrenal or extra-adrenal pheochromocytoma o Renal cell carcinoma
- Multiple renal and pancreatic cysts

  Note: Other lesions characteristic of VHL are endolymphatic sac tumors (ELST) and pancreatic neuroendocrine tumors; however these are not typically used to make a clinical diagnosis of VHL. ELST presents as a mass on the posterior wall of the petrous part of the temporal bone and can be missed on standard MRI. MRI with contrast and high signal intensity with $T_1$, using thin slices of the internal auditory canal is recommended in symptomatic individuals.

Molecular testing approaches can include **single-gene testing**, use of a **multi-gene panel**, and **more comprehensive genomic testing**.

- **Single-gene testing.** Sequence analysis of *VHL* is performed first followed by gene-targeted deletion/duplication analysis if no pathogenic variant is found.
- **A multi-gene panel** that includes *VHL* and other genes of interest (see Differential Diagnosis) may also be considered. Note: The genes included and sensitivity of multi-gene panels vary by laboratory and over time.
- **More comprehensive genomic testing** (when available) including whole-exome sequencing (WES), whole-genome sequencing (WGS), and whole mitochondrial sequencing (WMitoSeq) may be considered if serial single-gene testing (and/or use of a multi-gene panel) fails to confirm a diagnosis in an individual with features of VHL syndrome.

**Table 1.** Molecular Genetic Testing Used in von Hippel-Lindau Syndrome

| Gene[1] | Test Method | Proportion of Probands with a Pathogenic Variant[2] Detectable by This Method |
|---|---|---|
| VHL | Sequence analysis[3] | ~72%[4] |
| | Gene-targeted deletion/duplication analysis[5] | ~28%[4, 6] |

1. See Table A. Genes and Databases for chromosome locus and protein.
2. See Molecular Genetics for information on allelic variants detected in this gene.
3. Sequence analysis detects variants that are benign, likely benign, of uncertain significance, likely pathogenic, or pathogenic. Pathogenic variants may include small intragenic deletions/insertions and missense, nonsense, and splice site variants; typically, exon or whole-gene deletions/duplications are not detected.

4. Stolle et al [1998]
5. Gene-targeted deletion/duplication analysis detects intragenic deletions or duplications. Methods that may be used include: quantitative PCR, long-range PCR, multiplex ligation-dependent probe amplification (MLPA), and a gene-targeted microarray designed to detect single-exon deletions or duplications.
6. Hoebeeck et al [2005], Banks et al [2006]

**Test characteristics.** See [Decker et al 2014] for information on test characteristics including sensitivity and specificity.

## CLINICAL CHARACTERISTICS

### Clinical Description

Von Hippel-Lindau (VHL) syndrome is characterized by hemangioblastomas of the brain, spinal cord, and retina; renal cysts and renal cell carcinoma; pheochromocytoma and paraganglioma; pancreatic cysts and neuroendocrine tumors; endolymphatic sac tumors; and epididymal and broad ligament cysts. Some clustering of tumors occurs, resulting in the designation of specific VHL syndrome phenotypes. The manifestations and severity are highly variable both within and between families, even among those with the same pathogenic variant.

**Hemangioblastomas**

CNS hemangioblastoma is the prototypic lesion of VHL syndrome [Catapano et al 2005, Gläsker 2005]. Multiple CNS tumors, occurring either synchronously or metachronously, are common. Roughly 80% develop in the brain and 20% in the spinal cord. Peripheral nerve hemangiomas may develop rarely [Giannini et al 1998].

Hemangioblastomas oscillate between periods of growth and stability [Wanebo et al 2003] and are generally slow growing, but on occasion include rapidly enlarging cysts that produce hydrocephaly with papilledema. Some hemangioblastomas do not cause symptoms and are discovered only on imaging.

Central nervous system hemangioblastoma growth appears to be associated with male sex and partial germline deletions [Lonser et al 2014, Huntoon et al 2015]. Growth patterns of these lesions can be saltatory (72%), linear (6%), or exponential (22%). Increased growth was associated with male sex, symptomatic tumors and hemangioblastoma-associated cysts.

- **Brain hemangioblastomas.** Within the brain, the vast majority are infratentorial, mainly in the cerebellar hemispheres. The pituitary stalk is the most common site for the development of supratentorial hemangioblastomas in individuals with VHL syndrome

[Lonser et al 2009]. Clinical symptoms depend on the site of the tumor: with infratentorial tumors, headache, vomiting, and gait disturbances or ataxia predominate; with tumors above the tentorium, symptoms depend on the location of the lesion.

- **Spinal hemangioblastomas** are generally intradural, most commonly occur in the cervical or thoracic regions, and occasionally may involve the entire cord. Most symptom-producing spinal hemangioblastomas are associated with cysts/syringomyelia/syrinx [Wanebo et al 2003]. Spinal hemangioblastomas usually present with pain; sensory and motor loss may develop with cord compression.
- **Retinal hemangioblastoma.** These retinal lesions, sometimes called retinal angiomas, are histologically identical to CNS hemangioblastomas. They may be the initial manifestations of VHL syndrome and may occur in childhood. About 70% of affected individuals are identified as having retinal angiomas [Webster et al 1999, Kreusel 2005] with mean age of detection about 25 years [Dollfus et al 2002]. The tumors are most often located in the temporal periphery of the retina with feeder and draining vessels going to and from the optic disc. However, they may develop in the posterior pole (1%) and optic disc (8%).
- Retinal hemangioblastomas may be asymptomatic and may be detected on routine ophthalmoscopy. Others present with a visual field defect or a loss of visual activity resulting from retinal detachment, exudation, or hemorrhage. Tests of retinal function may be abnormal even in the presence of quiescent retinal angiomas [Kreusel et al 2006]. While the number of retinal angiomas does not appear to increase with age, the probability of vision loss increases with age [Kreusel et al 2006].

**Renal lesions**

- **Multiple renal cysts** are common in VHL syndrome [Lonser et al 2003].
- **Renal cell carcinoma** (RCC), specifically of the clear cell subtype, developing either within a cyst or in the surrounding parenchyma, occurs in about 70% of affected individuals by age 60 years, and is a leading cause of mortality in VHL syndrome [Maher et al 1990, Maher et al 1991]. Pathogenic variants in *VHL* are the most common cause of familial and sporadic RCC. Overall survival for renal cell carcinoma in individuals with VHL is associated with tumor size (<3 cm or ≥3 cm) and patient age [Kwon et al 2014].

**Pheochromocytoma** may present with sustained or episodic hypertension or be totally asymptomatic, detected incidentally by an abdominal imaging procedure. Pheochromocytomas are usually located in one or both adrenal glands. They are usually benign, but malignant behavior has been reported [Chen et al 2001, Jimenez et al 2009].
**Paragangliomas.** Similar in etiology, paragangliomas can develop along the sympathetic axis in the abdomen or thorax [Schimke et al 1998, Boedeker et al 2014]; these tumors are mostly nonfunctional.

**Pancreatic lesions**

- **Pancreatic cysts.** Most pancreatic lesions are simple cysts; however, while they can be numerous in individuals with VHL, they rarely cause endocrine or exocrine insufficiency. Occasionally, cysts in the head of the pancreas cause biliary obstruction.
- **Neuroendocrine tumors.** 5%-17% of individuals with VHL develop neuroendocrine tumors of the pancreas [Lonser et al 2003, Maher et al 2011]. They are not usually hormonally active and are slow growing, but malignant behavior has been observed, particularly in tumors greater than 3 cm [Marcos et al 2002, Corcos et al 2008].

**Endolymphatic sac tumors** are seen in approximately 10%-16% of individuals with VHL syndrome, and in some instances the associated uni- or bilateral hearing loss is the initial feature of the syndrome [Kim et al 2005, Binderup et al 2013b]. The onset of hearing loss is typically sudden; severity varies, but it is often severe to profound [Choo et al 2004, Kim et al 2005]. Vertigo or tinnitus is the presenting complaint. Symptoms do not appear to be related to tumor size. Large endolymphatic sac tumors can involve other cranial nerves. Endolymphatic sac tumors are rarely malignant [Muzumdar et al 2006].

**Epididymal and broad ligament cystadenomas.** Epididymal or papillary cystadenomas are relatively common in males with VHL syndrome. They rarely cause problems, unless bilateral, in which case they may result in infertility. The equivalent, much less common, lesion in women is a papillary cystadenoma of the broad ligament.

## Genotype-Phenotype Correlations

Four general VHL syndrome phenotypes (type 1, type 2A, type 2B, type 2C) have been suggested based on the likelihood of pheochromocytoma or renal cell carcinoma. Many lines of research support the conclusion that the molecular etiology of pheochromocytomas appears to be distinct from other VHL lesions. Therefore, the most relevant genotype-phenotype correlations rely mostly on scoring the presence/absence of pheochromocytomas associated with a given allele. The following discussion summarizes the genotype-phenotype studies published to date, with the cautionary note that further investigation is needed. Note: Patterns are not clear-cut, and genotype-phenotype correlations have no current diagnostic or therapeutic value and are used for academic purposes only.

**VHL type 1. Retinal angioma, CNS hemangioblastoma, renal cell carcinoma, pancreatic cysts and neuroendocrine tumors.**

VHL type 1 is characterized by a low risk for pheochromocytoma. Truncating or missense pathogenic variants that are predicted to grossly disrupt the folding of the VHL protein [Stebbins et al 1999] are associated with VHL type 1.

**VHL type 2. Pheochromocytoma, retinal angiomas and CNS hemangioblastoma.**
VHL type 2 is characterized by a high risk for pheochromocytoma. Individuals with VHL type 2 commonly have a missense pathogenic variant. Some missense pathogenic variants appear to correlate with a specific type 2 VHL phenotype [Weirich et al 2002, Sansó et al 2004, Abbott et al 2006, Knauth et al 2006]. (See also Molecular Genetics).



VHL type 2 is further subdivided:

- **Type 2A.** Pheochromocytoma, retinal angiomas and CNS hemangioblastoma; low risk for renal cell carcinoma
- **Type 2B.** Pheochromocytoma, retinal angioma, CNS hemangioblastomas, pancreatic cysts and neuroendocrine tumor with a high risk for renal carcinoma
- **Type 2C.** Risk for pheochromocytoma only

Several groups report a reduced risk for renal cell carcinoma in individuals with a deletion of *VHL* [Cybulski et al 2002, Maranchie et al 2004, McNeill et al 2009]. In particular, individuals with a complete or partial deletion that extends 5' of *VHL* to include *C3orf10* have a significantly reduced risk of renal cell carcinoma [Maranchie et al 2004, McNeill et al 2009]. This genotype may constitute a distinct phenotype, VHL type 1B, characterized by a reduced risk for both renal cell carcinoma and pheochromocytoma.
Some individuals within families with apparent type 2C syndrome have developed hemangioblastomas [Neumann & Eng 2009].

## Penetrance

*VHL* pathogenic variants are highly penetrant. Almost all individuals who have a pathogenic variant in *VHL* are symptomatic by age 65 years [Maher et al 1991].

## Nomenclature

Obsolete terms for VHL syndrome include: angiophakomatosis retinae et cerebelli, familial cerebello-retinal angiomatosis, cerebelloretinal hemangioblastomatosis, Hippel disease, Hippel-Lindau syndrome, Lindau disease, and retinocerebellar angiomatosis [Molino et al 2006].

## Prevalence

The incidence of VHL syndrome is thought to be about one in 36,000 births with an estimated *de novo* mutation rate of $4.4x10^{-6}$ gametes per generation [Maher et al 1991].

## GENETICALLY RELATED (ALLELIC) DISORDERS

**Familial erythrocytosis type 2 (ECYT2)** (OMIM) is characterized by increased circulating red blood cell mass, increased serum levels of erythropoietin, and normal oxygen affinity. Familial erythrocytosis type 2 is caused by homozygous or compound heterozygous pathogenic variants in *VHL*. Although thrombosis and/or hemorrhage has occurred in many individuals with familial erythrocytosis type 2, no individuals with this disorder or their heterozygous relatives thus far described have developed VHL-related tumors [Gordeuk et al 2004].

Note: Congenital erythrocytosis is endemic in subpopulations worldwide; pathogenic variants in *VHL* are the most common cause of congenital erythrocytosis [Pastore et al 2003]. In the Chuvash Republic of the Russian Federation, where this condition is endemic, Ang et al [2002] identified homozygosity for the *VHL* pathogenic variant p.Arg200Trp.

## DIFFERENTIAL DIAGNOSIS

**Isolated hemangioblastoma, retinal angioma, or clear cell renal cell carcinoma**
The clinical sensitivity of molecular genetic testing of *VHL* makes it possible to effectively rule out von Hippel-Lindau (VHL) syndrome with a high degree of certainty in individuals with (1) isolated hemangioblastoma, retinal angioma, or clear cell renal cell carcinoma and (2) no detectable germline *VHL* pathogenic variant. Somatic mosaicism for a *VHL* pathogenic variant could still be considered in such individuals. A younger individual, especially one with multiple lesions, is more likely to have a germline *VHL* pathogenic variant than an older individual with a single lesion [Neumann et al 2002].

**Pheochromocytoma**
Approximately 25% of individuals with pheochromocytoma and no known family history of pheochromocytoma have a heterozygous pathogenic variant in one of several genes: *RET*, *VHL*, *SDHD*, *SDHB, SDHA*, *SDHC*, *SDHAF2*, *TMEM127*, or *MAX*. Germline *VHL* pathogenic variants are rare in simplex cases of unilateral pheochromocytoma (i.e., an affected individual with no family history of VHL syndrome), unless the individual is younger than age 20 years.

- **Multiple endocrine neoplasia type 2 (MEN2).** Individuals with MEN2A are at increased risk for medullary carcinoma of the thyroid, pheochromocytoma, and parathyroid adenoma or hyperplasia. Pheochromocytomas usually present after medullary thyroid cancer (MTC) or concomitantly; however, they are the first sign in 13%-27% of individuals with MEN2A [Inabnet et al 2000, Rodriguez et al 2008]. Features of MEN2B

include mucosal neuromas of the lips and tongue, distinctive facies with thick vermilion of the upper and lower lips, ganglioneuromatosis of the gastrointestinal tract, a 'marfanoid' habitus, and an increased risk for MTC and pheochromocytoma. Pheochromocytomas occur in 50% of individuals with MEN2B; about half are multiple and often bilateral. A heterozygous pathogenic variant of *RET* is associated with MEN2.

- **Hereditary paraganglioma-pheochromocytoma syndrome.** Approximately 8.5% of individuals with apparently nonfamilial nonsyndromic pheochromocytoma have been shown to have a pathogenic variant in one of the genes (*SDHD*, *SDHB, SDHA*, *SDHC*, and *SDHAF2*) encoding the succinate dehydrogenase subunits that cause the hereditary paraganglioma-pheochromocytoma syndromes [Neumann et al 2002, Neumann et al 2004]. Mutation of these genes is associated with familial paragangliomas, which are also known as extra-adrenal pheochromocytomas or glomus tumors [Baysal et al 2000, Astuti et al 2001]. Korpershoek et al [2011] found an *SDHA* germline pathogenic variant in 3% of individuals with apparently sporadic paragangliomas and pheochromocytomas. A *MAX* germline pathogenic variant is seen in approximately 1% of individuals with familial or nonfamilial pheochromocytoma [Burnichon et al 2012].
- ***TMEM127*-associated susceptibility to pheochromocytoma** (OMIM). Recent studies estimate that 1%-2% of individuals with familial or nonfamilial pheochromocytoma have a germline pathogenic variant in *TMEM127* [Yao et al 2010, Abermil et al 2012]. A few individuals with a germline pathogenic variant in *TMEM127* have paragangliomas of the head/neck or at extra-adrenal sites [Neumann et al 2011].
- Pheochromocytomas are observed on occasion in neurofibromatosis type 1 (NF1).

**Renal cell carcinoma (RCC).** Individuals with familial RCC should be examined for hereditary leiomyomatosis and renal cell cancer (HLRCC) and Birt-Hogg-Dubé (BHD) syndrome.

**Endolymphatic sac tumors** in VHL are often misdiagnosed as Menière disease.

## MANAGEMENT

### Evaluations Following Initial Diagnosis

To establish the extent of disease and needs in an individual diagnosed with von Hippel-Lindau (VHL) syndrome, the following evaluations are recommended:

- Neurologic history and physical examination for evidence of CNS or peripheral nerve hemangioblastomatosis. A baseline brain and spine MRI is considered standard procedure.

- Ophthalmologic evaluation for retinal hemangioblastomas
- Abdominal ultrasound examination after age 16 years. Suspicious lesions in the kidney, adrenal gland, or pancreas should be evaluated by more sophisticated techniques, such as CT scan or MRI.
- Blood pressure determination, supplemented by measurement of urinary catecholamine metabolites after age five years to evaluate for pheochromocytoma
- Audiologic evaluation for hearing loss associated with endolymphatic sac tumors
- Consultation with a clinical geneticist and/or genetic counselor

## Treatment of Manifestations

No guidelines exist for the management of VHL lesions.

**CNS hemangioblastoma**

- Most central nervous system hemangioblastomas can be surgically removed completely and safely [Lonser et al 2003].
- Some advocate early surgical removal of both symptomatic and asymptomatic CNS lesions, while others follow asymptomatic lesions with yearly imaging studies.
- Surgical intervention of cysts/syrinx in the spinal cord is recommended.
- Preoperative arterial embolization may be indicated, especially for extensive spinal tumors.
- The position of stereotactic therapy is still questionable [Oldfield 2015]. Gamma knife surgery may be useful with small solid tumors or those in inoperable sites [Asthagiri et al 2010, Simone et al 2011]. While this technique may reduce the size of the solid tumor, it does not appear to prevent cyst formation. In a study with nearly six years of follow up of 40 hemangioblastomas in 20 patients treated with stereotactic therapy, no progression was described in 33% [Asthagiri et al 2010]. Similar results are found when analyzing the natural history of the hemangioblastomas (25%) [Lonser et al 2014]. The unpredictable growth pattern makes it difficult to determine when to start stereotactic therapy, to avoid unnecessary intervention. A recent study demonstrates a local tumor control with stereotactic therapy of 93% after three years, 89% after five years, and 79% after ten years [Kano et al 2015]. Factors associated with tumor control are solid, smaller, VHL-associated lesions and higher margin dose. Thirteen of the 186 (7%) experienced complications, 11 patients needed steroid therapy and one person died of refractory peritumoral edema. Two patients required additional surgery.

**Retinal hemangioblastoma**

- Most ophthalmologists favor prospective treatment of retinal (but not optic nerve) angiomas to avoid blindness, although spontaneous regression has occurred.

- Therapeutic modalities used to treat retinal hemangioblastomas include diathermy, xenon, laser, and cryocoagulation, with variable degrees of success depending on the location, size, and number of lesions. Recurrent tumors have been noted, even after many years, but some may be new tumors in the same general area rather than recurrent disease.
- External beam radiotherapy has been shown to be useful when standard therapy has not prevented progression [Raja et al 2004].



**Renal cell carcinoma**

- Early surgery is the best option for renal cell carcinoma, although close monitoring is recommended for lesions smaller than 3 cm. Depending on the size and location of the tumor, nephron-sparing or partial nephrectomy may be possible without compromising survival [Grubb et al 2005].
- Nephrectomy should leave the adrenal gland in situ, as is done in individuals with renal cell carcinoma who do not have a confirmed diagnosis of VHL. If contralateral pheochromocytoma occurs, the remaining adrenal gland will prevent or delay steroid replacement therapy.
- Cryoablation is being increasingly used for small lesions or in individuals who are likely to require multiple surgical procedures [Shingleton & Sewell 2002].
- Radio frequency ablation therapy is often applied to smaller tumors, particularly <3 cm [Best et al 2012]. However, smaller lesions treated with radio frequency ablation need frequent intervention [Joly et al 2011]. The major complication rate (need for a radiologic, surgical, or endoscopic intervention) for laparoscopic and percutaneous radio frequency ablation therapy was 7.3% and 4.3%, respectively [Young et al 2012].
- Renal transplantation has been successful in individuals in whom bilateral nephrectomy has been necessary. It is imperative to evaluate any living related potential donor for VHL syndrome and to exclude those found to have VHL syndrome.

**Pheochromocytomas**

- Pheochromocytomas should be surgically removed. Laparoscopic approaches have been shown to be effective.
- Preoperative treatment with alpha-adrenergic blockade, and optional additional beta-adrenergic blockade for seven to ten days is appropriate even in individuals with no known hypertension.
- Partial adrenalectomy could be considered. One long-term follow-up study (9.25 years) of 36 affected individuals showed no metastatic disease; ipsilateral recurrence after partial adrenalectomy was seen in three individuals (11%) [Benhammou et al 2010].
- Partial adrenalectomy is also therapy of choice in children. In 10 VHL patients 18 successful operations were performed. After follow up (median 7.2 years), 2 patients developed a new tumor in the ipsilateral adrenal gland [Volkin et al 2012].

**Pancreatic cysts and neuroendocrine tumors**

- Pancreatic cysts are common, but rarely influence endocrine function and generally do not require surgical removal.
- Pancreatic neuroendocrine tumors need to be differentiated from cysts and serous cystadenomas. Pancreatic tumors are usually slow growing and are not hormonally active, although they can cause metastatic disease. Surgery should be considered when there is a high risk of metastases suggested by one of the following prognostic criteria [Blansfield et al 2007]:
  - A tumor of ≥3 cm
  - A pathogenic variant in exon 3
  - A tumor with a doubling rate <500 days

**Endolymphatic sac tumors (ELST)**

Consideration of surgical removal of these slow-growing tumors must include discussion of the possible complication of total deafness. Early intervention with small tumors has been shown to preserve both hearing and vestibular function [Kim et al 2005, Friedman et al 2013]. Friedman et al described two patients (2/18) with postoperative decreased facial nerve function and three (3/18) patients with recurrent ELSTs (with a mean follow up of 67 months). Kim et al [2013] studied 31 patients with VHL with 33 resected ELSTs. Twenty-nine patients were symptomatic. After surgery, hearing was stabilized or improved in 97% of individuals, and tumor resection was complete in 91%. Complications occurred in three tumors: cerebrospinal fluid leakage in two (6%) and transient lower cranial nerve palsy in one (3%).

**Epididymal or broad ligament papillary cyst adenomas**

These generally do not require surgery, unless they are symptomatic or are threatening fertility.

## Prevention of Secondary Manifestations

Early detection through surveillance and removal of tumors may prevent or minimize deficits such as hearing loss, vision loss, neurologic symptoms, and the need for renal replacement therapy.

## Surveillance

Individuals with known VHL syndrome, individuals without clinical manifestations but identified as having a *VHL* pathogenic variant, and first-degree relatives who have not undergone DNA-based testing need regular clinical monitoring by a physician or medical team familiar with the spectrum of VHL syndrome.

- Annual evaluation starting at age one year for neurologic symptoms, vision problems or hearing disturbance
- Annual examination starting at age one year for signs of nystagmus, strabismus, or white pupils
- Annual blood pressure monitoring starting at age one year



Monitoring for complications is as follows:

- **CNS lesions.** MRI of the brain and total spine every two years starting at age 16 years. Attention should be given to the inner ear/petrous temporal bone (for ELST) and the posterior fossa.
- **Visceral lesions.** Annual abdominal ultrasound; MRI scan of the abdomen (kidney, pancreas and adrenal glands) every two years starting at age 16 years
- **Retinal angiomas.** Annual ophthalmology evaluation with indirect ophthalmoscope starting at age one year
- **Pheochromocytoma.** Annual blood or urinary fractionated metanephrines starting at age five years
- **Endolymphatic sac tumors (ELST).** The best way to detect ELST is unknown.
  - ELST presents as a mass on the posterior wall of the petrous part of the temporal bone and can be missed on standard MRI. MRI with contrast and high signal intensity with $T_1$ (to detect hydrops), using thin slices of the internal auditory canal is recommended in symptomatic individuals. Butman et al [2013] found that
  - FLAIR MRI is useful to find ELST-associated hydrops.
  - Butman et al [2013] described three pathophysiologic ways in which ELST can cause symptoms: optic capsule invasion, hemorrhage, and endolymphatic hydrops. Symptoms can be caused by all three mechanisms and hemorrhage or hydrops can be present even without any lesion being visible on MRI (<3 mm).
  - Audiology assessment every two to three years (annually if hearing loss, tinnitus, or vertigo is present) starting at age five years. Audiology can be used to detect (early) hearing loss. Binderup et al [2013b] described a male patient with demonstrable hearing loss by audiometric data whose ELST was only detectable with MRI more than one year later, after the patient already suffered from complete right-sided hearing loss. Results from a large study on audiometric data in individuals with VHL are pending.

While current medical surveillance guidelines do not address structured psychological support for individuals with VHL, their partners, and their family members, research suggests a distinct need for psychosocial support [Lammens et al 2010, Lammens et al 2011b].

Note: The surveillance guidelines established for VHL are not evidence based and rely on experiential reporting, largely from North America. Guidelines may vary somewhat depending on the local standard of care.

In the United States, the VHL Alliance has worked extensively with healthcare professionals to assemble guidelines which are generally accepted throughout the world [VHL Handbook]. Other guidelines originate from Denmark and the Netherlands. For example, Dutch guidelines recommend screening for ELST only on indication. In addition, examination by a primary care physician and assessment of metanephrine levels start at age ten years, while ophthalmologic examination begins at age five years.

Two recent studies evaluated tumor progression. In one study, new tumor development was compared to age and genotype [Binderup et al 2013b]. According to their results, surveillance for retinal angiomas is essential during teenage years and central nervous system hemangioblastomas is mainly important in adults. In the other study, the optimal lesion-specific age to start surveillance and the optimal screening interval per organ system was analyzed [Kruizinga et al 2013]. The optimal time to start metanephrine measurements is age five years; retinal screening in patients with VHL can start at age 12 years. For central nervous system hemangioblastomas and visceral lesions, starting age was in line with current surveillance guidelines. Furthermore, to attain a 5% detection rate, surveillance intervals for retinal tumors can be twice as long, and for the adrenal gland, four times as long.

Improved surveillance guidelines have increased the life expectancy of individuals with VHL by more than 16 years since 1990 [Wilding et al 2012]. Two studies evaluated the implementation of national surveillance guidelines in Denmark and the Netherlands. One study showed that more than 90% of the 84 affected individuals included reported that they were familiar with their national VHL surveillance guidelines. However, daily practice showed that 64% of those individuals had received information that was only partially consistent with the Dutch guidelines [Lammens et al 2011a]. In a Danish study, compliance and frequency of follow up was surprisingly low with regard to the national VHL guidelines for individuals with VHL and subjects at risk [Bertelsen & Kosteljanetz 2011]. These studies collectively suggest that correct implementation of surveillance guidelines through a doctor- and patient-oriented information campaign could have an immediate positive impact for individuals with VHL.

## Agents/Circumstances to Avoid

- Tobacco products should be avoided since they are considered a risk factor for kidney cancer.
- Chemicals and industrial toxins known to affect VHL involved organs should be avoided.
- Contact sports should be avoided if adrenal or pancreatic lesions are present.

## Evaluation of Relatives at Risk

Early recognition of manifestations of VHL syndrome may allow for timely intervention and improved outcome; thus, clinical surveillance of asymptomatic at-risk individuals (including children) for early manifestations of VHL syndrome is appropriate. The American Society of Clinical Oncology identifies VHL syndrome as a Group 1 disorder – a hereditary disease for which genetic testing is considered part of the standard management for at-risk family members [American Society of Clinical Oncology 2010] (full text).



**If the *VHL* pathogenic variant in the family is known**, molecular genetic testing can be used for early identification of at-risk family members to improve diagnostic certainty and reduce the need for screening procedures in those at-risk family members who have not inherited the pathogenic variant [Priesemann et al 2006].

**If the *VHL* pathogenic variant in the family is not known** and/or at-risk individuals decline genetic testing for religious or financial reasons, continued screening for VHL lesions is warranted (see Surveillance).

The use of molecular genetic testing for determining the genetic status of presumably at-risk relatives when a family member with a clinical diagnosis of VHL syndrome is not available for testing is not straightforward. Such test results need to be interpreted with caution. A positive test result signals the presence of a *VHL* pathogenic variant in the at-risk family member and indicates that the same molecular genetic testing method can be used to assess the genetic status of other at-risk family members. However, a negative test for a *VHL* pathogenic variant under such circumstances suggests one of the following possibilities:

- The at-risk family member has not inherited a *VHL* pathogenic variant.
- The familial *VHL* pathogenic variant may not be detectable by the assays used.
- The clinical diagnosis of VHL syndrome in the affected family member is questionable.

In this situation, the presumably at-risk family member has a small, but finite, residual risk of having inherited a pathogenic allele (i.e., VHL syndrome or other hereditary disorder). In counseling such individuals, careful consideration should be given to the strength of the clinical diagnosis of VHL syndrome in the affected family member, the relationship of the at-risk individual to the affected family member, the perceived risk of an undetected *VHL* (or other gene) pathogenic variant, and the potential need for some form of continued clinical surveillance.

See Genetic Counseling for issues related to testing of at-risk relatives for genetic counseling purposes.

## Pregnancy Management

Recommended medical surveillance for pregnant women with VHL is still debated. Research by the French VHL Study Group showed a significantly higher complication rate of hemangioblastomas in individuals with VHL who had had at least one pregnancy [Abadie et al 2010]. Another study concluded that pregnancy has a significant influence on cerebellar hemangioblastoma growth and causes an overall high complication rate (17%) [Frantzen et al 2012]. Intensified surveillance could therefore be recommended in a specialized medical center during preconception care and pregnancy. Special attention should be paid to pheochromocytoma and cerebellar hemangioblastoma. In another study pregnancy was not related with the development of new hemangioblastomas or hemangioblastoma/cyst growth [Ye et al 2012]. Their data suggest no extra precautions need to be taken during gestation. The VHL Handbook recommends MRI of the cerebellum without contrast at four months' gestation.

## Therapies Under Investigation

Certain *VHL* pathogenic variants fail to downregulate HIFα, leading to overexpression of downstream effectors such as vascular endothelial growth factor (VEGF) which contribute to pathogenesis. Many experimental therapies target these misregulated signaling pathways. An intravitreal VEGF receptor inhibitor, ranibizumab, has been used with some success in individuals with retinal hemangioblastomas who have either failed local therapy or whose lesions are not amenable to local therapy [Wong et al 2008]. Intravitreal injections of bevacizumab, another VEGF inhibitor, have also been shown to be effective in treating retinal hemangioblastomas in patients with VHL [Hrisomalos et al 2010]. Stabilization of some (but not all) CNS hemangioblastomas has also been demonstrated [Madhusudan et al 2004].

A tyrosine kinase inhibitor that inhibits the action of growth factor receptors, sunitinib, has had some utility in the rare unresectable malignant pheochromocytomas, but simple surgical excision is clearly preferable for these usually benign tumors [Jimenez et al 2009]. Sunitinib has also been shown to effectively treat clear cell renal cell carcinomas – but not hemangioblastomas – in patients with VHL [Jonasch et al 2011].

Checkpoint inhibitors such as antibodies targeting PD-L1 have shown promise in managing tumor load; however, these treatments have unknown toxicity in patients with VHL, who will likely have dozens to thousands of small subclinical lesions present throughout their body. Sardi et al [2009] reported three-year stabilization of previously progressive multifocal spinal hemangioblastomas with thalidomide.

Gene replacement therapy and other curative treatment approaches are still in the early developmental phases. No such treatment for VHL currently exists, although it will be exciting to follow the example set by other monogenic diseases causing blindness.

Encouragingly, gene replacement therapy strategies have been used successfully for other diseases of the eye including Leber congenital amaurosis, retinitis pigmentosa, and Usher syndrome [Ashtari et al 2011, Trapani et al 2014, Deng et al 2015]. The medical and research communities are largely focused on ameliorating disease progression and on improvement of early detection methodology. Surgical techniques are rapidly improving and therapeutic options are broadening every year.



Premature termination codon 124 (PTC124), also known as ataluren, may benefit a subset of affected individuals in whom nonsense variants give rise to premature stop codons in the messenger RNA (mRNA) [Auld et al 2010]. There are three stop codons: UAA, UAG, and UGA. PTC124 promotes read-through of all three stop codons with different efficiencies. The highest read-through efficiency takes place at UGA, followed by UAG and then UAA. PTC124 has been successfully proven to promote read-through of nonsense variants in Duchenne muscular dystrophy (DMD), cystic fibrosis (CF), and Usher syndrome type 1C. Phase 1 and 2 clinical trials have shown no serious side-effects with PTC124 treatment, even after long-term use [Wilschanski et al 2011]. Preclinical investigation of PTC124 effects on VHL is ongoing.

Aminoglycosides such as gentamicin promote read-through of premature stop codons when they are supplied in high concentrations, but they have serious side effects.

Search ClinicalTrials.gov for access to information on clinical studies for a wide range of diseases and conditions.

## GENETIC COUNSELING

*Genetic counseling is the process of providing individuals and families with information on the nature, inheritance, and implications of genetic disorders to help them make informed medical and personal decisions. The following section deals with genetic risk assessment and the use of family history and genetic testing to clarify genetic status for family members. This section is not meant to address all personal, cultural, or ethical issues that individuals may face or to substitute for consultation with a genetics professional.* —ED.

### Mode of Inheritance

Von Hippel-Lindau (VHL) syndrome is inherited in an autosomal dominant manner.

### Risk to Family Members

**Parents of a proband**

- About 80% of individuals diagnosed with VHL syndrome have an affected parent.

- A proband with VHL syndrome may have the disorder as the result of *de novo VHL* pathogenic variant. The proportion of individuals with VHL syndrome due to a *de novo* pathogenic variant is about 20%.
- If the pathogenic variant found in the proband cannot be detected in leukocyte DNA of either parent, two possible explanations are germline mosaicism in a parent or *de novo* mutaiton in the proband. The incidence of germline mosaicism is as of yet unknown.
- However, some results suggest that mosaicism contributes more to VHL syndrome than is currently thought. Next-generation sequencing, with its improved sensitivity, will increase detection of mosaicism in VHL [Wu et al 2013, Coppin et al 2014].
- Molecular genetic testing is recommended for the parents of a proband with an apparent *de novo* pathogenic variant. If the *VHL* pathogenic variant in the proband is not known, ophthalmologic screening and abdominal ultrasound evaluation, at a minimum, should be offered to both parents.
- The family history of some individuals diagnosed with VHL syndrome may appear to be negative because of failure to recognize the disorder in family members, reduced penetrance, early death of the parent before the onset of symptoms, or late onset of the syndrome in the affected parent. Therefore, an apparently negative family history cannot be confirmed unless molecular genetic testing has been performed on the parents of the proband.

Note: If the parent is the individual in whom the pathogenic variant first occurred, (s)he may have somatic mosaicism for the pathogenic variant and may be mildly/minimally affected.

**Sibs of a proband**

- The risk to the sibs of the proband depends on the genetic status of the proband's parents.
- If a parent of the proband is affected and/or has the *VHL* pathogenic variant, the risk to the sibs of inheriting the variant is 50%.
- If the parents are clinically unaffected and are at least 35 years old, the risk to the sibs of a proband appears to be low.
- The sibs of a proband with clinically unaffected parents are still at increased risk for VHL syndrome because of the possibility of failure to recognize the disorder or late onset of the syndrome in an affected parent.
- If the *VHL* pathogenic variant found in the proband cannot be detected in the leukocyte DNA of either parent, the risk to sibs is low but greater than that of the general population because of the possibility of germline mosaicism.
- Mosaicism has been described; the incidence is not known [Murgia et al 2000, Sgambati et al 2000, Santarpia et al 2007, Wu et al 2013, Coppin et al 2014].

**Offspring of a proband.** Each child of an individual with VHL syndrome is at a 50% risk of inheriting the *VHL* pathogenic variant; the degree of clinical severity is not predictable.

**Other family members**

- The risk to other family members depends on the status of the proband's parents.
- If a parent is affected, his or her family members may be at risk.



## Related Genetic Counseling Issues

See Management, Evaluation of Relatives at Risk for information on evaluating at-risk relatives for the purpose of early diagnosis and treatment.

**Genetic cancer risk assessment and counseling.** For a comprehensive description of the medical, psychosocial, and ethical ramifications of identifying at-risk individuals through cancer risk assessment with or without molecular genetic testing, see Cancer Genetics Risk Assessment and Counseling – for health professionals (part of PDQ®, National Cancer Institute).

**Testing of at-risk asymptomatic family members.** Molecular genetic testing of at-risk family members is appropriate in order to determine the need for continued clinical surveillance. Interpretation of molecular genetic test results is most accurate when a germline *VHL* pathogenic variant has been identified in an affected family member (see Evaluation of Relatives at Risk).

Because early detection of at-risk individuals affects medical management, testing of asymptomatic individuals during childhood is beneficial [Hes et al 2001, Lonser et al 2003, Binderup et al 2013a, VHL Handbook]. As ophthalmologic screening for those at risk for VHL syndrome begins as early as possible, certainly before age five years, molecular genetic testing may be considered in young children. Molecular genetic testing may be performed earlier if the results would alter the medical management of the child.

Parents often want to know the genetic status of their children prior to initiating screening in order to avoid unnecessary procedures in a child who has not inherited the pathogenic variant. Special consideration should be given to education of the children and their parents prior to genetic testing. A plan should be established for the manner in which results are to be given to the parents and their children. The authors recommend the VHL handbook for children by the VHL Alliance [VHL Handbook - Kids' Edition].

**Other issues to consider.** It is recommended that physicians ordering *VHL* molecular genetic testing and individuals considering undergoing testing understand the risks, benefits, and limitations of the testing prior to sending a sample to a laboratory. A study

demonstrated that for almost one third of individuals assessed for familial adenomatous polyposis, an autosomal dominant colon cancer disease, the physician misinterpreted the test results [Giardiello et al 1997]. Referral to a genetic counselor and/or a center in which testing is routinely offered is recommended.

**Considerations in families with an apparent *de novo* pathogenic variant.** When neither parent of a proband has VHL syndrome and/or has the *VHL* pathogenic variant, the *VHL* pathogenic variant is likely *de novo*. However, possible non-medical explanations including alternate paternity or maternity (e.g., with assisted reproduction) or undisclosed adoption could also be explored.

**Family planning**

- The optimal time for determination of genetic risk and discussion of the availability of prenatal testing is before pregnancy.
- It is appropriate to offer genetic counseling (including discussion of potential risks to offspring and reproductive options) to young adults who are affected or at risk.
- Preconception considerations include possible male infertility due to cysts of the epididymis.

**DNA banking** is the storage of DNA (typically extracted from white blood cells) for possible future use. Because it is likely that testing methodology and our understanding of genes, allelic variants, and diseases will improve in the future, consideration should be given to banking DNA of affected individuals.

## Prenatal Testing and Preimplantation Genetic Diagnosis

Once the *VHL* pathogenic variant has been identified in an affected family member, prenatal testing and preimplantation genetic diagnosis (PGD) for a pregnancy at increased risk for VHL syndrome are possible options. PGD has been successfully used in pregnancies at risk for VHL syndrome [Rechitsky et al 2002, Simpson et al 2005].

Differences in perspective may exist among medical professionals and in families regarding the use of prenatal testing, particularly if the testing is being considered for the purpose of pregnancy termination rather than early diagnosis. Although most centers would consider decisions about prenatal testing to be the choice of the parents, discussion of these issues is appropriate.

## MOLECULAR GENETICS

*Information in the Molecular Genetics and OMIM tables may differ from that elsewhere in the GeneReview: tables may contain more recent information.* —ED.

**Table A.** Von Hippel-Lindau Syndrome: Genes and Databases

| Gene | Chromosome Locus | Protein | HGMD |
|---|---|---|---|
| VHL | 3p25.3 | Von Hippel-Lindau disease tumor suppressor | |

Data are compiled from the following standard references: gene from HGNC; chromosome locus, locus name, critical region, complementation group from OMIM; protein from UniProt.

**Table B.**

| | |
|---|---|
| 193300 | VON HIPPEL-LINDAU SYNDROME; VHL |
| 608537 | VHL GENE; VHL |

### Gene structure

*VHL*, which comprises three exons spanning about 10 kb of genomic DNA, is highly conserved among worms, flies, rodents, zebrafish, and humans [Kaelin 2002, Gossage et al 2015]. An mRNA about 4.5 kb in size is almost ubiquitously expressed and encodes proteins of 213 and 159 amino acid residues. The latter isoform is the major product in most tissues and results from initiation of translation from an internal methionine codon at position 54. Both protein isoforms appear to be functional. For a detailed summary of gene and protein information, see Table A, Gene.

### Pathogenic allelic variants

More than 500 germline pathogenic variants have been identified in families with von Hippel-Lindau (VHL) syndrome (see Table A) [Nordstrom-O'Brien et al 2010]. They consist of partial- and whole-gene deletions and frameshift, nonsense, missense, and splice site variants. Single nucleotide variants have been identified in all three exons. Codon 167 is considered a mutational "hot spot."

Nordstrom-O'Brien et al [2010] describes detailed phenotype and pathogenic variant information for 945 families with VHL. The spectrum of pathogenic variants found: 52% missense, 13% frameshift, 11% nonsense, 6% in-frame deletions/insertions, 11% large/complete deletions, and 7% splice site variants. In families whose described phenotype includes pheochromocytoma, 83.5% had a pathogenic missense variant. Families without pheochromocytoma had 6.6% more pathogenic truncating variants than pathogenic missense variants.

**Normal gene product**

Von Hippel-Lindau syndrome tumor suppressor (pVHL) has been implicated in a variety of functions including transcriptional regulation, post-transcriptional gene expression, apoptosis, extracellular matrix formation, and ubiquitinylation [Kaelin 2007, Roberts & Ohh 2008]. The role of pVHL in the regulation of hypoxia-inducible genes through the targeted ubiquitinylation and degradation of HIF1α has been described, leading to a model of how disruption of *VHL* results in renal cell carcinoma, hemangioblastoma, and the production of other highly vascularized tumors.

Normal pVHL binds to elongin C, which forms a complex with elongin B and cullin-2 (encoded by *TCEB2* and *CUL2*, respectively), and Rbx1 (see Figure 1). This complex resembles the SCF ubiquitin ligase or E3 complex in yeast that catalyzes the polyubiquitinylation of specific proteins and targets them for degradation by proteasomes. Under normoxic conditions, HIF1α is hydroxylated at one of two specific proline residues, catalyzed by a member of the EglN family of prolyl hydroxylase enzymes.

The VHL protein then binds to hydroxylated HIF1α and targets it for degradation. Under hypoxic conditions, HIF1α is not hydroxylated, pVHL does not bind, and HIF1α subunits accumulate. HIF1α forms heterodimers with HIF1β and activates transcription of a variety of hypoxia-inducible genes (i.e., *VEGF*, *EPO*, *TGFα*, *PDGFβ*). Likewise, when pVHL is absent or mutated, HIF1α subunits accumulate, resulting in cell proliferation and the neovascularization of tumors characteristic of VHL syndrome [Gossage et al 2015].

**Abnormal gene product**

Pathogenic variants in *VHL* either prevent its expression (i.e., deletions, frameshifts, nonsense variants, and splice site variants) or lead to the expression of an abnormal protein (i.e., pathogenic missense variants). The type of VHL that results from a pathogenic missense variant depends on its effect on the three-dimensional structure of the protein [Stebbins et al 1999]. Pathogenic variants in *VHL* cause misfolding and subsequent chaperonin-mediated breakdown [Feldman et al 2003]. Pathogenic missense variants that destabilize packing of the alpha-helical domains, decrease the stability of the alpha-beta domain interface, interfere with binding of elongin C and HIF1α, or disrupt hydrophobic core residues result in loss of HIF regulation and are more likely to result in VHL type 1. Pathogenic missense variants that result in pVHL that is normal with respect to HIF regulation are more likely to be associated with VHL type 2 (see Genotype-Phenotype Correlations).

Pathogenic missense variants that lead to pheochromocytoma with a low (or no) risk for RCC (types 2A and 2C) may encode a VHL protein that retains the ability to ubiquinate (and thereby downregulate) HIF1α in the presence of molecular oxygen to a greater degree than pathogenic variants that result in VHL syndrome with pheochromocytoma and RCC (type 2B). Furthermore, mutant pVHL may predispose to pheochromocytoma by altering

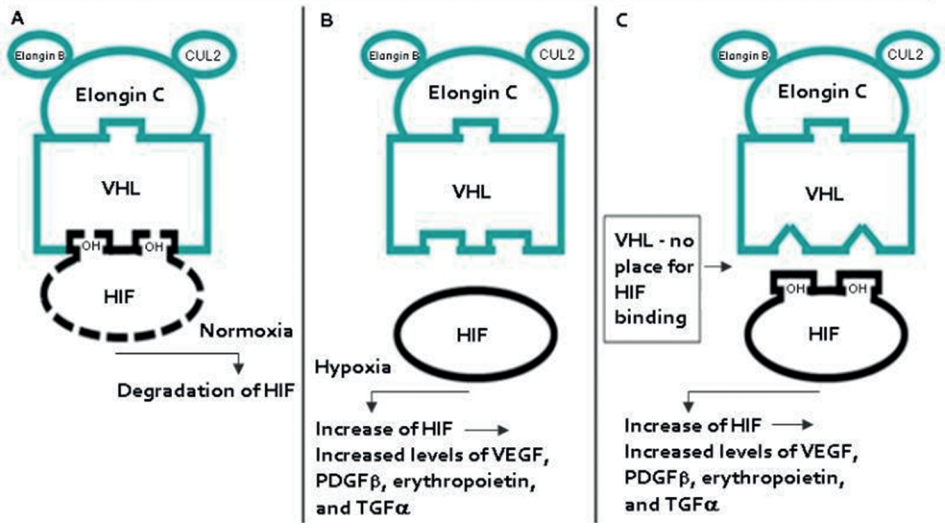


**Figure 1.** Schematic view of pVHL and HIF
**A.** Normoxia in a normal cell; HIF binds to pVHL. **B.** Hypoxia in a normal cell; HIF does not bind to pVHL. **C.** Cell with VHL pathogenic variant; HIF cannot bind to pVHL, therefore the cell acts as if there is constant hypoxia.

the balance among a group of proteins in a molecular pathway that controls apoptosis of sympatho-adrenal precursor cells during development. Such cells may be at increased risk of developing into pheochromocytomas at a later stage [Lee et al 2005, Kaelin 2007].

**Cancer and benign tumors**

Acquired somatic pathogenic variants in *VHL* may give rise to sporadic VHL-type tumors (i.e., clear cell RCC and hemangioblastoma) [Iliopoulos 2001, Kim & Kaelin 2004] without other associated tumors characteristic of the hereditary syndrome.

# REFERENCES

## Published Guidelines/Consensus Statements


1. American Society of Clinical Oncology. Policy statement update: genetic testing for cancer susceptibility. Available online. 2003. Accessed 5-13-16.
2. American Society of Clinical Oncology. Policy statement update: genetic testing for cancer susceptibility. Available online; registration or institutional access required. 2010. Accessed 5-13-16.
3. Binderup ML, Bisgaard ML, Harbud V, Møller HU, Gimsing S, Friis-Hansen L, Hansen Tv, Bagi P, Knigge U, Kosteljanetz M, Bøgeskov L, Thomsen C, Gerdes AM, Ousager LB, Sunde L; Danish vHL Coordination Group (2013b) Von Hippel-Lindau disease (vHL). National clinical guideline for diagnosis and surveillance in Denmark. 3rd edition. Dan Med J 60:B4763. [PubMed: 24355456]
4. Hes FJ, van der Luijt RB, Lips CJ. Clinical management of Von Hippel-Lindau (VHL) disease. Neth J Med. 2001;59:225–34. [PubMed: 11705642]
5. Lonser RR, Glenn GM, Walther M, Chew EY, Libutti SK, Linehan WM, Oldfield EH. von Hippel-Lindau disease. Lancet. 2003;361:2059–67. [PubMed: 12814730]
6. VHL Alliance. *The VHL Handbook*. 4 ed. Available for purchase online. 2012. Accessed 5-13-16.


## Literature Cited


1. Abadie C, Croupier I, Bringuier-Branchereau S, Mercies G, Deveaux S, Richard S. Role of pregnancy on hemangioblastomas in von Hippel-Lindau disease: A retrospective French study. Rio de Janeiro, Brazil: 9th International Medical Symposium on VHL. 2010.
2. Abbott MA, Nathanson KL, Nightingale S, Maher ER, Greenstein RM. The von Hippel-Lindau (VHL) germline mutation V84L manifests as early-onset bilateral pheochromocytoma. Am J Med Genet A. 2006;140:685–90. [PubMed: 16502427]
3. Abermil N, Guillaud-Bataille M, Burnichon N, Venisse A, Manivet P, Guignat L, Drui D, Chupin M, Josseaume C, Affres H, Plouin PF, Bertherat J, Jeunemaître X, Gimenez-Roqueplo AP. TMEM127 screening in a large cohort of patients with pheochromocytoma and/or paraganglioma. J Clin Endocrinol Metab. 2012;97:E805–9. [PubMed: 22419703]
4. American Society of Clinical Oncology. American Society of Clinical Oncology policy statement update: genetic and genomic testing for cancer susceptibility. J Clin Oncol. 2010;28:893–901. [PubMed: 20065170]
5. Ang SO, Chen H, Gordeuk VR, Sergueeva AI, Polyakova LA, Miasnikova GY, Kralovics R, Stockton DW, Prchal JT. Endemic polycythemia in Russia: mutation in the VHL gene. Blood Cells Mol Dis. 2002;28:57–62. [PubMed: 11987242]
6. Ashtari M, Cyckowski LL, Monroe JF, Marshall KA, Chung DC, Auricchio A, Simonelli F, Leroy BP, Maguire AM, Shindler KS, Bennett J. The human visual cortex responds to gene therapy-mediated recovery of retinal function. J Clin Invest. 2011;121:2160–8. [PMC free article: PMC3104779] [PubMed: 21606598]
7. Asthagiri AR, Metha GU, Zach L, Li X, Butman JA, Camphausen KA, Lonser RR. Prospective evaluation of radiosurgery for hemangioblastomas in von Hippel-Lindau disease. Neuro Oncol. 2010;12:80–6. [PMC free article: PMC2940550] [PubMed: 20150370]
8. Astuti D, Latif F, Dallol A, Dahia PL, Douglas F, George E, Sköldberg F, Husebye ES, Eng C, Maher ER. Gene mutations in the succinate dehydrogenase subunit SDHB cause susceptibility to familial pheochromocytoma and to familial paraganglioma. Am J Hum Genet. 2001;69:49–54. [PMC free article: PMC1226047] [PubMed: 11404820]
9. Auld DS, Lovell S, Thorne N, Lea WA, Maloney DJ, Shen M, Rai G, Battaile KP, Thomas CJ, Simeonov A, Hanzlik RP, Inglese J. Molecular basis for the high-affinity binding and stabilization of firefly luciferase by PTC124. Proc Natl Acad Sci U S A. 2010;107:4878–83. [PMC free article: PMC2841876] [PubMed: 20194791]
10. Banks RE, Tirukonda P, Taylor C, Hornigold N, Astuti D, Cohen D, Maher ER, Stanley AJ, Harnden P, Joyce A, Knowles M, Selby PJ. Genetic and epigenetic analysis of von Hippel-Lindau (VHL) gene alterations and relationship with clinical variables in sporadic renal cancer. Cancer Res. 2006;66:2000–11. [PubMed: 16488999]
11. Baysal BE, Ferrell RE, Willett-Brozick JE, Lawrence EC, Myssiorek D, Bosch A, van der Mey A, Taschner PE, Rubinstein WS, Myers EN, Richard CW 3rd, Cornelisse CJ, Devilee P, Devlin B. Mutations in SDHD, a mitochondrial complex II gene, in hereditary paraganglioma. Science. 2000;287:848–51. [PubMed: 10657297]
12. Benhammou JN, Boris RS, Pacak K, Pinto PA, Linehan WM, Bratslavsky G. Functional and oncologic outcomes of partial adrenalectomy for pheochromocytoma in patients with von Hippel-Lindau syndrome after at least 5 years of follow-up. J Urol. 2010;184:1855– 9. [PMC free article: PMC3164541] [PubMed: 20846682]
13. Bertelsen M, Kosteljanetz M. An evaluation of Danish national clinical guidelines for von Hippel-Lindau (VHL). Acta Neurochir (Wien) 2011;153:35–41. [PubMed: 20865287]
14. Best SL, Park SK, Youssef RF, Olweny EO, Tan YK, Trimmer C, Cadeddu JA. Long-term outcomes of renal tumor radio frequency ablation stratified by tumor diameter: size matters. J Urol. 2012;187:1183–9. [PubMed: 22335865]
15. Binderup ML, Bisgaard ML, Harbud V, Møller HU, Gimsing S, Friis-Hansen L, Hansen Tv, Bagi P, Knigge U, Kosteljanetz M, Bøgeskov L, Thomsen C, Gerdes AM, Ousager LB, Sunde L; Danish vHL Coordination Group (2013a) Von Hippel-Lindau disease (vHL). National clinical

guideline for diagnosis and surveillance in Denmark. 3rd edition. Dan Med J 60:B4763. [PubMed: 24355456]
16. Binderup ML, Gimsing S, Kosteljanetz M, Thomsen C, Bisgaard ML. von Hippel-Lindau disease: deafness due to a non-MRI-visible endolymphatic sac tumor despite targeted screening. Int J Audiol. 2013b;52:771–5. [PubMed: 24003980]
17. Blansfield JA, Choyke L, Morita SY, Choyke PL, Pingpank JF, Alexander HR, Seidel G, Shutack Y, Yuldasheva N, Eugeni M, Bartlett DL, Glenn GM, Middelton L, Linehan WM, Libutti SK. Clinical, genetic and radiographic analysis of 108 patients with von Hippel-Lindau disease (VHL) manifested by pancreatic neuroendocrine neoplasms (PNETs). Surgery. 2007;142:814–8. [PubMed: 18063061]
18. Boedeker CC, Hensen EF, Neumann HP, Maier W, van Nederveen FH, Suárez C, Kunst HP, Rodrigo JP, Takes RP, Pellitteri PK, Rinaldo A, Ferlito A. Genetics of hereditary head and neck paragangliomas. Head Neck. 2014;36:907–16. [PubMed: 23913591]
19. Burnichon N, Abermil N, Buffet A, Favier J, Gimenez-Roqueplo AP. The genetics of paragangliomas. Eur Ann Otorhinolaryngol Head Neck Dis. 2012;129:315–8. [PubMed: 23078982]
20. Butman JA, Linehan WM, Lonser RR. Neurologic manifestations of von Hippel-Lindau disease. JAMA. 2008;300:1334–42. [PMC free article: PMC3487164] [PubMed: 18799446]
21. Butman JA, Nduom E, Kim HJ, Lonser RR. Imaging detection of endolymphatic sac tumor-associated hydrops. J Neurosurg. 2013;119:406–11. [PubMed: 23472846]
22. Catapano D, Muscarella LA, Guarnieri V, Zelante L, D'Angelo VA, D'Agruma L. Hemangioblastomas of central nervous system: molecular genetic analysis and clinical management. Neurosurgery. 2005;56:1215–21. [PubMed: 15918937]
23. Chen MY, Chew EY, Reynolds JC, Chao DL, Oldfield EH. Metastatic brainstem pheochromocytoma in a patient with von Hippel-Lindau disease. J Neurosurg. 2001;94:138. [PubMed: 11147885]
24. Choo D, Shotland L, Mastroianni M, Glenn G, van Waes C, Linehan WM, Oldfield EH. Endolymphatic sac tumors in von Hippel-Lindau disease. J Neurosurg. 2004;100:480–7. [PubMed: 15035284]
25. Coppin L, Grutzmacher C, Crépin M, Destailleur E, Giraud S, Cardot-Bauters C, Porchet N, Pigny P. VHL mosaicism can be detected by clinical next-generation sequencing and is not restricted to patients with a mild phenotype. Eur J Hum Genet. 2014;22:1149–52. [PMC free article: PMC4135403] [PubMed: 24301059]
26. Corcos O, Couvelard A, Giraud S, Vullierme MP. Dermot O'Toole, Rebours V, Stievenart JL, Penfornis A, Niccoli-Sire P, Baudin E, Sauvanet A, Levy P, Ruszniewski P, Richard S, Hammel P. Endocrine pancreatic tumors in von Hippel-Lindau disease: clinical, histological, and genetic features. Pancreas. 2008;37:85–93. [PubMed: 18580449]
27. Cybulski C, Krzystolik K, Murgia A, Gorski B, Debniak T, Jakubowska A, Martella M, Kurzawski G, Prost M, Kojder I, Limon J, Nowacki P, Sagan L, Bialas B, Kaluza J, Zdunek M, Omulecka A, Jaskolski D, Kostyk E, Koraszewska-Matuszewska B, Haus O, Janiszewska H, Pecold K, Starzycka M, Slomski R, Cwirko M, Sikorski A, Gliniewicz B, Cyrylowski L, Fiszer-Maliszewska L, Gronwald J, Toloczko-Grabarek A, Zajaczek S, Lubinski J. Germline mutations in the von Hippel-Lindau (VHL) gene in patients from Poland: disease presentation in patients with deletions of the entire VHL gene. J Med Genet. 2002;39:E38. [PMC free article: PMC1735187] [PubMed: 12114495]
28. Decker J, Neuhaus C, Macdonald F, Brauch H, Maher ER. Clinical utility gene card for: von Hippel-Lindau (VHL). Eur J Hum Genet. 2014;22(4) [PMC free article: PMC3953906] [PubMed: 23982691]
29. Deng WT, Dyka FM, Dinculescu A, Li J, Zhu P, Chiodo VA, Boye SL, Conlon TJ, Erger K, Cossette T, Hauswirth WW. Stability and Safety of an AAV Vector for Treating RPGR-ORF15 X-Linked Retinitis Pigmentosa. Hum Gene Ther. 2015;26:593–602. [PMC free article: PMC4575541] [PubMed: 26076799]
30. Dollfus H, Massin P, Taupin P, Nemeth C, Amara S, Giraud S, Beroud C, Dureau P, Gaudric A, Landais P, Richard S. Retinal hemangioblastoma in von Hippel-Lindau disease: a clinical and molecular study. Invest Ophthalmol Vis Sci. 2002;43:3067–74. [PubMed: 12202531]
31. Feldman DE, Spiess C, Howard DE, Frydman J. Tumorigenic mutations in VHL disrupt folding in vivo by interfering with chaperonin binding. Mol Cell. 2003;12:1213–24. [PubMed: 14636579]
32. Frantzen C, Kruizinga RC, van Asselt SJ, Zonnenberg BA, Lenders JWM, de Herder WW, Walenkamp AME, Giles RH, Hes FJ, Sluiter WJ, van Pampus MG, Links TP. Pregnancy-related hemangioblastoma progression and complications in von Hippel-Lindau disease. Neurology. 2012;79:793–6. [PubMed: 22875085]
33. Friedman RA, Hoa M, Brackmann DE. Surgical management of endolymphatic sac tumors. J Neurol Surg B Skull Base. 2013;74:12–9. [PMC free article: PMC3699165] [PubMed: 24436884]
34. Giannini C, Scheithauer BW, Hellbusch LC, Rasmussen AG, Fox MW, McCormick SR, Davis DH. Peripheral nerve hemangioblastoma. Mod Pathol. 1998;11:999–1004. [PubMed: 9796730]
35. Giardiello FM, Brensinger JD, Petersen GM, Luce MC, Hylind LM, Bacon JA, Booker SV, Parker RD, Hamilton SR. The use and interpretation of commercial APC gene testing for familial adenomatous polyposis. N Engl J Med. 1997;336:823–7. [PubMed: 9062090]
36. Gläsker S. Central nervous system manifestations in VHL: genetics, pathology and clinical phenotypic features. Fam Cancer. 2005;4:37–42. [PubMed: 15883708]
37. Gordeuk VR, Sergueeva AI, Miasnikova GY, Okhotin D, Voloshin Y, Choyke PL, Butman JA, Jedlickova K, Prchal JT, Polyakova LA. Congenital disorder of oxygen sensing: association of the homozygous Chuvash polycythemia VHL mutation with thrombosis and vascular abnormalities but not tumors. Blood. 2004;103:3924–32. [PubMed: 14726398]
38. Gossage L, Eisen T, Maher ER. VHL, the story of a tumour suppressor gene. Nat Rev Cancer. 2015;15:55–64. [PubMed: 25533676]

39. Grubb RL III, Choyke PL, Pinto PA, Linehan WM, Walther MM. Management of von Hippel-Lindau-associated kidney cancer. Nat Clin Pract Urol. 2005;2:248–55. [PubMed: 16474836]
40. Hes FJ, van der Luijt RB, Lips CJ. Clinical management of Von Hippel-Lindau (VHL) disease. Neth J Med. 2001;59:225–34. [PubMed: 11705642]
41. Hoebeeck J, van der Luijt R, Poppe B, De Smet E, Yigit N, Claes K, Zewald R, de Jong GJ, De Paepe A, Speleman F, Vandesompele J. Rapid detection of VHL exon deletions using real-time quantitative PCR. Lab Invest. 2005;85:24–33. [PubMed: 15608663]
42. Hrisomalos FN, Maturi RK, Pata V. Long-term use of intravitreal bevacizumab (avastin) for the treatment of von hippel-lindau associated retinal hemangioblastomas. Open Ophthalmol J. 2010;4:66–9. [PMC free article: PMC3032222] [PubMed: 21293730]
43. Huntoon K, Oldfield EH, Lonser RR. Dr. Arvid Lindau and discovery of von Hippel-Lindau disease. J Neurosurg. 2015;123:1093–7. [PubMed: 25748307]
44. Iliopoulos O. von Hippel-Lindau disease: genetic and clinical observations. Front Horm Res. 2001;28:131–66. [PubMed: 11443850]
45. Inabnet WB, Caragliano P, Pertsemlidis D. Pheochromocytoma: inherited associations, bilaterality, and cortex preservation. Surgery. 2000;128:1007–11. [PubMed: 11114636]
46. Jimenez C, Cabanillas ME, Santarpia L, Jonasch E, Kyle KL, Lano EA, Matin SF, Nunez RF, Perrier ND, Phan A, Rich TA, Shah B, Williams MD, Waguespack SG. Use of the tyrosine kinase inhibitor sunitinib in a patient with von Hippel-Lindau disease: targeting angiogenic factors in pheochromocytoma and other von Hippel-Lindau disease-related tumors. J Clin Endocrinol Metab. 2009;94:386–91. [PubMed: 19017755]
47. Joly D, Méjean A, Corréas JM, Timsit MO, Verkarre V, Deveaux S, Landais P, Grünveld JP, Richard S. Progress in Nephron Sparing Therapy for Renal Cell Carcinoma and von Hippel-Lindau Disease. J Urol. 2011;185:2056–60. [PubMed: 21496837]
48. Jonasch E, McCutcheon IE, Waguespack SG, Wen S, Davis DW, Smith LA, Tannir NM, Gombos DS, Fuller GN, Matin SF. Pilot trial of sunitinib therapy in patients with von Hippel-Lindau disease. Ann Oncol. 2011;22:2661–6. [PMC free article: PMC4542805] [PubMed: 22105611]
49. Kaelin WG. von Hippel-Lindau disease. Annu Rev Pathol. 2007;2:145–73. [PubMed: 18039096]
50. Kaelin WG Jr. Molecular basis of the VHL hereditary cancer syndrome. Nat Rev Cancer. 2002;2:673–82. [PubMed: 12209156]
51. Kano H, Shuto T, Iwai Y, Sheehan J, Yamamoto M, McBride HL, Sato M, Serizawa T, Yomo S, Moriki A, Kohda Y, Young B, Suzuki S, Kenai H, Duma C, Kikuchi Y, Mathieu D, Akabane A, Nagano O, Kondziolka D, Lunsford LD. Stereotactic radiosurgery for intracranial hemangioblastomas: a retrospective international outcome study. J Neurosurg. 2015;122:1469–78. [PubMed: 25816088]
52. Kim HJ, Butman JA, Brewer C, Zalewski C, Vortmeyer AO, Glenn G, Oldfield EH, Lonser RR. Tumors of the endolymphatic sac in patients with von Hippel-Lindau disease: implications for their natural history, diagnosis, and treatment. J Neurosurg. 2005;102:503–12. [PubMed: 15796386]
53. Kim HJ, Hagan M, Butman JA, Baggenstos M, Brewer C, Zalewski C, Linehan WM, Lonser RR. Surgical resection of endolymphatic sac tumors in von Hippel-Lindau disease: findings, results, and indications. Laryngoscope. 2013;123:477–83. [PubMed: 23070752]
54. Kim WY, Kaelin WG. Role of VHL gene mutations in human cancer. J Clin Oncol. 2004;22:4991–5004. [PubMed: 15611513]
55. Knauth K, Bex C, Jemth P, Buchberger A. Renal cell carcinoma risk in type 2 von Hippel-Lindau disease correlates with defects in pVHL stability and HIF-1alpha interactions. Oncogene. 2006;25:370–7. [PubMed: 16261165]
56. Korpershoek E, Favier J, Gaal J, Burnichon N, van Gessel B, Oudijk L, Badoual C, Gadessaud N, Venisse A, Bayley JP, van Dooren MF, de Herder WW, Tissier F, Plouin PF, van Nederveen FH, Dinjens WN, Gimenez-Roqueplo AP, de Krijger RR. SDHA immunohistochemistry detects germline SDHA gene mutations in apparently sporadic paragangliomas and pheochromocytomas. J Clin Endocrinol Metab. 2011;96:E1472–6. [PubMed: 21752896]
57. Kreusel KM. Ophthalmological manifestations in VHL and NF 1: pathological and diagnostic implications. Fam Cancer. 2005;4:43–7. [PubMed: 15883709]
58. Kreusel KM, Bechrakis NE, Krause L, Neumann HP, Foerster MH. Retinal angiomatosis in von Hippel-Lindau disease: a longitudinal ophthalmologic study. Ophthalmology. 2006;113:1418–24. [PubMed: 16769118]
59. Kruizinga RC, Sluiter WJ, de Vries EG, Zonnenberg BA, Lips CJ, van der Horst-Schrivers AN, Walenkamp AM, Links TP. Calculating optimal surveillance for detection of von Hippel-Lindau-related manifestations. Endocr Relat Cancer. 2013;21:63–71. [PubMed: 24132471]
60. Kwon T, Jeong IG, Pak S, You D, Song C, Hong JH, Ahn H, Kim CS. Renal tumor size is an independent prognostic factor for overall survival in von Hippel-Lindau disease. J Cancer Res Clin Oncol. 2014;140:1171–7. [PubMed: 24671227]
61. Lammens CR, Aaronson NK, Hes FJ, Links TP, Zonnenberg BA, Lenders JW, Majoor-Krakauer D, Van Os TA, Gomez-Garcia EB, de Herder W, van der Luijt RB, van den Ouweland AM, Van Hest LP, Verhoef S, Bleiker EM. Compliance with period surveillance for von Hippel-Lindau disease. Genet Med. 2011a;13:519–27. [PubMed: 21415761]
62. Lammens CR, Bleiker EM, Verhoef S, Ausems MG, Majoor-Krakauer D, Sijmons RH, Hes FJ, Gómez-García EB, Van Os TA, Spruijt L, van der Luijt RB, van den Ouweland AM, Ruijs MW, Gundy C, Nagtegaal T, Aaronson NK. Distress in partners of individuals diagnosed with or at high risk of developing tumors due to rare hereditary cancer syndromes. Psychooncology. 2011b;20:631–8. [PubMed: 21384469]

63. Lammens CR, Bleiker EM, Verhoef S, Hes FJ, Ausems MG, Majoor-Krakauer D, Sijmons RH, van der Luijt RB, van den Ouweland AM, Van Os TA, Hoogerbrugge N, Gómez García EB, Dommering CJ, Gundy CM, Aaronson NK. Psychosocial impact of Von Hippel-Lindau disease: levels and sources of distress. Clin Genet. 2010;77:483–91. [PubMed: 20184621]
64. Lee S, Nakamura E, Yang H, Wei W, Linggi MS, Sajan MP, Farese RV, Freeman RS, Carter BD, Kaelin WG Jr, Schlisio S. Neuronal apoptosis linked to EglN3 prolyl hydroxylase and familial pheochromocytoma genes: developmental culling and cancer. Cancer Cell. 2005;8:155–67. [PubMed: 16098468]
65. Lonser RR, Butman JA, Huntoon K, Asthagiri AR, Wu T, Bakhtian KD, Chew EY, Zhuang Z, Linehan WM, Oldfield EH. Prospective natural history study of central nervous system hemangioblastomas in von Hippel-Lindau disease. J Neurosurg. 2014;120:1055–62. [PMC free article: PMC4762041] [PubMed: 24579662]
66. Lonser RR, Butman JA, Kiringoda R, Song D, Oldfield EH. Pituitary stalk hemangioblastomas in von Hippel-Lindau disease. J Neurosurg. 2009;110:350–3. [PMC free article: PMC2770699] [PubMed: 18834262]
67. Lonser RR, Glenn GM, Walther M, Chew EY, Libutti SK, Linehan WM, Oldfield EH. von Hippel-Lindau disease. Lancet. 2003;361:2059–67. [PubMed: 12814730]
68. Madhusudan S, Deplanque G, Braybrooke JP, Cattell E, Taylor M, Price P, Tsaloumas MD, Moore N, Huson SM, Adams C, Frith P, Scigalla P, Harris AL. Antiangiogenic therapy for von Hippel-Lindau disease. JAMA. 2004;291:943–4. [PubMed: 14982909]
69. Maher ER, Iselius L, Yates JR, Littler M, Benjamin C, Harris R, Sampson J, Williams A, Ferguson-Smith MA, Morton N. Von Hippel-Lindau disease: a genetic study. J Med Genet. 1991;28:443–7. [PMC free article: PMC1016952] [PubMed: 1895313]
70. Maher ER, Neumann HP, Richard S. von Hippel-Lindau disease: a clinical and scientific review. Eur J Hum Genet. 2011;19:617–23. [PMC free article: PMC3110036] [PubMed: 21386872]
71. Maher ER, Yates RJ, Harries R, Benjamin R, Moorre AT, Ferguson-Smith MA. Clinical features and natural history of von Hippel-Lindau disease. Q J Med. 1990;77:1151–63. [PubMed: 2274658]
72. Maranchie JK, Afonso A, Albert PS, Kalyandrug S, Phillips JL, Zhou S, Peterson J, Ghadimi BM, Hurley K, Riss J, Vasselli JR, Ried T, Zbar B, Choyke P, Walther MM, Klausner RD, Linehan WM. Solid renal tumor severity in von Hippel Lindau disease is related to germline deletion length and location. Hum Mutat. 2004;23:40–6. [PubMed: 14695531]
73. Marcos HB, Libutti SK, Alexander HR, Lubensky IA, Bartlett DL, Walther MM, Linehan WM, Glenn GM, Choyke PL. Neuroendocrine tumors of the pancreas in von Hippel-Lindau disease: spectrum of appearances at CT and MR imaging with histopathologic comparison. Radiology. 2002;225:751–8. [PubMed: 12461257]
74. McNeill A, Rattenberry E, Barber R, Killick P, MacDonald F, Maher ER. Genotype-phenotype correlations in VHL exon deletions. Am J Med Genet A. 2009;149A:2147–51. [PubMed: 19764026]
75. Molino D, Sepe J, Anastasio P, De Santo NG. The history of von Hippel-Lindau disease. J Nephrol. 2006;19 Suppl 10:S119–23. [PubMed: 16874724]
76. Murgia A, Martella M, Vinanzi C, Polli R, Perilongo G, Opocher G. Somatic mosaicism in von Hippel-Lindau Disease. Hum Mutat. 2000;15:114. [PubMed: 10612832]
77. Muzumdar DP, Goel A, Fattepurkar S, Goel N. Endolymphatic sac carcinoma of the right petrous bone in Von Hippel-Lindau disease. J Clin Neurosci. 2006;13:471–4. [PubMed: 16678727]
78. Neumann HP, Bausch B, McWhinney SR, Bender BU, Gimm O, Franke G, Schipper J, Klisch J, Altehoefer C, Zerres K, Januszewicz A, Eng C, Smith WM, Munk R, Manz T, Glaesker S, Apel TW, Treier M, Reineke M, Walz MK, Hoang-Vu C, Brauckhoff M, Klein-Franke A, Klose P, Schmidt H, Maier-Woelfle M, Peczkowska M, Szmigielski C, Eng C. Germ-line mutations in nonsyndromic pheochromocytoma. N Engl J Med. 2002;346:1459–66. [PubMed: 12000816]
79. Neumann HP, Eng C. The approach to the patient with paraganglioma. J Clin Endocrinol Metab. 2009;94:2677–83. [PMC free article: PMC2730863] [PubMed: 19657044]
80. Neumann HP, Pawlu C, Peczkowska M, Bausch B, McWhinney SR, Muresan M, Buchta M, Franke G, Klisch J, Bley TA, Hoegerle S, Boedeker CC, Opocher G, Schipper J, Januszewicz A, Eng C., European-American Paraganglioma Study Group. Distinct clinical features of paraganglioma syndromes associated with SDHB and SDHD gene mutations. JAMA. 2004;292:943–51. [PubMed: 15328326]
81. Neumann HP, Sullivan M, Winter A, Malinoc A, Hoffmann MM, Boedeker CC, Bertz H, Walz MK, Moeller LC, Schmid KW, Eng C. Germline mutations of the TMEM127 gene in patients with paraganglioma of head and neck and extraadrenal abdominal sites. J Clin Endocrinol Metab. 2011;96:E1279–82. [PubMed: 21613359]
82. Nordstrom-O'Brien M, van der Luijt RB, van Rooijen E, van den Ouweland AM, Majoor-Krakauer DF, Lolkema MP, van Brussel A, Voest EE, Giles RH. Genetic analysis of von Hippel-Lindau disease. Hum Mutat. 2010;31:521–37. [PubMed:20151405]
83. Oldfield EH. Editorial: Management of hemangioblastomas in patients with von Hippel-Lindau disease: stereotactic radiosurgery compared to surgical excision. J Neurosurg. 2015;122:1466–8. [PubMed: 25816089]
84. Pastore Y, Jedlickova K, Guan Y, Liu E, Fahner J, Hasle H, Prchal JF, Prchal JT. Mutations of von Hippel-Lindau tumor-suppressor gene and congenital polycythemia. Am J Hum Genet. 2003;73:412–9. [PMC free article: PMC1180379] [PubMed: 12844285]
85. Priesemann M, Davies KM, Perry LA, Drake WM, Chew SL, Monson JP, Savage MO, Johnston LB. Benefits of screening in von Hippel-Lindau disease--comparison of morbidity associated with initial tumours in affected parents and children. Horm Res. 2006;66:1–5. [PubMed: 16651847]

86. Raja D, Benz MS, Murray TG, Escalona-Benz EM, Markoe A. Salvage external beam radiotherapy of retinal capillary hemangiomas secondary to von Hippel-Lindau disease: visual and anatomic outcomes. Ophthalmology. 2004;111:150–3. [PubMed: 14711727]
87. Rechitsky S, Verlinsky O, Chistokhina A, Sharapova T, Ozen S, Masciangelo C, Kuliev A, Verlinsky Y. Preimplantation genetic diagnosis for cancer predisposition. Reprod Biomed Online. 2002;5:148–55. [PubMed: 12419039]
88. Roberts AM, Ohh M. Beyond the hypoxia-inducible factor-centric tumour suppressor model of von Hippel-Lindau. Curr Opin Oncol. 2008;20:83–9. [PubMed: 18043261]
89. Rodriguez JM, Balsalobre M, Ponce JL, Ríos A, Torregrosa NM, Tebar J, Parrilla P. Pheochromocytoma in MEN 2A syndrome. Study of 54 patients. World J Surg. 2008;32:2520–6. [PubMed: 18795243]
90. Sansó G, Rudaz MC, Levin G, Barontini M. Familial isolated pheochromocytoma presenting a new mutation in the von Hippel-Lindau gene. Am J Hypertens. 2004;17:1107–11. [PubMed: 15607616]
91. Santarpia L, Sarlis NJ, Santarpia M, Sherman SI, Trimarchi F, Benvenga S. Mosaicism in von Hippel-Lindau disease: an event important to recognize. J Cell Mol Med. 2007;11:1408–15. [PMC free article: PMC4401302] [PubMed: 18205710]
92. Sardi I, Sanzo M, Giordano F, Buccoliero AM, Mussa F, Aricò M, Genitori L. Monotherapy with thalidomide for treatment of spinal cord hemangioblastomas in a patient with von Hippel-Lindau disease. Pediatr Blood Cancer. 2009;53:464–7. [PubMed: 19415739]
93. Schimke RN, Collins DL, Rothberg PG. Functioning carotid paraganglioma in the von Hippel-Lindau syndrome. Am J Med Genet. 1998;80:533–4. [letter] [PubMed: 9880225]
94. Sgambati MT, Stolle C, Choyke PL, Walther MM, Zbar B, Linehan WM, Glenn GM. Mosaicism in von Hippel-Lindau disease: lessons from kindreds with germline mutations identified in offspring with mosaic parents. Am J Hum Genet. 2000;66:84–91. [PMC free article: PMC1288351] [PubMed: 10631138]
95. Shingleton WB, Sewell PE Jr. Percutaneous renal cryoablation of renal tumors in patients with von Hippel-Lindau disease. J Urol. 2002;167:1268–70. [PubMed: 11832711]
96. Simone CB, Lonser RR, Ondos J, Oldfield EH, Camphausen K, Simone NL. Infratentorial craniospinal irradiation for von Hippel-Lindau: a retrospective study supporting a new treatment for patients with CNS hemangioblastomas. Neuro Oncol. 2011;13:1030–6. [PMC free article: PMC3158017] [PubMed: 21798886]
97. Simpson JL, Carson SA, Cisneros P. Preimplantation genetic diagnosis (PGD) for heritable neoplasia. J Natl Cancer Inst Monogr. 2005;34:87–90. [PubMed: 15784832]
98. Stebbins CE, Kaelin WG Jr, Pavletich NP. Structure of the VHL-ElonginC-ElonginB complex: implications for VHL tumor suppressor function. Science. 1999;284:455–61. [PubMed: 10205047]
99. Stolle C, Glenn G, Zbar B, Humphrey JS, Choyke P, Walther M, Pack S, Hurley K, Andrey C, Klausner R, Linehan WM. Improved detection of germline mutations in the von Hippel-Lindau disease tumor suppressor gene. Hum Mutat. 1998;12:417–23. [PubMed: 9829911]
100. Trapani I, Colella P, Sommella A, Iodice C, Cesi G, de Simone S, Marrocco E, Rossi S, Giunti M, Palfi A, Farrar GJ, Polishchuk R, Auricchio A. Effective delivery of large genes to the retina by dual AAV vectors. EMBO Mol Med. 2014;6:194–211. [PMC free article: PMC3927955] [PubMed: 24150896]
101. Volkin D, Yerram N, Ahmed F, Lankford D, Baccala A, Gupta GN, Hoang A, Nix J, Metwalli AR, Lang DM, Bratslavsky G, Linehan WM, Pinto PA. Partial adrenalectomy minimizes the need for long-term hormone replacement in pediatric patients with pheochromocytoma and von Hippel-Lindau syndrome. J Pediatr Surg. 2012;47:2077–82. [PMC free article: PMC3846393] [PubMed: 23164001]
102. Wanebo JE, Lonser RR, Glenn GM, Oldfield EH. The natural history of hemangioblastomas of the central nervous system in patients with von Hippel-Lindau disease. J Neurosurg. 2003;98:82–94. [PubMed: 12546356]
103. Webster AR, Maher ER, Moore AT. Clinical characteristics of ocular angiomatosis in von Hippel-Lindau disease and correlation with germline mutation. Arch Ophthalmol. 1999;117:371–8. [PubMed: 10088816]
104. Weirich G, Klein B, Wohl T, Engelhardt D, Brauch H. VHL2C phenotype in a German von Hippel-Lindau family with concurrent VHL germline mutations P81S and L188V. J Clin Endocrinol Metab. 2002;87:5241–6. [PubMed: 12414898]
105. Wilding A, Ingham SL, Lalloo F, Clancy T, Huson SM, Moran A, Evans DG. Life expectancy in hereditary cancer predisposing diseases: an observational study. J Med Genet. 2012;49:264–9. [PubMed: 22362873]
106. Wilschanski M, Lovell S, Thorne N, Lea WA, Maloney DJ, Shen M, Rai G, Battaile KP, Thomas CJ, Simeonov A, Hanzlik RP, Inglese J. Chronic ataluren (PTC124) treatment of nonsense mutation cystic fibrosis. Eur Respir J. 2011;38:59–69. [PubMed: 21233271]
107. Wong WT, Liang KJ, Hammel K, Coleman HR, Chew EY. Intravitreal ranibizumab therapy for retinal capillary hemangioblastoma related to von Hippel-Lindau disease. Ophthalmology. 2008;115:1957–64. [PMC free article: PMC3034164] [PubMed: 18789534]
108. Wu P, Zhang N, Wang X, Li T, Ning X, Bu D, Gong K. Mosaicism in von Hippel-Lindau disease with severe renal manifestations. Clin Genet. 2013;84:581–4. [PubMed: 23384228]
109. Yao L, Schiavi F, Cascon A, Qin Y, Inglada-Pérez L, King EE, Toledo RA, Ercolino T, Rapizzi E, Ricketts CJ, Mori L, Giacchè M, Mendola A, Taschin E, Boaretto F, Loli P, Iacobone M, Rossi GP, Biondi B, Lima-Junior JV, Kater CE, Bex M, Vikkula M, Grossman AB, Gruber SB, Barontini M, Persu A, Castellano M, Toledo SP, Maher ER, Mannelli M, Opocher G, Robledo M, Dahia PL. Spectrum and prevalence of FP/TMEM127 gene mutations in pheochromocytomas and paragangliomas. JAMA. 2010;304:2611–9. [PubMed: 21156949]
110. Ye DY, Bakhtian KD, Asthagiri AR, Lonser RR. Effect of pregnancy on hemangioblastoma development and progression in von Hippel-Lindau disease. J Neurosurg. 2012;117:818–24. [PubMed: 22937928]
111. Young EE, Castle SM, Gorbatiy V, Leveillee RJ. Comparison of safety, renal function outcomes and efficacy of laparoscopic and percutaneous radio frequency ablation of renal masses. J Urol. 2012;187:1177–82.

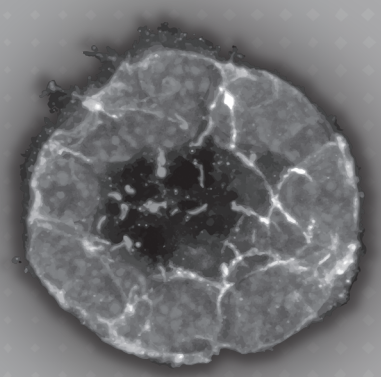

# CHAPTER 4

# Pre-clinical models to validate combination therapy approaches to reduce pathophysiological angiogenesis

Manuscript submitted

**Klasson TD**, Brandt M, van Rooijen E, Verhulst D, Verhaar MC, Knoers NV, Groenewegen G, Cheng CL, Giles RH

## ABSTRACT

The most common form of kidney cancer is clear cell renal cell carcinoma (ccRCC). Current treatment strategies focus on reducing pathophysiologic angiogenesis which accompanies ccRCC to reduce tumor burden and slow cancer progression. Although the drugs used for ccRCC such as first-line treatments sunitinib or pazopanib are initially effective, patients invariably display resistance to individual therapies after a period of successful treatment. One possible method for reducing resistance is to use combination therapy instead of serial monotherapies. By attacking multiple aspects of angiogenesis at once, combination therapy can reduce the risk of resistance while maintaining effectiveness and keeping drug concentration, and therefore toxicity, low. However, testing the effectiveness of combination therapy is difficult in traditional mammalian models. Here we use a *vhl*-/- zebrafish model of pathophysiological angiogenesis alongside a human-derived co-culture *in vitro* model to assess the effectiveness of combination therapy in combatting angiogenesis. Using a proof-of-principle combination of vascular endothelial growth factor receptor tyrosine kinase inhibitor cediranib and endothelin receptor antagonist zibotentan, we show that combination therapy is a feasible drug treatment modality and, in addition, zebrafish along with *in vitro* models are attractive systems to test therapies in a more high-throughput manner than traditional drug-testing models.


**Abbreviations**
ccRCC = clear cell Renal Cell Carcinoma
VEGF = Vascular Endothelial Growth Factor
VEGFR = Vascular Endothelial Growth Factor Receptor
TKI = Tyrosine Kinase Inhibitor
ET = Endothelin
HUVEC = Human Umbilical Vein Endothelial Cell
ISV = Intersomitic Vessel
DMSO = Dimethyl Sulfoxide

## INTRODUCTION

Angiogenesis, the post-development growth of new blood vessels from existing vasculature, is required for cancer progression of solid tumors. One angiogenesis pathway frequently found upregulated in cancer is the Vascular Endothelial Growth Factor (VEGF) pathway. The VEGF family of factors are key promoters of angiogenesis whose expression is regulated by the von Hippel-Lindau (VHL) tumor suppressor which is the most commonly mutated gene in clear cell renal cell carcinoma (ccRCC). VEGF factors bind to two receptor tyrosine kinases (VEGFRs), specifically VEGF Receptor 1 (also known as Flt-1) and VEGF receptor 2 (also called Flk-1), which are found on endothelial cells. The binding of a VEGF factor to a VEGFR promotes VEGFR dimerization and tyrosine phosphorylation causing priming of the endothelium for angiogenesis and activation of downstream effector pathways including the Raf-Mek-Erk and PI3K-Akt pathways, two key cellular signaling systems that promote cell survival, mitogenesis and chemotaxis [1]. VEGF signaling is frequently found upregulated in cancer –through loss of *VHL* or other mechanisms- because of its pro-angiogenic effects, which are hijacked to deliver nutrients and oxygen to the growing tumor, in a process commonly referred to as the "angiogenic switch" [2]. VEGFR tyrosine kinase inhibitors (TKIs) are a class of drugs designed to take advantage of this treatment strategy by blocking the phosphorylation of tyrosines at the signaling end of VEGFRs and thereby reducing the ability of tumor cells to promote aberrant angiogenesis. Before 2007, when the first anti-angiogenesis drugs were approved for ccRCC, two-year survival for patients with late-stage ccRCC was less than 20%. After these treatments began being commonly prescribed, two-year survival improved to over 50%, demonstrating the effectiveness of anti-angiogenesis as a treatment strategy. Despite improved progression-free survival and evidence of overall survival benefits [3], VEGFR TKIs are associated with serious toxicities, including hypertension, cardiac cell death, cutaneous reactions, proteinuria, and impaired wound healing as well as hemorrhagic, hepatotoxicity and thromboembolic events. Moreover, almost all patients treated with VEGFR TKIs will eventually display insensitivity to their treatment and their cancer will begin to progress again [4]. The possible value of drug treatment sequencing and the potential of drug re-challenge is an ongoing discussion, with many sources agreeing that combination therapy may be the best chance for long-term benefit to the patient. Indeed, the first combination therapy using an mTOR inhibitor with a VEGFR TKI has recently been FDA-approved for ccRCC [5].

Endothelins (ETs) are a group of signaling molecules which play a related role in the complex cellular signaling networks that control angiogenesis. Endothelin binding to its receptors promotes the activity of a wide variety of downstream pathways including the Raf-Mek-Erk and the cAMP-PKA-mTOR pathways. Endothelin's most well characterized role is in promoting vasoconstriction. Endothelin binds one of two receptors, $ET_A$ or $ET_B$.

Binding of ET to $ET_A$ has a potent vasoconstrictive effect, while binding of ET to $ET_B$ receptors produces a vasodilative effect by promoting the release of nitric oxide and other relaxing factors. Endothelin signaling plays an important role in mediating the blood pressure of the body [6]. In addition to its vital regulatory role in vascular homeostasis, ET signaling leads to the modulation of apoptosis and chemoresistance, cell growth and migration, neovascularization and angiogenesis as well as epithelial to mesenchymal transition [7]. Excessive ET signaling has also been implicated in tumorigenesis and inhibitors have been tested as anti-cancer drugs in a few cancers, including colorectal [8] and prostate cancer [9, 10]. Unlike VEGFR TKIs, endothelin antagonists are not regularly used in cancer treatment although one exploratory study in metastatic RCC patients indicates that combination therapy using the ET receptor antagonist atrasantan with interferon-α may provide a survival benefit over interferon-α alone [11]. However, interferon-α is no longer given as first- or second-line treatment for renal cell carcinoma. There is also recent evidence that endothelin signaling is involved in the side-effects patients experience while on other angiogenesis inhibitors [12]. More research into the antiangiogenic potential of endothelin inhibitors in cancer patients is therefore warranted. Currently, combination therapy for ccRCC is under-researched due to the fact that it can be difficult to optimize, especially because there are no preclinical ccRCC murine models available for drug testing. We have previously described a zebrafish model of *VHL* deficiency with quantifiable pathophysiological angiogenesis which responds to VEGFR TKI sunitinib [13]. This zebrafish model is -to the best of our knowledge- the only genetic animal model that manifests aberrant angiogenic sprouting with leaky vessels and allows fast, easy, and high-throughput screening of chemicals. This model allows us to test different therapies and quantify their effects on angiogenesis in a relevant *in vivo* environment. Here, we assess the effects of combination therapy of a VEGFR TKI, cediranib (also known as AZD2171), in combination with zibotentan (also known as ZD4054), a drug which inhibits the binding of ET to the ET receptor $ET_A$, on *vhl-/-* zebrafish (Figure 1B). Our results show that combination therapy decreases angiogenesis significantly at concentrations at which no toxicity is observed and where no significant effect is observed for either treatment alone. Further testing in an *in vitro* co-culture of human umbilical vein endothelial cells (HUVECs) with human pericytes to model human angiogenesis recapitulates this effect *in vitro*. We conclude that combination therapy may be a more effective alternative than treatment with individual drugs and show that zebrafish can be used alongside *in vitro* assays as a powerful model for developing anti-angiogenesis therapies *in vivo* and in higher throughput than in mammalian models.

## METHODS

**Danio rerio (Zebrafish) lines**

*vhl* mutant lines possessing the previously described [14] mutant *vhl* allele *vhl*$^{hu2117}$ were used for this study. We have crossed these zebrafish to *vhl*$^{hu2117}$ zebrafish with Tg(*kdrl*:GFP) to visualize the vasculature of the developing zebrafish [15]. Mutant *vhl* embryos were phenotyped according to previously established guidelines [13]. All embryos were confirmed by genotyping. For all drug experiments, embryos were treated at 3 days post-fertilization (dpf) because zebrafish vasculogenesis is complete at this time, ensuring that the drugs did not interfere with normal developmental process. Experiments were conducted in accordance with Dutch guidelines for the care and use of laboratory animals, with the approval of the Animal Experimentation Committee (DEC) of the Royal Netherlands Academy of Arts and Sciences (KNAW).



**Zebrafish drug treatments**

Stock solutions of both drugs (cediranib Cat# S1017 and zibotentan Cat# S1456, both from Seleckchem, 9330 Kirby Drive, STE 200, Houston, TX 77054 USA) were prepared by dissolving in dimethylsulfoxide (DMSO) and stored at -20 °C. The dose concentration range for zibotentan tested was 100, 40, 20, 10 and 5 nM, while the range for cediranib was 400, 200, 100, 50, 10 and 1 nM. A DMSO control group was also tested. Embryos were selected at 3 dpf phenotypically and placed into E3 medium containing the drug. Each drug concentration was administered to 4 phenotypically wild-type and 6 phenotypically mutant embryos per experiment (n=5). At 5 dpf embryos were examined for any anatomical or behavioral deficiencies. Based on our observations, the maximal non-toxic doses of cediranib and zibotentan were set at 20nM and 200nM, respectively.

In order to perform the angiogenesis assay, zebrafish embryos were treated with 20nM zibotentan and 200nM cediranib in the combination therapy group, or 20nM zibotentan or 200nM cediranib in each monotherapy group. A DMSO control group was also included (all groups received the same total volume of DMSO), along with an untreated control group and a small group of untreated sibling embryos for comparison. Embryos were selected based on phenotype at 3dpf. 10 mutant embryos were included in each experimental group and 5 untreated siblings were included in each experiment (n=5). Embryos were imaged by confocal microscope z-stacks without bias (blinded) and then genotyped before angiogenic sprouting was quantified.

**Confocal imaging of zebrafish intersomitic blood vessels**

Embryos were imaged with the 20x objective on a LSM700 confocal laser scanning microscope (Carl Zeiss AG, Carl-Zeiss-Straße 22, 73447 Oberkochen, Germany) at 5 dpf to examine the tail vasculature. Embryos were anesthetized with MS222 (final concentration 0.17 mg/ml) before imaging. Z-stacks were made of the zebrafish tail centered on the cloaca (Fig. 2), and sprouts from 10-12 vessels were counted per embryo. Zebrafish were then euthanized and collected for genotyping (see below). Z-stacks were converted into maximum-intensity projections using Zeiss Zen software to facilitate scoring.

**Genotyping vhl zebrafish embryos**

Collected *vhl* mutant zebrafish were genotyped by Sanger sequencing using the following primers: Forward: 5'- TAA GGG CTT AGC GCA TGT TC. Reverse: 5'-CGA GTT AAA CGC GTA GAT AG. Sequences were read using Chromas software (Technelysium Pty Ltd, Unit 701, 8 Cordelia St, South Brisbane QLD 4101, Australia) and examined for mutations described previously [16].

**Scoring and statistical analysis**

After genotyping, z-stacks of confirmed mutant embryo tails were scored for sprouting. Between 10-12 intersomitic blood vessels (ISVs) were counted per image using Image J. The total number of sprouts visible was then divided by the number of ISVs present in the image to produce an average number of sprouts per ISV. The mean ISV for each treatment group was calculated and compared by ANOVA using Graphpad Prism 6 (GraphPad Software, Inc. 7825 Fay Avenue, Suite 230, La Jolla, CA 92037 USA) Data are presented as mean ± SEM. P-values where $p<0.05$ are considered significant and represented with *.

**In vitro co-culture angiogenesis assay**

HUVECs (Lonza Group Ltd, Muenchensteinerstrasse 38, CH-4002 Basel, Switzerland) and Human Brain Vascular Pericytes (Cat#1200, Sciencell, 6076 Corte Del Cedro, Carlsbad, CA USA 92011) were cultured on gelatin-coated plates in EGM2 medium (Lonza Cat# cc-3156) and DMEM (10% FCS; Lonza), respectively, in 5% $CO_2$ at 37˚C. Lentiviral transfected HUVECs expressing green fluorescent protein (GFP) and pericytes expressing red fluorescent protein (RFP) were used between passage 6-8. HUVECs were transfected with siRNA at 100nM final concentration using DharmaFECT 1 transfection reagent (cat# T-2001, 2650 Crescent Dr, Lafayette, CO USA 80026). The following siRNAs were used: ON-TARGETplus non-targeting control pool (Cat# D-001810-10, Dharmacon) and si-human VHL silencer select pre-designed siRNA (Dharmacon, Cat# 4392420). Transfected HUVEC-GFP and Pericytes-dsRed were suspended in a 2 mg/ml collagen type I (BD Biosciences) as described by Stratman *et al* [17]. Co-cultures were imaged after 48h and

120h incubation in 5% $CO_2$ at 37˚C by fluorescence microscopy, followed by analysis using a commercial analysis system (Angiosys, Caltag Medsystems Ltd. Whiteleaf Business Centre 11 Little Balmer Buckingham UK MK18 1TF). Maximal non-toxic dosages were determined to be 200 nM zibotentan and 1nM cediranib based on toxicity and drug response. The co-culture experiment was performed in the same experimental groups as the zebrafish: DMSO control, untreated control, cediranib and zibotentan monotherapies and the combination therapy group. These treatments were performed on both siCtrl-treated and siVHL-treated co-cultures. Each experimental condition was performed in duplicate except for the untreated control group, which was performed in quadruplicate. Statistics were performed using Graphpad Prism 6 software.



## RESULTS

**Zebrafish ISV sprouting assay**

*vhl-/-* mutant zebrafish do not exhibit a vasculogenesis defect, but do manifest a marked increase in the number of blood vessels throughout the embryo [13]. Zooming in on the trunk of *vhl-/-* embryos, we observe aberrant but specific angiogenic sprouting which mainly eminates from the intersomitic vessels (ISVs). ISV sprouting is quantifiable as an *in vivo* assay for angiogenesis; aberrant sprouts are most prominent on the dorsal half of the embryo which are never observed in wild-type siblings (Figure 1A, Supplemental Figure 1). To address the hypothesis whether combination treatment of cedinranib and zibotentan might be effective as anti-angiogenic therapy (Figure 1B), we first tested the maximal non-toxic dose of cediranib and zibotentan separately in zebrafish embryos in a dose-response experiment. For all drug experiments, embryos were treated at 3 days post-fertilization (dpf) because zebrafish vasculogenesis is complete at this time, ensuring that the drugs did not interfere with normal developmental process. Zibotentan (100, 40, 20, 10 and 5 nM) or cediranib (400, 200, 100, 50, 10 and 1 nM) was administered to four phenotypically wild-type and 6 phenotypically mutant embryos per experiment (n=5). A DMSO control group was also tested for each concentration. At 5 dpf embryos were examined for any anatomical or behavioral deficiencies. The maximal non-toxic doses of cediranib and zibotentan were set at 20nM and 200nM, respectively, and no evident abnormalities were externally observed in the DMSO control group or when cediniranib (200nM) and zibotentan (20nM) were given together (not shown).

We next asked whether these concentrations of cediniranib (200nM) and zibotentan (20nM) had an effect on ISV sprouting in *vhl-/-* mutant embryos, either individually or in combination, as compared to DMSO treated controls. Images of embryos from an in-cross of *vhl*+/- adult fish with a Tg(*kdrl*:GFP) were taken without prior knowledge of the offspring genotype (blinded), and then euthanized and subjected to genotyping. Sprouts were counted

on each ISV fully visible in a z-stack of images centered on the cloaca of the zebrafish embryo (Figure 2A). Whereas neither cediniranib (200nM) and zibotentan (20nM) significantly decreased sprouting, combination therapy did significantly decrease the aberrant angiogenic sprouting in the *vhl* mutant embryos, (Figure 2B). Of note, none of the conditions affected the development of the parachordal vessel or vertebral artery which also happens in the 3-5 dpf time window.

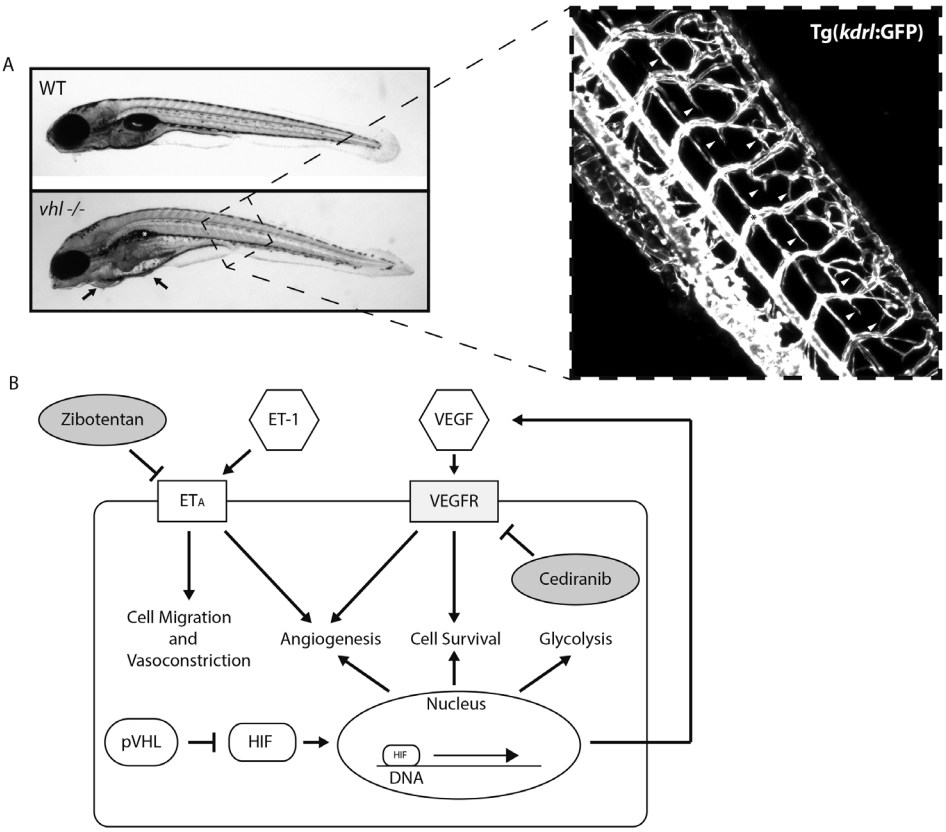


**Figure 1. *VHL* deficiency causes excessive angiogenic sprouting.** A*: vhl -/-* zebrafish embryos (lower image) display a visible phenotype which can be used to sort embryos without initial genotyping. Note bent body axis, edema, swim bladder deficiency (white asterisk), reduced pigmentation, an enlarged heart with visible polycythemia (arrows). The dashed box indicates the area of the zebrafish embryos which is imaged for angiogenesis assays (right insert, shows fluorescent image of GFP-labelled kdrl endothelial cell marker, Tg(*kdrl*:GFP). A representative z-stack maximum projection of this area is also shown. White arrowheads denote sprouts counted during the assay, but is not comprehensive for clarity's sake. Embryos are 5dpf, magnification is 10x, embryo anterior and ventral is to the left in image. B: schematic diagram representing the downstream effects of endothelin (ET-1), vascular endothelial growth factor (VEGF), and hypoxia-inducible factor (HIF) signaling. The diagram also indicates the inhibitory effects of Zibotentan and Cediranib used in this study on the endothelin A receptor ($ET_A$) and vascular endothelial growth factor (VEGF) receptor (VEGFR), respectively (shaded), as well as the von Hippel-Lindau tumor suppressor protein (pVHL).

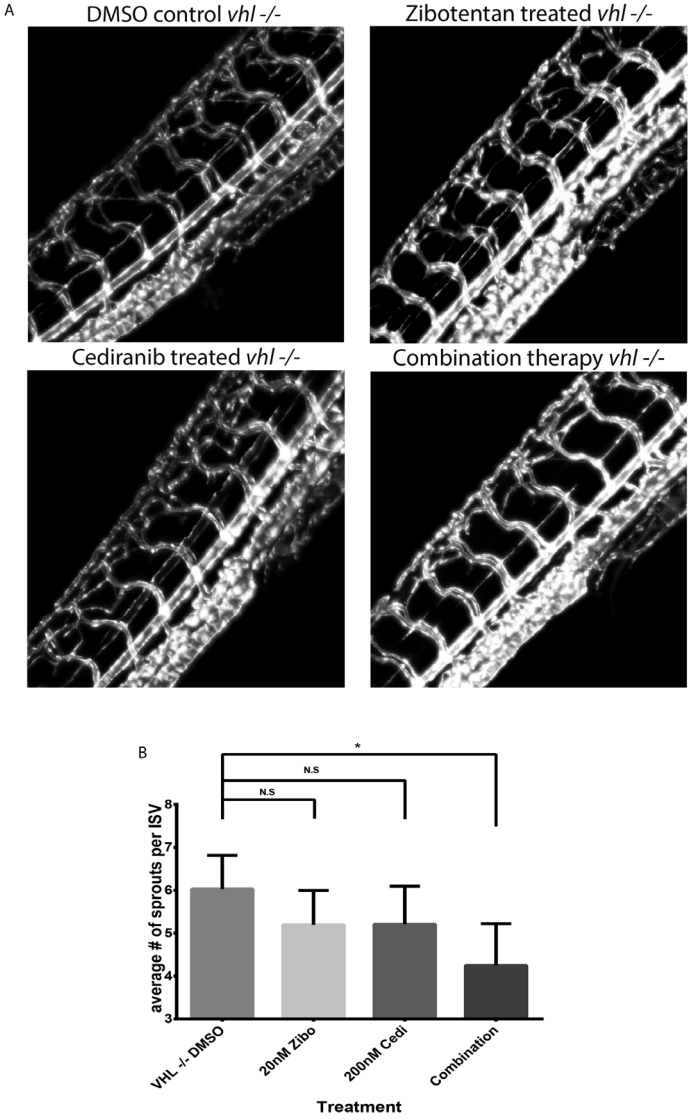


**Figure 2. Combination therapy reduces pathophysiological angiogenesis in a *Danio rerio* (zebrafish) model of *VHL* deficiency.** A: Representative images of *vhl-/-* zebrafish embryo tails (as shown in Fig. 1A) in each treatment group used for quantification of angiogenesis. B: Quantification of sprouting in the zebrafish angiogenesis assay. Untreated siblings (n=7; phenotypically normal *vhl+/-* or *+/+*) are included for reference, all other groups are *vhl-/-* mutants. The effect of combination therapy (n=12) is significantly different from DMSO treated mutant embryos (n=10; p<0.0001). Neither cediranib monotherapy (n=8; p=0.152) nor zibotentan monotherapy (n=9; p=0.115) significantly reduced sprouting. This experiment was repeated 4 times with 10 phenotypically mutant embryos in each treatment group and 5 untreated phenotypically wild-type sibling fish. The resulting images were scored for sprouting and then pooled based on genotype. Significance was determined by one-way ANOVA with Sidak's multiple comparison's test. Data is presented as mean+S.E.M. Embryos are all 5dpf, anterior and ventral is to the right in all images.

**In vitro co-culture angiogenesis assay**

To further investigate the effect these drugs have individually and in combination on vascular growth, we performed an *in vitro* neovascularization assay using human umbilical vascular endothelial cells (HUVECa) and pericytes in a co-culture assay (Figure 3A). To this end, we reduced endogenous levels of *VHL* in HUVEC cells by siRNA (siVHL or siControl) transfection (Supplemental Figure 2A) and co-cultured with pericytes, and measured the length and number of of tubules formed, as well as the propensity the tubules had to spout (junctions). We observed that siVHL significantly increased the number of junctions, sprouting events, and the length of the tubules (Figure 3B) in the co-culture assay. With this phenotype as a readout, we then treated siVHL or siControl co-cultures with either cediranib, zibotentan or a combination of both. A new dose-response curve had to be established for this assay, and we determined that cediranib (1nM) and zibotentan (200nM), were the highest tolerable concentrations not toxic to the cells. We observed that, similar to the zebrafish *in vivo* assay, combination therapy is more effective at reducing the number of junctions, the number of tubules and the total tubule length than either monotherapy at the same concentrations (Figure 3C). Cediranib also significantly reduced the total tubule length at the same concentration as the combination therapy (Figure 3C). The effect of the two drugs was determined to be additive by two-way ANOVA (data not shown). Cediranib had a greater effect than zibotentan, as can be seen by the significant effect on total tubule length, especially at higher concentrations (Supplemental Figure 2B). Maximal non-toxic zibotentan concentration was also much higher in the co-culture assay than in the zebrafish, while the effective cediranib concentration was much lower. These differences are probably due to underlying biological differences between the two models.

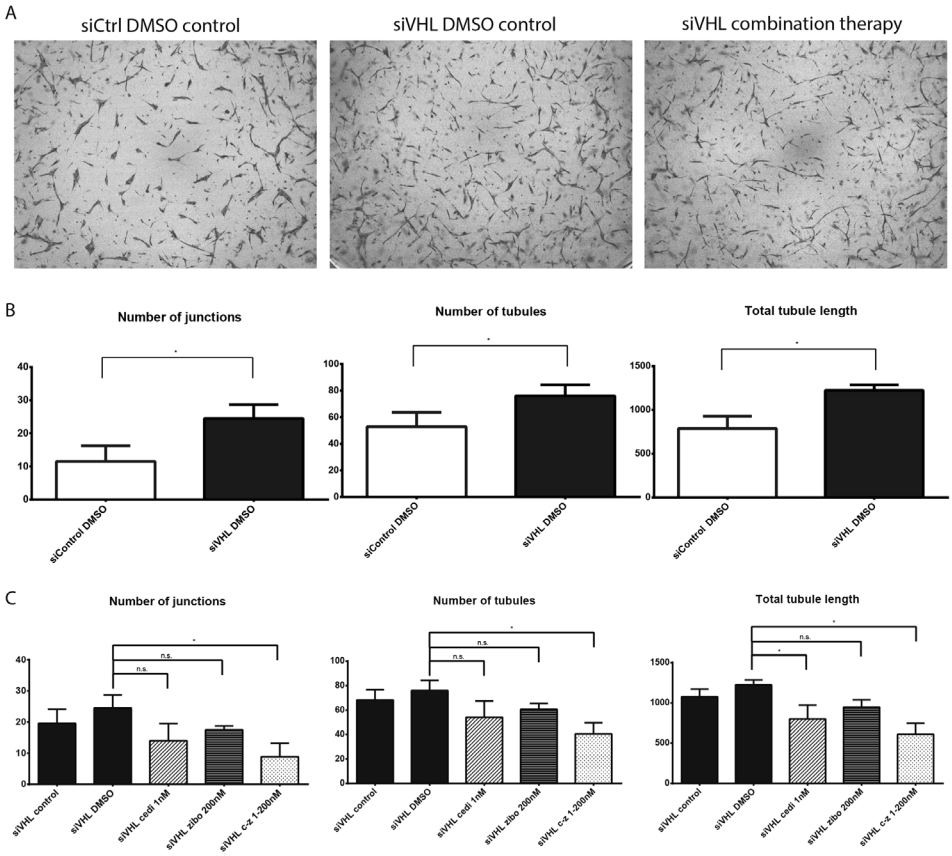


**Figure 3. Cediranib and Zibotentan combination therapy reduces angiogenic sprouting in an *in vitro* co-culture model** A: Representative images of selected conditions from co-culture of human vascular endothelial cells (HUVECs) with pericytes used for scoring after 5 days of co-culture. Note increased sprouting after treatment with siVHL (Supplemental Figure 2A) and reduced sprouting after treatment with combination therapy. N=2, in triplicate. B: Quantification of increase in number of junctions (p=0.015), number of tubules (p=0.002) and total tubule length (p=0.002) after treatment with siRNA against *VHL*. All changes were mathematically significant by student's T-Test ($p<0.05$). N=3, in triplicate. C: Quantification of the results of the co-culture angiogenesis assay. Numbers of junctions was significantly reduced by combination therapy (p=0.01) but not by cediranib (p=0.135) or zibotentan (p=0.0325) monotherapy. Number of tubules was similarly reduced significantly by combination therapy (p=0.002) but not by cediranib (p=0.066) or zibotentan (p=0.194) monotherapy. Total tubule length is significantly affected by both cediranib monotherapy (p=0.029) and combination therapy (p=0.001), although the effect of combination therapy is stronger. Zibotentan monotherapy did not significantly reduce total tubule length (p=0.115). n=6 for each monotherapy combination therapy, while n=12 for untreated controls. This experiment was repeated 3 times. Each condition was performed in duplicate except for untreated control which was performed in quadruplicate. Significance was determined by student's t-test using the Bonferroni correction for multiple comparisons. Data is presented as mean+S.E.M. Cedi, cediranib treatment; zibo, zibotentan; c-z; cediranib and zibotentan combination (DMSO concentrations equal in all conditions).

## DISCUSSION

Here we present two complementary models, one *in vitro* and one *in vivo*, in which the underlying biological efficacy of combination therapy can be tested for regulation of pathophysiological angiogenesis. We show that combination therapy can be effective in reducing angiogenesis at drug concentrations at which monotherapy has no effect and there is no evident increase in toxicity from combination therapy. The fish model is excellent for an *in vivo* screen for potent new combinatorial treatments, and is amenable to treatment matrices with different drugs. Exploring combination therapy read-out may be also relevant because patients may not develop resistance at the same rate as monotherapies because of the multiple overlapping concomitant drug strategies, although more research is needed to confirm this hypothesis. Unfortunately, our models are unsuitable to address the question of resistance. In addition, the co-culture model and the zebrafish model reacted differently in some ways to the drugs, especially zibotentan. The lower efficiency of zibotentan in the *in vitro* co-culture model is probably due to the underlying biology of endothelin signaling. Endothelin signaling involves feedback loops between the endothelial cells present in the assay and vascular smooth muscle cells, which are not included in the co-culture assay, but are present in the zebrafish, underscoring the value of *in vivo* modelling. Future versions of this co-culture drug assay could also include vascular smooth muscle cells in order to more accurately represent the *in vivo* action of processes such as endothelin signaling. However, the two models we have presented have the potential to be scaled up to allow for high-throughput screening of different combination therapies, which is not feasible in traditional mammalian models. This allows us to screen for promising combinations which can then be validated in other models for use in patients.

In addition to the suite of VEGFR TKIs available for first- or second-line systemic therapy for metastatic ccRCC, several other therapies have been tried with varying levels of success in ccRCC patients. Inhibitors of the mammalian target of rapamycin (mTOR) signaling pathway, such as everolimus, have been used to treat ccRCC [18-20]. Unlike more specific tyrosine kinase inhibitors, there is evidence that combination therapy combining lenvatinib with everolimus gives better results than everolimus alone and can improve outcomes even in patients who already display resistance to VEGFR TKI therapy, although more study is needed [21]. Cabozantinib is another inhibitor of tyrosine kinases including the MET pathway in addition to the VEGFR pathway. The recent METEOR phase-III trial showed its superiority in progression-free survival over everolimus in patients who have displayed progression of the disease after VEGFR tyrosine-kinase inhibitor treatment [22]. There is also evidence that immune system modulating treatments may be highly effective, especially as part of combination therapy [23]. The emerging evidence that different types of combination therapy may be effective for treating kidney cancer underlines its promise as

a treatment strategy while the previous failure of mTOR and VEGF inhibitor combination therapy after lengthy and expensive research emphasizes the need for a more convenient and powerful models to assess the feasibility of such treatments.

Here we have shown that zebrafish represent a promising model for this type of drug testing. Unlike typical mammalian models, such as mice, zebrafish are comparatively easy to genetically manipulate, develop rapidly and outside the body of the parent animal. Because of these features, development of phenotypes can be observed easily in a short period of time without any loss of adult animals. Zebrafish are lower vertebrates but despite this fact they possess many of the same genes and pathways as humans. This makes zebrafish models a convenient and powerful system for testing drugs, especially for testing new ways of using drugs which have already been approved for phase I trials [24]. Because the toxicity of these drugs is already known in humans, zebrafish can be used to quickly assess the feasibility of new treatment modalities, such as combination therapies, in order to quickly progress them to phase II. In this case, we have shown that zebrafish can be used to model pathophysiological angiogenesis caused by the same genetic dysfunction which causes the same phenotype in humans. By combining this zebrafish model with an *in vitro* model we can test the feasibility of different treatment regimens in comparatively less time. The *in vitro* model allows us to provide physiologically relevant human context to our *in vivo* zebrafish results. Different patients may have different responses to different drugs in a wide variety of combinations and sequences. Therefore, a large amount of data is needed to quickly assess the viability of different regimens before further work on personalized medicine is initiated. Higher throughput models, such as those used in this study, can provide the data necessary to tailor treatments to patients and lead to the development of treatments with improved outcomes.



**Acknowledgements**

The Cell Microscopy Center at the UMC Utrecht and the zebrafish facility at the Hubrecht institute provided expert services. We are grateful for technical support from Zhiyong Lei (Experimental Cardiology, UMC Utrecht).

**Competing Interests**

The authors declare no competing or financial interests.

**Author contributions**

TDK performed zebrafish experiments, performed data analysis and wrote the manuscript. MB performed and interpreted the co-culture experiments and contributed to the manuscript. DV and EvR performed, interpreted and analyzed the data from initial zebrafish

pilot experiments. RHG, GG, CLC, MCV, NVK conceived of experiments and supervised work. All authors discussed and reviewed the manuscript.

**Funding**
This work was supported by the European Union FP7/2009 Consortia "SYSCILIA" [grant number 241955 to RHG] and "EURenOmics" [grant number 305608 to RHG and NK]; the Dutch Kidney Foundation "KOUNCIL" [CP11.18 to RHG and NK].

## REFERENCES


1. Hoeben, A., et al., *Vascular endothelial growth factor and angiogenesis.* Pharmacol Rev, 2004. **56**(4): p. 549-80.
2. Giles, R.H., et al., *Interplay between VHL/HIF1alpha and Wnt/beta-catenin pathways during colorectal tumorigenesis.* Oncogene, 2006. **25**(21): p. 3065-70.
3. Powles, T., et al., *European Association of Urology Guidelines for Clear Cell Renal Cancers That Are Resistant to Vascular Endothelial Growth Factor Receptor-Targeted Therapy.* Eur Urol, 2016.
4. Ravaud, A., et al., *VEGFR TKI 'resistance' or transient clinical insensitivity to VEGFR TKI in metastatic renal cell carcinoma.* Ann Oncol, 2010. **21**(2): p. 431-2.
5. *FDA Approves Drug Combo for Kidney Cancer.* Cancer Discov, 2016. **6**(7): p. 687-8.
6. Hynynen, M.M. and R.A. Khalil, *The vascular endothelin system in hypertension--recent patents and discoveries.* Recent Pat Cardiovasc Drug Discov, 2006. **1**(1): p. 95-108.
7. Rosano, L., F. Spinella, and A. Bagnato, *Endothelin 1 in cancer: biological implications and therapeutic opportunities.* Nat Rev Cancer, 2013. **13**(9): p. 637-51.
8. Haque, S.U., et al., *Efficacy of the specific endothelin a receptor antagonist zibotentan (ZD4054) in colorectal cancer: a preclinical study.* Mol Cancer Ther, 2013. **12**(8): p. 1556-67.
9. Quinn, D.I., et al., *Docetaxel and atrasentan versus docetaxel and placebo for men with advanced castration-resistant prostate cancer (SWOG S0421): a randomised phase 3 trial.* Lancet Oncol, 2013. **14**(9): p. 893-900.
10. Fizazi, K., et al., *Phase III, randomized, placebo-controlled study of docetaxel in combination with zibotentan in patients with metastatic castration-resistant prostate cancer.* J Clin Oncol, 2013. **31**(14): p. 1740-7.
11. Groenewegen, G., et al., *Targeting the endothelin axis with atrasentan, in combination with IFN-alpha, in metastatic renal cell carcinoma.* Br J Cancer, 2012. **106**(2): p. 284-9.
12. Lankhorst, S., A.H. Danser, and A.H. van den Meiracker, *Endothelin-1 and antiangiogenesis.* Am J Physiol Regul Integr Comp Physiol, 2016. **310**(3): p. R230-4.
13. van Rooijen, E., et al., *von Hippel-Lindau tumor suppressor mutants faithfully model pathological hypoxia-driven angiogenesis and vascular retinopathies in zebrafish.* Dis Model Mech, 2010. **3**(5-6): p. 343-53.
14. van Rooijen, E., et al., *Zebrafish mutants in the von Hippel-Lindau tumor suppressor display a hypoxic response and recapitulate key aspects of Chuvash polycythemia.* Blood, 2009. **113**(25): p. 6449-60.
15. Bussmann, J., et al., *Zebrafish VEGF receptors: a guideline to nomenclature.* PLoS Genet, 2008. **4**(5): p. e1000064.
16. van Rooijen, E., et al., *A zebrafish model for VHL and hypoxia signaling.* Methods Cell Biol, 2011. **105**: p. 163-90.
17. Stratman, A.N., et al., *Pericyte recruitment during vasculogenic tube assembly stimulates endothelial basement membrane matrix formation.* Blood, 2009. **114**(24): p. 5091-101.
18. Hainsworth, J.D., et al., *Phase II trial of bevacizumab and everolimus in patients with advanced renal cell carcinoma.* J Clin Oncol, 2010. **28**(13): p. 2131-6.
19. Logan, J.E., et al., *Systemic therapy for metastatic renal cell carcinoma: a review and update.* Rev Urol, 2012. **14**(3-4): p. 65-78.
20. Motzer, R.J., et al., *Efficacy of everolimus in advanced renal cell carcinoma: a double-blind, randomised, placebo-controlled phase III trial.* Lancet, 2008. **372**(9637): p. 449-56.
21. Motzer, R.J., et al., *Lenvatinib, everolimus, and the combination in patients with metastatic renal cell carcinoma: a randomised, phase 2, open-label, multicentre trial.* Lancet Oncol, 2015. **16**(15): p. 1473-82.
22. Choueiri, T.K., et al., *Cabozantinib versus everolimus in advanced renal cell carcinoma (METEOR): final results from a randomised, open-label, phase 3 trial.* Lancet Oncol, 2016. **17**(7): p. 917-27.
23. Albiges, L., et al., *Efficacy of targeted therapies after PD-1/PD-L1 blockade in metastatic renal cell carcinoma.* Eur J Cancer, 2015. **51**(17): p. 2580-6.
24. Cutler, C., et al., *Prostaglandin-modulated umbilical cord blood hematopoietic stem cell transplantation.* Blood, 2013. **122**(17): p. 3074-81.

## SUPPLEMENTAL

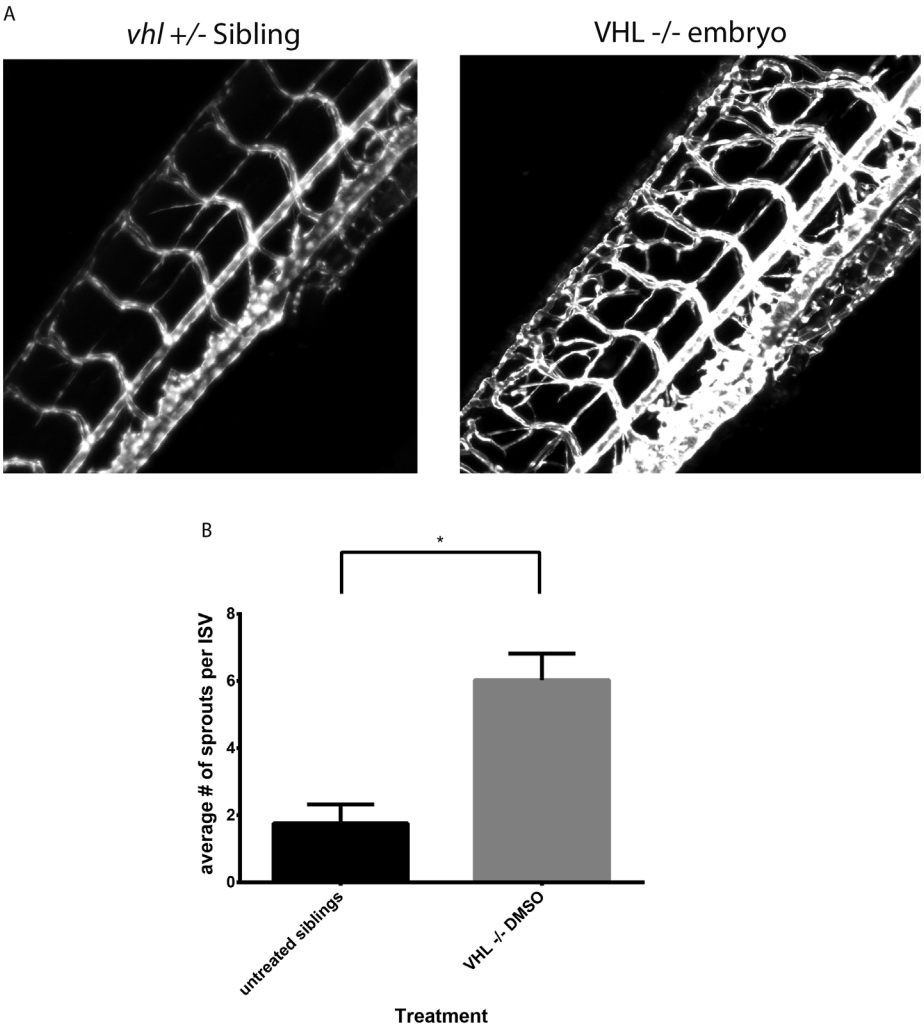


**Supplemental Figure 1.** *vhl-/-* mutant zebrafish embryos display an increased angiogenic response compared to phenotypically normal *vhl+/-* or *+/+* clutch siblings. A: Confocal analysis of the trunk vasculature in Tg(*kdrl:gfp*) embryos at 5dpf, anterior and ventral are to the right in these images. B: Quantification of the sprouts from the intersomitic vessels. n=8 animals per condition, *p<0.001, error bars show SEM.

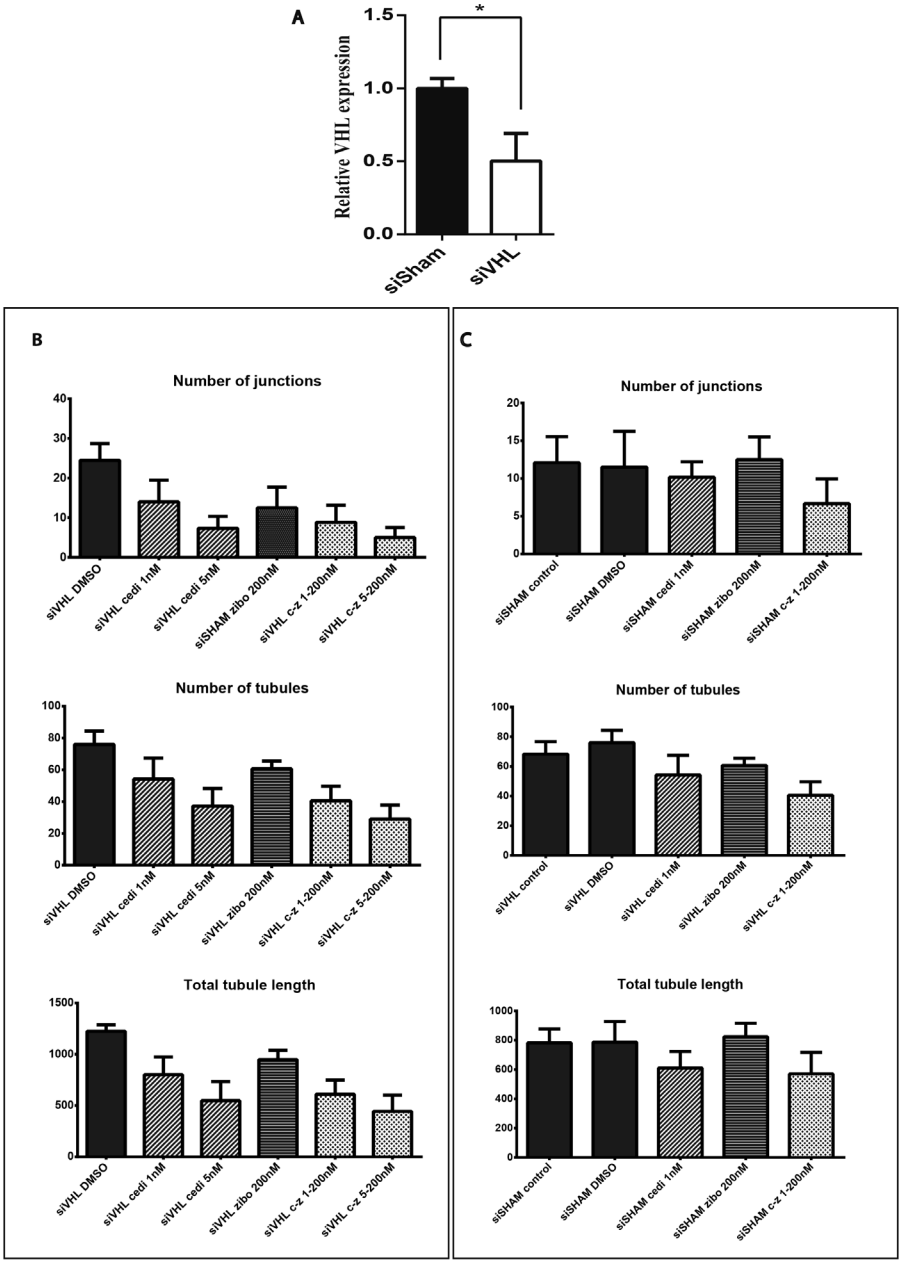


**Supplemental Figure 2. Quantification of remaining data from the co-culture assay** A: Effect of different concentrations of the two drugs on angiogenesis. B: Effect of the drug treatments on DMSO treated control cells treated with siCtrl. Cedi, cediranib treatment; zibo, zibotentan; c-z; cediranib and zibotentan combination. DMSO levels were identical in all experimental conditions.

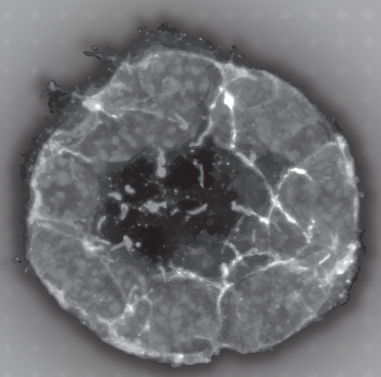

# CHAPTER 5

# Inhibition of miRNA-132/212 Suppresses VHL-Regulated Pathophysiological Angiogenesis

Manuscript submitted

Lei Z*, **Klasson TD***, Brandt MM, van de Hoek G, Logister I, Cheng C, Doevendans PAF, Sluijter JPG*, Giles RH*

*these authors contributed to this work equally

## ABSTRACT

**Objective**

Clear cell renal cell carcinoma (ccRCC) is the most common form of sporadic and inherited kidney cancer, both of which are highly associated with biallelic mutations in the *von Hippel-Lindau* (*VHL*) tumor suppressor gene and an activated PI3k-AKT pathway. Although upregulation of the miR-212/132 and disturbed VHL signaling have both been linked with pathogenic angiogenesis, no evidence of a possible connection between the two has yet been made.

**Approach and Results**

We show that miRNA132/212 levels are increased after loss of functional pVHL, the protein product of the *VHL* gene, *in vivo* and *in vitro*. We also show that PTEN levels are downregulated in models lacking endogenous *VHL* or after *VHL* knockdown in wild-type cells, at least partially due to the action of miRNA132/212. Furthermore, we show that blocking miRNA132/212 with anti-miRs can significantly alleviate the excessive vascular branching phenotype characteristic of *vhl*$^{-/-}$ mutant zebrafish. Moreover, using human umbilical vascular endothelial cells (HUVECs) and an endothelial cell/pericyte coculture system, we observed that *VHL* knockdown promotes endothelial cells' neovascularization capacity *in vitro*, an effect which can be inhibited by anti-miR-212/132 treatment.

**Conclusions**

Taken together, our results demonstrate an important role for miRNA132/212 in angiogenesis induced by loss of VHL and suggest an interesting opportunity for pharmaceutical intervention using an inhibitor of miR-212/132 to inhibit tumor growth for ccRCC patients.


**Abbreviations**

| | |
|---|---|
| ccRCC | Clear cell renal cell carcinoma |
| VHL | von Hippel-Lindau |
| pVHL | The protein product of the von Hippel-Lindau gene |
| HIF | Hypoxia-Inducible Factor |
| CREB | cAMP response element binding protein |
| PTEN | phosphatase and tensin Homologue |
| dpf | days post fertilization |
| HUVEC | human umbilical vascular endothelial cells |

## INTRODUCTION

Clear cell renal cell carcinoma (ccRCC), the most common form of sporadic and inherited kidney cancer, is highly associated with mutations in the von Hippel-Lindau (*VHL*) gene. [1, 2] The protein product of the *VHL* gene (pVHL) is an E3 ubiquitin ligase involved in the degradation of hypoxia-inducible transcription factor subunits (HIFα). Under normal oxygen tension, hydroxylated HIFα can be recognized by a ubiquitin ligase complex containing pVHL and rapidly degraded. Upon hypoxia or loss of functional pVHL, HIFα-subunits can no longer be hydroxylated and begin to accumulate. Stabilized HIFα activates the expression of a large suite of downstream target genes (*EPO*, *VEGF* etc), the actions of which are vital to promote angiogenesis. However, many of the changes initiated by the stabilization of HIFα, such as increased angiogenesis, an upregulation of anti-apoptotic signaling and a shift to anaerobic glycolosis, can contribute to tumor growth and survival. People born with a mutation in one *VHL* allele will acquire somatic mutations in the second allele, resulting in consequent angiogenic symptoms and a variety of tumors, including ccRCC [3]. Another hallmark of ccRCC is activated PI3k/AKT pathway signaling, higher levels of which is significantly correlated with a worse survival rate[2], although the mechanism by which this occurs is still not fully understood.

MicroRNAs (miRNAs) are small non-coding RNAs that post-transcriptionally regulate the expression of groups of target genes by inhibition of the translation of their targeting messenger RNAs (mRNAs) or marking these mRNAs for degradation. miRNAs are key regulators in many physiological and pathological processes [4], including the dynamic regulation of ccRCC during tumor progression[2]. By promoting the expression of vascular endothelial growth factor (*VEGF*), VHL/HIF signaling increases cAMP response element binding protein (CREB) levels, a transcription factor which upregulates the expression of pro-angiogenic miR-212/132 [5]. This implies that pVHL loss-of-function would stimulate miR-212/132 expression and thereby contribute to excessive angiogenesis. In this study, using a combination of cellular models, patient ccRCC material with biallelic loss of *VHL* and a previously described *vhl*$^{-/-}$ mutant zebrafish model, we show that miR-212/132 is upregulated after *VHL* knockdown or mutation and that this upregulation is at least partially responsible for increased angiogenesis, possibly by targeting phosphatase and tensin homolog (*PTEN)*. A scarcity of functional pVHL induces excessive vascular outgrowth which can be inhibited by pharmaceutical inhibition of miR-212/132, thereby providing an exciting potential therapy target for reducing the growth and burden of tumors associated with *VHL* mutations.

## MATERIALS AND METHODS

Materials and Methods are available in the online-only data supplement.

## RESULTS

We first examined the expression of miR-132 in relation to VHL loss-of-function and (pseudo)-hypoxia signaling. We found that endothelial cells grown in hypoxic conditions display significantly elevated levels of miR-132 expression (Figure 1.A). We observe similar effects in HUVECs transfected with siRNA targeting *VHL* mRNA relative to those treated with non-targeting siRNA (Figure 1.B). To confirm the effect *in vivo,* we used a previously established zebrafish model of *VHL* deficiency [6-8]. miR-212/132 are well conserved in most species, including zebrafish (Supplementary Figure 1.A). Like our cell models, *vhl*$^{-/-}$ zebrafish also show an increased level of expression of miR-132 (Figure 1.C). In isogenic cell lines taken from human ccRCC *VHL*$^{-/-}$ tumors, the expression of miR-132 is reduced upon *VHL* reconstitution with ectopic *VHL* (Figure 1.D). Lastly, we examined miR-132 expression in histology slides taken from ccRCC tumors using microRNA *in situ* hybridization. In agreement with our previous qPCR results, we observed widespread overexpression of miR-132 in tumor material from ccRCC samples with biallelic *VHL* mutations proven by sequencing (Figure 1.E). These results demonstrate that miR-212/132 are increased in response to the (pseudo-)hypoxia induced by the lack of functional pVHL which eventually leads to overexpression of miR-212/132.

To assess the functional consequences of miR-212/132 expression in a *VHL*-null environment, we used an *in vitro* co-culture assay designed to gauge angiogenesis. In agreement with the important role of VHL in HIFa degradation, knockdown of VHL in HUVEC/pericyte coculture shows significantly more vascular junctions, tubule number, and total tubular length as compared to siSham control treatment (Figure 2.A-C). To evaluate whether the pro-angiogenic effects of *VHL* silencing are mediated by a downstream increase in miR-212/132, GFP-labelled HUVECs were treated with anti-miRs against miR-212/132 in combination with siRNA targeting *VHL*. Inhibiting the action of miR-212/132 reduced the excessive angiogenesic response induced by the silencing of *VHL* significantly (Figure 2.D), suggesting that VHL-regulated angiogenesis is at least partially mediated by the upregulation of miR-212/132.

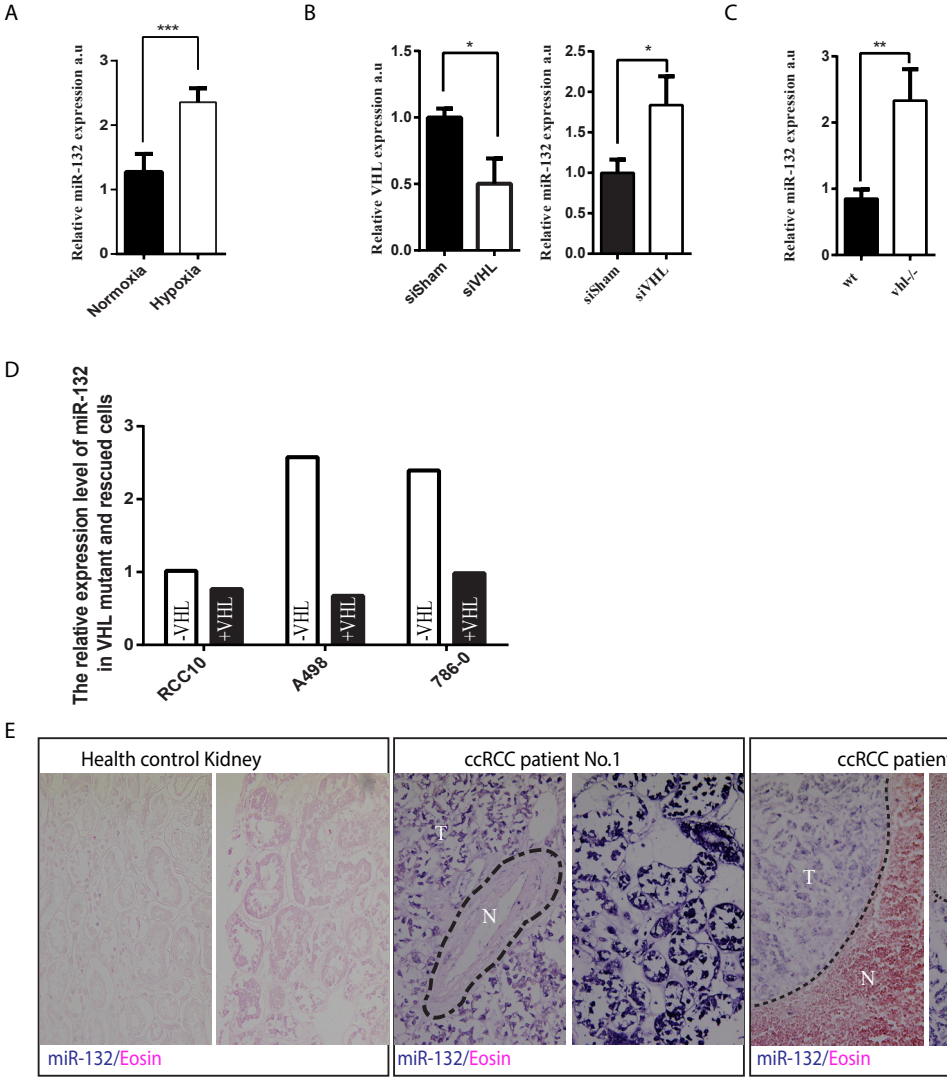


**Figure 1.** Characterization of miR-132 expression under hypoxic and pseudo-hypoxic conditions. **A.** The expression of miR-132 in HUVECs cells under normoxia and hypoxia as compared by qPCR. **B.** The expression of miR-132 in siSham and siVHL transfected HUVECs as compared by qPCR. **C.** The expression of miR-132 in WT and vhl-/- mutant zebra_sh as compared by qPCR. **D.** The expression of miR-132 in established VHL-/- lines RCC10, A498 and 786-0 as well as the same lines reconstituted with ectopic VHL. **E.** The expression of miR-132 in healthy kidney tissue and ccRCC from two patients with known bilateral VHL mutations in their tumor as shown by miR-132 in situ hybridization. miR-132 in situ in purple blue. Light eosin counterstaining appears pink. Dashed line in Patient 2 indicates normal parenchyma (N) vs ccRCC tumor

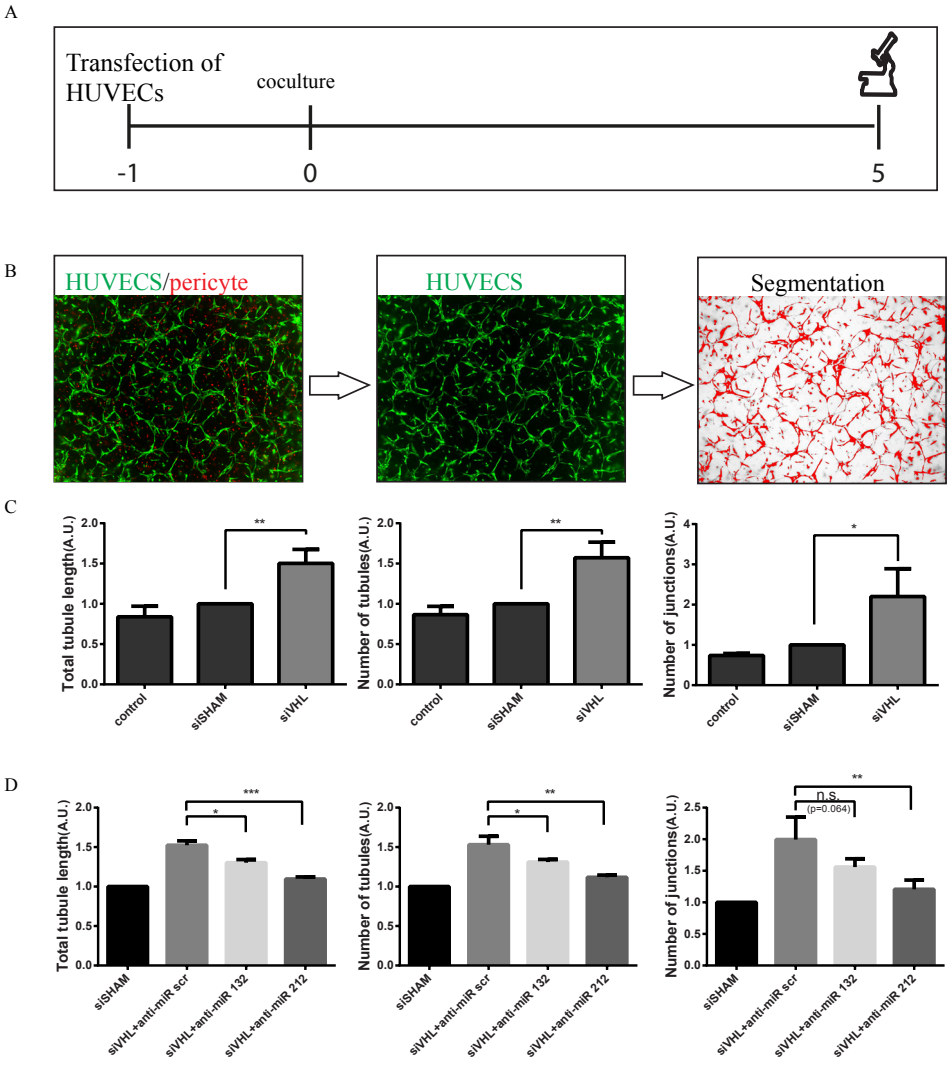


**Figure 2.** Reduced levels of VHL enhances endothelial cell neovascularization capacity and can be inhibited by blocking miR-132 or miR-212.
**A.** Schematic outline of the coculture experiment with HUVECs and pericytes. **B.** Schematic cartoon showing the analysis process of tubular structures in the endothelial cells and pericytes coculture assay. **C.** VHL siRNA knockdown in HUVECs enhances endothelial cell neovascularization capacity. **D.** Blocking miR-132/212 inhibits VHL-induced neovascularization enhancement.

*vhl*$^{-/-}$ zebrafish embryos display a phenotype of post-vascularization branching/sprouting around the intersomitic vessels. Counting these sprouts is a quantitative measure of angiogenesis in zebrafish [7]. *vhl*$^{-/-}$ zebrafish were injected at a one-cell stage with anti-miRs directed against miR-132 or miR-212 and four days later tails of the living fish were imaged with a confocal microscope (Figure 3.A). The cloaca of the zebrafish is placed in the center of the image and the branches sprouting from the inter-somitic vessels were counted for the four vessels anterior and the four vessels posterior to the cloaca (Figure 3.B). Anti-miR injections against miR-212/132 significantly reduced the extent of inter-somitic vessel sprouting in *vhl*$^{-/-}$ fish (Figure 3.C-D). In addition, injecting wild-type zebrafish with miRNA132/212 mimics partially recapitulated the *vhl* mutant vessel sprouting phenotype (supplemental figure B,C).



Therefore, in light of the fact that miR-212/132 expression is linked to vessel sprouting in *vhl*$^{-/-}$ zebrafish, which phenocopies zebrafish with loss of both *ptena* and *ptenb* [9], we proceeded to look at the expression of PTEN in our VHL-null models. PTEN, a phosphatidylinositol-3,4,5-trisphosphate 3-phosphatase, antagonizes the activity of phosphatidylinositol-4,5-bisphosphate 3-kinase (PI3K), suppressing cellular proliferation, cell survival and angiogenesis by inactivating the PI3K-driven AKT signaling pathway [10]. *PTEN* has been predicted to be a potential target of miR-212/132 in humans by targetscan (Figure 4.A) and the rat homologue of *PTEN* has been shown to be targeted by miR-212/132 in rat vascular smooth muscle cells [11]. Moreover, downregulation of PTEN has been significantly correlated with lower survival rate in ccRCC patients [2]. We reasoned that upregulated miR-212/132 upon mutation or silencing of *VHL* could result in the subsequent reduction of PTEN. We therefore first looked at the regulation of PTEN in *vhl*$^{-/-}$ zebrafish and in HUVECs after knockdown of *VHL*. Zebrafish, as opposed to mammals, have two copies of the *pten* gene: *ptena* and *ptenb. ptenb* is a predicted target of miRNA132/212 in targetscan, but not *ptena* (Figure 4.B). Accordingly, we found significantly reduced *ptenb* expression in *vhl*$^{-/-}$ zebrafish with no significant changes observed in *ptena* (Figure 4.C). In HUVECs, overexpression of miR-132 or miR-212 combined with *VHL* knockdown caused a reduction in PTEN mRNA (Figure 4.D) and protein levels (Figure 4.E-F) showing that PTEN is indeed targeted by miR-212/132 in our *in vitro* as well as *in vivo* models.

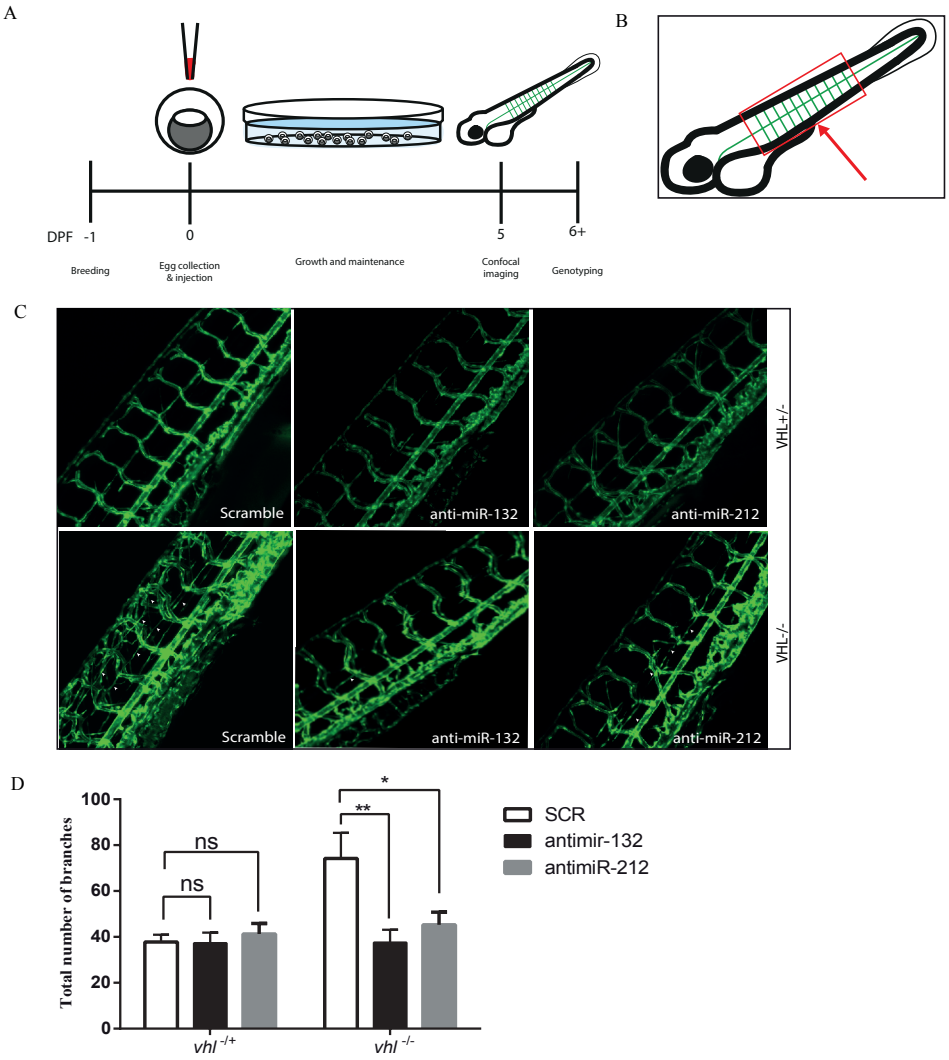


**Figure 3.** Overexpression of miR-132 induces vasculature outgrowth in wildtype zebra_sh
**A.** Schematic outline of the zebra_sh embryo microinjection experiment. microRNA mimics and antimiRs are injected into the yolk of the eggs on day 0 and imaged with a confocal microscope on day 5. **B.** Schematic cartoon showing the area of the zebra_sh embryo that is imaged after microinjection. The cloaca is marked with a red arrow. The imaging area is shown with a red box. The vessels of the tail are shown in green. **C.** Representative images of zebra_sh tail vascular structures in vhl+/- and vhl-/- zebra_sh after injection with scrambled or miR-132, miR-212 inhibitors. White arrows designate examples of structures which have been scored as branches. **D.** Quanti_cation of vascular branching in zebra_sh tail structures after injection with scrambled control inhibitors, miR-132 inhibitors or miR-212 inhibitors.

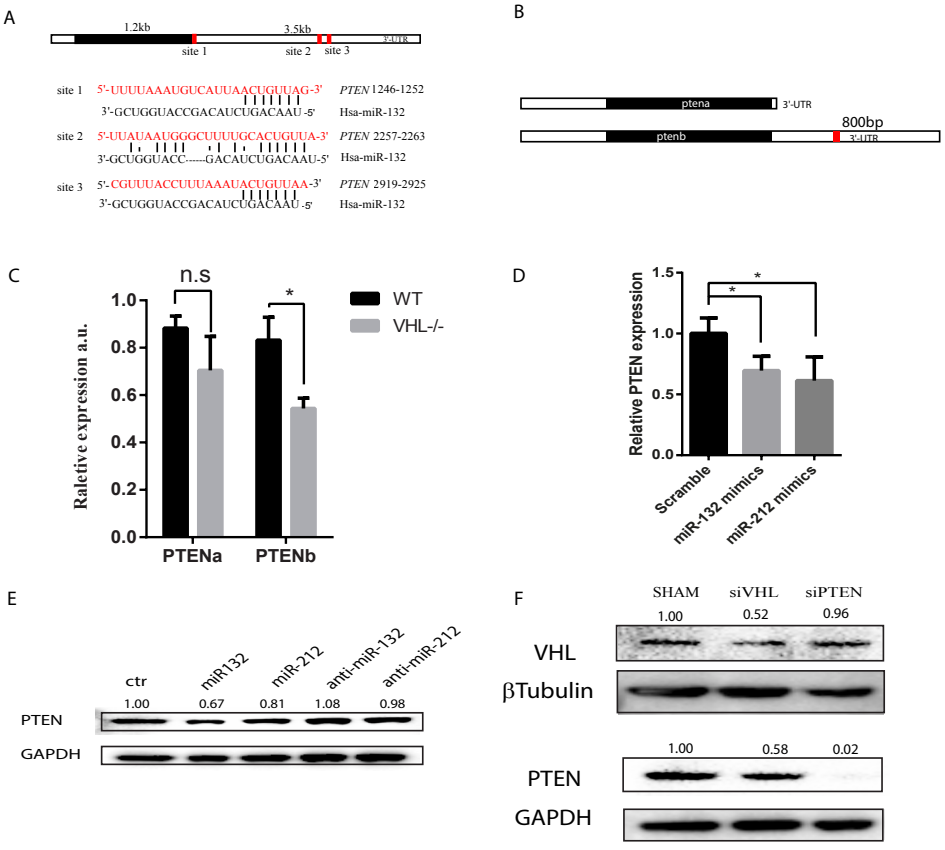


**Figure 4.** PTEN is a potential target of miR-132/212
**A.** Three predicted miR-132 target sites of PTEN predicted by Targetscan in human. Target sites and sequences are shown in red. **B.** The position of predicted miR-132 targets on zebra_sh orthologues ptena and ptenb by Targetscan. Note only ptenb has a predicted miR-132 targeting site on the 3'-UTR (red). **C.** The expression levels of ptena and ptenb in WT and vhl-/- zebra_sh determined by qPCR. **D.** PTEN mRNA expression after miR-132 and miR-212 overexpression in HUVECs determined by qPCR. **E.** PTEN protein levels after miR-132 and miR-212 overexpression and inhibition in HUVECs. The numbers above the bands indicate the relative expression compared with the control band, normalized by GAPDH. **F.** PTEN and VHL protein levels in HUVECs after transfection with scrambled control siRNA, siRNA targeting VHL and siRNA targeting PTEN. The numbers above the bands indicate the relative expression compared with the control band, normaled by GAPDH.

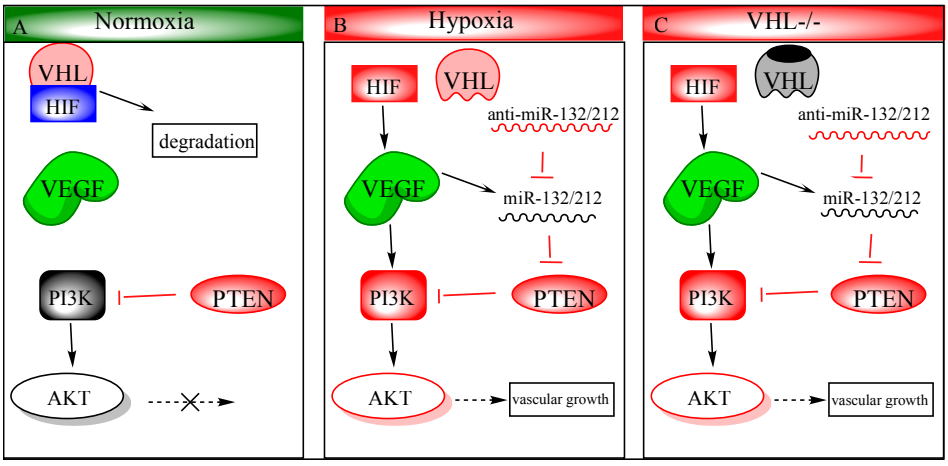


**Figure 5.** Proposed mechanism of miR-132/212 in modulation of VHL/PI3K/AKT pathways.
**A.** During normoxia, HIF_ is ubiquitinated by the VHL-ubiquinition complex, targeting it for degradation. PTEN antagonizes PI3K to prevent AKT from being activated. **B.** Upon hypoxia, HIF_ can no longer be hydroxylated, which prohibits VHL-regulated degradation, and allows stabilized HIF_ to translocate to the nucleus upregulate its downstream targets such as VEGF. VEGF in turn activates PI3K-AKT pathway and upreguates miR-132/212 expression as well. Upregulated miR-132/212 inhibits PTEN expression which in turn prolongs AKT activity. **C.** VHL loss-of-function phenocopies hypoxic conditions even in the presence of oxygen (pseudo-hypoxia).

## DISCUSSION

In this study we used patient material, human cells and zebrafish to examine the role of the miRNA132/212 family in the pathophysiology of neovascularization caused by the loss of functional pVHL. We observed that miR-212/132 is upregulated in response to *VHL* mutation both in zebrafish model systems and in human patient ccRCC tumor material carrying biallelic inactivating *VHL* mutations. We demonstrated that the excessive angiogenesis attributable to *VHL* mutation is strongly affected by miRNA132/212. Indeed, targeting these miRNAs with anti-miRs can significantly reduce angiogenesis in both *in vitro* and *in vivo* models of *VHL* deficiency. We identified the tumor suppressor PTEN as one of the targets affected by miRNA132/212 in *VHL*-null models. Taken together, our results implicate miRNA132/212 as an important intermediate in pathological angiogenesis after loss of functional pVHL or tissue hypoxia. In addition, the effects of miRNA132/212 on *PTEN* suggest a possible role for these miRNAs in tumorigenesis.

The miRNA132/212 family is clustered in the genome and is highly conserved in vertebrates. miR-212/132 are initially expressed as one primary miRNA and then processed into two mature miRNA with the same target-defining “seed” sequence [12]. This miRNA family plays a number of roles in the promotion of angiogenesis. Mice without functional miR-

212/132 show impaired arteriogenesis response after hindlimb ischemia [13]. The pro-angiogenic potential of miR-132 has been used to increase angiogenesis in endothelial cell grafts and after ischemic injury [14]. miR-212/132 frequently act as a promoter of cell proliferation and increases in their expression levels have also been suggested as contributors to tumorigenesis in addition to their angiogenic role. miR-132 has previously been shown to induce pathological neovascularization in the endothelium by targeting p120 Ras GTPase activating protein [5]. In addition, anti-miR-132 has also been shown to reduce tumor burden in a mouse xenograft model of human breast carcinoma [5].

This study supports the previously reported role of miRNA132/212 in pathophysiological angiogenesis and expands upon its role in the context of VHL-regulated hypoxia signaling. When VHL is mutated or downregulated, miRNA132/212 and PI3K are consequently upregulated. miR-212/132 targeting of *PTEN* mRNA ensures that PI3K has a chance to activate AKT (Figure 5). Uncontrolled proliferation and angiogenesis are hallmarks of cancer and many tumors contain mutations leading to hyperactivation of the RAS or AKT signaling networks which act to promote these processes[15-17]. Differential expression of miRNA has been previously reported in tumors including ccRCC [18] and is widely believed to be an important player in tumorigenesis [19-21]. miR132/212 is therefore an interesting potential target for the treatment of cancer.

In human patients, ccRCC is almost always associated with *VHL* mutations. However, von Hippel-Lindau patients born with a single germline mutation in *VHL* initially develop non-cancerous cysts in the kidney and do not develop ccRCC until around 35 years of age on average[22]. In addition, mouse models with *Vhl* mutations do not develop renal tumors[23]. In contrast, zebrafish *vhl* mutants develop dysplastic lesions within 6 days post fertilization (dpf) (citation #8 goes here) . Therefore it is believed that *VHL* mutations in mammals create a pre-cancerous cystic phenotype but an additional mutation to another ancillary oncogene is required before tumor formation[24]. Although the recently developed *Vhl* mutant mouse with heterozygous mutations in BRCA1 associated protein 1 (*Bap1*) is perhaps the most physiologically relevant mouse model of human ccRCC [25], *Pten* $^{-/-}$ *Vhl* $^{-/-}$ double mutant mice develop benign squamous metaplasia and cystadenoma [24] and display kidney cysts that are very similar to those taken from the kidneys of human VHL patients, implying that activation of the AKT signaling pathway is important in the development of pre-cancerous cysts. Indeed, cysts taken from VHL patients display hyper-activation of PI3K signaling [24]. miR-212/132 mediated reduction of PTEN, which is an important suppressor of the PI3K/AKT pathway, may at least partially explain this expression pattern. In addition, biallelic *PTEN* mutations are rare in ccRCC [26, 27] but loss of a single *PTEN* allele through mutation is not uncommon [28]. miR-212/132 expression may be the reason that this is sufficient to cause hyper-activation of AKT signaling despite the presence of a functional PTEN allele. Hyper-activation of AKT

signaling and loss of *PTEN* are common in many other tumor types because tumor growth requires angiogenesis. Thus, miR-212/132 expression may fulfill an important role in the development of ccRCC tumors.

One of the hallmarks of ccRCC is resistance to cytotoxic treatment. Anti-apoptotic signaling is upregulated after HIFα hyper-stabilization in ccRCC tumors. Many experimental treatments focus on inhibiting the action of downstream anti-apoptosis proteins such as mammalian target of rapamycin (mTOR), an important pro-survival protein induced by activated AKT signaling [29]. Our results and the results of other studies suggest that miR-212/132 may act as a promoter of tumorigenesis by targeting inhibitors of proliferation, survival and angiogenesis presenting an interesting opportunity for pharmaceutical intervention. Treatments which inhibit the action of miR-212/132 might therefore be a useful method to inhibit tumor growth by targeting angiogenesis and increase the sensitization of tumors to apoptotic signaling, increasing the effectiveness of cytotoxic therapies for ccRCC.

**Acknowledgements**

Z.L., T. K., J. S. and R.G. conceived and designed the experiments. **:** T. K., Z.L., M. B. performed the experiments. T. K., Z.L., and M.B. analysed the data. T. K., Z.L., J. S. and R.G. wrote the paper.

**Sources of Funding**

This research forms part of the Project P1.05 LUST of the research program of the BioMedical Materials institute, co-funded by the Dutch Ministry of Economic Affairs. We furthermore acknowledge the financial support of the European Community's Seventh Framework Programme FP7 under grant agreement numbers 305608 (EURONOMICS) and 241955 (SYSCILIA), the Dutch Kidney Foundation Consortium CP11.18 "KOUNCIL", and the Netherlands CardioVascular Research Initiative (CVON): the Dutch Heart Foundation, Dutch Federation of University Medical Centers, the Netherlands Organization for Health Research and Development, and the Royal Netherlands Academy of Sciences

**Significance**

Aberrant angiogenesis is an important feature of the pathogenesis of kidney cancer. The loss of the *VHL* gene is frequently associated with kidney tumors and leads to abnormal neovascularization. Our results demonstrate a vital role for the miRNA132/212 family in this process. We show that targeting these miRNAs can reduce pathological angiogenesis associated with the loss of functional VHL. We also show that miRNA132/212 targets PTEN, an important tumor suppressor and growth regulator, in both *in vitro* and *in vivo*

models. These results suggest that the upregulation of miR-212/132 may act as a promoter of tumorigenesis. Therefore, drugs which target the action of this miRNA family could present an important and novel opportunity for the treatment of tumors associated with VHL mutations.

# REFERENCES


1. Baldewijns, M.M., et al., *VHL and HIF signalling in renal cell carcinogenesis.* J Pathol, 2010. **221**(2): p. 125-38.
2. Cancer Genome Atlas Network, *Comprehensive molecular characterization of human colon and rectal cancer.* Nature, 2012. **487**(7407): p. 330-337.
3. Frantzen, C., et al., *Pregnancy-related hemangioblastoma progression and complications in von Hippel-Lindau disease.* Neurology, 2012. **79**(8): p. 793-6.
4. Shen, J. and M.C. Hung, *Signaling-Mediated Regulation of MicroRNA Processing.* Cancer Res, 2015.
5. Anand, S., et al., *MicroRNA-132-mediated loss of p120RasGAP activates the endothelium to facilitate pathological angiogenesis.* Nat Med, 2010. **16**(8): p. 909-14.
6. van Rooijen, E., et al., *Zebrafish mutants in the von Hippel-Lindau tumor suppressor display a hypoxic response and recapitulate key aspects of Chuvash polycythemia.* Blood, 2009. **113**(25): p. 6449-60.
7. van Rooijen, E., et al., *von Hippel-Lindau tumor suppressor mutants faithfully model pathological hypoxia-driven angiogenesis and vascular retinopathies in zebrafish.* Dis Model Mech, 2010. **3**(5-6): p. 343-53.
8. van Rooijen, E., et al., *A zebrafish model for VHL and hypoxia signaling.* Methods Cell Biol, 2011. **105**: p. 163-90.
9. Choorapoikayil, S., et al., *Loss of Pten promotes angiogenesis and enhanced vegfaa expression in zebrafish.* Dis Model Mech, 2013. **6**(5): p. 1159-66.
10. Jiang, B.H. and L.Z. Liu, *PI3K/PTEN signaling in angiogenesis and tumorigenesis.* Adv Cancer Res, 2009. **102**: p. 19-65.
11. Jin, W., et al., *Small RNA sequencing reveals microRNAs that modulate angiotensin II effects in vascular smooth muscle cells.* J Biol Chem, 2012. **287**(19): p. 15672-83.
12. Remenyi, J., et al., *Regulation of the miR-212/132 locus by MSK1 and CREB in response to neurotrophins.* Biochem J, 2010. **428**(2): p. 281-91.
13. Lei, Z., et al., *MicroRNA-132/212 family enhances arteriogenesis after hindlimb ischaemia through modulation of the Ras-MAPK pathway.* J Cell Mol Med, 2015.
14. Gomes, R.S., et al., *Efficient pro-survival/angiogenic miRNA delivery by an MRI-detectable nanomaterial.* ACS Nano, 2013. **7**(4): p. 3362-72.
15. Kumar, A., et al., *AKT kinase pathway: a leading target in cancer research.* ScientificWorldJournal, 2013. **2013**: p. 756134.
16. Hubbard, P.A., C.L. Moody, and R. Murali, *Allosteric modulation of Ras and the PI3K/AKT/mTOR pathway: emerging therapeutic opportunities.* Front Physiol, 2014. **5**: p. 478.
17. Samatar, A.A. and P.I. Poulikakos, *Targeting RAS-ERK signalling in cancer: promises and challenges.* Nat Rev Drug Discov, 2014. **13**(12): p. 928-42.
18. Ge, Y.Z., et al., *A tumor-specific microRNA signature predicts survival in clear cell renal cell carcinoma.* J Cancer Res Clin Oncol, 2015.
19. Acunzo, M., et al., *MicroRNA and cancer - A brief overview.* Adv Biol Regul, 2015. **57**: p. 1-9.
20. Braicu, C., et al., *Clinical and pathological implications of miRNA in bladder cancer.* Int J Nanomedicine, 2015. **10**: p. 791-800.
21. Qin, X., et al., *The Tumor Cytosol miRNAs, Fluid miRNAs, and Exosome miRNAs in Lung Cancer.* Front Oncol, 2014. **4**: p. 357.
22. Shuch, B., et al., *Defining early-onset kidney cancer: implications for germline and somatic mutation testing and clinical management.* Journal of Clinical Oncology, 2014. **32**(5): p. 431-437.
23. Ma, W., et al., *Hepatic vascular tumors, angiectasis in multiple organs, and impaired spermatogenesis in mice with conditional inactivation of the VHL gene.* Cancer Research, 2003. **63**(17): p. 5320-5328.
24. Frew, I.J., et al., *Combined VHLH and PTEN mutation causes genital tract cystadenoma and squamous metaplasia.* Mol Cell Biol, 2008. **28**(14): p. 4536-48.
25. Wang, S.S., et al., *Bap1 is essential for kidney function and cooperates with Vhl in renal tumorigenesis.* Proc Natl Acad Sci U S A, 2014. **111**(46): p. 16538-43.
26. Alimov, A., et al., *Somatic mutation and homozygous deletion of PTEN/MMAC1 gene of 10q23 in renal cell carcinoma.* Anticancer Res, 1999. **19**(5B): p. 3841-6.
27. Kondo, K., et al., *PTEN/MMAC1/TEP1 mutations in human primary renal-cell carcinomas and renal carcinoma cell lines.* Int J Cancer, 2001. **91**(2): p. 219-24.
28. Velickovic, M., et al., *Intragenic PTEN/MMAC1 loss of heterozygosity in conventional (clear-cell) renal cell carcinoma is associated with poor patient prognosis.* Modern pathology, 2002. **15**(5): p. 479-485.
29. Lin, Y.C., et al., *SCP phosphatases suppress renal cell carcinoma by stabilizing PML and inhibiting mTOR/HIF signaling.* Cancer Res, 2014. **74**(23): p. 6935-46.

## DETAILED MATERIALS AND METHODS

**MicroRNA in situ hybridization**

microRNA *in situ* hybridization was performed with a modified microRNA *in situ* hybridization method. Formalin-fixed paraffin-embedded tumor tissue from two ccRCCs and one healthy donor kidney dating from September 2006 were collected from the pathology archives of the University Medical Centre Utrecht (UMCU) after authorization of the UMCU institutional review board in accordance with Dutch medical ethical guidelines. Sequencing results of *VHL* identified no variants in the normal healthy kidney. However in ccRCC #1, in addition to the already known germline deletion of *VHL* exons 1 and 2 (c.1-?_463+?del), an additional somatic mutation was found in the tumor (c.277delG /p.Gly93Ala_fs_x158). ccRCC #2 has a germline mutation c.266T> p.Leu89Pro and a somatic mutation of c.419-420delTC/p.Leu140Gln_fs_x142. Mutation analysis of these tumors has been previously published [1].

Paraffin samples were first deparaffinized with tissue clear (Cat# 1426, SAKURA) followed with 10 min proteinase K treatment (5 mg/ml, Cat# 03115828001, Roche). Hybridization was performed with 10nM DIG labeled miRCURY LNA miRNA detection probes in hybridization buffer (Urea (2 M), 2.5x SSC, 1x Denhardt's, 200 µg/ml yeast tRNA, 0.1% CHAPS, 0.1% Tween, 50 mg/ml heparin) for miR-132 (Cat# 38031-15, Exiqon). Sections were subsequently incubated with anti-DIG alkaline phosphatase antibody (1:1,500, Cat# 1093274, Roche). To block endogenous alkaline phosphatase activity, sections were incubated with levamisole solution (Cat. X3021, DAKO), followed by NBT/BCIP (Cat# K0598 DAKO) incubation for visualization. A light Eosin counter staining was performed to visualize histology of the tissue. Images were taken with an Olympus microscope (BX53) under bright field.

**Cell culture and transfection**

HUVECs were cultured in EGM2 (Lonza, cat# cc-3156) according to manufacturer's instructions, and all experiments were performed before passage 7. HUVECS were either transfected with validated siVHL (ID: s14790), siPTEN (ID: s61222), Silencer select negative control #1 (cat# 4390843), mirVana miRNA mimic negative control (cat# 4464085), hsa-miR-132-3p mimics (ID: MC10166), hsa-miR-212-3p mimics (ID: MC10340), mirVana miRNA inhibitor control1 (cat# 4464077), hsa-miR-132-3p inhibitor (ID: AM10166), or hsa-miR-212-3p inhibitor (ID: AM10340) (all from Life Technologies) using Lipofectamine 2000 (Life Technologies). The transfection was performed with a final concentration of 20nM in opti-MEM reduced-serum medium (Cat# 31985062, Life Technologies) and replaced with fresh EGM2 after 6 hours. Cells were harvested 72 hours after transfection for protein or RNA analysis.

**RNA isolation and RT-PCR**

Total RNA was isolated with Tripure Isolation Reagent following manufactory's instructions (Roche Applied Science) and treated with Dnase to remove potential genome DNA contaminations. cDNA was synthesized using the iScript™ cDNA Synthesis Kit (Bio-Rad). Quantitative real-time polymerase chain reaction (qRT-PCR) was performed with iQ SYBR Green Supermix (Bio-Rad). The following primers were used for detection of human genes: *GAPDH* forward 5'-GGCATGGACTGTGGTCATGA-3' and reverse 5'-TTCACCACCATGGAGAAGGC-3'; *PTEN* forward 5'-TGGATTCGACTTAGACTTGACCT-3' and reverse 5'-GGTGGGTTATGGTCTTCAAAAGG-3'; *VHL* forward 5'-CAGCTACCGAGGTCACCTTT-3' and reverse 5'- CCGTCAACATTGAGAGATGG-3'; the following primers are used for *zebrafish*: *ptena* forward 5'-CCAGCCAGCGCAGGTATGTGTA-3' and reverse 5'-GCGGCTGAGGAAACTCGAAGATC-3'; *ptenb* forward 5'-GCTACCTTCTGAGGAATAAGCTGG-3' and reverse 5'- CTTGATGTCCCCACACACAGGC-3'; *rpl13α* forward 5'-TCTGGAGGACTGTAAGAGGTATGC-3' and reverse 5'-AGACGCACAATCTTGAGAGCAG-3'(All primers from Integrated DNA Technologies, Coralville, Iowa, USA).

**Western blotting**

Total protein was isolated with protein lysis buffer (50 mM Tris-HCl, pH 7.4, 100 mM NaCl, 1% NP-40, 0.1% SDS, 0.5% sodium deoxycholate). Protein concentration was determined using the Pierce BCA Protein Assay (Cat. 23225, Thermo Scientific). 10mg protein were loaded and separated with the Novex® NuPAGE® SDS-PAGE Gel System and transferred to a PVDF membrane with the iBlot® Transfer System (Invitrogen). Membranes were subsequently blocked in 5% non-fat dry milk dissolved in TBS with 0.1% tween-20 (TBST) for 1 hour. Blocked membranes were washed 3 times with TBST before primary antibody incubation overnight. The following antibodies and dilution were used in this study: anti-VHL (1:500, Cat. 556347, BD Pharmingen) anti-GAPDH (1:1000, Cat. 5174, Cell signaling) and anti-PTEN(1:1000, Cat. 9188, Cell signaling), anti-_Tubulin(1:1000, Cat. 2128, Cell signaling), and subsequently probed with horseradish peroxidase-conjugated goat-anti-rabbit (1:2000, Dako, P0448) or goat-anti-mouse (1:1000, Dako, P0447). The signal was detected with Chemiluminescent Peroxidase Substrate (Sigma) and the ChemiDoc XRS System (Bio-Rad). Bio-Rad Image Lab software was used for analysis.

**In vitro angiogenesis assay**

HUVECs (Lonza) and Human Brain Vascular Pericytes (Cat#1200, Sciencell) were cultured on gelatin-coated plates in EGM2 medium (Lonza cat# cc-3156) and DMEM (10% FCS; Lonza), respectively, in 5% $CO_2$ at 37˚C. Lentiviral transfected HUVECs expressing green fluorescent protein (GFP) and pericytes expressing red fluorescent protein (RFP) were used between passage 6-8. HUVECs were transfected either with siRNA or antimiRs as described above. In order to monitor the effects of miR-132 and miR-212 in angiogenesis, transfected HUVEC-GFP and Pericytes-dsRed were suspended in a 2.5 mg/ml collagen type I (BD Biosciences) as described by Stratman [2]. Co-cultures were imaged after 48h and 120h incubation in 5% $CO_2$ at 37 ˚C by fluorescence microscopy, followed by analysis using a commercial analysis system (Angiosys, Buckingham, UK).



**Zebrafish**

Experiments were conducted in accordance with Dutch guidelines for the care and use of laboratory animals, with the approval of the Animal Experimentation Committee (DEC) of the Royal Netherlands Academy of Arts and Sciences (KNAW). Mutant *zebrafish* possessed the previously described vhl$^{hu2117}$ mutation[3]. For RNA collection, *zebrafish* embryos were collected at 5 dpf based on these phenotypes and RNA was collected using Trizol reagent (Ambion) as per manufacturer's instructions.

**Injections and visualizations**

Wild type and mutant *Zebrafish* embryos were injected at the 1-2 cell stage with 1nL of 5uM of the same miRNA mimics and antagonists used for the cell culture experiments described above. Mimics and antagonists were diluted in pure water with 0.1% phenol red for visualization and injected using a nanoject2000 microinjector (World Precision Instruments). *Zebrafish* were selected without bias at 5dpf and then imaged using an LSM700 microscope (Zeiss). DNA was then collected from theses embryos using lysis buffer and then embryos were genotyped using a KASP™ genotyping system (LGC Genomics, Teddington, Middlesex, England) kit designed against the *vhl$^{hu2117}$* mutation or by sanger sequencing using the following primers:
Fw: 5'- TAA GGG CTT AGC GCA TGT TC -3'
Rv: 5'- CGA GTT AAA CGC GTA GAT AG -3'

**Statistical analysis**

Data was analyzed with Graphpad Prism 6 and comparisons were performed with student t-test or paired t-test between two groups, and ANOVA for more than two groups. Data are presented as mean ± SEM. P-values are indicated as follows: *p<0.05; **p<0.01;***p<0.001, p<0.05 is considered significant.

# REFERENCES

1. Nordstrom-O'Brien, M., et al., *Genetic analysis of von Hippel-Lindau disease.* Human mutation, 2010. **31**(5): p. 521-537.
2. Stratman, A.N., et al., *Pericyte recruitment during vasculogenic tube assembly stimulates endothelial basement membrane matrix formation.* Blood, 2009. **114**(24): p. 5091-101.
3. van Rooijen, E., et al., *Zebrafish mutants in the von Hippel-Lindau tumor suppressor display a hypoxic response and recapitulate key aspects of Chuvash polycythemia.* Blood, 2009. **113**(25): p. 6449-60.

# SUPPLEMENTAL

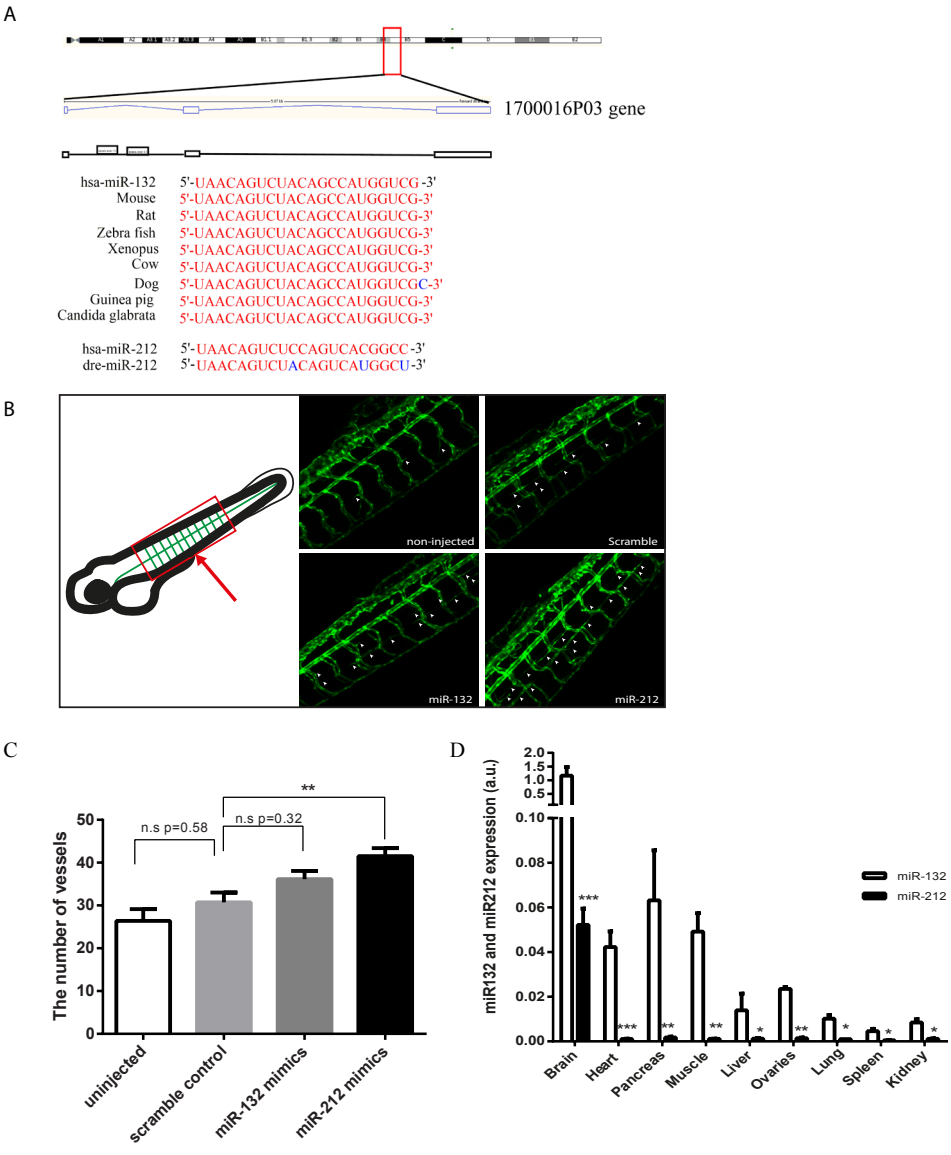


**Supplementary Figure 1.**
**A.** miR-132/212 location in human genome and conservation of miR-132/212 between different species. **B.** Representative images of tail vascular structures in WT zebrafish after being injected with scrambled, miR-132, or miR-212 mimics. Schematic cartoon shows the area of the zebrafish embryo shown (cloaca marked with red arrow, imaging area marked with red box). **C.** Quantification of vascular branching after injected with scrambled, miR-132, or miR-212 mimics. **D.** Relative expression of miR-132 and 212 in different tissues in mouse. Note miR-132 expression is considerably higher than miR-212. n=3

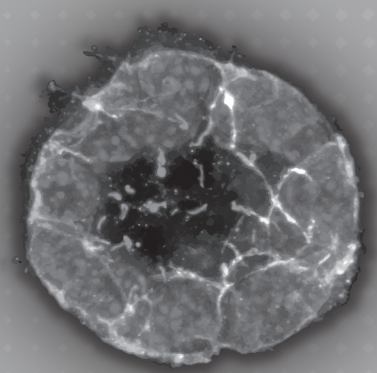

## CHAPTER 6

# The von Hippel-Lindau tumor suppressor regulates programmed cell death 5 mediated degradation of Mdm2

Oncogene. 2015 Feb 5;34(6):771-9.

**Klasson TD***, Essers PB*, Pereboom TC, Mans DA, Nicastro M, Boldt K, Giles RH, Macinnes A

*these authors contributed to this work equally

## ABSTRACT

Functional loss of the von Hippel–Lindau (VHL) tumor suppressor protein (pVHL), which is part of an E3-ubiquitin ligase complex, initiates most inherited and sporadic clear-cell renal cell carcinomas (ccRCC). Genetic inactivation of the *TP53* gene in ccRCC is rare, suggesting that an alternate mechanism alleviates the selective pressure for *TP53* mutations in ccRCC. Here we use a zebrafish model to describe the functional consequences of pVHL loss on the p53/Mdm2 pathway. We show that p53 is stabilized in the absence of pVHL and becomes hyperstabilized upon DNA damage, which we propose is because of a novel *in vivo* interaction revealed between human pVHL and a negative regulator of Mdm2, the programmed cell death 5 (PDCD5) protein. PDCD5 is normally localized at the plasma membrane and in the cytoplasm. However, upon hypoxia or loss of pVHL, PDCD5 relocalizes to the nucleus, an event that is coupled to the degradation of Mdm2. Despite the subsequent hyperstabilization and normal transcriptional activity of p53, we find that zebrafish *vhl* $^{-/-}$ cells are still as highly resistant to DNA damage-induced cell cycle arrest and apoptosis as human ccRCC cells. We suggest this is because of a marked increase in expression of *birc5a*, the zebrafish homolog of *Survivin*. Accordingly, when we knock down *Survivin* in human ccRCC cells we are able to restore caspase activity in response to DNA damage. Taken together, our study describes a new mechanism for p53 stabilization through PDCD5 upon hypoxia or pVHL loss, and reveals new clinical potential for the treatment of pathobiological disorders linked to hypoxic stress.

## INTRODUCTION

Biallelic inactivation of the von Hippel–Lindau tumor suppressor gene (*VHL*) causes the majority of inherited and sporadic kidney cancers, in particular, of the clear-cell renal cell carcinoma (ccRCC) subtype. Recent deep-genomic sequencing efforts on sporadic ccRCCs from unrelated individuals have demonstrated that loss of function of the *VHL* gene by somatic mutation is very often the initiating event of ccRCC.[1–3] ccRCC is the seventh most common malignancy that is responsible for 3% of all adult cancers.[4] Metastasized ccRCC is associated with a poor prognosis in large part because of the resistance of these tumors to chemo- and radiotherapy.[5]

VHL tumor suppressor protein (pVHL) is best known for its role in oxygen sensing, where it performs a critical function in an E3-ubiquitin ligase complex. In this complex, pVHL targets the transcription factors hypoxia inducible factor 1a and 2a (HIF1a/ HIF2a) for degradation under normoxic conditions. Under hypoxic conditions, HIFa is no longer ubiquitinated by pVHL, resulting in its stabilization and the upregulation of target genes such as *VEGF, EPO* and *c-MYB*.[6] Mutations in pVHL may consequently result in a failure to recognize HIFa subunits, inducing a constitutive hypoxic response. The excessive blood vessel formation and metabolic switch to glycolysis as a result of this response can clearly assist tumorigenesis,[7] but several studies have concluded that HIFa dysregulation alone is not sufficient to drive tumorigenesis.[8–10] The p53 tumor suppressor, normally kept at low levels by association with the E3-ubiquitin ligase Mdm2, performs a central role in the DNA damage response pathway.[11] In response to numerous types of cellular stress, p53 stabilizes and translocates as a tetramer to the nucleus to upregulate the expression of genes involved in cell cycle arrest and/or apoptosis.[12] The stabilization of p53 has been widely reported as a result of low oxygen levels,[13] and there is evidence to suggest that this is coupled to the hypoxia- mediated degradation of Mdm2.[14] However, despite a number of hypotheses proposed,[15] current understanding has not yet resolved the precise mechanisms of the p53 response to hypoxia.

Programmed cell death 5 (PDCD5) is a protein that functions in the apoptotic pathway to enhance caspase-3 activity through Bax translocation from the cytosol to the mitochondrial membrane resulting in cytochrome *c* release.[16] PDCD5 also rapidly translocates to the nucleus in an early response to DNA damage, where in addition to its effects on Bax localization has been shown to have a role in p53-induced apoptosis through the co-activation of Tip60 (a protein required for an acetylation event on p53 that leads to the transcription of apoptosis-related genes), the stabilization of p53 and the degradation of Mdm2.[17–19] The expression of PDCD5 is substantially reduced in several tumor types, including (but not limited to) breast tumors, gastric tumors, lung tumors and ccRCCs compared with corresponding normal tissues.[20–23] In fact, immunohistological studies have

concluded that the extent of PDCD5 expression loss is a major indicator of the tumor grade, stage and prognosis in ccRCC patient samples.[24] However, despite the potential significance of PDCD5 expression in characterizing ccRCC, no studies of PDCD5 in relation to pVHL have been reported to date.

There is also little known about the relationship between p53 and pVHL. It has been demonstrated in engineered mice that the functional loss of both proteins can cause dysregulation of cellular proliferation and result in the formation of cysts and neoplastic lesions in kidneys, as well as tumors in genital tract organs.[25,26] In line with the fact that most tumor cells maintaining wild-type *TP53* have devised alternate mechanisms to impair p53 function, it has been reported that pVHL is able to directly bind to p53 *in vitro,* and that this binding is required for p53 stabilization and induction of target gene expression.[27] However, there is significant evidence to suggest that the p53 pathway has a limited role in the impaired DNA damage response that is the hallmark of ccRCC. This is mainly owing to the fact that the genetic mutation of *TP53* in ccRCC is an extremely rare event. One recent study found only 3 ccRCCs out of 106 (2.8%) to have *TP53* mutations,[2] whereas another study of 385 ccRCCs found only 10 cases (2.2%). This is compared with other human tumor types where the mutation rate of *TP53* is between 50–70%.[28] ccRCC cells maintaining wild-type *TP53* must therefore devise alternate mechanisms to evade apoptosis. Many other inhibitors of apoptosis are expressed during hypoxia, including the IAP-2 and Survivin genes,[29] that are well known to inhibit caspase activation.[30] In a study using ccRCC cells devoid of functional pVHL, it was demonstrated that the observed caspase inhibition was largely because of the increased expression of anti-apoptotic nuclear factor-kB target genes such as c-*FLIP*, *Survivin*, *c-IAP-1* and *cIAP-2*.[31]

Here we used a zebrafish model of pVHL loss to investigate the relationship between pVHL and the p53/Mdm2 pathway in cells that do not carry compounding oncogenic mutations. Our study reveals a mechanism by which p53 is stabilized upon hypoxia or pVHL loss through PDCD5, a novel binding partner of pVHL.

## RESULTS

### p53 is hyperstabilized in vhl mutant zebrafish upon DNA damage

To investigate whether pVHL is required for p53 stabilization *in vivo*, we exposed 5 days post-fertilization (d.p.f.) wild-type and *vhl* $^{-/-}$ embryos to 25 Gy of ionizing radiation and performed western blotting with a zebrafish-specific p53 antibody.[32] Our results show that p53 becomes hyperstabilized in *vhl* $^{-/-}$ embryos upon irradiation compared with wild-type embryos (Figures 1a and b). Moreover, an increase of p53 stabilization was observed in the *vhl* $^{-/-}$ embryos even in the absence of irradiation compared with wild-type control embryos.

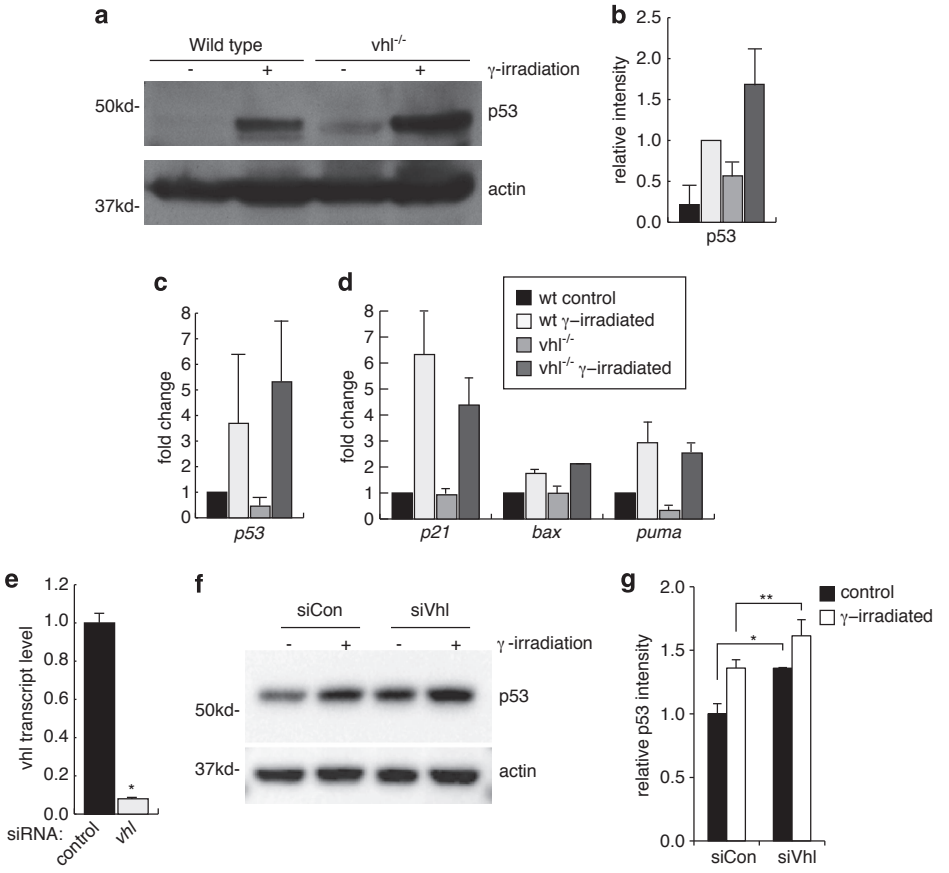


**Figure 1.** Loss of vhl stabilizes p53. (a) Western blot analysis of p53 levels in wild-type and vhl$^{-/-}$ embryos at 5 d.p.f., 6 h after g-irradiation. (b) Quantification of western blot band intensity showing the results from three independent experiments. (c, d) qPCR analysis of p53 transcript levels (c) and p53 target gene expression (d) in wild-type and vhl$^{-/-}$ embryos at 5 d.p.f., 6 h after g-irradiation. (e) qPCR confirming the knockdown of Vhl transcripts normalized to Rpl27 expression. (f) Western blot analysis of p53 levels in IMCD3 cells treated with siRNAs against Vhl (siVhl) vs control oligos (siCon) in the presence or absence of g-irradiation. (g) Quantification of western blot band intensity from f, showing the results from three independent experiments. *Po0.02, **Po0.05.

*p53* transcript levels were not significantly different between wild-type and mutant embryos after irradiation, indicating that the increase of p53 protein is not because of increased *p53* transcription but because of increased p53 stabilization (Figure 1c). This *in vivo* data suggests that, in contrast to the previous finding that overexpressed pVHL is able to regulate p53 expression *in vitro*,[27] in a physiological context an additional layer of regulation of endogenous p53 stability upon *VHL* loss must exist.

To determine whether loss of zebrafish *vhl* affected transcription of p53 target genes, we measured transcript levels of the p53 target genes *p21*, *bax* and *puma* by quantitative PCR (qPCR). No significant differences were observed in the expression of these genes upon *vhl* loss (Figure 1d), indicating that functional *vhl* is not required for the transcriptional activity of p53. We found no statistical increase in the transcription of p53 target genes as a result of p53 hyperstabilization. To ensure that these observations are not specific to zebrafish vhl and p53, we measured the p53 response after *Vhl* small interfering RNA (siRNA) knockdown in murine collecting duct IMCD3 cells. The siRNAs we used were successful in knocking down *Vhl* transcripts levels by 90% (Figure 1e). We observed an increased stabilization of p53 upon acute loss of pVHL that was augmented by DNA damage induced by g-irradiation (Figures 1f and g). In addition, we analyzed p53 protein expression in isogenic *VHL*-null ccRCC cells (RCC10) and RCC10 cells in which wild-type pVHL has been stably reconstituted at near-endogenous levels (RCCp30d10 cells[33]). Upon irradiation with 1.5 mJ/cm$^2$ UV, western blotting analysis shows that p53 is stabilized to equivalent levels in both cell systems, supporting the notion that functional pVHL is not required for the p53 response (Supplementary Figure S1).

**pVHL interacts directly with PDCD5**

To gain insight into the regulation of p53 by pVHL on protein level, we performed tandem-affinity purifications of TAP-tagged pVHL (full-length; UniProt ID P40337-1) in HEK293 cells, followed by mass spectrometry in duplicate. We were able to identify established binding partners of pVHL, for example, components of the E3-ubiquitin ligase complex (cullin-2, elongin B, elongin C and Rbx1[34–36]), VHL-binding protein[37] and collagens[38] (Supplementary Table 1 and Figure 2a). We did not observe an interaction between pVHL and p53, but we did identify a robust interaction in several independent experiments between pVHL and PDCD5, an important positive regulator of apoptosis.

We repeated this experiment with a pVHL isoform lacking amino acids 114–154 (pVHL isoform 2; UniProt ID P40337-2), and although the resulting interactome identified by mass spectrometry largely overlapped, PDCD5 was absent in this data set (Figure 2b and Supplementary Table 1). To investigate whether this interaction is direct, we performed yeast two-hybrid experiments and identified robust binding of pVHL to PDCD5 (Figure 2c). Moreover, this assay revealed that the pVHL-PDCD5 interaction is limited to the first 178 amino acids of pVHL.

Finally, we immunoprecipitated endogenous pVHL in HEK293 kidney cell lysate and found endogenous PDCD5 to be bound in a complex with pVHL by western blotting (Figure 2d).

**Loss of *vhl* or hypoxia results in nuclear relocalization of PDCD5 and subsequent Mdm2 degradation**

Western blot analysis in 5 d.p.f. zebrafish embryos and ccRCC lysates indicates that vhl does not target PDCD5 for degradation, as PDCD5 protein levels remain constant in the absence of *vhl*/pVHL (Supplementary Figure S2). Immunocytochemical analysis revealed that PDCD5 localizes to the membrane in RCCP30d10 cells, and this membranous staining is lost in the RCC10 cells that are devoid of pVHL (Figure 3a). Cells were scored for membranous and cytosolic staining patterns to quantify this effect (Figure 3b). To verify that pVHL determines PDCD5 localization directly, and is not the result of clonal drift, we used siRNA to knock down *Vhl* in mIMCD3 cells. Immunocytochemical analysis in these cells shows that murine PDCD5 localizes to the cell membrane and is absent from the nucleus in the cells transfected with a control siRNA (Figure 3c). In cells transfected with the siRNA against *vhl*, PDCD5 is largely devoid from the cell membrane and is instead found localized in the nucleus (Figure 3c). In order to determine whether this PDCD5 nuclear relocalization is because of the stabilization of HIF in the absence of pVhl, we repeated the immunocytochemistry experi- ments with cells exposed to hypoxia (1% $O_2$) compared with normoxia (21% $O_2$). We recapitulated the same shift of PDCD5 from the plasma membrane to the nucleus of hypoxic cells, indicating that the relocalization of PDCD5 can be regulated by oxygen loss (Figure 3e). Staining of these cells with HIF antibodies illustrates the expected increase of HIF expression in response to hypoxia (Supplementary Figure S3). qPCR was used to confirm that knockdown of *Vhl* was effective in mIMCD3 cells (Figure 3d). We then used western blot analysis to determine how this relocalization of PDCD5 upon pVHL loss affects Mdm2 expression. The transfection of mlMCD3 cells with siRNAs against *Vhl*, but not control siRNAs, resulted in a substantial reduction (56±2%) of Mdm2 protein (Figure 3f). Consistent with these results, we found that Mdm2 protein levels were significantly reduced in *vhl* $^{-/-}$ zebrafish embryos as well (Figure 3g). In order to test whether PDCD5 is required for the p53 stabilization resulting from pVHL loss (as surrogate for Mdm2 function), we knocked down *Vhl* alone or in combination with siRNAs against the *PDCD5* gene in IMCD3 cells. We observed that in the absence of PDCD5, p53 is not stabilized by the reduction of *Vhl* and instead remains at baseline levels (Figures 3h and i). Moreover, Figures 3h and i illustrate that the knockdown of PDCD5 alone reduces the baseline level of p53 stabilization, confirming the role of PDCD5 as a regulator of p53. Together, these data suggest that the stabilization of p53 in the absence of pVHL or in the presence of hypoxia is because of the degradation of Mdm2 upon relocalization of PDCD5 to the nucleus, and that PDCD5 is a required protein for the p53 response to pVHL loss (model illustrated in Supplementary Figure S4).

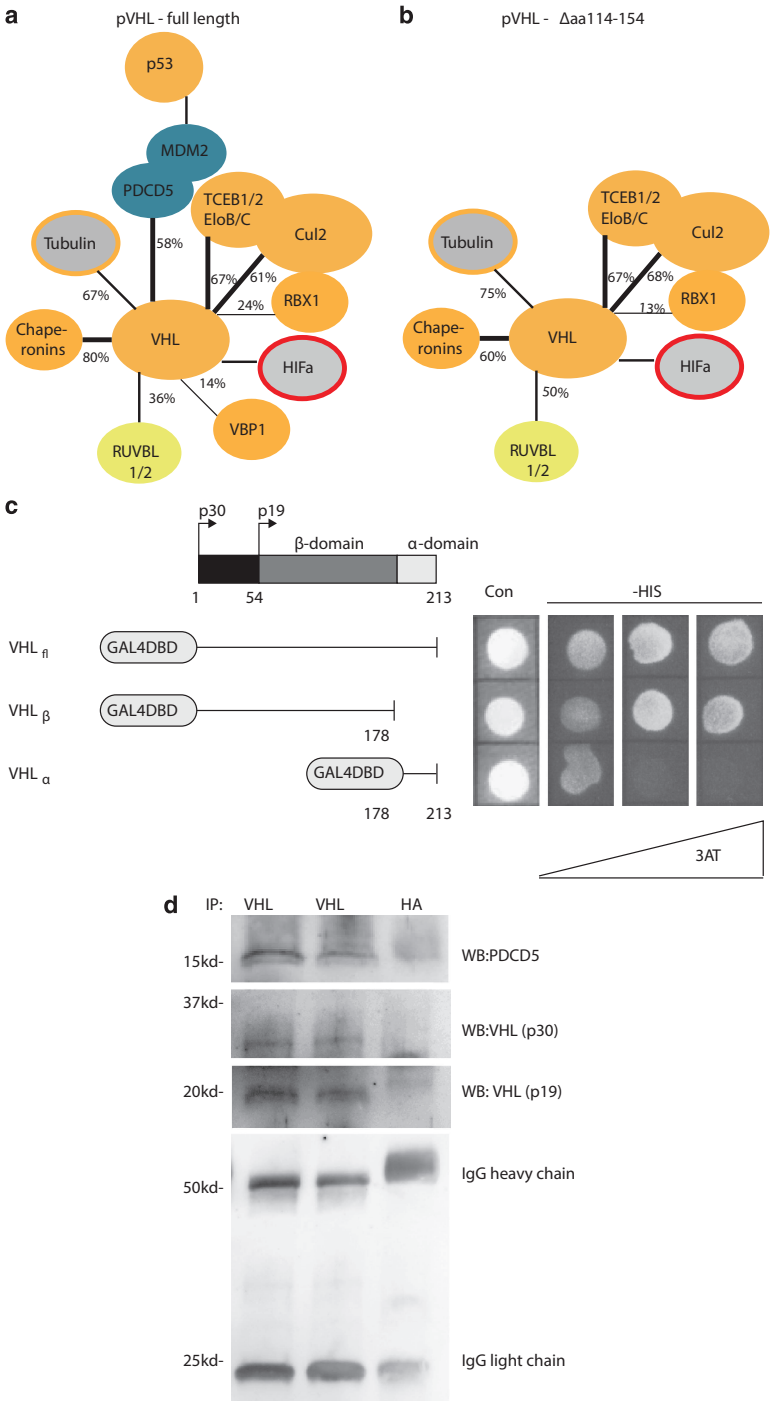

◀ **Figure 2.** VHL directly binds to PDCD5 at endogenous levels. (a, b) Schematic representation of protein–protein interaction data revealed from mass spectrometry of four independent pVHL tandem-affinity purification pull-down assays using either full-length pVHL (a) or an isoform lacking amino acids 114–154, Dexon2 (b). Previously identified direct interactions are provided as orange nodes, previously identified and possibly indirect interactions are shown as gray nodes, and nodes with a red outline indicate proteins whose stability/turnover is regulated by pVHL. This study focuses on the novel interactors PDCD5 and indirectly Mdm2 (blue nodes). An additional novel and robust finding is that VHL interacts with the RUVBL1/2 complex (yellow node). Percentages on the edges between nodes represent the peptide coverage, which is often used as a surrogate for binding confidence. (c) Yeast two-hybrid assay with Gal4 DNA-binding domain fused to: full-length pVHL (VHLfl), the acidic and b-domain of pVHL (VHLb) or the a-domain of pVHL (VHLa) used as bait and PDCD5 used as prey. Right panel: colony growth of transformed yeast, using increasing 3-aminotriazole (0, 12.5 and 25mM) without histidine (_HIS). Control colony (Con) in the presence of HIS. (d) Immunoprecipitation of endogenous pVHL in HEK293 cells using anti-pVHL (biological duplicates are shown) or anti-HA (mock) antibody. Anti-pVHL specifically immunoprecipitates both the p30 and p19 isoforms of pVHL and co-immunoprecipitates PDCD5, shown by western blotting with anti-PDCD5.

### *Vhl* is required for p53-mediated cell cycle arrest and apoptosis

To investigate whether loss of *vhl* affects p53-mediated cell cycle arrest and apoptosis in our zebrafish model, we first measured the number of dividing cells in embryos after g-irradiation at 5 d.p.f. The application of g-irradiation normally leads to cell cycle arrest and a decrease of the number of cells undergoing mitosis, which can be detected by labeling cells with a phospho-specific histone 3 (pH3) antibody.[40] Although g-irradiation led to an approximately threefold decrease in the number of mitotic cells in wild-type embryos, we observed a significantly greater number of mitotic cells in *vhl* $^{-/-}$ mutant embryos, indicating an impaired cell cycle arrest response to DNA damage (Figures 4a and b). To examine the *in vivo* apoptotic response of the *vhl* $^{-/-}$ embryonic cells subjected to the same DNA damage, we performed measure- ments of activated caspase-3/7 and caspase-2 activity. Figure 4c demonstrates that the loss of *vhl* prevents the activation of either caspase-3/7 or caspase-2. Consistent with these results, Figures 4d and e illustrate that *vhl* loss prevents the normal accumulation of apoptotic cells upon DNA damage as detected by acridine orange (AO) staining (Figures 4d and e). RCC10 cells were likewise resistant to UV-induced caspase activation, whereas RCCp30d10 cells that reconstituted with pVHL were not (Figure 4f). As it has been shown in ccRCC cells that the nuclear factor-kB-dependent anti-apoptotic pathway can prevent tumor necrosis factor-a- induced cytotoxicity,[31] we measured levels of nuclear factor-kB targets in the *vhl* $^{-/-}$ embryos. We found that expression levels of *birc5a,* the zebrafish homolog of Survivin, are substantially elevated in *vhl* $^{-/-}$ mutants (Figure 4g). To explore this observation further in human cells, we first determined that RCC10 cells express B10-fold the levels of *Survivin* compared with RCCp30d10 cells (Figure 4h). siRNAs against *Survivin* transfected into RCC10 cells substantially reduced the levels of the transcript, as shown in Figure 4i. This knockdown of Survivin resulted in a significant increase in the levels of caspase-3/7 activity when RCC10 cells were exposed to g-irradiation (Figure 4j).

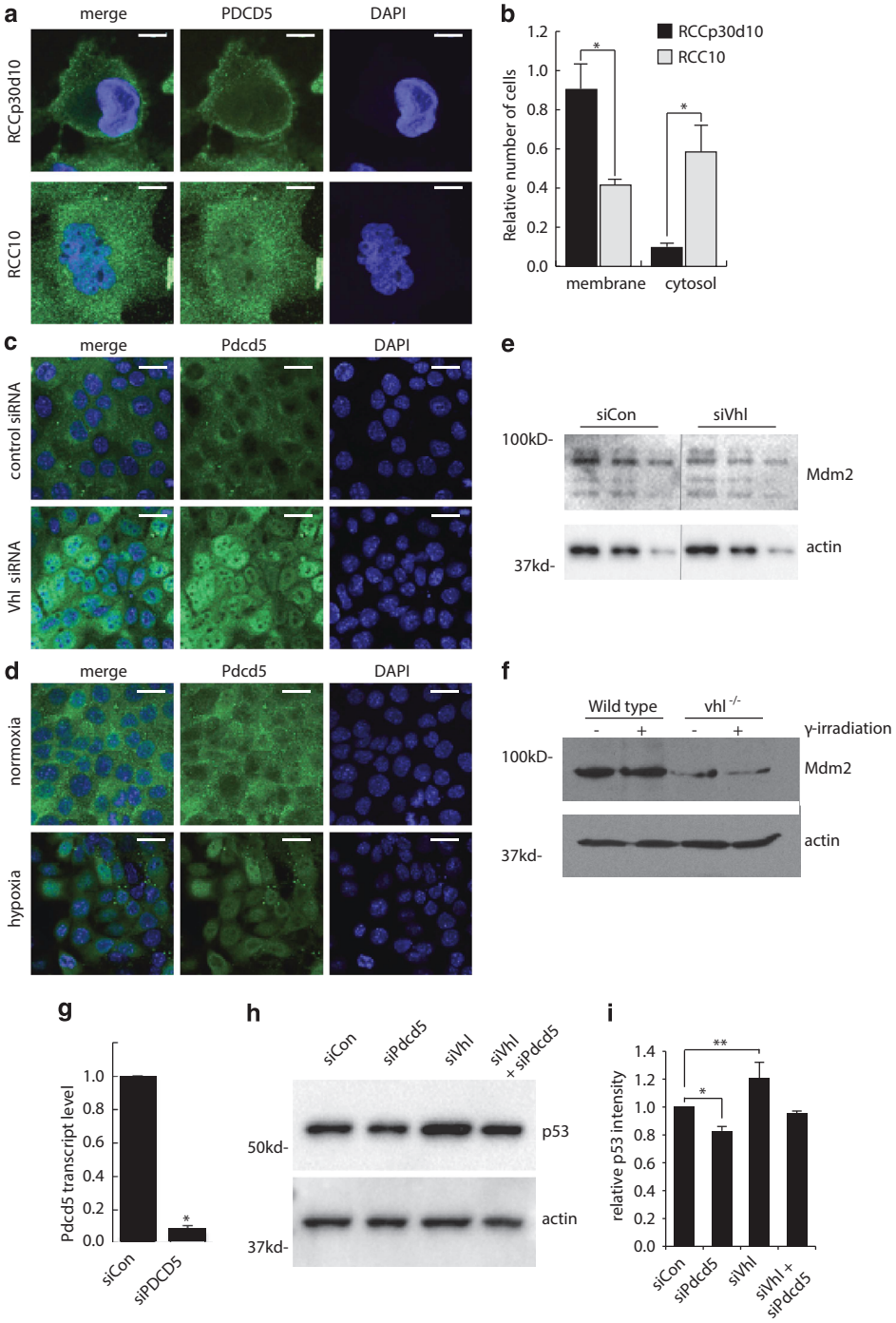

Taken together, these data suggest that the resistant *VHL* mutant cells confer to DNA damage-induced apoptosis is modulated at least partly by an increase in *Survivin* expression, and this resistance may be overcome by Survivin inhibition.

## DISCUSSION

In human cancer research, pVHL and p53 are both extensively studied tumor suppressors. However, scarcely any information is known about their relationship between one another. The advantages of studying pVHL loss in the zebrafish model are multiple. One reason is that we are able to bypass the embryonic lethality problem that is inherent in mouse models of Vhl loss (the zebrafish embryos remain alive for at least 5 d.p.f.). Another more important reason is that the lack of other oncogenic mutations in the mutant embryos that are invariably present in the tumor suppressor pathways of immortalized cancer cell lines provides us with an opportunity to clearly gauge what amount of influence the p53 pathway has on the DNA damage response of cells in the absence of pVHL. The hyperstabilization of p53 that we found in the zebrafish *vhl* $^{-/-}$ embryos may have been expected to produce a normal, or even augmented, DNA damage response. However, we do not observe a difference in p53 transcriptional target mRNA levels between irradiated wild-type zebrafish embryos and irradiated *vhl* $^{-/-}$ embryos. Moreover, when cell cycle arrest and apoptosis were examined, it became clear that the mutation of *vhl* blocks these pathways downstream of p53 activation. These observations are possibly explained by the acetylation status of p53 and the subsequent changes in affinity to downstream promoters,[41] leaving the relationship between pVHL and Tip60 as an interesting area of future study.



◀ **Figure 3.** Loss of VHL causes PDCD5 to be released from the cell membrane and translocated into the nucleus. (a) Immunocytochemical stain for PDCD5 protein (green) and nuclei (blue) in RCC cells, showing membranous staining in RCCp30d10 but not RCC10 cells. Scale bars, 10 mm. (b) Manual quantification of the proportion of cells with membranous and cytoplasmic PDCD5 localization. (c) Immunocytochemical analysis of PDCD5 (green) and nuclei (blue) in IMCD3 cells treated with siRNA against Vhl, showing PDCD5 nuclear translocation in the absence of Vhl. Scale bars, 20 mm. (d) Immunocytochemical analysis of PDC5 (green) and nuclei (blue) in IMCD3 cells cultured under hypoxic conditions. Scale bars, 20 mm. (e) Western blot analysis of Mdm2 levels in IMCD3 cells treated with siRNA against Vhl. The middle dividing line indicates where several lanes were removed from the blot. (f) Western blot analysis of Mdm2 levels in wild-type and vhl$^{-/-}$ zebrafish embryos. (g) qPCR confirming the knockdown of PDCD5 transcripts, normalized to Rpl27 expression. (h) Western blots showing p53 levels in IMCD3 cells treated with siRNA oligos against Vhl, PDCD5 or both. (i) measurements of western blot band intensity from h, showing the results for three independent experiments. *Po0.01, **Po0.05.

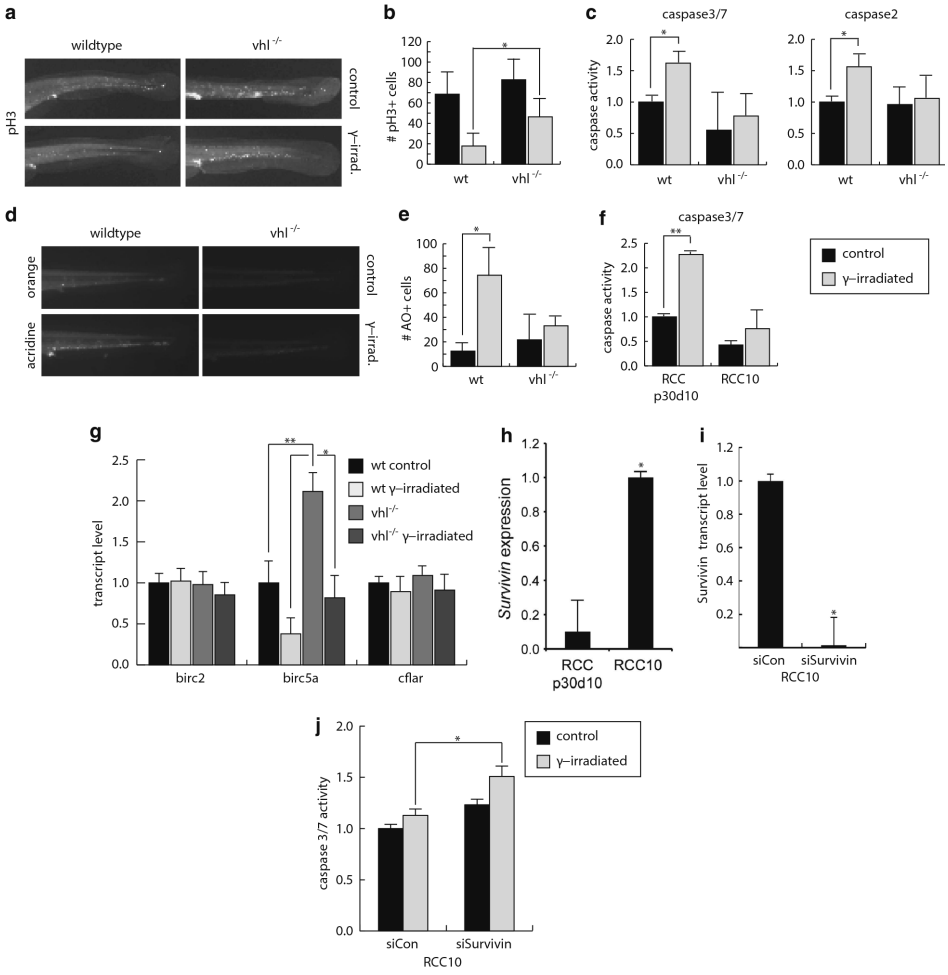


**Figure 4.** DNA damage fails to induce cell cycle arrest and apoptosis in vhl$^{-/-}$ embryos. (a) Immunohistochemical analysis of pH3 in the tails of 5 d.p.f. embryos after g-irradiation. The tails of the embryo were used for quantification of positive cells. (b) Quantification of the number of pH3-positive cells in the tails of at least four embryos per condition. (c) Measurement of caspase-3/7 activity in 5 d.p.f. embryos after g-irradiation. (d) Measurement of caspase activity in RCC cell lines after UV irradiation. (e) AO stain of apoptotic cells in the tails of 5 d.p.f. embryos after g-irradiation. (f ) Quantification of the number of AO-positive cells in the tails of at least nine embryos per condition. (g) qPCR analysis of the transcript levels of several inhibitors of apoptosis in 5 d.p.f. embryos, 6 h after g-irradiation. (h) qPCR analysis of Survivin transcript levels in RCC10 and RCCp30d10 cells shown relative to expression of RPLp0. (i) qPCR analysis of Survivin transcript levels in RCC10 cells transfected with siRNA oligos directed against Survivin or control oligos (siCon). (j) Measurement of caspase-3/7 activity after g-irradiation in RCC10 cells transfected with siRNA oligos directed against Survivin or control oligos (siCon). *Po0.01, **Po0.00001.

Despite enormous efforts to date, there are very few validated models of murine kidney cancer. Initial murine studies of *VHL*- driven ccRCC tumorigenesis were limited to heterozygous mice because of the embryonic lethality observed in homozygous mutant animals.[42,43] In these mice, liver vascular lesions were the only phenotype observed and an increased incidence of ccRCC was not found,[42] even when mice were treated with high doses of carcinogens.[43] When pVHL was conditionally knocked out in the renal proximal tubule, occasional renal cysts were observed, but not ccRCC.[44] Alternatively, mutating the hydroxylation sites in HIF1a in mice results in a kidney histology that is similar to human ccRCC[45] with concomitant upregulation of proliferation markers and the presence of genomic instability in abnormal proximal tubule cells, but no ccRCC development has been reported.[45] Although loss of p53 itself is a rare event in RCC (2–3%[23]), ccRCC development in an animal model was only recently demonstrated for the first time by the simultaneous deletion of murine *p53* and *Vhl*.[46] These findings support the idea that the loss of signaling pathways downstream of p53 is still an important event for malignant transformation of *VHL* $^{-/-}$ cells.



Our findings regarding the hyperstabilization of p53 upon loss of pVHL are in contrast to a previous study in which pVHL was found to bind p53 and to be required for its stabilization.[47] The discrepancy between these findings and our own is likely to be explained by the experimental setup. Most findings by Roe *et al.*[47] were based on experiments using overexpression of pVHL in non- kidney cell lines. In contrast, the models used in the current study represent either a loss of endogenous pVHL, namely in the zebrafish embryos lacking a functional *vhl* gene and siRNA- mediated knockdown of *Vhl* in the murine kidney cell line IMCD3, or exogenous expression of near-endogenous levels of pVHL in the case of the isogenic sister-paired cell lines RCC10 and p30d10RCC10.[48] Overexpression of pVHL beyond endogenous levels possibly revealed effects that are not representative in the *in vivo* situation. Allowing for the fact that pVHL binds to p53, our results could indicate that the interaction we describe between PDCD5 and Mdm2 has a much larger influence on p53 stabilization in the pathophysiological context of pVHL loss. In addition, it has been reported that increased levels of pVHL increase acetylation of p53,[47] thereby increasing the affinity of p53 for its target sites.[47,49] Therefore, the loss of pVHL may hyperstabilize unacetylated p53 that consequently does not result in increased levels of p53 target genes as observed in our models. This mechanism also possibly explains the low baseline level of *puma* observed in *vhl* $^{-/-}$ embryos.

In recent years it has become clear that pVHL is not only involved in HIFa regulation, but functions as an adaptor protein in many other processes, including stress response, survival, senescence, adhesion, invasion and primary cilium function.[50] In line with this, we found that PDCD5 is a novel *in vivo*-binding partner of pVHL, and that this interaction dictates the cellular localization of PDCD5 and the levels of Mdm2 in response to the loss of pVHL

or oxygen. These results establish an as of yet unappreciated role for PDCD5 in the apoptotic response to hypoxia. Moreover, we show that in the pathophysiological context of *VHL* inactivation, pVHL binding to PDCD5 is lost and the subsequent nuclear localization of PDCD5 leads to an atypical stabilization of p53 with few downstream p53 effects. We conclude that the functional significance is primarily in the mislocalization of PDCD5. Challenging *vhl* $^{-/-}$ zebrafish embryos or RCC10 cells with g-irradiation fails to induce apoptosis, which is not surprising given the resistance patients with ccRCC retain against chemo- and radiotherapy. The substantial increase in the expression of *birc5a/ Survivin* is likely playing an important role in this evasion of apoptosis. Not only do we see a large increase in *birc5a/Survivin* expression in *vhl* $^{-/-}$ mutant zebrafish and RCC10 cells, respectively, we are also able to restore caspase-3/7 activity to the RCC10 cells upon reducing the expression of *Survivin*. Several pathways likely co- modulated this effect; nevertheless, these results are in line with previous work demonstrating that 786-0 ccRCC cells with knocked down expression of *Survivin* show reduced colony formation and express an increase of cleaved poly ADP ribose polymerase, a marker of apoptosis.[51]

We provide with this work a novel mechanism for the stabilization of p53 upon hypoxia or pVHL loss through the relocalization of PDCD5 to the nucleus coupled to the degradation of Mdm2. Given the multifunctional role of PDCD5 in driving apoptosis, it is possible that one or more of its downstream functions (such as relocalizing Bax to the mitochondria and releasing cytochrome *c*) may be exploited clinically, such that PDCD5 expression and/or activity is enhanced to overcome the apoptosis inhibition in ccRCC. Conversely, the inhibition of PDCD5 may be a promising treatment for conditions that arise from prolonged systemic hypoxia, such as neurodegeneration and Alzheimer's disease. We also include in this work evidence that despite the hyperstabilization of p53 upon DNA damage in ccRCC cells, the mutation of pVHL singularly exerts a powerful inhibition of apoptosis that includes the increase of *Survivin* expression. Finally, our results indicating that caspase activity is restored upon the loss of *Survivin* in ccRCC cells reiterates the potential clinical advantage of using DNA-damaging agents for patients with ccRCC in combination with Survivin inhibitors. Taken all together, this study reveals promising new avenues for the treatment of a wide-spanning range of diseases.

## MATERIALS AND METHODS

### Zebrafish strains

Zebrafish were maintained as previously described.[52] Animal experiments were conducted in accordance with the Dutch guidelines for the care and use of laboratory animals, with the approval of the Animal Experimentation Committee (Dier Experimenten Commissie) of

the Royal Netherlands Academy of Arts and Sciences (Koninklijke Nederlandse Akademie van Wetenschappen (protocol no. 08.2001). The *vhl* $^{hu21}$ mutant zebrafish line was previously described, and mutants were initially selected at 5 d.p.f. according to the phenotypes described therein, followed by genotyping after use.[53] Where indicated, embryos were exposed to 25 Gy of ionizing radiation and used for analysis after 4–6 h.

**Cell culture**

RCC10 and RCCp30d10 cells[33] were grown in RPMI 1640 supplemented with glutamax (Life Technologies, Carlsbad, CA, USA), 10% fetal calf serum and 1% penicillin and streptomycin (Pen/Strep) (Sigma, St Louis, MO, USA). mIMCD3 cells (CRL-2123, American Type Culture Collection) were cultured in DMEM/Ham's F12 (1:1) supplemented with glutamax (Life Technologies), 10% fetal calf serum and 1% Pen/Strep. g-irradiation was performed using a Gammacell 1000 (Atomic Energy of Canada Limited, Mississauga, Southern Ontario, Canada) according the manufacturer's instructions. Zebrafish embryos were irradiated with 25 Gy and cell lines were irradiated at 10 or 20 Gy for western blotting and 25 Gy for caspase assays. For UV irradiation, culture medium was removed from cells, and cells were irradiated in a UV Stratalinker 2400 (Stratagene, La Jolla, CA, USA) using 1.5 mJ/cm$^2$. Following UV irradiation, fresh medium was added to the cells.



**Western blotting**

Western blots were performed using five zebrafish embryos or 30 mg cell line protein lysate per sample as described.[54] The following antibodies were used: zebrafish-specific anit-p53,[32] anti-p53 FL-393 (SC-6243, Santa Cruz Biotechnology, Santa Cruz, CA, USA), anti-Mdm2 (SC-812, Santa Cruz Biotechnology), anti-p21 (EA10, Abcam, Cambridge, UK), anti-PDCD5 (1:500; SAB3500258, Sigma-Aldrich, St Louis, MO, USA), anti-VHL (1:500, IG32, BD Thermo Scientific, Rockford, IL, USA), anti-b-actin (1:500; A5441. Sigma-Aldrich), donkey anti-rabbit IgG (1:5000; NA934V, GE Healthcare, Chalfont St Giles, UK) and sheep anti-mouse IgG (1:5000; NXA931, GE Healthcare). Visualization was performed with a Molecular Imager ChemiDoc XRS þ system (Bio-Rad, Hercules CA, USA) as per the manufacturer's instructions. Protein band quantification was done using ImageJ v1.44 (Bethesda, MD, USA).

**Strep/FLAG tandem-affinity purification and mass spectrometry**

HEK293T were transfected using polyethyleneimine[55] for 48 h with N-terminally Strep/FLAG-tagged pVHL30, before being lysed in 30 mM Tris-HCl (pH 7.4), 150 mM NaCl, 0.5% Nonidet-P40, protease inhibitor cocktail (Roche, Basel, Switzerland) and phosphatase inhibitor cocktail 2 and 3 (Sigma) for 20 min at 4 1C. The Streptavidin- and FLAG-based purification steps were performed as previously described.[56] Five percent of final eluates were separated by SDS-PAGE and silver stained. Remaining samples were protein precipitated

with chloroform and methanol and stored at — 80 1C. Further processing of protein precipitates, mass spectrometry analysis and peptide identification was carried out as reported previously.[57] Proteins identified in control Strep/FLAG tandem- affinity purification experiments were manually removed from the analysis.

**Yeast two-hybrid experiments**

A human fetal brain cDNA library (Matchmaker, Clontech, Mountain View, CA, USA) was co-transfected with VHL-pMD4 into *Saccharomyces cerevisiae* strain Hf7c. Plasmids were recovered from His þ /LacZ þ clones and tested for specificity with irrelevant baits and 2.5 or 25 mM of 3-aminotriazole (Sigma).

**Immunoprecipitations**

HEK293 cells were lysed in 30 mM Tris-HCl (pH 7.4), 150 mM NaCl, 0.5% Nonidet-P40, protease inhibitor cocktail (Roche) for 20 min at 4 1C. The insoluble material was separated by centrifugation and the supernatants (containing 2.7 mg total protein) were rotated with 2 mg of anti-VHL or anti- HA (sc-57592, Santa Cruz Biotechnology) at 4 1C overnight. Samples were incubated with protein A/G-PLUS agarose beads (sc-2003, Santa Cruz Biotechnology) for 2 h at 4 1C. The beads were then washed with ice-cold lysis buffer three times, and proteins were resuspended in loading buffer and boiled for 5 min. The resulting samples were used to perform western blotting using anti-PDCD5 and anti-VHL antibodies.

**qPCR analysis**

Total RNA was isolated using trizol (Invitrogen, Carlsbad, CA, USA) and cDNA was made using iScript (Bio-Rad). qPCRs were run using iQ SYBR Green Supermix (Bio-Rad) on a myIQ iCycler (Bio-Rad). The following primers were used: *p21* fw: $5^0$-tgtcaggaaaagcagcagaa-$3^0$, *p21* rv: $5^0$-ctggtgttttcgggatgttt-$3^0$, *bax* fw: $5^0$-gcaagttcaactggggaaga-$3^0$, *bax* rv: $5^0$-gtcaggaaccctggttgaaa-$3^0$, *puma* fw: $5^0$-tcccctccagcttaaggaat-$3^0$, *puma* rv: $5^0$-atcccagaatcgtgatgtcc-$3^0$, *birc2* fw: $5^0$-ccagtcccatttcatctcgt-$3^0$, *birc2* rv: $5^0$-agtgtcaaggcgttcctgtt-$3^0$, *birc5a* fw: $5^0$-ttgaagacgcagtgaagctc-$3^0$, *birc5a* rv: $5^0$-aaaaggaccacagccaaatg-$3^0$, *cflar* fw: $5^0$-ggatcacagaagccccagta-$3^0$, *cflar* rv: $5^0$-ggcattggaacacttcctgt-$3^0$, *p53* fw: $5^0$-ttaagtgatgtggtgcctgcct-$3^0$, *p53* rv: $5^0$-agcttctttccctgtttgggct-$3^0$, *Vhl* fw: $5^0$-ctcagccctacccgatcttac-$3^0$, *Vhl* rv $5^0$-acattgagggatggcacaaac-$3^0$, *Rpl27* fw: $5^0$-ggtgccatcgtcaatgttctt-$3^0$, *Rpl27* rv: $5^0$-cgccctcctttcctttctgc-$3^0$. *Pdcd5* fw: $5^0$-atggcggacgaagaacttgag-$3^0$, *Pdcd5* rv: $5^0$-gggctgactgatccagaact-$3^0$, *RPLp0:* fw: 5'-tgcacaatggcagcatctac-3'. *RPLp0* rv: 5'-atccgtctccacagacaagg-3'. Survivin fw: $5^0$-agaactggcccttcttg- gagg-$3^0$, Survivin rv: $5^0$-ctttttatgttcctctatggggtc-$3^0$. Three biological replicates and at least two technical replicates were performed for each measurement.

**Immunohistochemistry and AO staining**

Zebrafish embryos were grown in 200 mM of 1-phenyl 2-thiourea from 28 hours post fertilization (hpf) onwards. For pH3 staining, embryos were irradiated and fixed overnight in 4% paraformaldehyde.[58] Embryos were then dehydrated by successive incubation in 25, 50, 75 and 100% methanol. The next day, embryos were rehydrated, washed in phosphate buffered saline (PBS) with 0.1% Tween (PBST) four times and digested with 10 mg/ml of proteinase K at room temperature for 20 min. Then, embryos were washed in PBST and refixed in 4% paraformaldehyde for 20 min, washed in PBST five times and blocked in blocking buffer (PBST containing 10% lamb serum, 1% DMSO and 0.1% Tween-20) for at least 2 h and incubated in rabbit a-pH3 antibody (1:200; Upstate Biotechnology, Lake Placid, NY, USA) in blocking buffer overnight at 4 1C. The embryos were washed extensively in PBST and incubated in Alexa-594 donkey a-rabbit IgG (1:200; Invitrogen) at 4 1C overnight, washed extensively in PBST and mounted in 70% glycerol. For AO staining, embryos were irradiated and soaked in 10 mg/ml AO (Sigma) for 30 min, washed six times in E3 embryo water and sedated with Tricane (MS- 222).[52] Photos were taken with a Leica MZ FLIII microscope (Leica, Wetzlar, Germany) and cells were counted using ImageJ v1.44. Embryos were genotyped afterwards using Sanger sequencing, as previously described.[59]



**siRNA treatments**

Cells were seeded onto coverslips sterilized with 70% ethanol. mIMCD3 cells were transfected using the Lipofectamine RNAiMAX reagent (Invitrogen) according to the manufacturer's instructions. Mouse *Vhlh* siRNA pool (L-040755), mouse *PDCD5* siRNA pool (target Gm3837, L-168868), human *Survivin* siRNA pool (target BIRC5332, L-0034459) and control siRNA pool (D–001206–13) were purchased from Dharmacon (Layfayette, CO, USA).

**Immunocytochemistry**

Coverslips with cells were rinsed with PBS and fixed with 4% PFA for 15 min at room temperature followed by permeabilization with 1% bovine serum albumin (BSA) plus 0.1% Triton X-100 in PBS. Cells were then subjected to immunofluorescence staining with anti-PDCD5 (1:500; SAB3500258, Sigma) for 3 h at room temperature. Secondary antibody Alexa Fluor-488 anti-rabbit (1:500; Invitrogen) was incubated at room temperature for 2 h. Nuclei were counterstained with $4^0$,6-diamidino-2- phenylindole (DAPI) (1:5000) and mounted on slides using Fluoromount G (Southern Biotech, Birmingham, AL, USA). Cells were examined using a Zeiss LSM700 confocal microscope and photographed using Zeiss Zen black edition software (Jena, Germany).

**Caspase assays**

Three 5 d.p.f. zebrafish embryos per sample were lysed in an opaque 96- well plate (Greiner Bio-One, Alphen a/d Rijn, The Netherlands) as previously described.[54] For cells, $2 \times 10^4$ cells per well were seeded in 96-well plates and allowed to grow overnight. Medium was aspirated and the cells were lysed directly in the Caspase-Glo 3/7 or Caspase-Glo 2 reagent (Promega, Madison, WI, USA). Lysates were then transferred to an opaque 96-well plate. Luminescence resulting from caspase activity was measured using a Berthold Centro $XS^3$ LB960 microplate reader (Berthold Technologies, Bad Wildbad, Germany).

**Conflict of interest**

The authors declare no conflict of interest.

**Acknowledgements**

This research was supported by grants from the European Community's Seventh Framework Programme FP7/2009 under grant agreement 241955, SYSCILIA and 305608, EURenOmics (RHG). We would like to thank Susanne Lens for the kind gift of siRNA against *Survivin*, the animal caretakers of the Hubrecht Institute, and www.art- 4-science.com for the creation of the graphic illustration.

## REFERENCES


1. Gerlinger M, Rowan AJ, Horswell S, Larkin J, Endesfelder D, Gronroos E *et al.* Intratumor heterogeneity and branched evolution revealed by multiregion sequencing. *N Engl J Med* 2012; 366: 883–892.
2. Sato Y, Yoshizato T, Shiraishi Y, Maekawa S, Okuno Y, Kamura T *et al.* Integrated molecular analysis of clear-cell renal cell carcinoma. *Nat Genet* 2013; 45: 860–867.
3. Cancer Genome Atlas Research Network. Comprehensive molecular characterization of clear cell renal cell carcinoma. *Nature* 2013; 499: 43–49.
4. Cohen HT, McGovern FJ. Renal-cell carcinoma. *N Engl J Med* 005;353:2477–2490
5. Motzer RJ, Bander NH, Nanus DM. Renal-cell carcinoma. *N Engl J Med* 1996; 335: 865–875.
6. Hsu T. Complex cellular functions of the von Hippel-Lindau tumor suppressor gene: insights from model organisms. *Oncogene* 2012; 31: 2247–2257.
7. Semenza GL. Targeting HIF-1 for cancer therapy. *Nat Rev Cancer* 2003; 3: 721–732.
8. Kondo K, Klco J, Nakamura E, Lechpammer M, Kaelin Jr WG. Inhibition of HIF is necessary for tumor suppression by the von Hippel-Lindau protein. *Cancer Cell* 2002; 1: 237–246.
9. Mack FA, Rathmell WK, Arsham AM, Gnarra J, Keith B, Simon MC. Loss of pVHL is sufficient to cause HIF dysregulation in primary cells but does not promote tumor growth. *Cancer Cell* 2003; 3: 75–88.
10. Maranchie JK, Vasselli JR, Riss J, Bonifacino JS, Linehan WM, Klausner RD. The contribution of VHL substrate binding and HIF1-alpha to the phenotype of VHL loss in renal cell carcinoma. *Cancer Cell* 2002; 1: 247–255.
11. Horn HF, Vousden KH. Coping with stress: multiple ways to activate p53. *Onco-gene* 2007; 26: 1306–1316.
12. Kubbutat MH, Jones SN, Vousden KH. Regulation of p53 stability by Mdm2. *Nature* 1997; 387: 299–303.
13. Graeber TG, Peterson JF, Tsai M, Monica K, Fornace Jr AJ, Giaccia AJ. Hypoxia induces accumulation of p53 protein, but activation of a G1-phase checkpoint by low-oxygen conditions is independent of p53 status. *Mol Cell Biol* 1994; 14: 6264–6277.
14. Alarcon R, Koumenis C, Geyer RK, Maki CG, Giaccia AJ. Hypoxia induces p53 accumulation through MDM2 down-regulation and inhibition of E6-mediated degradation. *Cancer Res* 1999; 59: 6046–6051.
15. Sermeus A, Michiels C. Reciprocal influence of the p53 and the hypoxic pathways. *Cell Death Dis* 2011; 2: e164.
16. Chen LN, Wang Y, Ma DL, Chen YY. Short interfering RNA against the PDCD5 attenuates cell apoptosis and caspase-3 activity induced by Bax overexpression. *Apoptosis* 2006; 11: 101–111.
17. Xu L, Chen Y, Song Q, Xu D, Wang Y, Ma D. PDCD5 interacts with Tip60 and functions as a cooperator in acetyltransferase activity and DNA damage-induced apoptosis. *Neoplasia* 2009; 11: 345–354.
18. Xu L, Hu J, Zhao Y, Hu J, Xiao J, Wang Y *et al.* PDCD5 interacts with p53 and functions as a positive regulator in the p53 pathway. *Apoptosis* 2012; 17: 1235–1245.
19. Chen Y, Sun R, Han W, Zhang Y, Song Q, Di C *et al.* Nuclear translocation of PDCD5 (TFAR19): an early signal for apoptosis? *FEBS Lett* 2001; 509: 191–196.
20. Zucchi I, Mento E, Kuznetsov VA, Scotti M, Valsecchi V, Simionati B *et al.* Gene expression profiles of epithelial cells microscopically isolated from a breast- invasive ductal carcinoma and a nodal metastasis. *Proc Natl Acad Sci USA* 2004; 101: 18147–18152.
21. Yang YH, Zhao M, Li WM, Lu YY, Chen YY, Kang B *et al.* Expression of programmed cell death 5 gene involves in regulation of apoptosis in gastric tumor cells. *Apoptosis* 2006; 11: 993–1001.
22. Spinola M, Meyer P, Kammerer S, Falvella FS, Boettger MB, Hoyal CR *et al.* Association of the PDCD5 locus with lung cancer risk and prognosis in smokers. *J Clin Oncol* 2006; 24: 1672–1678.
23. Xiong L, Tan WL, Yu ZC, Wu YD, Huang H, Zhao GZ *et al.* [Expression of TFAR19(PDCD5) in normal human kidney, renal clear cell carcinoma, normal human bladder and bladder carcinoma]. *Nan Fang Yi Ke Da Xue Xue Bao* 2006; 26: 805–809.
24. Tan WL, Xiong L, Zheng SB, Yu ZC, Qi H, Du YJ *et al.* [Relationship between programmed cell death 5 protein expression and prognosis of renal clear cell carcinoma]. *Nan Fang Yi Ke Da Xue Xue Bao* 2006; 26: 1316–1318.
25. Szymanska K, Moore LE, Rothman N, Chow WH, Waldman F, Jaeger E *et al.* TP53, EGFR, and KRAS mutations in relation to VHL inactivation and lifestyle risk factors in renal-cell carcinoma from central and eastern Europe. *Cancer Lett* 2010; 293: 92–98.
26. Albers J, Rajski M, Schonenberger D, Harlander S, Schraml P, von Teichman A *et al.* Combined mutation of Vhl and Trp53 causes renal cysts and tumours in mice. *EMBO Mol Med* 2013; 5: 949–964.
27. Roe JS, Kim H, Lee SM, Kim ST, Cho EJ, Youn HD. p53 stabilization and transac- tivation by a von Hippel-Lindau protein. *Mol Cell* 2006; 22: 395–405.
28. Lane DP. Exploiting the p53 pathway for the diagnosis and therapy of human cancer. *Cold Spring Harb Symp Quant Biol* 2005; 70: 489–497.
29. Dong Z, Nishiyama J, Yi X, Venkatachalam MA, Denton M, Gu S *et al.* Gene promoter of apoptosis inhibitory protein IAP2: identification of enhancer elements and activation by severe hypoxia. *Biochem J* 2002; 364: 413–421.
30. Dong Z, Wang JZ, Yu F, Venkatachalam MA. Apoptosis-resistance of hypoxic cells: multiple factors involved and a role for IAP-2. *Am J Pathol* 2003; 163: 663–671.
31. Qi H, Ohh M. The von Hippel-Lindau tumor suppressor protein sensitizes renal cell carcinoma cells to tumor necrosis factor-induced cytotoxicity by suppressing the nuclear factor-kappaB-dependent antiapoptotic pathway. *Cancer Res* 2003; 63: 7076–7080.
32. MacInnes AW, Amsterdam A, Whittaker CA, Hopkins N, Lees JA. Loss of p53 synthesis in zebrafish tumors with ribosomal protein gene mutations. *Proc Natl Acad Sci USA* 2008; 105: 10408–10413.

33. Esteban MA, Tran MG, Harten SK, Hill P, Castellanos MC, Chandra A *et al.* Regulation of E-cadherin expression by VHL and hypoxia-inducible factor. *Cancer Res* 2006; 66: 3567–3575.
34. Kibel A, Iliopoulos O, DeCaprio JA, Kaelin Jr WG. Binding of the von Hippel-Lindau tumor suppressor protein to Elongin B and C. *Science* 1995; 269: 1444–1446.
35. Pause A, Lee S, Worrell RA, Chen DY, Burgess WH, Linehan WM *et al.* The von Hippel-Lindau tumor-suppressor gene product forms a stable complex with human CUL-2, a member of the Cdc53 family of proteins. *Proc Natl Acad Sci USA* 1997; 94: 2156–2161.
36. Kamura T, Koepp DM, Conrad MN, Skowyra D, Moreland RJ, Iliopoulos O *et al.* Rbx1, a component of the VHL tumor suppressor complex and SCF ubiquitin ligase. *Science* 1999; 284: 657–661.
37. Tsuchiya H, Iseda T, Hino O. Identification of a novel protein (VBP-1) binding to the von Hippel-Lindau (VHL) tumor suppressor gene product. *Cancer Res* 1996; 56: 2881–2885.
38. Lai Y, Song M, Hakala K, Weintraub ST, Shiio Y. Proteomic dissection of the von Hippel-Lindau (VHL) interactome. *J Proteome Res* 2011; 10: 5175–5182.
39. Xu L, Hu J, Zhao Y, Xiao J, Wang Y, Ma D *et al.* PDCD5 interacts with p53 and functions as a positive regulator in the p53 pathway. *Apoptosis* 2012; 17: 1235–1245.
40. Sansam CL, Cruz NM, Danielian PS, Amsterdam A, Lau ML, Hopkins N *et al.* A vertebrate gene, ticrr, is an essential checkpoint and replication regulator. *Genes Dev* 2010; 24: 183–194.
41. Cui D, Li L, Lou H, Sun H, Ngai S-M, Shao G *et al.* The ribosomal protein S26 regulates p53 activity in response to DNA damage. *Oncogene* 2014; 33: 2225–2235.
42. Haase VH, Glickman JN, Socolovsky M, Jaenisch R. Vascular tumors in livers with targeted inactivation of the von Hippel-Lindau tumor suppressor. *Proc Natl Acad Sci USA* 2001; 98: 1583–1588.
43. Kleymenova E, Everitt JI, Pluta L, Portis M, Gnarra JR, Walker CL. Susceptibility to vascular neoplasms but no increased susceptibility to renal carcinogenesis in Vhl knockout mice. *Carcinogenesis* 2004; 25: 309–315.
44. Rankin EB, Tomaszewski JE, Haase VH. Renal cyst development in mice with conditional inactivation of the von Hippel-Lindau tumor suppressor. *Cancer Res* 2006; 66: 2576–2583.
45. Fu L, Wang G, Shevchuk MM, Nanus DM, Gudas LJ. Generation of a mouse model of Von Hippel-Lindau kidney disease leading to renal cancers by expression of a constitutively active mutant of HIF1alpha. *Cancer Res* 2011; 71: 6848–6856.
46. Albers J, Rajski M, Schonenberger D, Harlander S, Schraml P, von Teichman A *et al.* Combined mutation of *Vhl* and *Trp53* causes renal cysts and tumours in mice. *EMBO Mol Med* 2013; 5: 949–964.
47. Roe JS, Kim H, Lee SM, Kim ST, Cho EJ, Youn HD. p53 stabilization and transac- tivation by a von Hippel-Lindau protein. *Mol Cell* 2006; 22: 395–405.
48. Mans DA, Vermaat JS, Weijts BG, van Rooijen E, van Reeuwijk J, Boldt K *et al.* Regulation of E2F1 by the von Hippel-Lindau tumour suppressor protein predicts survival in renal cell cancer patients. *J Pathol* 2013; 231: 117–129.
49. Roe JS, Kim HR, Hwang IY, Ha NC, Kim ST, Cho EJ *et al.* Phosphorylation of von Hippel-Lindau protein by checkpoint kinase 2 regulates p53 transactivation. *Cell Cycle* 2011; 10: 3920–3928.
50. Frew IJ, Krek W. pVHL: a multipurpose adaptor protein. *Sci Signal* 2008; 1: pe30.
51. Yuen JS, Sim MY, Siml HG, Chong TW, Lau WK, Cheng CW *et al.* Inhibition of angiogenic and non-angiogenic targets by sorafenib in renal cell carcinoma (RCC) in a RCC xenograft model. *Br J Cancer* 2011; 104: 941–947.
52. Westerfield M. *The Zebrafish Book. A Guide for the Laboratory Use of Zebrafish (Danio rerio)*. 4th edn (Univ. of Oregon Press: Eugene, OR, USA, 2000).
53. van Rooijen E, Santhakumar K, Logister I, Voest E, Schulte-Merker S, Giles R *et al.* A zebrafish model for VHL and hypoxia signaling. *Methods Cell Biol* 2011; 105: 163–190.
54. Pereboom TC, van Weele LJ, Bondt A, MacInnes AW. A zebrafish model of dys- keratosis congenita reveals hematopoietic stem cell formation failure resulting from ribosomal protein-mediated p53 stabilization. *Blood* 2011; 118: 5458–5465.
55. Kim EL, Wustenberg R, Rubsam A, Schmitz-Salue C, Warnecke G, Bucker EM *et al.* Chloroquine activates the p53 pathway and induces apoptosis in human glioma cells. *Neuro Oncol* 2010; 12: 389–400.
56. Coene KL, Mans DA, Boldt K, Gloeckner CJ, van Reeuwijk J, Bolat E *et al.* The ciliopathy-associated protein homologs RPGRIP1 and RPGRIP1L are linked to cilium integrity through interaction with Nek4 serine/threonine kinase. *Hum Mol Genet* 2011; 20: 3592–3605.
57. Boldt K, Mans DA, Won J, van Reeuwijk J, Vogt A, Kinkl N *et al.* Disruption of intraflagellar protein transport in photoreceptor cilia causes Leber congenital amaurosis in humans and mice. *J Clin Invest* 2011; 121: 2169–2180.
58. Shepard JL, Stern HM, Pfaff KL, Amatruda JF. Analysis of the cell cycle in zebrafish embryos. *Methods Cell Biol* 2004; 76: 109–125.
59. van Rooijen E, Voest EE, Logister I, Korving J, Schwerte T, Schulte-Merker S *et al.* Zebrafish mutants in the von Hippel-Lindau tumor suppressor display a hypoxic response and recapitulate key aspects of Chuvash polycythemia. *Blood* 2009; 113: 6449–6460.

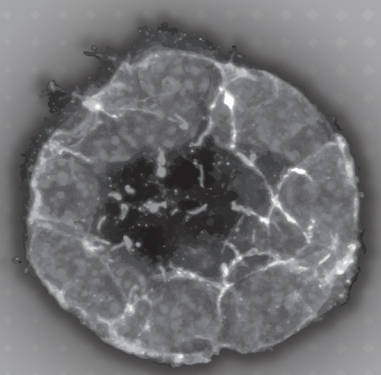

# CHAPTER 7

# Validation of novel regulators of renal ciliogenesis: HUWE1, STARD3NL, ANAPC4 and FAM110A

Manuscript submitted

**Klasson TD***, Slaats GG*, Chen Z, Noordegraaf S, Custers L, Logister I, Johnson CA, Knoers NV, Devuyst O, Giles RH

*these authors contributed to this work equally

## ABSTRACT

We recently performed an siRNA-based reverse genetics screen of all coding genes in the mouse genome in murine inner medullary collecting duct cells, which resulted in the identification of a list of unvalidated hits. We show here that siRNA knockdown of four of these hits with previously unidentified roles in ciliary regulation specifically reduces cells' ciliogenesis potential: *HUWE1*, *FAM110A*, *STARD3NL*, and *ANAPC4*. We further report that exogenous expression of human cDNAs of *HUWE1*, *FAM110A* and *STARD3NL* rescue ciliogenesis after siRNA-mediated depletion of endogenous murine mRNA. Our data suggest that these four genes have a novel role in renal ciliogenesis, with potential implication in ciliopathy pathophysiology. We further demonstrate that zebrafish with genome-edited *huwe1* appear to be haploinsufficient with chimeric animals manifesting phenotypes consistent with ciliopathies. Secondly, we speculate that STARD3NL may regulate ciliary membrane dynamics based on localization, but this hit requires specialized functional testing for further insight. We also demonstrate the function of ANAPC4 in the anaphase promoting complex/cyclosome (APC/C) does not seem to be redundant with its role in ciliogenesis in our assays, but invites further investigation. Lastly, we show that FAM110A has a role in microtubule stability and G1/S phase cell cycle progression, which may contribute to a role in ciliary initiation and/or maintenance. Ciliary roles of a subset of the hits from this large-scale screen provide new insights into the disease pathogenesis of ciliopathies and in particular opens up new areas of research in the molecular mechanisms by which these four proteins work.

## INTRODUCTION

Primary cilia are found on the apical/luminal surface of most renal cells, where they are thought to transduce extracellular signals and regulate proliferation, differentiation, transcription, migration, polarity and tissue morphology [1, 2]. Renal cilia integrate many developmental and pathological signalling pathways, including Wnt-, Hedgehog-, and GPCR-signalling [3]. Outside of the kidneys, primary cilia are essential for the development and healthy physiology of many different organ systems, including eye, liver, brain, pancreas, heart, and bone, and abnormal ciliary function can result in a large variety of diseases, known as ciliopathies, affecting different tissues and organ systems [4]. Renal cystic lesions are common across ciliopathies, typically arising from the distal end of the nephron in an area of the kidney corresponding to the inner medulla [4].

We have recently published an siRNA-based reverse genetics screen of all coding genes in murine inner medullary collecting duct (mIMCD3) cells that revealed several genes with an effect on ciliogenesis, but not on cell number [5]. One of the advantages of this approach is the ability to subsequently perform subset analyses. For example, we have used the initial screen data to demonstrate that the function of a subset of ion channels regulates renal ciliogenesis [6]. In the current study, we took four additional candidates from the reverse genetics screen for validation and initial functional testing, and found all four to robustly regulate cilia numbers: *Huwe1* (HECT, UBA and WWE Domain Containing 1, E3 Ubiquitin Protein Ligase), *Stard3nl* (START domain-3 containing N-terminal like protein), *Anapc4* (Anaphase-promoting complex subunit 4), and *Fam110a* (family with sequence similarity 110, member A). *Huwe1* and *Anapc4* were also significant hits from a ubiquitin proteasome screen (UPS) subset analysis that interrogated the role of UPS subunits in ciliary biology. In contrast, *Fam110a* and *Stard3nl* made the first cut-off for the siRNA reverse genetics screen but not the second. Despite this, we show that both *Fam110a* and *Stard3nl* functionally regulate ciliogenesis in IMCD3 cells and that FAM110A plays a role in microtubule dynamics. Based on these results, we conclude that our cut-off criteria was arguably too stringent and that the genome screen we published probably has a higher false negative rate than previously estimated.

While our analysis is not exhaustive, elucidating the role of these four genes in primary cilia offers new insights into the molecular networks regulating cilia initiation and/or maintenance, in addition to extending the known functions of these proteins, and will possibly supply functional data supporting a ciliopathy phenotype in patients with variant alleles in any of these genes.

## RESULTS

**Reverse genetics screen**

We performed an siRNA-based reverse genetics screen of coding genes in the mouse genome in mouse inner medullary collecting duct cells (mIMCD3 cells). This screen identified 112 new candidate ciliogenesis and ciliopathy genes, of which 44 components of the ubiquitin-proteasome system that, when down-regulated, impair cilium biogenesis. The effect of siRNA knockdown on ciliogenesis was assessed by calculating the percentage of cells with a single cilium, with the statistical significance of this effect assessed by calculating *z* scores ($z_{cilia}$). *z* scores were also calculated for the effect of the knockdown on cell number ($z_{cell}$), to exclude effects of cell proliferation or apoptosis on ciliogenesis, since these could be due to non-specific secondary processes [5]. Based on this analysis, we identified that the following four candidates had a significant negative effect on ciliogenesis but not on cell number: *Huwe1, Fam110a, Stard3nl, Anapc4* (Figure 1).

**HUWE1 is required for ciliation**

We started by asking whether endogenous Huwe1, the mouse homologue of HUWE1, is expressed in the cilium. Using immunofluorescence, we did not observe ciliary staining of endogenous Huwe1 or HUWE1 in ciliated murine IMCD3 cells or retinal pigment epithelial cells, respectively. Instead, we observed speckled cytoplasmic staining with some nuclear staining as well (data not shown). However, we hypothesized that HUWE1 localization might be more specific in polarized epithelial cells. To that end, we grew IMCD3 cells in polarized 3D spheroids and stained for endogenous Huwe1. Huwe1 was observed gathering at the apical edge of the lumen in spheroids, but again not in the cilia (Figure 2A). siRNA mediated knockdown of *Huwe1*in IMCD3 cells was validated by qPCR (Supplemental Figure 1A, n= 2 in triplicate, p= 0.017). Reducing the cellular levels of *Huwe1* in IMCD3 cells leads to a defect in ciliation in 3D cell culture (Figure 2B-C, n= 30 spheroids over two experiments, p<0.0001). We attempted to rescue this phenotype with ectopic transfection of human HUWE1 constructs resistant to the siRNA targeted to the murine Huwe1 orthologue to show specificity. However, after multiple attempts we concluded that IMCD3 cells cannot be transfected with full-length HUWE1 due to its size (482kDa). We therefore moved to another murine ciliated cell type, 3T3 fibroblasts, which are easier to transfect with large constructs. Knockdown of *Huwe1* in these cells by siRNA transfection was also confirmed by qPCR (Supplemental Figure 1B, n=2 in triplicate, p= 0.0018). Knockdown of endogenous *Huwe1* (si*Huwe1* vs si*Control*) in 3T3 cells also leads to a ciliation defect (n=600 cells scored over 3 experiments, p=0.0018, Figure 2D) which can be rescued by transfection with either full-length HUWE1 (n=30 spheroids over 3 experiments, p=0.0036) or a truncated version of HUWE1 (Figure 2D-E, n=30 spheroids over 3 experiments,

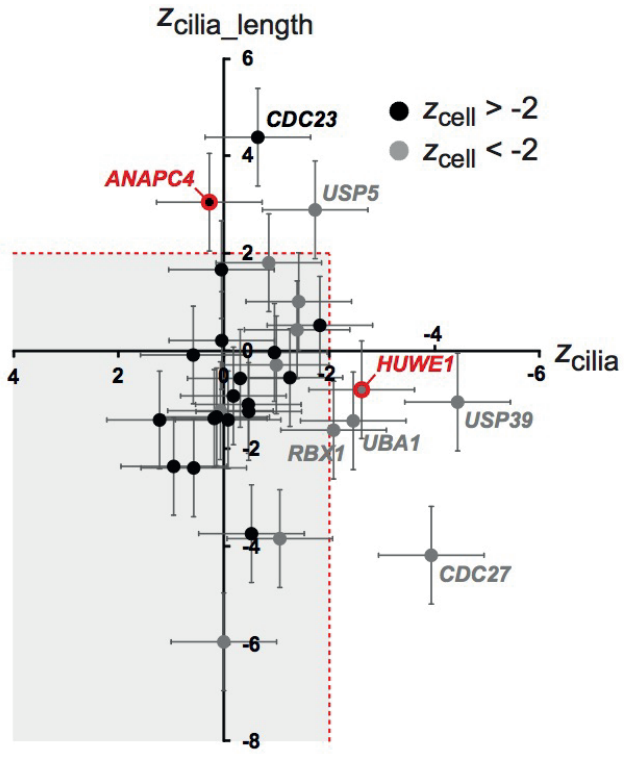


**Figure 1. Scatter-plot and images of the siRNA-based UPS screen.** (**A**) Scatter-plot of *z*-scores from both runs of the screen. The cut-offs of *z* cilia <-2 for both run 1 and run 2 are shown with dotted red lines. Grey and black points discriminate between *z* cell >-2 or <-2 (grey means exclusion).

p=0.034,) which retains its function [7]. To address the *in vivo* relevance of HUWE1, we attempted to create a stable *huwe1* mutant zebrafish using TALEN genome editing. Zebrafish embryos chimeric for an in-frame 6 nucleotide deletion-insertion mutation (resulting in 2 amino acid missense changes) in *huwe1* displayed a putative mild phenotype, including bent body axis in a proportion of the embryos, swim bladder development defects, and abnormalities of the gut and liver (Figure 2F). Attempts to create outcross F0 fish possessing nonsense mutations to generate a germline *huwe1*+/- zebrafish line were unsuccessful. Although injected mosaic animals survived and could breed, any offspring possessing a germline truncating mutation in *huwe1* did not reach adulthood (Figure 2G). This indicates that *huwe1* mutant alleles may be heterozygous lethal. We therefore did not pursue these zebrafish lines.

HUWE1 is a known interaction partner of Disheveled 2 (DVL2), a component of the canonical Wnt signaling pathway. Wnt signaling is an important modulator of many cellular

processes including cell fate determination, cell proliferation, cell polarity, cell motility and others [8, 9]. HUWE1 ubiquitinylates DVL2, inhibiting its multimerization, which is important for its function. Thus, HUWE1 usually acts as an modulator of Wnt signaling [7]. Wnt signaling passes through the primary cilium and components of the Wnt pathway have previously been shown to be involved in ciliogenesis, including DVL2, which was shown to be required for apical docking of the basal body [10]. Reduction of endogenous levels of *Huwe1* by siRNA does not cause a downstream change in *Axin2* (a Wnt-pathway target) signaling in IMCD3 cells (Figure 2H).

C. elegans *eel-1(okt1575)/huwe1* mutants do not have obvious ciliary defects as tested by dye-filling with lipophilic dye DiI, which is specifically taken up by the exposed ciliary endings of the amphid and phasmid neurons (not shown, data kindly provided by Marco Betist and Rik Korswagen, Hubrecht Institute, Utrecht, the Netherlands). Although this assay does not rule out any subtle defects in cilia function, the overall morphology and function of the amphid and phasmid ciliary endings appears intact.

**Figure 2. HUWE1 regulates ciliogenesis.** (**A**) Immunostaining of 3D spheroids of mIMCD3 cells for endogenous Huwe1 (green), beta-catenin (red), tight junctions (ZO-1, white), with DAPI counterstaining (blue) shows apical staining of Huwe1 in polarized cells. Scale bars 5 $\mu$m. (**B**) Immunostaining of 3D spheroids of mIMCD3 cells for cilia (Acetylated tubulin, red) beta-catenin (green), tight junctions (ZO-1, white), with DAPI counterstaining (blue), shows loss of cilia after *Huwe1* siRNA transfection. (**C**) Quantification of ciliary frequency in mIMCD3 spheroids after *Huwe1* siRNA transfection. 30 spheroids were scored per condition (n=2, p<0.0001. p value determined by student's t-test). (**D**) Quantification of ciliary frequency in murine 3T3 cells depleted for *Huwe1* also shows a significant reduction of cilia (400 cells scored for ciliation per condition, over 2 experiments. p=0.0018 as determined by student's t-test with multiple test correction), which can be resucued by exogenous expression of both a construct encoding full-length human HUWE-1 (n=30 spheroids over 2 experiments, p=0.0036 as determined by student's t-test with multiple test correction) and another construct encoding an N-terminal truncated HUWE1 that maintains its catalytic activity(n=30 spheroids over 2 experiments, p=0.034 as determined by student's t-test with multiple test correction). (**E**) Western blot showing endogenous (first two lanes) and overexpression of both full-length and truncated HUWE1 in 3T3 cells after transfection (middle and third lane). Western blots also showed expression of FLAG-tag (full-length HUWE1, H-FL) and HA-tag (truncated HUWE1, H-Tr or HUWE-Tr). Cep290 is used as a loading control because of the large size of full length HUWE1. (**F**) Sibling and genotyped insertion-deletion *huwe* mutant zebrafish embryos. Pictures taken at 5 days post fertilization. Mutant fish display frequent body axis abnormalities (half the embryos), abnormalities in the gut and possibly liver (arrows), as well as swim bladder agenesis (white asterisks). Anterior is to the right. (**G**) Table showing the results of matings from attempted outcross of *huwe* mutant fish with early stop mutations. No mutant alleles were found in genotypes of surviving adult fish. P value was determined by student's t-test. (**H**) Relative expression of *AXIN2*, a downstream target of Wnt signaling. No difference is observed after transfection of siRNA against *Huwe1*in mIMCD3 cells.

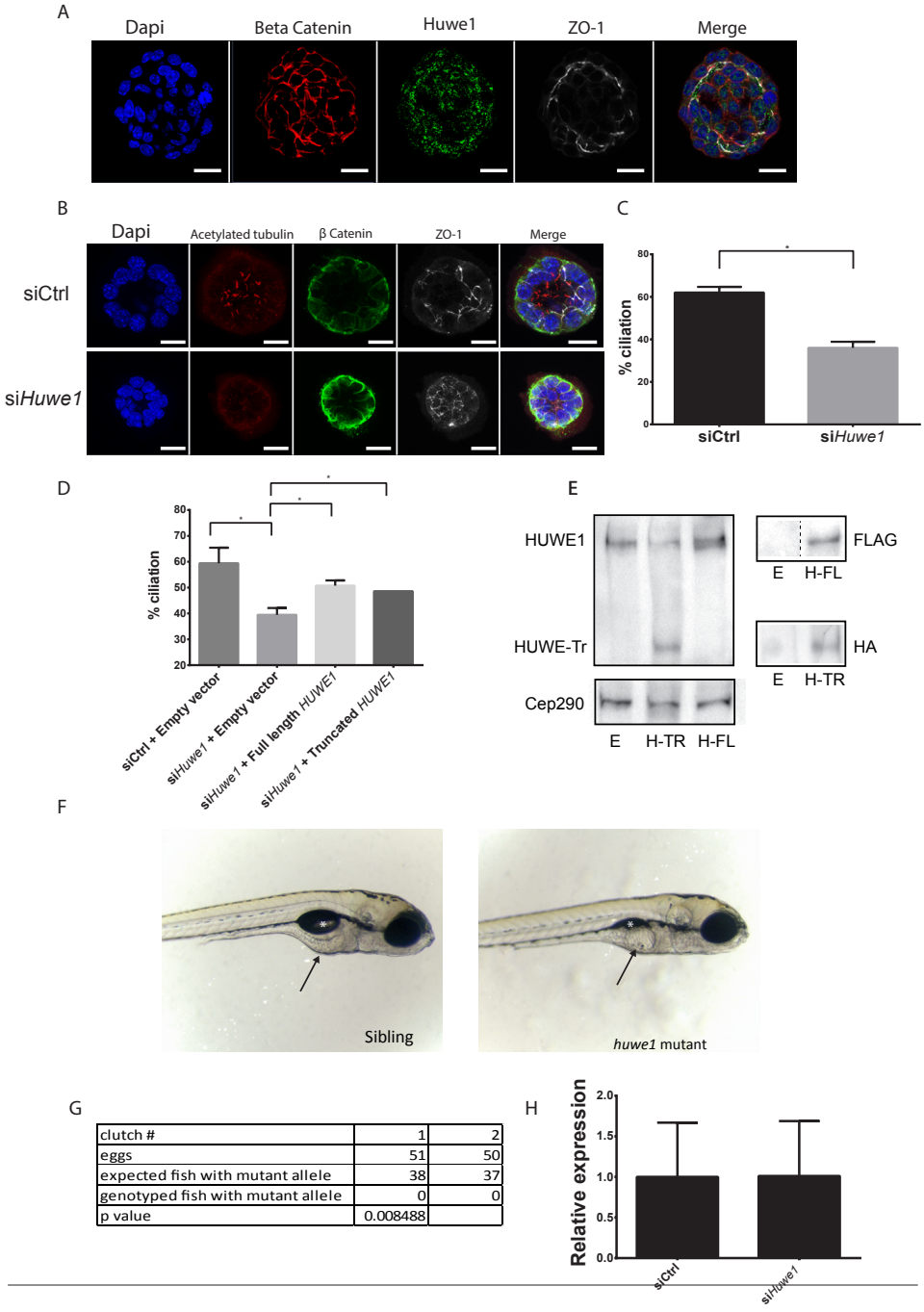


| | | |
|---|---|---|
| clutch # | 1 | 2 |
| eggs | 51 | 50 |
| expected fish with mutant allele | 38 | 37 |
| genotyped fish with mutant allele | 0 | 0 |
| p value | 0.008488 | |

◀ **Figure 2. HUWE1 regulates ciliogenesis**

**STARD3NL regulates ciliogenesis**

STARD3 [StAR (steroidogenic acute regulatory protein)-related lipid transfer domain-3] and its paralogue STARD3NL (STARD3 N-terminal like) are widely expressed proteins involved in cholesterol transport. STARD3NL is expressed in the endosome, where it binds cholesterol and forms heterodimers with STARD3, assisting in cholesterol transport and helping it to associate with STARD3 [11-13]. To validate the screen result that STARD3NL may regulate ciliogenesis, we first closely examined the localization of GFP-labelled exogenously transfected STARD3NL in ciliated human RPE-hTERT cells. We observed that STARD3NL-GFP localized to the endosomal membranes, as might be expected based on its known function. STARD3NL-positive endosomes were also sometimes found in close association with the base of the cilium, possibly the ciliary pocket (Figure 3A). siRNA mediated knockdown of the mouse homologue of STARD3NL, *Stard3nl,* via transfection with si*Stard3nl* was first confirmed via qPCR (Supplemental Figure 1C, n=2 in triplicate, $p<0.0001$). siRNA reduction of endogenous murine *Stard3nl* showed a significant reduction of ciliary frequency in 3D IMCD3 cultures compared with siControl transfected spheroids (Figure 3B-C n=25 spheroids over 2 experiments, $p=0.014$). Counting only GFP-positive spheroids, we were able to rescue the ciliogenesis defect with the STARD3NL-GFP construct shown in Figure 3A (Figure 3D, n=20 spheroids over 2 experiments, $p=0.022$). We postulate that STARD3NL is involved in the transport of cholesterol to the ciliary membrane.

**ANAPC4 regulates ciliogenesis**

The anaphase-promoting complex (APC/C; also known as the cyclosome) promotes metaphase-anaphase transition through ubiquitination of specific substrates such as mitotic cyclins, which are subsequently degraded by the proteasome. Evaluation of our siRNA screen dataset identified six proteins from the APC/C complex as hits in our knockdown-screen: APC4, APC5, CDC16, CDC20, CDC23=APC8, CDC27=APC3. Depletion of *Anapc4* which encodes APC4, was the only knockdown of an APC/C subunit to not be detrimental to overall cell numbers, and therefore the most interesting as a potential cilia gene. We validated the UPS and original screen with siRNA depletion of *Anapc4* in IMCD3 cells (Supplemental Figure 1D, n=3 in triplicate, $p<0.0001$) and observed a significant decrease in cilia not observed in the siControl experimental comparator (Figure 4A-4B, n=50 spheroids, experiment was repeated twice, $p=0.0019$). Rescue of this phenotype was not possible with overexpression of human ANAPC4 construct, because overexpression of any APC/C subunit has been shown to obstruct the function of the APC/C cyclosome complex [14]. Without the possible rescue of this target, we decided to focus on other targets and did not pursue additional functional studies of ANAPC4.

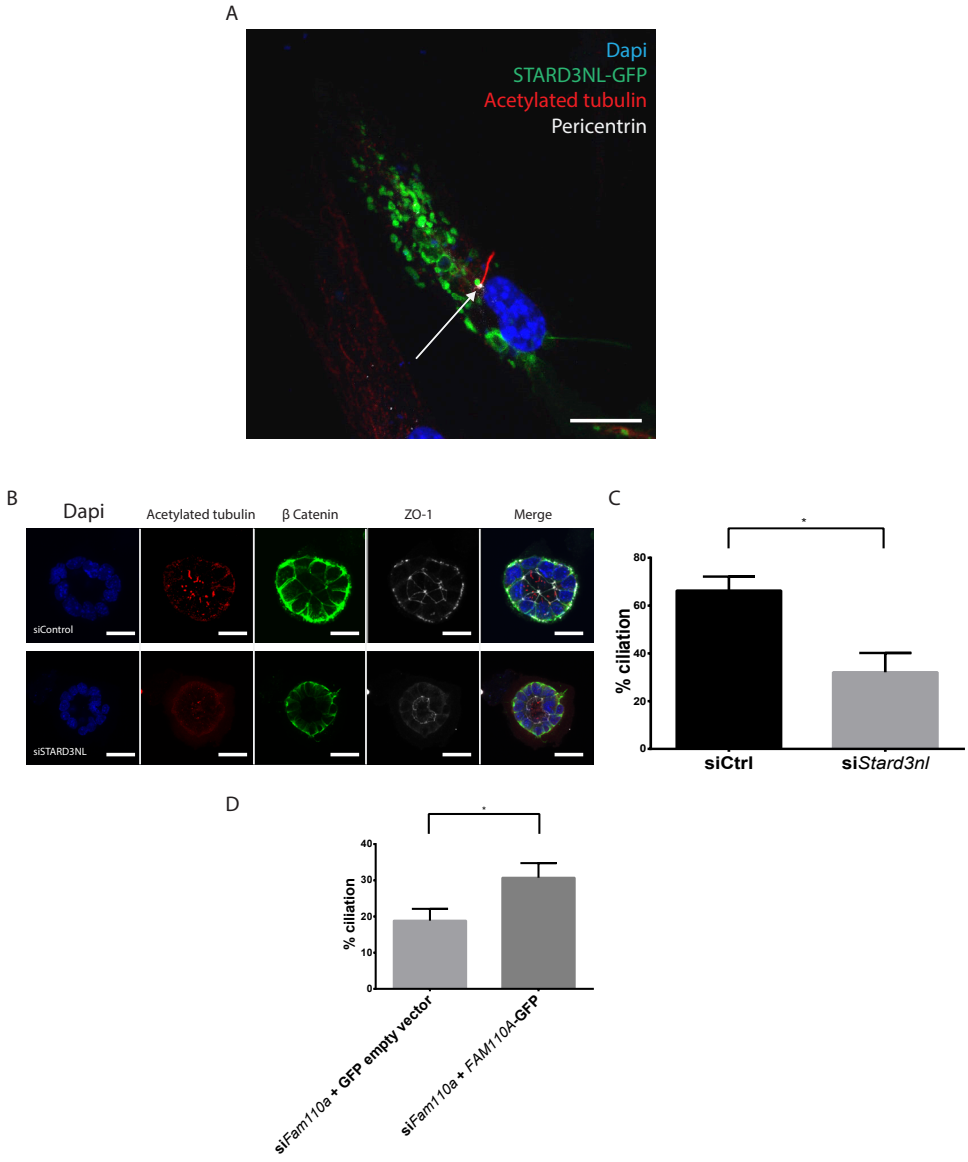


**Figure 3. STARD3NL regulates ciliogenesis.** (**A**) Staining of RPE-hTERT cells transfected with a human STARD3NL-GFP construct for cilia (acetylated tubulin, red) and the basal body (pericentrin, white) with DAPI counterstaining (blue) shows expression of ectopic STARD3NL-GFP in edosomal membranes, some of which are found near the base of the cilium (arrow). (**B**) Immunostaining of 3D spheroids of mIMCD3 cells for cilia (Acetylated tubulin, red) beta-catenin (green), tight junctions (ZO-1, white), with DAPI counterstaining (blue), shows loss of cilia after *Stard3nl* siRNA transfection. (**C**) Quantification of ciliation frequency in mIMCD3 spheroids after *Stard3nl* or Control (siCtrl) siRNA transfection. 25 spheroids were scored per condition over 2 experiments. p=0.014 as determined by student's t-test). (**D**) Quantification of rescue of ciliary frequency in mIMCD3 cells transfected with a human STARD3NL-GFP or empty-GFP construct. 20 spheroids were scored over 2 experiments. p=0.022 as determined by student's t-test.

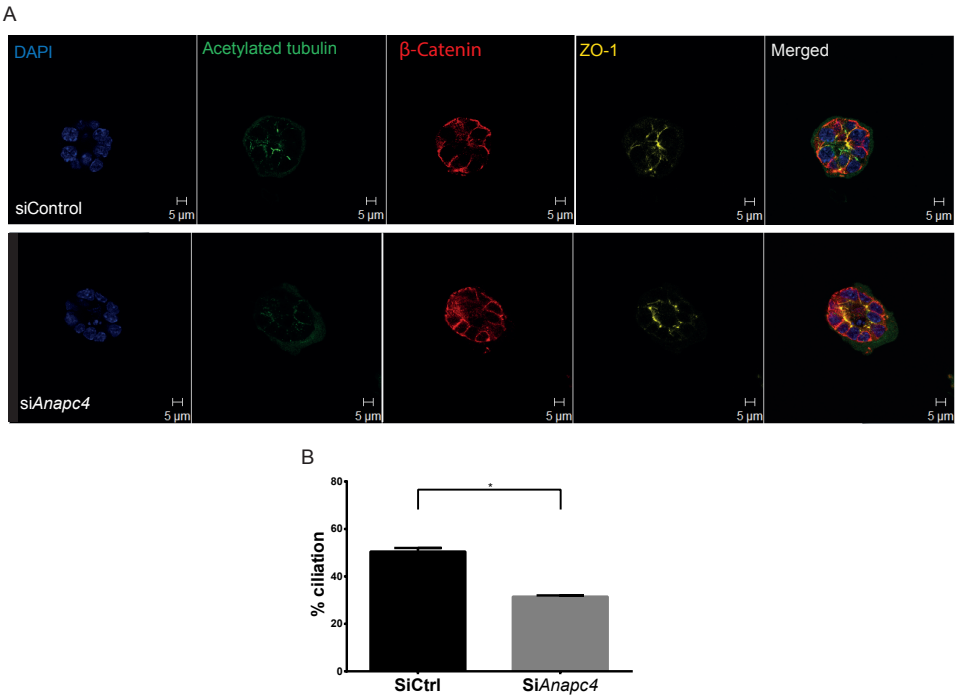


**Figure 4. ANAPC4 regulates ciliogenesis.** (**A**) Immunostaining of 3D spheroids of mIMCD3 cells for cilia (Acetylated tubulin, green), beta-catenin (red), tight junctions (ZO-1, yellow), with DAPI counterstaining (blue) shows loss of cilia after *Anapc4* siRNA transfection Scale bar 5 $\mu$m. (**B**) Quantification of ciliary frequency in mIMCD3 spheroids after *Anapc4* siRNA transfection. 50 spheroids were scored per condition (n=2). p=0.0019.

**FAM110A regulates ciliogenesis**

Not much is known about FAM110A, except that it localizes to centrosomes where it putatively binds known ciliopathy protein Centrosome And Spindle Pole Associated Protein 1 (CSPP1), and that it accumulates at the microtubule organization center in interphase and at spindle poles in mitosis, suggesting a centrosomal function [15]. Thus, we were interested in validating and obtaining some functional data on this hit, even though it did not make the final 112 hits from the screen [5]. A GFP-labeled construct of human FAM110A localized to the base of cilia in IMCD3 cells (Figures 5A). We then validated the screen by siRNA knockdown of *Fam110a* in IMCD3 3D spheroids (Figure 5B) which resulted in a significant reduction of cilia (Figure 5C, n=50 spheroids per experiment, repeated twicep=0.0006,). Despite this observation, we did not see a significant reduction in *Fam110a* expression after treating IMCD3 cells with siRNA directed against *Fam110a*, although a trend was visible (Supplemental Figure 1E, n=3 in triplicate, p=0.15). However, overexpression of a GFP-labelled construct of human FAM110A in IMCD3 spheroids

treated with si*Fam110a* to reduce the endogenous levels of this target resulted in a rescue of the ciliogenesis defect, suggesting this hit is specific (Figure 5D, n=50 spheroids per experiment, repeated twice, p=0.00414,). RPE-hTERT are amenable to cell cycle analyses [16, 17], so we next asked whether siRNA knockdown of the human FAM110A in RPE-hTERT cells would affect cell cycle progression. To this end we BrDU-pulsed the cells to label cells undergoing replication, and then FACSed the cells on BrDU positivity and DNA content to quantify the percentage of cells in G1 phase of the cell cycle (Figure 5E). Firstly we synchronized the cells in S-phase on two consecutive days with thymidine and then release the cells in regular medium for 16 hours before prior to harvesting and we observed a significant increase in the number of cells in G1. RPE-hTERT cells starved for serum also accumulate in G1, but when we stimulate the cells to enter the cell cycle by addition of serum, we note that the cells with reduced endogenous levels of FAM110A are slower to leave G1. Collectively, we observed that cells with lower levels of FAM110A showed a significant increase of cells in G1 compared to siControl transfected cells (Figure 5E, $p<0.05$, n=40,000 cells in 2 experiments).

Because FAM110A localizes to the spindle poles during mitosis, we hypothesized that FAM110A may be involved in microtubule dynamics, which may explain its effect on ciliogenesis. We therefore examined the effect of microtubule stability effecting agents on COS-7 cells transfected with *FAM110A*-GFP. Cells transfected with either empty vector or *FAM110A*-GFP were either untreated, or treated with taxol as a positive control or treated with nocodazol (Figure 5F n=60 cells scored over 2 experiments). FAM110A overexpression caused microtubule stabilization on its own to a slightly lesser degree than taxol, which taxol further increased in the cells transfected with *FAM110A*-GFP. FAM110A overexpression also causes a nocodazol protection phenotype, as nocodazol was unable to rescue the hyperstabilization of microtubules in transfected cells. Ice treatment caused a reduction of microtubule stabilization as a negative control (supplemental figure 1F). FAM110A is therefore likely to play a role in microtubule stabilization. It is possible that the ciliogenesis defect after siRNA depletion of FAM110A is due to the loss of this microtubule stabilization activity.

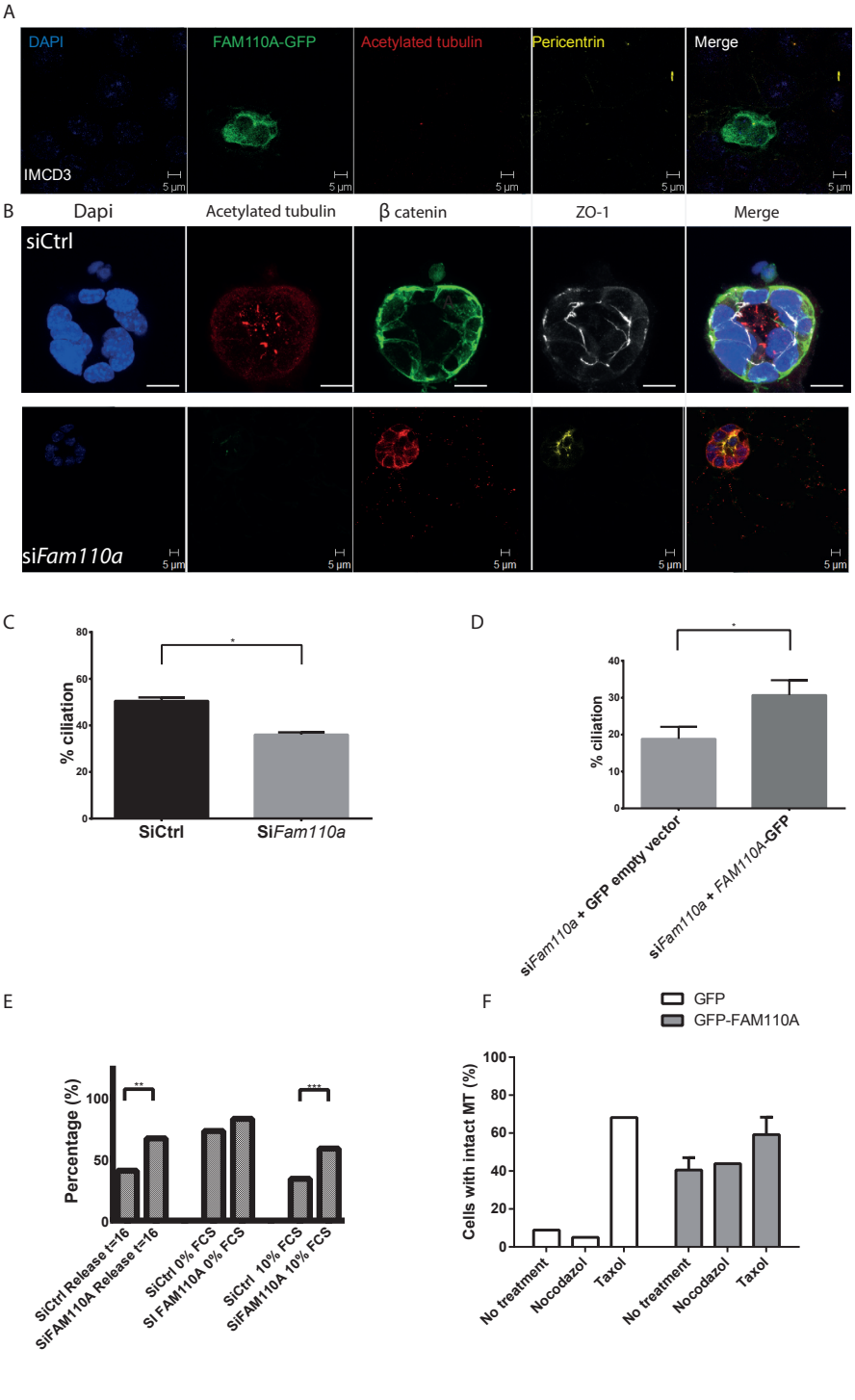

## DISCUSSION

Here we have employed the data derived from an unbiased siRNA knockdown screen in a mouse ciliated cell renal line and identified four proteins previously unlinked to ciliary function that we validated in our *in vitro* systems. With the exception of ANAPC4, the ciliogenesis defect seen in 3D spheroids after knockdown of these candidates can be rescued by exogenous overexpression of the WT human orthologs, which are not targeted by the mouse siRNA, suggesting biological specificity. For two candidates, HUWE1 and FAM110A, we performed additional functional experiments to elucidate the functional significance of these proteins in ciliogenesis.

Human genetic data acquired from patients or animal models with ciliopathies has generated a list of ciliopathy genes which we know is far from comprehensive [18]. Not even one third of patients with a clinically evident ciliopathy have a known causal mutation. In this work we have demonstrated that previous guidelines for determining possible ciliopathy genes may have been too stringent, that many more possible candidate ciliopathy genes probably exist in the original data. The results of screens such as these may serve the research community better as guidelines or lists of priorities. Stringent cut-off points in screens may not accurately reflect the more subtle biology when hits are investigated individually.



▶ **Figure 5. FAM110A regulates ciliogenesis.** (**A**) Overexpression of GFP-FAM110A in mIMCD3 cells reveals a centrosomal (PCNT, yellow) localization at the base of the primary cilium ( AcTub, red). Scale bar 5 $\mu$m. (**B**) Immunostaining of 3D spheroids of mIMCD3 cells for cilia (Acetylated tubulin, red), beta-catenin (green), tight junctions (ZO-1, white), with DAPI counterstaining (blue) shows loss of cilia after control (siCtrl) or *Fam110a* siRNA (si*Fam100a*) transfection. (**C**) Quantification of ciliary reduction in 3D IMCD3 spheroids. n=3, 50 spheroids counted per experiment. p=0.0006. (**D**) FAM110A-GFP overexpression in si*Fam100a*-treated IMCD3 3D spheroids significantly increased ciliary frequency as compared to spheroids transfected with an empty GFP vector. 50 green fluorescent spheroids were scored per condition (n=2). p=0.00414). (**E**) RPE-hTERT cells were pulse-labeled with BrDU to visualize S-phase and counterstained with DAPI and FACS sorted for cell cycle profiling (% cells in G1 shown on y-axis). RPE-hTERT cells were synchronized in S-phase by double thymidine (10mM) block and then released with normal medium for 16 hours (t=16). However, RPE cells serum-starved (0% FCS) for 24 hours did not show a difference in % G1. When those same cells re-enter the cell cycle by addition of 10% FCS for 16 hours, FAM110A depletion causes an arrest in G1. 40,000 events measured per condition; $n = 2$, **p<0.01 or ***p<0.001. Means are shown, S.E.M. are calculated in the statistics but are not shown here as error bars (**F**) FAM110A-GFP stabilizes microtubules. % of cells with intact stable microtubules in COS-7 cells overexpressing either empty-GFP or FAM110A-GFP treated with either nothing, 10 $\mu$M nocodazol for 20 minutes, or 10 $\mu$M taxol for 20 minutes. (60 cells, n=2). Means are graphed and S.E.M. are error bars.

Patient genetic data have guided researchers to many of the obvious ciliary genes such as required structural components and other genes that, when mutated, cause severe anomalies without the presence of other mutations. The current challenge is to identify genes that have more subtle regulatory effects such as control of post-translational modification and temporo-spatial aspects of ciliogenesis, as well as ciliary function and signalling pathways. For example, here we examined the function of a subset of ubiquitin ligases and concluded that the two we selected both have robust effects on ciliogenesis. This is an example of using forward genetics to identify novel regulators. Interestingly, we also found that two unrelated targets also affect ciliogenesis even though they have previously been removed from our screens. Our functional approach is somewhat limited in terms of its ability to detect genes that are directly involved in ciliogenesis. Nonetheless, here we have shown that some genes can affect cilia number, even though we previously dismissed them as candidates.

Taking each hit individually, there are several caveats to this study to be considered. Firstly, HUWE1 is a known tumor suppressor and interactor with Wnt regulator Dishevelled. Our data are in accordance with the published data that suggests that knockdown of *Huwe1* does not affect canonical Wnt target genes [7]. Nevertheless, C. elegans mutants for an ortholog of *Huwe1*, *eel-1*, do not have ciliopathy phenotype and our zebrafish chimeric F0 lines had a complex phenotype only partially overlapping with ciliopathies as well. Our data suggests that levels of *huwe1* in zebrafish are critical and that it may be haploinsufficient, at least in the two lines analyzed here. Additional experiments are warranted. For example, creating inducible lines could regulate the temporal and organ-specific deletion of Huwe1 *in vivo*.

Secondly, we have identified members of the APC/C cell cycle master regulator complex to be high confidence and well validated hits in our siRNA ciliogenesis screen although there were noticeably variable effects on the overall cell numbers, with ANAPC4 being the only subunit not detrimental to overall cell numbers. This is surprising since it would be anticipated that any APC/C subunit's depletion would cause cell cycle arrest because they all should be found in the complex; immunoprecipitating one subunit likewise clears cellular extracts of all the other subunits [19]. However, the strongest knockdown we observed only constituted a 50% reduction of endogenous *Anapc4* levels, which may explain the difference with the other APC/C components. A really efficient *ANAPC4* knockdown would likely disrupt the APC/C complex and should ultimately result in a mitotic block. We therefore hypothesize that our ANAPC4 effect is either caused by subtly reduced APC/C activity in interphase and a concomitant specific rise of an APC/C substrate, or ANAPC4 has a ciliary function as a non-complexed subunit. For the former scenario, the most attractive substrate to test first would be NEK1, a target of APC/C and a known regulator of ciliary resorption upon serum-starvation [20, 21]. We will follow this up also by examining the role of Cdh1 and Aurora A in the context of *Anapc4* depletion [19].

Thirdly, we only briefly examined the role of STARD3NL in ciliogenesis, observing only a novel association with the base of the cilium (possibly the ciliary pocket) and testing the fidelity of the siRNA knockdown with a rescue construct. Our data suggest a role for STARD3NL in the delivery of membrane lipoproteins for the generation or extension of the ciliary membrane. It is possible that the effect of reduction of *Stard3nl* in IMCD3 cells affects all membrane structures and that our effect is not specific to the cilium. We would like to test this hypothesis by fluorescently labelling cholesterol *in vitro* and filming the generation of the cilium with a counter marker such as ARL13b [22]. Fluorescence recovery after photobleaching (FRAP) experiments would also be excellent follow-up experiments to pinpoint this function.

Lastly, we observed that FAM110A regulates ciliogenesis and that it has a role in microtubule stability. Very little is known about this member of the FAM110 family, except that it is a putative interaction partner with CSPP1 [23], whose gene is known to be mutated in ciliopathy patients [24]. We were able to validate the role of FAM110A in ciliogenesis as a specific and robust phenotype rescuable by ectopic expression of FAM110A, even though we were only able to modestly (and insignificantly) decrease the endogenous levels of mRNA by siRNA treatment. It is known that *FAM110A* mRNA expression is regulated by the cell cycle [15] which probably explains the inefficient siRNA knockdown in unsynchronized cells. It would be interesting to test the effects of *CSPP1* mutation on FAM110A function in the future, for example in patient cells, to determine whether FAM110A function is independent or downstream of CSPP1.

In conclusion, this manuscript validates and explores four genes from a siRNA ciliogenesis screen. Two of these genes did not make the stringency settings for the screen, but still provided a significant and specific effect on ciliary frequency in renal IMCD3 cells. We conclude that settings for the screen were possibly too stringent and that additional hypothesis-generating hits can be harvested from the initial screen data. Each of the genes we superficially explored are indeed hypothesis-generating are worthy of follow-up functional studies of a more extensive nature.



## MATERIAL AND METHODS

**Cell culture**

Mouse inner medullary collecting duct (mIMCD3) cells were cultured as previously described [17].

**Reverse genetics visual screen**

The reverse genetics visual screen was performed as described previously [5].

**Antibodies and reagents**

Antibodies used are rabbit anti-HUWE1 (Novus biologicals, NBP1-76795), mouse anti-acetylated tubulin (Sigma T6793) and mouse anti-β-actin (AC-15 Sigma A5441, 1;20000), rat anti-ZO-1 (Santa Cruz, 1:500), rabbit anti-β-catenin (BD Bioscience, 1:500), rabbit anti-pericentrin (Abcamm Ab4448 1:400), anti-CEP290 (Novus Biologicals NB100-86991, 1:500)

Plasmid DNA transfection was performed with Lipofectamine2000 (Invitrogen, 11668-019), according to the supplier's protocol. Opti-MEM (Invitrogen, 31985-062) was used to dilute the plasmids. Plasmids were generous gifts from Dr. Erica Davis (FAM110A and STARD3NL) or Dr. Rik Korswagen (HUWE1).

Lipofectamine RNAimax (Invitrogen, 13778-075) was used for siRNA transfection, according to the supplier's protocol. Opti-MEM (Invitrogen, 31985-062) was used to dilute the ON-TARGETplus siRNA SMARTpools (Thermo Scientific Dharmacon):

Non-targeting pool (D-001810-10),
mouse Ift88(21821) (L-050417-00),
mouse Huwe1(59026)(L-059037-02),
mouse Fam110a (73847)(L-065039-01),
mouse Stard3nl (760205)(L-056118-01) and
mouse Anapc4 (52206)(L-051472-01) to 20 nM.

**RT-qPCR**

RNA was isolated, cDNA was synthesized, and RT-qPCR analysis was performed as previously described [17]. The mouse primer sequences (Sigma) used are:

Mouse *Rpl27* (housekeeping):
Fw: GGTGCCATCGTCAATGTTCTT
Rv: CGCCCTCCTTTCCTTTCTGC

Mouse *Huwe1*:
Fw: TCTTCCACTAGAGATTCTGCCG
Rv: TGATACCAGCAAGGGGATCTTC

Mouse *Stard3nl*:
Fw: TGCCCATCATTTCATTCATCCTT
Rv:AAAAGCGGTTTCTCACTCTCC

Mouse *Anapc4*:
Fw: CTGCGCTTTCCGACCTGTT
Rv: AAAACCTCGCCTGTAGTGTTG

Mouse *Fam110a*:
Fw: ACTCCCGCCCTACCTTTTC
Rv: CCACAGCACTCGGTTTCCT

**Immunofluorescence**
For immunostaining, mIMCD3 cells were grown on coverslips and confocal imaging was performed using Zeiss Confocal laser microscope and images were processed with the ZEN 2012 software [6]. 3D spheroids matrigel assays with mIMCD3 cells were performed as previously described [25].
**Western blots** were performed as previously described [6]. Protein lysates were prepared using RIPA lysis buffer and sonicated. To correct for protein content a BCA protein assay (Pierce) was performed. After blotting, the PVDF membranes were blocked in 5% BSA or 5% dried skim milk in TBS with 0.5% Tween. The primary antibodies Anti-Huwe1 (1:500), anti-CEP290 (1:500), Anti-Flag (clone M2 Sigma, 1:2000) or anti-HA (clone 12CA5 hybridoma supernatant, 1:3) were diluted and incubated with the membrane overnight at 4 degrees C. The secondary HRP conjugates swine anti-rabbit and swine anti-mouse antibodies (DAKO, dilution 1:200) were incubated for 1 hour at RT. And submitted to the ECL chemiluminescence kit (Sigma CPS1120-1KT). Scans of the blots were made with the BioRad ChemiDoc XRS+ device.



**FACS**
Performed as previously described.

**Statistics**
P-values (*p,0.05, ** p<0.01, ***p<0.001) were calculated from normally distributed data sets using a two-tailed Student's t test. Statistical analyses represent the mean of all experiments and error bars represent SEM.

**Zebrafish**
Talens were designed against a region in exon 9 of the zebrafish *huwe1* gene that contained a restriction site which could be used for genotyping. The target sequence of the forward talen was ATATTTTTTGTGCAGTGTACTCCAA, while the target sequence of the reverse talen was AGCCAATAGCATACTCTATA. The restriction enzyme site sequence was ctccag, corresponding to the restriction enzyme BpmI. The following primers were used for genotyping:
Fw: CCCCTCTGAGATCATGGAGT
Rv: AGACCTTGGCTTAAACAGTGC

**Acknowledgements**
We would like to thank R. Korswagen for the HUWE1 constructs used in this paper, and for information about the phenotype of mutant worms. We would also like to thank E. Davis for the FAM110A- and STARD3NL-GFP constructs used in this work. This work was supported by the European Union FP7/2009 Consortia "SYSCILIA" [grant number 241955 to RHG, CAJ] and "EURenOmics" [grant number 305608 to NK/RHG and OD]; the Dutch Kidney Foundation "KOUNCIL" [CP11.18 to NVK, ML, RHG]; and by the Medical Research Council [MR/M000532/1 to CAJ].
The Cell Microscopy Center and the Flow Cytometry Core Facility at the UMC Utrecht provided expert services.

## REFERENCES


1. Oh, E.C. and N. Katsanis, *Cilia in vertebrate development and disease.* Development, 2012. **139**(3): p. 443-8.
2. D'Angelo, A. and B. Franco, *The primary cilium in different tissues-lessons from patients and animal models.* Pediatr Nephrol, 2011. **26**(5): p. 655-62.
3. Basten, S.G. and R.H. Giles, *Functional aspects of primary cilia in signaling, cell cycle and tumorigenesis.* Cilia, 2013. **2**(1): p. 6.
4. Baker, K. and P.L. Beales, *Making sense of cilia in disease: the human ciliopathies.* Am J Med Genet C Semin Med Genet, 2009. **151C**(4): p. 281-95.
5. Wheway, G., Schmidts, M., Mans, D. A., Szymanska, K., Nguyen, T. T., Racher, H., Phelps, I. G., Toedt, G., Kennedy, J., Wunderlich, K. A., et. al., *An siRNA-based functional genomics screen for the identification of regulators of ciliogenesis and ciliopathy genes.* Nat Cell Biol, 2015. **17**(8): p. 1074-87.
6. Slaats, G.G., et al., *Screen-based identification and validation of four new ion channels as regulators of renal ciliogenesis.* J Cell Sci, 2015. **128**(24): p. 4550-9.
7. de Groot, R.E., et al., *Huwe1-mediated ubiquitylation of dishevelled defines a negative feedback loop in the Wnt signaling pathway.* Sci Signal, 2014. **7**(317): p. ra26.
8. Komiya, Y. and R. Habas, *Wnt signal transduction pathways.* Organogenesis, 2008. **4**(2): p. 68-75.
9. MacDonald, B.T., K. Tamai, and X. He, *Wnt/beta-catenin signaling: components, mechanisms, and diseases.* Dev Cell, 2009. **17**(1): p. 9-26.
10. Park, T.J., et al., *Dishevelled controls apical docking and planar polarization of basal bodies in ciliated epithelial cells.* Nat Genet, 2008. **40**(7): p. 871-9.
11. Alpy, F., et al., *Functional characterization of the MENTAL domain.* J Biol Chem, 2005. **280**(18): p. 17945-52.
12. Alpy, F., et al., *MENTHO, a MLN64 homologue devoid of the START domain.* J Biol Chem, 2002. **277**(52): p. 50780-7.
13. Alpy, F., et al., *STARD3 or STARD3NL and VAP form a novel molecular tether between late endosomes and the ER.* J Cell Sci, 2013. **126**(Pt 23): p. 5500-12.
14. Lehman, N.L., et al., *Overexpression of the anaphase promoting complex/cyclosome inhibitor Emi1 leads to tetraploidy and genomic instability of p53-deficient cells.* Cell Cycle, 2006. **5**(14): p. 1569-73.
15. Hauge, H., S. Patzke, and H.C. Aasheim, *Characterization of the FAM110 gene family.* Genomics, 2007. **90**(1): p. 14-27.
16. Chaki, M., et al., *Exome capture reveals ZNF423 and CEP164 mutations, linking renal ciliopathies to DNA damage response signaling.* Cell, 2012. **150**(3): p. 533-48.
17. Slaats, G.G., et al., *Nephronophthisis-associated CEP164 regulates cell cycle progression, apoptosis and epithelial-to-mesenchymal transition.* PLoS Genet, 2014. **10**(10): p. e1004594.
18. van Dam, T.J., et al., *The SYSCILIA gold standard (SCGSv1) of known ciliary components and its applications within a systems biology consortium.* Cilia, 2013. **2**(1): p. 7.
19. van Leuken, R., et al., *Polo-like kinase-1 controls Aurora A destruction by activating APC/C-Cdh1.* PLoS One, 2009. **4**(4): p. e5282.
20. Evangelista, M., et al., *Kinome siRNA screen identifies regulators of ciliogenesis and hedgehog signal transduction.* Sci Signal, 2008. **1**(39): p. ra7.
21. Monroe, G.R., et al., *Compound heterozygous NEK1 variants in two siblings with oral-facial-digital syndrome type II (Mohr syndrome).* Eur J Hum Genet, 2016.
22. Slaats, G.G., et al., *MKS1 regulates ciliary INPP5E levels in Joubert syndrome.* J Med Genet, 2016. **53**(1): p. 62-72.
23. Boldt, K., et al., *An organelle-specific protein landscape identifies novel diseases and molecular mechanisms.* Nat Commun, 2016. **7**: p. 11491.
24. Shaheen, R., et al., *Mutations in CSPP1, encoding a core centrosomal protein, cause a range of ciliopathy phenotypes in humans.* Am J Hum Genet, 2014. **94**(1): p. 73-9.
25. Giles, R.H., H. Ajzenberg, and P.K. Jackson, *3D spheroid model of mIMCD3 cells for studying ciliopathies and renal epithelial disorders.* Nat Protoc, 2014. **9**(12): p. 2725-31.

# SUPPLEMENTAL

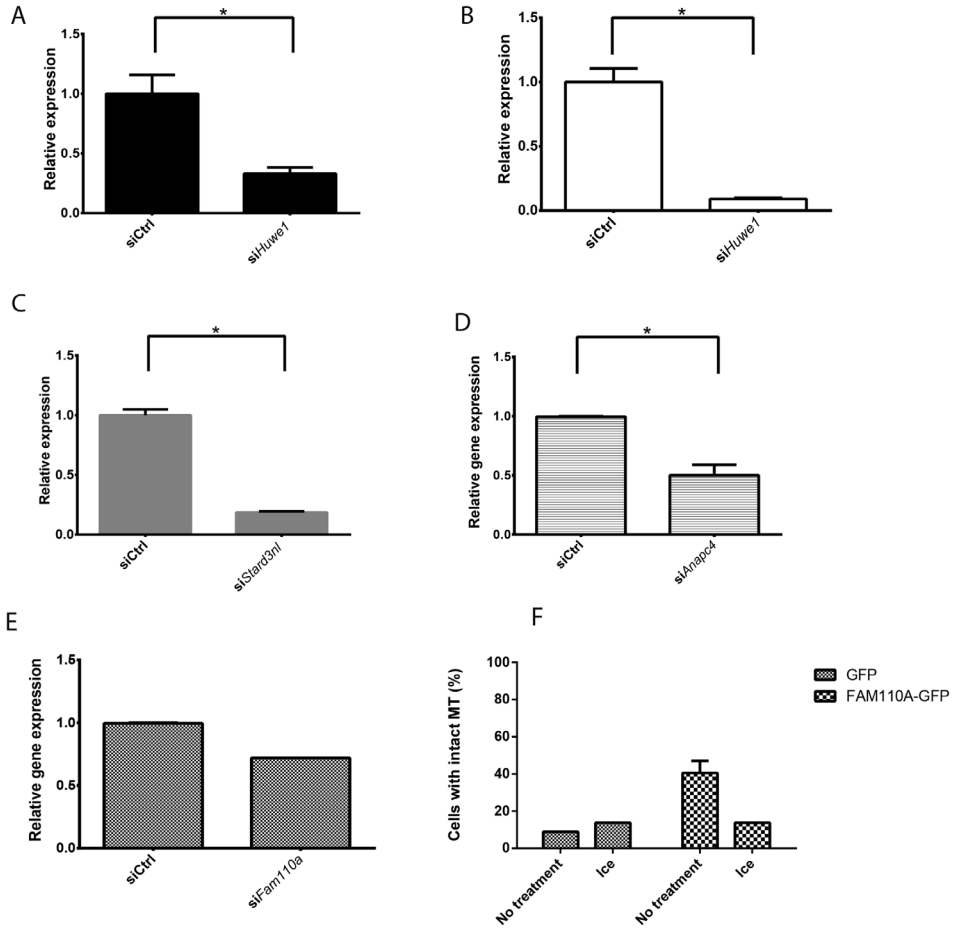


**Supplemental Figure 1:** (A) qPCR of endogenous *Huwe1* mRNA levels indicates siRNA efficacy of si*Huwe1* in IMCD3 cells at 72 hours after transfection normalized to siControl transfected cells. n=2, in triplicate. p==0.017. (**B**) qPCR of endogenous *HUWE1* mRNA levels indicates siRNA efficacy of si*HUWE1* in RPE-hTERT cells at 48 hours after transfection normalized to siControl transfected cells. n=2, in triplicate. p=0.00018. (**C**) qPCR of endogenous *Stard3nl* mRNA levels indicates siRNA efficacy of si*Stard3nl* in IMCD3 cells at 72 hours after transfection normalized to siControl transfected cells. n=2, in triplicate. p<0.0001. (**D**) qPCR of endogenous *Anapc4* mRNA levels indicates siRNA efficacy of si*Anapc4* in IMCD3 cells at 72 hours after transfection normalized to siControl transfected cells. n=3, in triplicate. p<0.0001. (**E**) qPCR of endogenous *Fam110a* mRNA levels indicates siRNA efficacy of si*Fam100a* in IMCD3 cells at 72 hours after transfection normalized to siControl transfected cells. n=3, in triplicate. p=0.15.(**F**) Ice treatment of COS-7 cells transfected with either empty-GFP construct or with FAM110A-GFP show that microtubule cystoskeleton can be collapsed by incubating the plates on ice for 15 minutes.

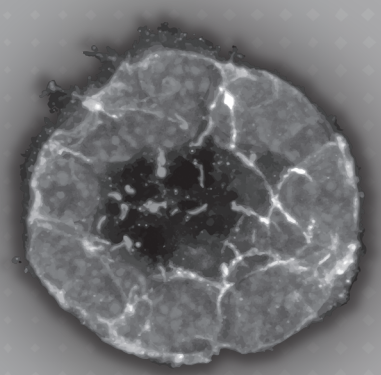

## CHAPTER 8

# DCDC2 mutations cause a renal-hepatic ciliopathy by disrupting Wnt signaling

The American Journal of Human Genetics. 2015 Jan 8;96(1):81-92. doi: 10.1016/j.ajhg.2014.12.002. Epub 2014 Dec 31.

Schueler M, Braun DA, Chandrasekar G, Gee HY, **Klasson TD**, Halbritter J, Bieder A, Porath JD, Airik R, Zhou W, LoTurco JJ, Che A, Otto EA, Böckenhauer D, Sebire NJ, Honzik T, Harris PC, Koon SJ, Gunay- Aygun M, Saunier S, Zerres K, Bruechle NO, Drenth JP, Pelletier L, Tapia-Páez I, Lifton RP, Giles RH, Kere J, Hildebrandt F

## ABSTRACT

Nephronophthisis-related ciliopathies (NPHP-RC) are recessive diseases characterized by renal dysplasia or degeneration. We here identify mutations of *DCDC2* as causing a renal-hepatic ciliopathy. DCDC2 localizes to the ciliary axoneme and to mitotic spindle fibers in a cell-cycle-dependent manner. Knockdown of *Dcdc2* in IMCD3 cells disrupts ciliogenesis, which is rescued by wild-type (WT) human *DCDC2*, but not by constructs that reflect human mutations. We show that DCDC2 interacts with DVL and *DCDC2* overexpression inhibits b-catenin-dependent Wnt signaling in an effect additive to Wnt inhibitors. Mutations detected in human NPHP-RC lack these effects. A Wnt inhibitor likewise restores ciliogenesis in 3D IMCD3 cultures, emphasizing the importance of Wnt signaling for renal tubulogenesis. Knockdown of *dcdc2* in zebrafish recapitulates NPHP-RC phenotypes, including renal cysts and hydrocephalus, which is rescued by a Wnt inhibitor and by WT, but not by mutant, *DCDC2*. We thus demonstrate a central role of Wnt signaling in the pathogenesis of NPHP-RC, suggesting an avenue for potential treatment of NPHP-RC.

## INTRODUCTION

Cilia are microtubule-based structures that project from the cell surface of numerous mammalian cells and mediate key pathways of development such as Wnt and Shh signaling. Many ciliary proteins participate in functional protein sub- complexes,[1] which localize to primary cilia, centrosomes, the mitotic spindle, or the abscission structure in a cell-cycle-dependent manner.[2] Mutations in genes that encode these ciliary proteins lead to developmental and degenerative diseases, which show a broad phenotypic spectrum. This complex of disorders has collectively been termed "ciliopathies" due to their localization to primary cilia and centrosomes.[3] Moreover, numerous cilia-mediated signaling pathways have been implicated in the pathogenesis of ciliopathies, such as canonical Wnt/b-catenin,[4] Shh,[5] and DNA damage response (DDR).[6,7]

In this context, the term nephronophthisis-related ciliopathies (NPHP-RC) summarizes a group of rare autosomal-recessive cystic kidney diseases including nephronophthisis (NPHP [MIM 256100]), Senior-Loken syndrome (SLS [MIM 266900]), Joubert syndrome (JBTS [MIM 213300]), and Meckel Gruber syndrome (MKS [MIM 249000]). NPHP accounts for the majority of genetically caused end-stage renal disease (ESRD) during the first three decades of life. The most prominent diagnostic hallmarks are increased echogenicity and the presence of corticomedullary cysts upon renal ultrasound. Histologically, NPHP is characterized by tubular atrophy, basement membrane disintegration, interstitial fibrosis, and cyst formation. About 15% of the affected individuals with NPHP-RC exhibit extra-renal organ involvement, in particular hepatobiliary ductal plate malformation, progressive retinal dystrophy, and cerebellar vermis hypoplasia/aplasia as the hallmark of JBTS. The most severe manifestation of the NPHP-RC spectrum is MKS, a perinatally lethal ciliopathy.

Similar to the vast pleiotropy, NPHP-RC show broadly heterogeneous genotypes with monogenic ciliopathies established to be caused by recessive mutations in more than 90 genes.[3–5,8–15] We recently demonstrated in a large cohort of 1,056 families with NPHP-RC that in more than 50% of cases the underlying disease-causing mutation is un- known.[16,17] In order to identify additional single gene causes of NHPH-RC, we here applied homozygosity map- ping and whole-exome sequencing in 100 affected individuals of consanguineous parents or sibling cases fulfilling the diagnostic criteria of NPHP-RC. In combination with high- throughput exon sequencing in a cohort of 800 individuals with NPHP-RC, we identified recessive truncating mutations in *DCDC2* as a hitherto unknown cause of renal-hepatic variant of NPHP-RC. We demonstrate that DCDC2 interacts with the mediator of Wnt signaling dishevelled, and that *DCDC2* overexpression inhibits b-catenin-dependent Wnt signaling. Thus, we demonstrate a central role of Wnt signaling in the pathogenesis of NPHP-RC, suggesting an avenue for potential treatment of NPHP-RC.

## MATERIALS AND METHODS

**Research Subjects**

Blood samples and pedigrees were obtained from individuals with diagnosed NPHP-RC and informed consent. Approval for human subject research was obtained from Institutional Review Boards of the University of Michigan and the Boston Children's Hospital.

**Linkage Analysis**

For genome-wide homozygosity mapping GeneChip® Human Mapping 250k StyI Array (Affymetrix) was used. Regions of homozygosity were identified using GENEHUNTER 2.1[18,19] and ALLEGRO[20] with a disease allele frequency of 0.0001 and marker allele frequencies of European descent.[12,21]

**Whole-Exome Sequencing**

Whole exome sequencing (WES) and variant burden analysis was performed as previously described[22] using Agilent SureSelect human exome capture arrays (Life Technologies™) with next generation sequencing (NGS) on an Illumina™ sequencing platform. Sequence reads were mapped against the human reference genome (NCBI build 36/hg18) using CLC Genomics Workbench (version 4.7.2) software (CLC bio). Mutation calling (Tables S1 and S2) was performed by geneticists/cell biologists, who had knowledge of clinical phenotypes, pedigree structure, homozygosity mapping, and WES evaluation.

**High-Throughput Mutation Analysis by Array-Based Multiplex PCR and NGS**

For 48 DNA samples simultaneously, 672 amplicons (592 exons) of 32 candidate genes, including *DCDC2*, were sequenced in a cohort of 800 individuals with NPHP-RC using a PCR-based 48.48 Access Array microfluidic technology (Fluidigm) with consecutive NGS as previously described.[16,17] Detected variants were confirmed by Sanger sequencing and evaluated for segregation. Additional 21 individuals with early onset liver fibrosis were Sanger sequenced for coding regions of *DCDC2* (Table S3).

**cDNA and Splice Mutation**

RNA of A4435-21 and healthy control was purified from whole blood, cDNA was synthesized (Agilent Technologies) and Sanger sequenced, using primers flanking exon 4 in order to confirm skip- ping of exon 4 (Figure S1; Table S3).

**cDNA Cloning**

Human full-length (Hs-FL) *DCDC2* cDNA was subcloned by PCR from Hs-FL cDNA (origene SC114336). Full-length and partial clones were subcloned into pRK5-N-Myc using

the gateway system (Invitrogen). Mutations were introduced at position c.649A>T to represent p.Lys217* (Figure S2C) and at c.123_124 delGT to represent p.Ser42Glnfs*72 (Figure S2A) using "QuikChange II XL Site-Directed Mutagen- esis" (Agilent Technologies). Using the same technique the nucleotides 349 to 425 of exon 4 were deleted in order to represent the splice mutation c.349-2A>G (Figure S2B). *MAP- K8IP1* (*JIP1*) full-length was subcloned from Hs-FL cDNA (NM_005456, origen sc124125) into pDEST40 (gateway). *PAFAH1B1* (*LIS1*) (NM_000430.3 [MIM 601545]), open reading frame was amplified from Hs-FL cDNA (clone ID HsCD00378475) and subcloned to pDEST40. Human *Disheveled 1,2,3* (NM_004421.2, NM_004422.2, NM_004423.3) full-length clones and fragment of *DVL3* were a gift from Vita Bryja, Masaryk University.

**Coimmunoprecipitation**

Coimmunoprecipitation experiments upon co-overexpression in NIH 3T3 and HEK293T cells were performed as described previously.[23]

**Luciferase Reporter Gene Assay**

The Wnt/b-catenin reporter assay has been performed as described.[23] In brief, NIH 3T3 cells were transfected with pcDNA3/S33Y b-catenin, pTOPFLASH, pGL4.74[hRluc/TK] (Prom- ega) and *DCDC2* (WT/mutants) or the empty vectors. At 36 hr posttransfection, luciferase activities were measured using a Dual-Luciferase® Reporter Assay and GloMax™ 96 microplate luminometer (Promega) according manufacturer's instruction. The luciferase activities were normalized to Renilla luciferase activities and protein concentration.



**Antibodies**

For immunofluorescence studies, the following primary anti- bodies were used: Mouse anti-DCDC2 (Abcam, ab 157186), goat-anti-DCDC2 (Santa Cruz, sc-50728), rabbit anti-Kif3a (Abcam ab11259), mouse anti-Jip-1 (Santa Cruz sc-25267), mouse anti-DVL3 (Santa Cruz sc-365581), mouse anti-SDCCAG8 (Abcam, ab67098), rabbit anti-Cep164 (Sigma, hpa037606), mouse anti-Pericentrin (Abcam, ab28144), rabbit anti-PCNT (Atlas Antibodies, 019887), rabbit anti-PCM-1 (Cell Signaling, 5259), and rabbit anti-IFT88 (ProteinTech, 13967-1-AP). For immunoblotting, the following primary antibodies were used: rabbit anti-DCDC2 (Sigma Aldrich D2945), and mouse anti-Jip- 1 (Santa Cruz sc-25267).

**Immunofluorescence and Confocal Microscopy in Cell Lines**

Cells were prepared for immunofluorescence as previously described[24], incubated in primary antibodies (see above) over- night at 4°C, and imaged using Leica SP5X system with an upright DM6000 microscope and A1R confocal microscope (Nikon Instruments).

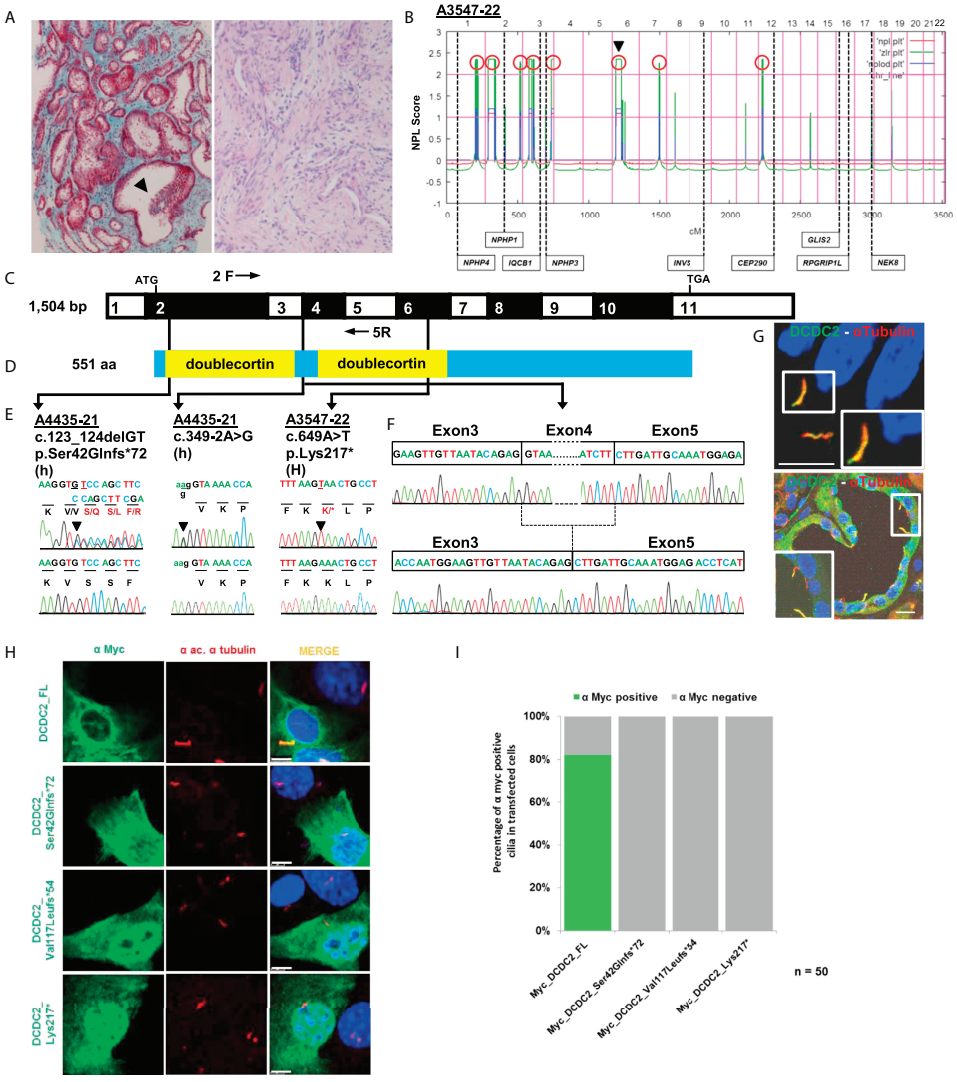


**Figure 1.** Homozygosity Mapping and WES Detect *DCDC2* Mutations in Individuals with Renal-Hepatic Ciliopathy. In A3547-22 with a renal-hepatic ciliopathy renal histology (left panel; Masson trichrome staining) reveals tubulointerstitial fibrosis and tubular dilation with epithelial luminal budding (arrowhead). Hepatic histology (right panel; H&E staining) of A3547-22 shows areas of florid fibrosis with destruction of bile ducts, focal ductular proliferation with cholestasis, and bile plugging. For individual A3547-22 nonparametric LOD (NPL) scores from whole-genome mapping are plotted across the human genome. The x axis shows Affymetrix 250K *Styl* array SNP positions on human chromosomes concatenated from pter (left) to qter (right). Genetic dis- tance is given in cM. Eight maximum NPL peaks (red circles) indicate candidate regions of homozygosity by descent. Note that the *DCDC2* locus (arrow head) is positioned within a maximum NPL peaks on chromosome 6p. Exon structure of human *DCDC2* cDNA. Positions of start codon (ATG) and stop codon (TGA) are indicated. Protein domain structure of DCDC2. The N terminus contains two doublecortin domains. Three homozygous (H) or compound-heterozygous (h) *DCDC2* mutations detected in two families with a ▶▶

**Immunofluorescence and Confocal Microscopy on Tissues**

Human and murine paraffin-embedded samples were obtained from Zyagen. Paraffin-embedded tissue sections of 5–7 mm were deparaffinized, rehydrated, stained after heat-induced antigen retrieval, and imaged on a LSM510 confocal microscope (Carl Zeiss Microimaging), and on an A1R confocal microscope (Nikon Instruments).

**Knockdown of *Dcdc2***

Transfection of non-target siRNA was performed in parallel to tar- geted siRNA using Lipofectamine RNAimax (Invitrogen) following manufacturer's instructions. Experiments were performed 48 hr after siRNA transfection. For all knockdown experiments, Dharmacon ON-TARGETplus siRNA 11 and 12 against murine *Dcdc2a* were used (Table S3). The knockdown efficiency was shown by immunoblot (Figure S12) and by qPCR (Figure S10).

**Spheroid Assay**

Spheroid assays were performed as previously described.[6] In brief, IMCD3 cells were transfected with human *DCDC2* cDNA constructs at day 1. After 24 hr, cells were transfected with siRNA against murine *Dcdc2a.* 24 hr after the second transfection, cells were resuspended in matrigel (BD Bioscience) and seeded on Lab TekII chambered coverglasses. After 72 hr, cells that had formed spheroids with visible cleared lumens were stained and imaged us- ing a Zeiss LSM700 confocal microscope. In each spheroid, nuclei were counted, followed by cilia. The percentage of "ciliated nuclei" in each spheroid was used as a distinct value in the results. To detect the presence of cilia, we scored 200–2,000 cells per condition for the presence of cilia. GraphPad Prism 6.0 (GraphPad Soft- ware) was used to graph results and perform statistical tests using ANOVA statistical analysis. Experiments were repeated at least two times independently and data combined, graphs show mean value and SEM.

◀ *Figure 1. continued*
renal-hepatic ciliopathy (see Table 1). Family number (underlined), mutation, and predicted translational changes are indicated. Healthy control sequence is shown underneath. Sequenced RT-PCR product from cDNA of lymphocytes of A4435-21 with obligatory splice mutation (c.349-2A>G) using primers located in exons 2 (2F) and 5 (5R). Positions of primers are indicated in (C). Hepatic and renal localization of DCDC2. Coimmunofluorescence using anti-DCDC2 or anti-a-acetylated tubulin antibodies dem- onstrates DCDC2 at the ciliary axoneme in cilia of cholangiocytes (upper panel) and of renal epithelial cells (lower panel). Immunoflu- orescence was performed on human paraffin embedded sections. Nuclei are stained with DRAQ5. Scale bars are 20 mm. Upon overexpression in NIH 3T3 cells WT DCDC2 decorates the ciliary axoneme, whereas all three mutant clones reflecting muta- tions in NPHP-RC families lack ciliary localization.
Quantitation of ciliary staining in 50 transfected cells per clone. Scale bars are 5 mM.

Table 1. Mutations of DCDC2 in Two Families with Nephronophthisis-Related Ciliopathies

| Family-Individual | Ethnic Origin | Nucleotide Alteration [a] (Segregation) | Deduced protein Change | Exon/intron (state) | Parental Consanguinity | Kidney Phenotype | Liver Phenotype | Other (Clinical Characteristics) |
|---|---|---|---|---|---|---|---|---|
| A3547 –22 | UK | c.649A >T (M: het, P: het) | p.Lys217* | 6 (Hom) | Yes | Increased echogenicity, severe interstitial fibrosis, tubular dilation with prominent epithelial luminal budding, ESRD at 14 yr. died at 16 yr. from esophageal bleeding | Hepatosplenomegaly, extensive florid fibrosis with destruction of bile ducts, bile focal duct proliferation with cholestasis | Left terminal ICA region aneurysm, foci of signal abnormality in subcortical and deep white matter |
| A4435 –21 | Czech | c.123_124 delGT (M: het) c.349-2A >G (P: het) | p.Ser42Glnfs*72 [b] 3$^0$ splice site (100% conserved) (p.Val117Leufs*54) [c] | 2 (het) 4 (het) | No | No renal involvement current age 9 yr. | Hepatosplenomegaly, ductal plate malformation, hepatic fibrosis, scant cholestasis, LTX at 2 yr. | N/A |

CRF, chronic renal failure; ESRD, end-stage renal disease; het, heterozygous; Hom, homozygous; ICA, internal carotid artery; LTX, liver transplantation; M, maternal; N/A, not applicable; P, paternal; yr., years.
[a]DCDC2: cDNA mutations are numbered according to human cDNA reference sequence NM_001195610.1.
[b]The allele appears 12/8,242 in the EVS-Server database.
[c]G is not among alternative nucleotides in the splice site consensus (3 $^0$ acceptor splice site position). The allele appears 3/67366 in the ExAC Browser database.

**Zebrafish Embryos and Microinjections of Morpholinos and mRNA**

Zebrafish embryos were staged 24 hr post fertilization (hpf) and 1- phenyl-2-thiourea (PTU, Sigma) was used to block pigmentation in embryos older than 24 hpf. A morpholinooligonucleotide (MO) against the translation start site of *dcdc2b* (AUGMO) (Table S3) was designed (Gene Tools, LLC), dissolved in 13 Danieau's buffer and injected at varying concentrations (50, 100, 150, 200, and 250 mM) into WT zebrafish embryos at the one-cell stage. $5^0$- capped sense mRNA of human *DCDC2* WT and the two mutant clones *hDCDC2_Lys217** and *hDCDC2_Ser42Glnfs*72* were synthesized using SP6 mMessage mMachine Kit (Ambion) and was coinjected (approximately 100 pg) with *dcdc2b* MO for rescue experiments. Two additional MOs targeting splice sites were not efficient in *dcdc2b* knockdown as evidenced by RT PCR (data not shown). All zebrafish experiments were performed in accordance with ethical permits approved by Stockholm North Experimental Animal Committee (Dnr N29-12).

Treatment with WNT/b-Catenin Inhibitor iCRT14 Zebrafish embryos injected with AUGMO were exposed to 500 nM or 750 nM or 1 mM or 5 mM concentrations of iCRT14 at the beginning of gastrulation. Compound treated embryos were raised at 28.5$^{O}$C in Petri dishes for 48 hr and screened for the rescue of ciliopathy phenotypes. As solvent control, 1% DMSO was used.

**Whole-Mount In Situ Hybridization, Histology, and Immunohistochemistry**

Digoxigenin-labeled antisense probe for *foxa3* was synthesized as described previously.[25] For in situ hybridization staged embryos were fixed in 4% PFA for 24 hr and processed.[26] Immunohistochemistry and histology experiments on Zebrafish embryos have been performed as described.[27,28]

**Transmission Electron Microscopy**

For electron microscopy, 3.5-day-old control and morphant embryos were fixed in 2% glutaraldehyde solution containing 1% PFA in 0.1 M phosphate buffer (PB), pH 7.4. Sectioning was per- formed using a Leica EM UC 6 (Leica) and stained with uranyl acetate and lead citrate. Electron micrographs were examined and acquired using a Tecnai 10 transmission electron microscope with a veleta camera.

**Statistical Analysis**

Results in Figure 2 are presented as scattergrams with means and error bars for SD for the indicated number of values. Statistical analysis of continuous data was performed with a two-tailed Student's t test. $p < 0.05$ was considered statistically significant.

**Bioinformatics**

Genetic location is according to the February 2009 Human Genome Browser data.

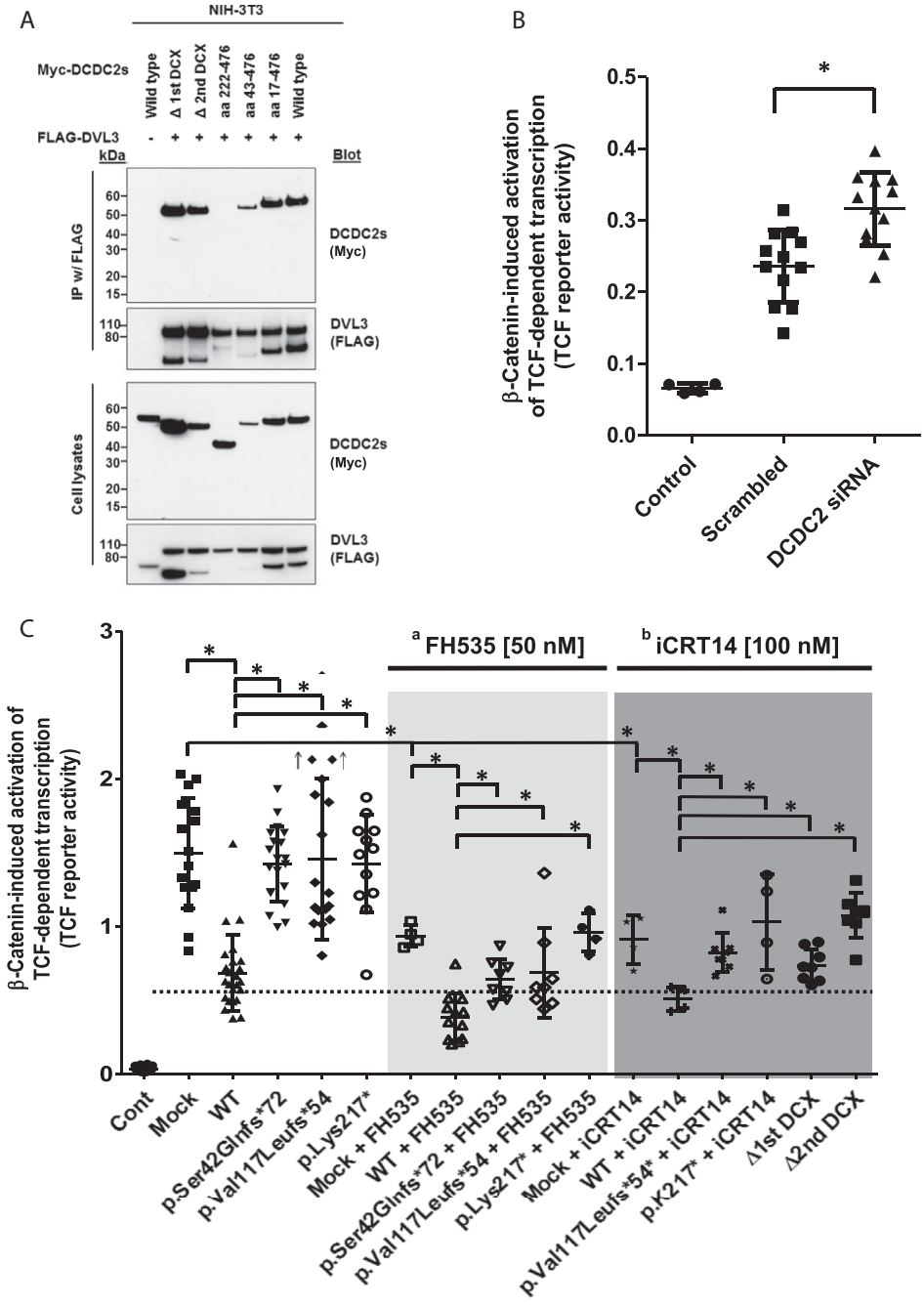

## RESULTS

### DCDC2 Mutations Cause a Renal-Hepatic Ciliopathy

To elucidate pathomechanisms of NPHP-RC, we sought additional causative mutations and performed homozygosity mapping[21] and whole-exome sequencing[24] in 100 consanguineous cases or sibling cases fulfilling the diagnostic criteria of NPHP-RC. In consanguineous individual A3547-22, who had hepatic fibrosis (Figure 1A) at age 11 months and end-stage renal disease (ESRD) from NPHP at age 14 years (Table 1), we obtained by homozygosity mapping eight candidate regions of homozygosity by descent (Figure 1B). Whole-exome sequencing yielded a homozygous truncating mutation (c.649A>T, p.Lys217*) in *DCDC2* (double cortin domain-containing 2) (Figures 1C–1E; Table 1). No additional homozygous truncating mutations were detected in any other gene within the mapped candidate regions (Tables S1 and S2). Direct inspection of sequence alignments did not yield a mutation in any of the >90 genes with a known connection to NPHP-RC. By high-throughput exon sequencing[16,17] in a large worldwide cohort of 800 additional families with NPHP-RC, in whom mutations in known genes were excluded, we sequenced all exons of *DCDC2*. In less than ten of these individuals liver fibrosis was present. We detected in individual A4435-21, who had hepatic fibrosis requiring liver transplantation at 2 years of age, two com- pound heterozygous mutations: A frameshift mutation (c.123_124 delGT, p.Ser42Glnfs*72) (Table 1; Figure 1E) and an obligatory splice site mutation (c.349-2A>G) that we show produces the frameshift product p.Val117Leufs*54 (Table 1; Figure 1F; Figures S1 and S2).



**Figure 2.** DCDC2 Interacts with Dishev- elled and Inhibits b-Catenin-Dependent Wnt Signaling Synergistically with Wnt Inhibitors. DCDC2 interacts with DVL3 when both are transiently overexpressed in NIH 3T3 cells. A construct (aa 222-476) lacking both doublecortin (DCX) domains (see Figure S2 for constructs) does not interact with DVL3, whereas the deletion of either DCX domain alone is not sufficient to abrogate the interaction. Knockdown of *DCDC2* in NIH 3T3 activates the b-catenin-dependent WNT pathway. Cells were transfected with an empty vector pcDNA3 (Control) or pcDNA3-S33Y-b-catenin together with scrambled or *DCDC2* siRNA. The ratio be- tween the luciferase activity obtained from the cotransfected TCF-responsive re- porter and the control luciferase reporter gene construct (pGL4.74[hRluc/YK]) was calculated and designated as "TCF reporter activity." Cells were transfected with an empty vector pcDNA3 (Control) or pcDNA3- S33Y-b-catenin (Mock) together with *DCDC2* constructs. Left panel: Overexpression of WT, but not mutant, *DCDC2* inhibits b-catenin-induced activation of TCF-dependent reporter gene. Light gray panel: The Wnt inhibitor FH535 sup- presses TCF reporter activity. Overexpression of WT *DCDC2*, but not three mutant *DCDC2* clones, inhibits TCF reporter activity additively to the effect of FH535. Dark gray panel: Likewise, the Wnt inhibitor iCRT14 suppresses TCF reporter activity. Overexpression of WT *DCDC2*, but not mutants, inhibits TCF reporter activity additively to the effect of iCRT14. Two cDNA clones lacking the first or second DCX domain, respectively (D1st DCX and D2nd DCX), also fail to suppress TCF re- porter activity. A dotted horizontal line is drawn for easier interpretation of results. [ indicates two outliers at 2.4 and 2.7. [a]FH535 (middle light gray panel) is known to suppress b-catenin/TCF-mediated transcription and to inhibit b-catenin and GRIP-1 recruitment to PPARg; [b]iCRT14 (left dark gray panel) is known to modulate interaction between b-catenin and TCF and inhibit b-catenin/TCF-mediated transcription.

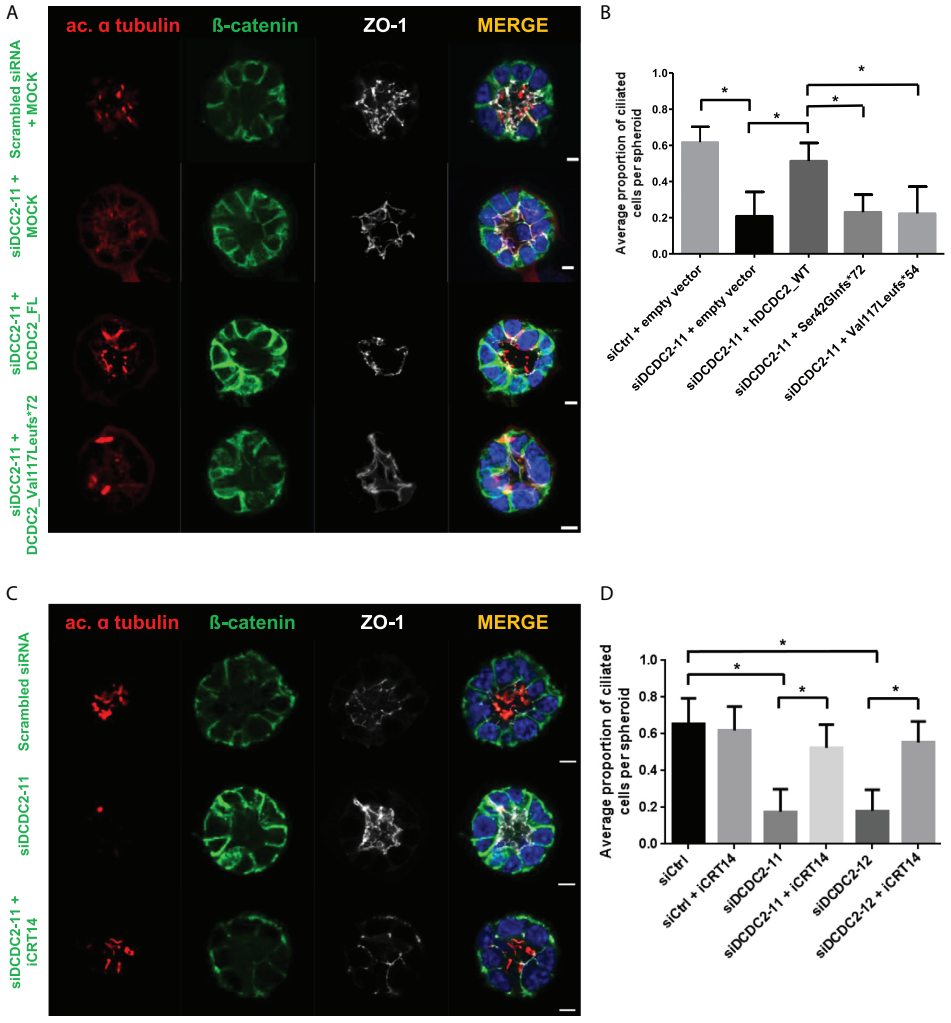


**Figure 3.** Lack of *Dcdc2* Is Rescued by Full-Length *DCDC2* and by Wnt Inhibition, but Not by Mutants Detected in NPHP-RC. siRNA (siDcdc2-11) mediated knockdown of *Dcdc2* in IMCD3 cells grown in 3D spheroid culture causes a ciliogenesis defect that is rescued by overexpression of human WT *DCDC2,* but not by mutants found in humans with NPHP-RC. For each condition >50 spheroids were evaluated for the percentage of ciliated cells and the experiment was repeated three times independently. Note that the red structures visible in the mutant-transfected spheroid are midbodies of dividing cells, not cilia. Scale bars are 5 mm.
Ratio of ciliated cells per nuclei within each spheroid upon knockdown and after attempted rescue with WT *DCDC2* and two mutants. *p < 0.001, as determined by ANOVA analysis. Experiments were repeated at least two times independently and the data combined. Graphs show mean value and standard error of the mean (SEM). The ciliogenesis defect was rescued by growing spheroids in medium treated with Wnt inhibitor iCRT14 (100 mM). Scale bars are 5 mm. Quantification for two siRNAs of rescue of ciliogenesis defect by iCRT14 treatment. *p < 0.001, as determined by ANOVA analysis. Experiments were repeated at least two times independently and the data combined. Graphs show mean value and SEM.

None of the affected individuals had retinal degeneration, cerebellar vermis hypoplasia, hydrocephalus, obesity, or bone dis- ease. An additional 21 individuals with early onset liver fibrosis were screened for variants in the coding region of *DCDC2* by Sanger sequencing (Table S3). No additional mutations were detected. We generated cDNA clones reflecting the human *DCDC2* mutations (Figure S2). When re-evaluating the *Dcdc2* knockout mouse model,[29] we found that there was periportal fibrosis at age 11 months consistent with the phenotype seen in humans with *DCDC2* mutations (Figure S3).

**DCDC2 Colocalizes with Other NPHP-RC Proteins to the Cilia-Centrosome-Spindle Complex**

To elucidate the role of DCDC2 in the pathogenesis of NPHP-RC, we examined its localization in epithelia of different tissues that are involved in NPHP-RC phenotypes, using indirect immunofluorescence studies. In kidney and liver, we observed that DCDC2 colocalizes with acetylated a-tubulin to the axoneme of primary cilia of human renal tubule cells and cholangiocytes in liver (Figure 1G) and to multiciliated ependymal cells and pia mater cells in mouse brain (Figure S4). However, DCDC2 did not localize to the basal body (Figure S4).

Because NPHP-RC proteins localize to primary cilia, centrosomes, the mitotic spindle, and the abscission structure in a cell-cycle-dependent manner,[2] we performed colocalization studies for DCDC2 and other NPHP-RC proteins using confocal laser immunofluorescence microscopy in MDCK-II and hTERT-RPE1 cells (Figures S6 and S7). We found that within the different phases of mitosis DCDC2 fully or partially colocalizes with acetylated a-tubulin during metaphase and anaphase to the spindle microtubules, during late telophase/diakinesis to the abscission structure, and in ciliated cells during interphase to the ciliary axoneme (Figures S5–S7). Throughout those cell-cycle phases, DCDC2 is excluded from the basal body (in inter- phase) and the mitotic spindle poles (in metaphase and anaphase), as well as the midbody (in diakinesis) (Figures S5–S7), in contrast to other NPHP-RC proteins, which preferentially stain basal body and spindle poles, reciprocally omitting the axoneme and mitotic spindle fibers. These NPHP-RC proteins include SDCCAG8/NPHP10 (Figure S6) and CEP164/NPHP15 (Figure S7). In metaphase, DCDC2 is absent from the interpolar spindle domain of the mitotic spindle (Figure S5). Three proteins that had been described as interacting with DCDC2, DVL3 (this study), JIP1,[30] and Kif3a[31] labeled basal bodies, mitotic spindle poles, and midbody rather than the ciliary axoneme (Figure S8).

Overexpression in hTERT-RPE1 cells revealed upon immunofluorescence that mutations observed in individuals with NPHP-RC and constructs, from which either of the two doublecortin domains are deleted (Figure S2) fail to localize to the primary cilia (Figure S9). These results are in accordance to observations made in rat hippocampal neurons.[31] Immunocytochemistry of cells overexpressing WT and the truncating mutants p.Lys217*,

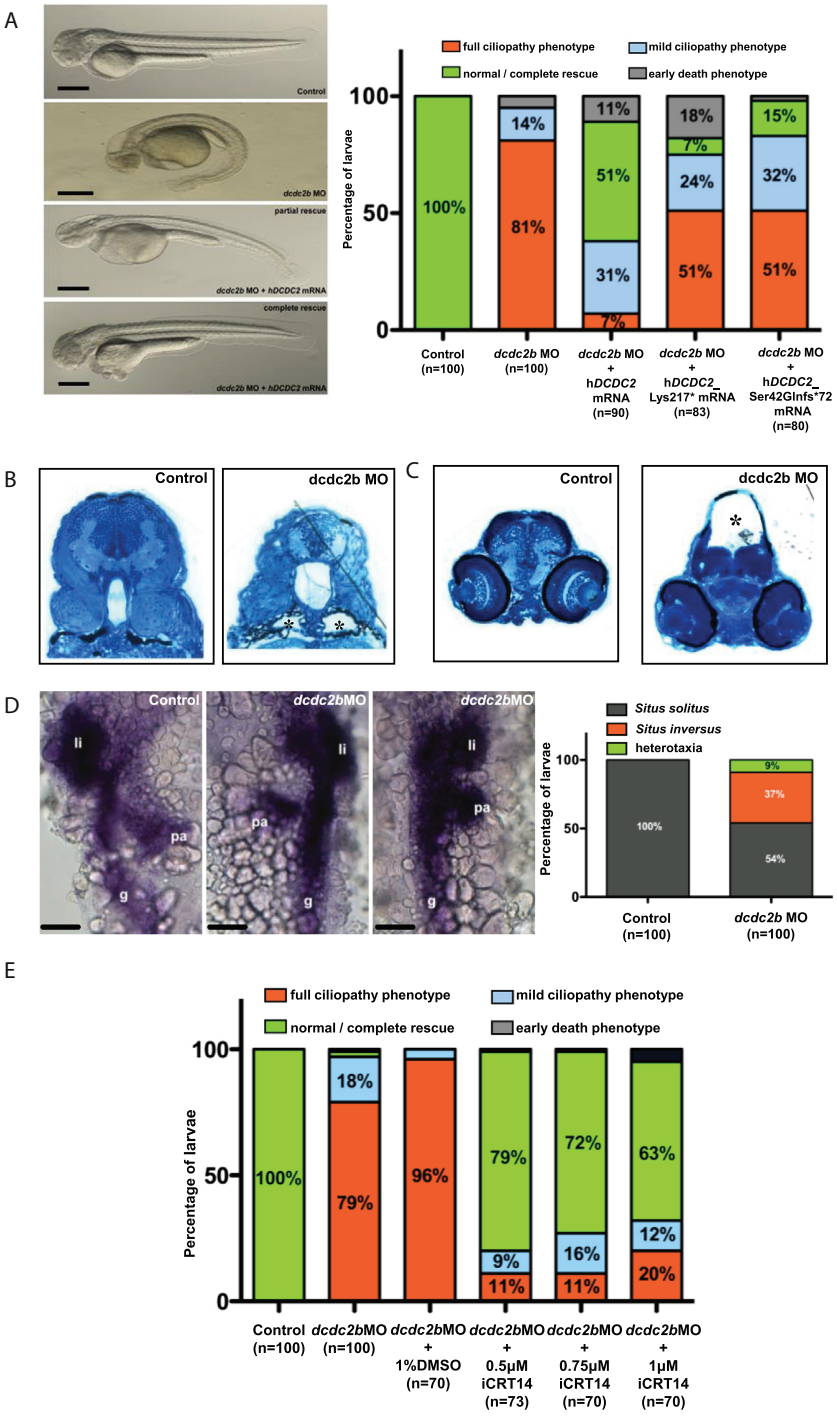

p.Val117Leufs*54, and p.Ser42Glnfs*72 shows that the mutations abrogate localization of DCDC2 to the primary cilium in NIH 3T3 (Figure 1H) and RPE1 cells (Figure S9).

**DCDC2 Interacts with DVL1-3, and Mutations Abrogate Wnt Signaling**

Because we have previously shown that INVS[4,32] and CEP164,[6] defects in which are associated with NPHP-RC, interact with proteins that participate in Wnt signaling, we tested whether DCDC2 interacts with the disheveled proteins (DVL1, DVL2, or DVL3), which act as regulators of Wnt signaling.[31,33]

We performed coimmunoprecipitation studies in NIH 3T3 cells demonstrating that full-length DCDC2 interacts with all three dishevelled proteins, DVL1, DVL2, and DVL3. This interaction was not abrogated in cDNA constructs representing the mutations that we identified in individuals with NPHP-RC (Figure S11). However, a construct (aa 222-476) lacking both doublecortin (DCX) domains (see Figure S2) failed to interact with DVL3, whereas deletion of either DCX domain alone did not abrogate interaction with DVL3 (Figure 2A). (An overview on cDNA clones is given in Figure S2, where p.Ser42Glnfs* 72 represents the shortest variant of A4435-21).

As DVL regulates Wnt signaling, we examined signaling effects downstream of DCDC2 and found that siRNA knockdown of *Dcdc2a* in NIH 3T3 cells increases b-catenin-induced activation of T cell factor (TCF)-dependent transcription (Figure 2B). Reciprocally, overexpression of *DCDC2* WT reduced b-catenin-induced activation of TCF-dependent transcription (Figure 2C, left panel). This effect was abrogated by all three mutations (Table 1, Figures 1C–1E) that we detected in individuals with NPHP-RC (Figure 2C, left panel). Two different Wnt inhibitors (FH535 and iCRT14) reduced b-catenin-induced activation of TCF-dependent transcription with an effect that was additive when combined with *DCDC2* overexpression (Figure 2C, middle and right panels).



**Figure 4.** MO Knockdown of *dcdc2b* Replicates Ciliopathy Phenotypes in Zebrafish that Cannot Be Rescued by cDNA Clones Representing Human Ciliopathy Mutants. Zebrafish embryos injected with AUGMO at one-cell stage produced defects characteristic of cilia dysfunction. Lateral view of 2-day-old control and morphant embryos. *dcdc2b* morphant developed ventrally bent body axis, hydrocephalus, tail kinks, and pericardial edema ("full ciliopathy phenotype"). Morphologically visible ciliopathy phenotypes in *dcdc2b* morphants were completely or partially rescued (lacking at least one phenotype) by coinjection of $5^0$capped mRNA of WT human *DCDC2*. Coinjection of AUGMO with capped mRNA of either of the two human *DCDC2* mutant clones h*DCDC2_Lys217** or h*DCDC2_Ser42Glnfs*72* mostly failed to rescue ciliary defects. Scale bar is 100 mm. Histological sections of pronephros from control and morphant embryo at 3.5 dpf. *dcdc2b* morphants clearly showed dilation of the pronephric duct (asterisks) compared to control embryos.
Transverse brain sections shows hydrocephalus (asterisk) in *dcdc2b* morphants as compared to control brain sections (methylene blue and silver stain). Left-right asymmetry defects in liver, gut, and pancreas as visualized by in situ hybridization for the expression of *foxa3* with quantitation by histogram (li, liver; pa, pancreas; g, gut). Scale bar is 50 mm. Treatment with b-catenin inhibitor iCRT14 within the dose range of 0.5–1 mM rescued *dcdc2b* knockdown ciliopathy phenotypes in the morphants. Histograms are representation of two or three independent experiments.

**DCDC2 Interacts with JIP1**

Previous studies showed that DCDC2 interacts with the protein JIP1 (mitogen-activated protein kinase 8 interacting protein 1).[30,34] JIP1 plays a role in aggregating components of the MAP kinase module (MLK, MKK7, JNK), in facilitating JNK signal transduction[35] activating JNK,[36] thereby mediating MAPK activation. We therefore performed coimmunoprecipitation in HEK293T cells (Figure S12A). Whereas WT DCDC2 and the mutant p.Val117Leufs*54 still interacted with full-length JIP1, the DCDC2 truncated mutant p.Ser42Glnfs*72 that we had detected in individual A4435-21 lacked interaction with JIP1. (For DCDC2 constructs see Figure S2.) When phosphorylation of the JNK downstream targets c-Jun and ATF2 was assayed in NIH 3T3 cells, knockdown of *DCDC2* in NIH 3T3 cells did not affect JNK pathway activation (Figure S12B). It was previously shown that lissencephaly-1 (LIS1) interacts with doublecortin (DCX), a protein that belongs with DCDC2 to a family of doublecortin domain-containing proteins.[37] When performing coimmunoprecipitation to test for interaction of DCDC2 with LIS1 we did not detect an interaction between the two proteins (Figure S13).

**Loss of Dcdc2 Function Disturbs Renal Epithelial Ciliation in 3D Cultures**

In order to test the effects of DCDC2 on ciliation, we assessed the result of *Dcdc2* siRNA knockdown in a 3D cell culture system. IMCD3 cells cultured in 3D matrigel mimic the normal processes of renal tubulogenesis by forming spheroids or small tubules composed of polarized cells, which exhibit a lumen and a ciliated apical membrane. Counting the number of cilia present on this apical mem- brane is an established model of ciliogenesis.[38] Spheroids grown from cells treated with two different RNAi oligonucleotides targeted against *Dcdc2* displayed significantly fewer cilia than spheroids grown from cells treated with a non-target control RNAi but did not display any severe architectural changes in lumen formation (Figure 3). In both cases, this ciliation defect could be rescued by concurrent transfection of WT human *DCDC2* but not by any of the mutant *DCDC2* clones Ser42Glnfs*72 and Val117- Leufs*54 that were derived from the affected individuals (Figures 3A–3C). ). The third mutant (Lys217*) was not efficiently expressed in the spheroids. The overexpression of empty vector, human WT *DCDC2*, or either of the mutants did not produce a significant difference in ciliation, excluding a dominant-negative or overexpression effect caused by these alleles (Figure 3; Figure S10). We conclude that DCDC2 is important for the generation and maintenance of renal cilia, but knockdown of *DCDC2* does not recapitulate the spheroid defects commonly observed after the loss of function of other NPHP proteins.[1,24]

Because loss of *Dcdc2* constitutively activates Wnt signaling (Figure 2B), we hypothesized that treating spheroids grown from renal cells depleted for *Dcdc2* with Wnt inhibitors would restore the frequency of cilia. We grew IMCD3 spheroids in the presence of either 50 nM

FH535 or 100 nM iCRT14 for 72 hr and scored for cilia per nucleus in 3D structures. The cells exposed to 50 nM FH535 failed to thrive and resulted in no viable spheroids (data not shown). However, the cells treated with 100 nM iCRT14 did generate well-polarized spheroids with lu- mens. The Wnt inhibitor treatment noticeably rescued the effects of *Dcdc2* knockdown in the cells growing in 3D structures by restoring cilia numbers (Figures 3C and3D). This suggests a role for Wnt signaling in the process of ciliation.

***Dcdc2* Knockdown Replicates Ciliopathy Phenotypes in Zebrafish**

To examine the renal cystic phenotype in an in vivo vertebrate model, we studied loss-of-function of *dcdc2b* in zebra- fish using a morpholino targeted against the start codon (AUGMO) to suppress the translation of *dcdc2b* mRNA. The knockdown efficiency of the AUGMO was dose dependent, producing clear visible phenotypes in higher percentage of embryos at 200 mM. In comparison with WT control embryos, knockdown of *dcdc2b* resulted in typical ciliopathy-related defects such as ventrally curved body axis, hydrocephalus, kidney cysts, kinky tails, and occasionally pericardial edema (Figure 4). At 2 days postfertilization (dpf), 81% of the morphants showed body-axis defects with kinks or waviness in the tail (Figure 4A). Hydrocephalus was observed in 58% of morphants at 2 dpf, and kidney cysts were prominantly visible in 31% of the morphants at 3.5 dpf (Figures 4A–4C). In addition, *dcdc2b* morphants also showed malformation in otolith assembly(Figure S14). Compared to control embryos that normally had two otoliths, some of the *dcdc2b* morphants had one or two fused or three otoliths (Figure S14F). These results demonstrate that *dcdc2b* in zebrafish might have a vital role in cilia formation or function. We further observed that suppression of *dcdc2b* caused laterality defects in liver, gut, and pancreas, which was visualized by whole-mount in situ hybridization for the expression of *foxa3* (Figure 4D). Interestingly, immunohistochemical staining with an anti-acetylated tubulin anti- body revealed that knockdown of *dcdc2b* does not alter motile cilia length in zebrafish kidney or spinal cord (Figure S14A–S14D). Electronmicrographs of the motile pronephric cilia of *dcdc2b* morphants showed no structural defects in comparison to WT pronephric cilia (Figure S14E). To confirm the specificity of the phenotype and to determine whether the biological function of DCDC2 is evolutionarily conserved between human and zebrafish, we performed an mRNA rescue experiment by coinjecting human WT *DCDC2* mRNA along with *dcdc2b* MO into one-cell-stage embryos. Injection of WT human *DCDC2* mRNA rescued morphologically visible ciliary phenotypes in 51% of the morphants, suggesting a similar role for *dcdc2b* as for DCDC2 in cilia function (Figure 4A). We further tested the pathogenicity of the *DCDC2* mutations identified in individuals diagnosed for NPHP-RC by a similar rescue approach where *dcdc2b* MO was coinjected with capped mRNA of the human mutation representing clones hDCDC2_Lys217* or hDCDC2_Ser42Glnfs*72 into one-cell-stage embryos. Both mutations were unable to completely

rescue the phenotype of *dcdc2b* morphants, confirming that these mutations indeed affect the function of the protein (Figure 4A).

**Zebrafish Ciliopathy Phenotype Is Rescued by a β-Catenin Inhibitor**

Since knockdown or overexpression of *Dcdc2* in NIH 3T3 cells altered the Wnt/b-catenin pathway, we hypothesized that the ciliopathy phenotype observed in zebrafish *dcdc2b* morphants might be a result of derailed Wnt signaling pathway. To test this hypothesis, we exposed the morphants to 0.5 mM, 0.75 mM, and 1 mM of a potent b-catenin inhibitor, iCRT14 at the beginning of gastrulation. After 48 hr period of exposure, the embryos were scored for body curvature, hydrocephalus, tail kinks, and pericardial edema. Interestingly, iCRT14 was able to effectively rescue the phenotype in higher percentage of embryos at doses ranging from 0.5 to 1 mM (Figure 4E). However, concentrations higher than 1 mM were toxic to the embryos (data not shown). Our in vivo and in vitro results strongly suggest a role of Wnt signaling pathway in the pathogenesis of NPHP-RC.

## DISCUSSION

We here identified mutations of *DCDC2* as a previously un- known cause of a renal-hepatic ciliopathy in humans that is characterized by severe early-onset liver fibrosis within the first year of life. DCDC2 localized to the ciliary axoneme and to mitotic spindle fibers in a cell-cycle- dependent manner. We showed that DCDC2 interacts with DVL, and *DCDC2* overexpression inhibited b-catenin-dependent Wnt signaling in an effect additive to Wnt inhibitors. Mutations detected in human NPHP-RC lacked these effects. A Wnt inhibitor restored ciliogenesis in 3D IMCD3 cultures, emphasizing the importance of Wnt signaling for renal tubulogenesis. The fact that knock- down of DCDC2 reduces the number of cilia in cell culture, but not in dcdc2b zebrafish morphants might be explained by the biological differences between primary cilia of IMCD3 cells and multiciliated, motile cilia of zebrafish larval pronephric duct. Finally, knockdown of *dcdc2b* in zebrafish recapitulated NPHP-RC phenotypes, which were rescued by a Wnt inhibitor and by WT but not by mutant *DCDC2*. We thus demonstrate a central role of Wnt signaling in the pathogenesis of NPHP-RC, suggesting an avenue for potential treatment of NPHP-RC.

Broad pleiotropy is a common feature of NPHP-RC. In this context, the absence of renal involvement in individual A4435-21 at 9 years of age does not exclude that the affected individual might develop renal involvement later in life, because individual A3547-22 developed chronic kidney disease at 14 years of age with no signs of renal involvement earlier in life. Due to the significant overlap of the observed phenotype with other forms of NPHP-RC we introduce the term “NPHP19” for this variant of NPHP-RC.

By immunofluorescence studies, we show that DCDC2 localizes to the ciliary axoneme and to mitotic spindle fibers. This localization pattern is clearly distinct from other NPHP-RC proteins, such as CEP164 and SDCCAG8 (Figures S6 and S7), which preferentially stain the basal body and the mitotic spindle poles. Interestingly, the interaction partners of DCDC2, DVL3 and JIP1,[34] and KIF3a[31] show a localization pattern that resembles CEP164 and SDCCAG8. The finding that there was no tight subcellular colocalization for these proteins could be due to the fact that the proteins bind to tubulin as suggested by Figure S8. The specific subcellular compartments to which NPHP-RC proteins localize are very small and often extremely dynamic during different phases of cell cycle, making colocalization experiments difficult to interpret. This holds true for many of the >90 NPHP-RC that are known so far.

Our in vitro studies in cell lines, spheroids, and our in vivo studies in zebrafish clearly demonstrate a role of increased canonical Wnt signaling in the pathogenesis of NPHP-RC. Loss-of-function mutations observed in individuals with NPHP-RC fail to reduce canonical Wnt signaling in vitro. The zebrafish phenotype observed upon knockdown of *dcdc2b* is reminiscent of the one seen in the zebrafish *apc*$^{-/-}$ mutant, a model of constitutively activated Wnt.[39] The fact that the phenotype of *dcdc2b* zebrafish morphants could be mitigated by treatment with Wnt inhibitors further supports the significance of dysregulated canonical Wnt signaling in this model.

Consistent with the observed human phenotype, our histological studies of *Dcdc2*$^{-/-}$ mice reveal periportal liver fibrosis and demonstrate biliary duct proliferation and extensive collagen deposition surrounding the portal tracts compared to WT control (Figure S3). It has been frequently reported that Wnt signaling regulates tubule formation (reviewed in[40]). Interestingly, the role of Wnt/b-catenin signaling during the development of liver fibrosis was recently analyzed.[41] It was shown that abnormal activation of Wnt/b-catenin signaling pro- motes tissue fibrogenesis while downregulation of Wnt signaling suppresses the activity of hepatic stellate cells and the collagen synthesis. Our data suggest that loss of DCDC2 function does not profoundly affect renal tubulogenesis but renders the tubules more responsive to Wnt modulation in the 3D polarized tubule state. Activated Wnt signaling has so far been implicated in human NPHP-RC in the presence of *INVS* mutations.[4] Our demonstration that Wnt inhibitors reverse the failure of *DCDC2* mutants to reduce canonical Wnt signaling opens a potential route toward treatment for certain forms of NPHP-RC.

**Supplemental Data**

Supplemental Data include fourteen figures and three tables and can be found with this article online at http://www.cell.com/ajhg.

**Acknowledgments**

We are grateful to families and study individuals for their contribution. We would like to thank Milan Elleder and Helena Hulkova (Institute for Inherited Metabolic Disorders) for histological preparation of liver biopsy specimen. We thank the zebrafish core facility, Karolinska Institutet for providing zebrafish embryos. We thank Kjell Hultenby, Eva Blomen, and Sally Cheung for technical support. We thank the Live Cell Imaging unit/Nikon Center of Excellence, Department of Biosciences and Nutrition, Karolinska Institutet for their support. This research was supported by grants from the National Institutes of Health to F.H. (DK1069274, DK1068306, DK064614), to P.C.H. (DK090728, DK059597), to R.A. (DK099434), and by the CIHR to L.P. (MOP130507). H.Y.G. is supported by the NephCure Foundation and by the ASN Foundation for Kidney Research. T.H. was supported by General University Hospital program RVO-VFN 64165/2012. This work was in part supported by grants to J.K. from Knut and Alice Wallenberg Foundation, the Swedish Research Council, the Centre for Biosciences, the Centre for Innovative Medicine, and Jonasson donation to the School of Technology and Health, Kungliga Tekniska Ho¨gskolan, Swedish Brain Foundation (Hja¨rnfonden) and Swedish Brain Foundations postdoc fellowship award to G.C., from the European Union Framework Programmes 241955 "SYSCILIA" and 305608 "EURenOmics" as well as the Dutch Kidney Foundation grants CP11.18 "KOUNCIL"/13A3D103 to R.H.G., and from the Deutsche Forschungs–gemeinschaft to K.Z. (ZE 205/14-1). F.H. is an Investigator of the Howard Hughes Medical Institute, a Doris Duke Distinguished Clinical Scientist, and the Warren E. Grupe Professor.

**Web Resources**

ExAC Browser Beta, http://exac.broadinstitute.org
Online Mendelian Inheritance in Man (OMIM), http://www. omim.org/
UCSC Genome Bioinformatics, http://genome.ucsc.edu/

## REFERENCES


1. Sang, L., Miller, J.J., Corbit, K.C., Giles, R.H., Brauer, M.J., Otto, E.A., Baye, L.M., Wen, X., Scales, S.J., Kwong, M., et al. (2011). Mapping the NPHP-JBTS-MKS protein network reveals ciliop- athy disease genes and pathways. Cell *145*, 513–528.
2. Hildebrandt, F., Benzing, T., and Katsanis, N. (2011). Ciliopa- thies. N. Engl. J. Med. *364*, 1533–1543.
3. Hildebrandt, F., Otto, E., Rensing, C., Nothwang, H.G., Vollmer, M., Adolphs, J., Hanusch, H., and Brandis, M. (1997). A novel gene encoding an SH3 domain protein is mutated in nephronophthisis type 1. Nat. Genet. *17*, 149–153.
4. Otto, E.A., Schermer, B., Obara, T., O'Toole, J.F., Hiller, K.S., Mueller, A.M., Ruf, R.G., Hoefele, J., Beekmann, F., Landau, D., et al. (2003). Mutations in INVS encoding inversin cause nephronophthisis type 2, linking renal cystic disease to the function of primary cilia and left-right axis determination. Nat. Genet. *34*, 413–420.
5. Attanasio, M., Uhlenhaut, N.H., Sousa, V.H., O'Toole, J.F., Otto, E., Anlag, K., Klugmann, C., Treier, A.C., Helou, J., Sayer, J.A., et al. (2007). Loss of GLIS2 causes nephronophthisis in humans and mice by increased apoptosis and fibrosis. Nat. Genet. *39*, 1018–1024.
6. Chaki, M., Airik, R., Ghosh, A.K., Giles, R.H., Chen, R., Slaats, G.G., Wang, H., Hurd, T.W., Zhou, W., Cluckey, A., et al. (2012). Exome capture reveals ZNF423 and CEP164 muta- tions, linking renal ciliopathies to DNA damage response signaling. Cell *150*, 533–548.
7. Zhou, W., Otto, E.A., Cluckey, A., Airik, R., Hurd, T.W., Chaki, M., Diaz, K., Lach, F.P., Bennett, G.R., Gee, H.Y., et al. (2012). FAN1 mutations cause karyomegalic interstitial nephritis, linking chronic kidney failure to defective DNA damage repair. Nat. Genet. *44*, 910–915.
8. Olbrich, H., Fliegauf, M., Hoefele, J., Kispert, A., Otto, E., Volz, A., Wolf, M.T., Sasmaz, G., Trauer, U., Reinhardt, R., et al. (2003). Mutations in a novel gene, *NPHP3*, cause adolescent nephronophthisis, tapeto-retinal degeneration and hepatic fibrosis. Nat. Genet. *34*, 455–459.
9. Otto, E., Hoefele, J., Ruf, R., Mueller, A.M., Hiller, K.S., Wolf, M.T., Schuermann, M.J., Becker, A., Birkenha¨ger, R., Sudbrak, R., et al. (2002). A gene mutated in nephronophthisis and retinitis pigmentosa encodes a novel protein, nephroretinin, conserved in evolution. Am. J. Hum. Genet. *71*, 1161–1167.
10. Mollet, G., Salomon, R., Gribouval, O., Silbermann, F., Bacq, D., Landthaler, G., Milford, D., Nayir, A., Rizzoni, G., Anti- gnac, C., and Saunier, S. (2002). The gene mutated in juvenile nephronophthisis type 4 encodes a novel protein that inter- acts with nephrocystin. Nat. Genet. *32*, 300–305.
11. Otto, E., Loeys, B., Khanna, H., Hellemans, J., Sudbrak, R., Fan, S., Muerb, U., O'Toole, J.F., Helou, J., Attanasio, M., et al. (2005). A novel ciliary IQ domain protein, NPHP5, is mutated in Senior-Loken syndrome (nephronophthisis with retinitis pigmentosa), and interacts with RPGR and calmodulin. Nat. Genet. *37*, 282–288.
12. Sayer, J.A., Otto, E.A., O'Toole, J.F., Nurnberg, G., Kennedy, M.A., Becker, C., Hennies, H.C., Helou, J., Attanasio, M., Fau- sett, B.V., et al. (2006). The centrosomal protein nephrocystin- 6 is mutated in Joubert syndrome and activates transcription factor ATF4. Nat. Genet. *38*, 674–681.
13. Valente, E.M., Silhavy, J.L., Brancati, F., Barrano, G., Krishnas- wami, S.R., Castori, M., Lancaster, M.A., Boltshauser, E., Boc- cone, L., Al-Gazali, L., et al.; International Joubert Syndrome Related Disorders Study Group (2006). Mutations in CEP290, which encodes a centrosomal protein, cause pleio- tropic forms of Joubert syndrome. Nat. Genet. *38*, 623–625.
14. Delous, M., Baala, L., Salomon, R., Laclef, C., Vierkotten, J., Tory, K., Golzio, C., Lacoste, T., Besse, L., Ozilou, C., et al. (2007). The ciliary gene RPGRIP1L is mutated in cerebello- oculo-renal syndrome (Joubert syndrome type B) and Meckel syndrome. Nat. Genet. *39*, 875–881.
15. Otto, E.A., Trapp, M.L., Schultheiss, U.T., Helou, J., Quarmby, L.M., and Hildebrandt, F. (2008). NEK8 mutations affect ciliary and centrosomal localization and may cause nephro- nophthisis. J. Am. Soc. Nephrol. *19*, 587–592.
16. Halbritter, J., Diaz, K., Chaki, M., Porath, J.D., Tarrier, B., Fu, C., Innis, J.L., Allen, S.J., Lyons, R.H., Stefanidis, C.J., et al. (2012). High-throughput mutation analysis in patients with a nephronophthisis-associated ciliopathy applying multi- plexed barcoded array-based PCR amplification and next-gen- eration sequencing. J. Med. Genet. *49*, 756–767.
17. Halbritter, J., Porath, J.D., Diaz, K.A., Braun, D.A., Kohl, S., Chaki, M., Allen, S.J., Soliman, N.A., Hildebrandt, F., and Otto, E.A.; GPN Study Group (2013). Identification of 99 novel mutations in a worldwide cohort of 1,056 patients with a neph- ronophthisis-related ciliopathy. Hum. Genet. *132*, 865–884.
18. Kruglyak, L., Daly, M.J., Reeve-Daly, M.P., and Lander, E.S. (1996). Parametric and nonparametric linkage analysis: a uni- fied multipoint approach. Am. J. Hum. Genet. *58*, 1347–1363.
19. Strauch, K., Fimmers, R., Kurz, T., Deichmann, K.A., Wienker, T.F., and Baur, M.P. (2000). Parametric and nonparametric multipoint linkage analysis with imprinting and two-locus- trait models: application to mite sensitization. Am. J. Hum. Genet. *66*, 1945–1957.
20. Gudbjartsson, D.F., Jonasson, K., Frigge, M.L., and Kong, A. (2000). Allegro, a new computer program for multipoint link- age analysis. Nat. Genet. *25*, 12–13.
21. Hildebrandt, F., Heeringa, S.F., Ru¨schendorf, F., Attanasio, M., Nu¨rnberg, G., Becker, C., Seelow, D., Huebner, N., Chernin, G., Vlangos, C.N., et al. (2009). A systematic approach to mapping recessive disease genes in individuals from outbred populations. PLoS Genet. *5*, e1000353.

22. Boyden, L.M., Choi, M., Choate, K.A., Nelson-Williams, C.J., Farhi, A., Toka, H.R., Tikhonova, I.R., Bjornson, R., Mane, S.M., Colussi, G., et al. (2012). Mutations in kelch-like 3 and cullin 3 cause hypertension and electrolyte abnormalities. Nature *482*, 98–102.
23. Zariwala, M.A., Gee, H.Y., Kurkowiak, M., Al-Mutairi, D.A., Leigh, M.W., Hurd, T.W., Hjeij, R., Dell, S.D., Chaki, M., Dougherty, G.W., et al. (2013). ZMYND10 is mutated in pri- mary ciliary dyskinesia and interacts with LRRC6. Am. J. Hum. Genet. *93*, 336–345.
24. Otto, E.A., Hurd, T.W., Airik, R., Chaki, M., Zhou, W., Stoetzel, C., Patil, S.B., Levy, S., Ghosh, A.K., Murga-Zamalloa, C.A., et al. (2010). Candidate exome capture identifies mutation of SDCCAG8 as the cause of a retinal-renal ciliopathy. Nat. Genet. *42*, 840–850.
25. Odenthal, J., and Nu¨sslein-Volhard, C. (1998). fork head domain genes in zebrafish. Dev. Genes Evol. *208*, 245–258.
26. Thisse, B., Heyer, V., Lux, A., Alunni, V., Degrave, A., Seiliez, I., Kirchner, J., Parkhill, J.P., and Thisse, C. (2004). Spatial and tem- poral expression of the zebrafish genome by large-scale in situ hybridization screening. Methods Cell Biol. *77*, 505–519.
27. Chandrasekar, G., Vesterlund, L., Hultenby, K., Tapia-Pa´ez, I., and Kere, J. (2013). The zebrafish orthologue of the dyslexia candidate gene DYX1C1 is essential for cilia growth and func- tion. PLoS ONE *8*, e63123.
28. Zhou, W., and Hildebrandt, F. (2009). Molecular cloning and expression of phospholipase C epsilon 1 in zebrafish. Gene Expr. Patterns *9*, 282–288.
29. Truong, D.T., Che, A., Rendall, A.R., Szalkowski, C.E., LoTurco, J.J., Galaburda, A.M., and Holly Fitch, R. (2014). Mutation of Dcdc2 in mice leads to impairments in auditory processing and memory ability. Genes Brain Behav. *13*, 802–811.
30. Shmueli, A., Gdalyahu, A., Sapoznik, S., Sapir, T., Tsukada, M., and Reiner, O. (2006). Site-specific dephosphorylation of dou- blecortin (DCX) by protein phosphatase 1 (PP1). Mol. Cell. Neurosci. *32*, 15–26.
31. Massinen, S., Hokkanen, M.E., Matsson, H., Tammimies, K., Ta- pia-Pa´ez, I., Dahlstro¨m-Heuser, V., Kuja-Panula, J., Burghoorn, J., Jeppsson, K.E., Swoboda, P., et al. (2011). Increased expres- sion of the dyslexia candidate gene DCDC2 affects length and signaling of primary cilia in neurons. PLoS ONE *6*, e20580.
32. Watnick, T., and Germino, G. (2003). From cilia to cyst. Nat. Genet. *34*, 355–356.
33. Giles, R.H., van Es, J.H., and Clevers, H. (2003). Caught up in a Wnt storm: Wnt signaling in cancer. Biochim. Biophys. Acta *1653*, 1–24.
34. Coquelle, F.M., Levy, T., Bergmann, S., Wolf, S.G., Bar-El, D., Sapir, T., Brody, Y., Orr, I., Barkai, N., Eichele, G., and Reiner, O. (2006). Common and divergent roles for members of the mouse DCX superfamily. Cell Cycle *5*, 976–983.
35. Yasuda, J., Whitmarsh, A.J., Cavanagh, J., Sharma, M., and Davis, R.J. (1999). The JIP group of mitogen-activated protein kinase scaffold proteins. Mol. Cell. Biol. *19*, 7245–7254.
36. Jaeschke, A., Czech, M.P., and Davis, R.J. (2004). An essential role of the JIP1 scaffold protein for JNK activation in adipose tissue. Genes Dev. *18*, 1976–1980.
37. Caspi, M., Atlas, R., Kantor, A., Sapir, T., and Reiner, O. (2000). Interaction between LIS1 and doublecortin, two lissencephaly gene products. Hum. Mol. Genet. *9*, 2205–2213.
38. Renkema, K.Y., Stokman, M.F., Giles, R.H., and Knoers, N.V. (2014). Next-generation sequencing for research and diagnos- tics in kidney disease. Nat. Rev. Nephrol. *10*, 433–444.
39. Hurlstone, A.F., Haramis, A.P., Wienholds, E., Begthel, H., Korving, J., Van Eeden, F., Cuppen, E., Zivkovic, D., Plasterk, R.H., and Clevers, H. (2003). The Wnt/beta-catenin pathway regulates cardiac valve formation. Nature *425*, 633–637.
40. Miller, R.K., and McCrea, P.D. (2010). Wnt to build a tube: contributions of Wnt signaling to epithelial tubulogenesis. Developmental dynamics: an official publication of the Amer- ican Association of Anatomists *239*, 77–93.
41. Ge, W.S., Wang, Y.J., Wu, J.X., Fan, J.G., Chen, Y.W., and Zhu, L. (2014). Beta-catenin is overexpressed in hepatic fibrosis and blockage of Wnt/beta-catenin signaling inhibits hepatic stellate cell activation. Molecular medicine reports *9*, 2145– 2151.

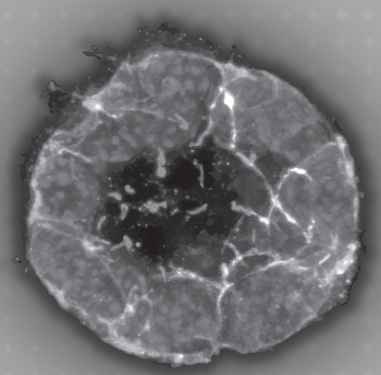

# CHAPTER 9

# The tumorigenic role of TCF21 hypermethylation in renal tumors

Manuscript submitted

**Klasson TD***, Gooskens SL*, Logister I, Pieters R, Perlman EJ, Giles RH, van den Heuvel-Eibrink MM

*these authors contributed to this work equally

## ABSTRACT

We recently identified increased methylation at the gene promotor of transcription factor 21 (*TCF21*) in clear cell sarcoma of the kidney (CCSK), a rare pediatric renal tumor. *TCF21* is a transcription factor involved in tubular epithelial development of the kidney that has been identified as a candidate tumor suppressor (located at chromosome 6q23-q24). As there are no *in vitro* models of CCSK, we employed a well-established clear cell renal cell carcinoma (ccRCC) cell line, 786-O, which also manifests high methylation at the *TCF21* promotor, with consequent low TCF21 protein expression. The tumor suppressor function of *TCF21* has not yet been functionally addressed in ccRCC cells, therefore we aimed to explore the functional potential of *TCF21* expression in ccRCC cells *in vitro*. 786-O cells were stably transfected with either a pBABE-TCF21-HA construct or pBABE vector alone and four clones were functionally analyzed from each transfection. We found that ectopic expression of *TCF21* in 786-O cells results in a trend towards decreased cell proliferation (not significant) and significant decreased migration compared to mock-transfected 786-O cells. Although the number of colonies established in colony formation assays was not different between 786-O clones, colony size was significantly reduced in 786-O cells expressing *TCF21*. To investigate whether the changes in migration were due to epithelial-to-mesenchymal transition changes, we interrogated the expression of selected epithelial and mesenchymal markers. Although we observed upregulation of the epithelial marker *CDH1* in clones overexpressing TCF21, this did not result in surface expression of E-cadherin as measured by FACS. Furthermore, the mesenchymal markers *VIM* and *SNAI1* were not altered in *TCF21*-expressing 786-O cells. We conclude that re-expression of *TCF21* in renal cancer cells that have silenced their endogenous *TCF21* locus through hypermethylation results in a reduction of clonogenic proliferation and migration, suggesting a tumor suppressor function for *TCF21*.


**Highlights**

We ectopically expressed *TCF21* in the clear cell renal cell carcinoma cell line 786-0.
786-0 clones exogenously expressing *TCF21* show reduced clonogenic proliferation.
786-0 clones exogenously expressing *TCF21* show reduced migration.
Ectopic expression of TCF21 upregulated *CDH1* mRNA levels.
However, the expression of surface E-Cadherin was unchanged by TCF21.

**Abbreviations**

CCSK, clear cell sarcoma of the kidney
EMT, epithelial-to-mesenchymal transition
FACS, fluorescence activated cell sorting
MET, mesenchymal-to-epithelial transition
RCC, renal cell carcinoma
TCF21, Transcription factor 21

## INTRODUCTION

Clear cell sarcoma of the kidney (CCSK) is an uncommon pediatric renal tumor that comprises between 2-5% of all primary renal tumors in children (Furtwangler et al., 2013; Gooskens et al., 2012; Mullen et al., 2014). This tumor is observed most often in children between 2 and 4 years of age and is characterized by a high malignant potential (Argani et al., 2000; Gooskens et al., 2012). Apart from internal tandem duplications within exon 16 of *BCOR* (reported in about 90% of CCSKs) and translocation t(10;17)(q22;p13) leading to a fusion of *YWHAE* and *NUTM2B/E* (reported in about 10% of CCSKs), the genome of CCSK seems to be rather stable (Astolfi et al., 2015; Gooskens et al., 2015; Karlsson et al., 2015; Roy et al., 2015; Ueno-Yokohata et al., 2015). This paucity of large genomic imbalances and the few detected somatic mutations in CCSK, prompted the investigation of the epigenome of CCSKs. Our study as part of the NCI-initiated TARGET project (Therapeutically Applicable Research to Generate Effective Treatment), identified hypermethylation of the promoter region of *TCF21* in all studied CCSK samples, except for samples harboring the *YWHAE-NUTM2* fusion transcript (Gooskens et al., 2015). This hypermethylation was negatively correlated with *TCF21* expression. Other tested 3 pediatric renal tumor samples and normal kidney samples showed significantly lower *TCF21* methylation levels.

*TCF21* (also referred to as *Pod-1, capsulin* and *epicardin*) encodes a basic helix-loop-helix transcription factor that binds DNA and regulates cell differentiation and cell-fate specification during development (Hidai et al., 1998). It is expressed in embryonic mesenchymal cells surrounding areas of epithelial development in the kidney, heart, lung and gastrointestinal tract (Hidai et al., 1998; Lu et al., 1998; Quaggin et al., 1998). *TCF21* expression rapidly decreases in postnatal tissues with the exception of a subset of interstitial cells in organs including the kidney, heart, lung and spleen (Plotkin and Mudunuri, 2008). Antisense inhibition of *TCF21* has been reported to disrupt epithelial differentiation and branching morphogenesis of the epithelium in murine embryonic kidney, suggesting a role for *TCF21* in epithelial-mesenchymal interactions (Quaggin et al., 1999). Gene deletion studies in chimeric mice have shown that loss of *TCF21* in the kidney results in decreased glomerulogenesis and tubulogenesis (Cui et al., 2003). Of note, suppression of *TCF21* expression by siRNA within a mouse kidney progenitor cell line that endogenously expresses *TCF21* resulted in increased cell proliferation and migration, as well as reduced expression of smooth muscle genes and myofibroblast secreted proteins (Plotkin and Mudunuri, 2008). Currently, no CCSK cell lines or models are available to functionally verify the role of *TCF21* hypermethylation in this renal tumor type. Therefore, we searched for an alternative model. A literature search revealed that *TCF21* hypermethylation is also present in clear cell renal cell carcinomas (ccRCC): renal tumors with another biology and phenotype, that most

often occur in adults (Costa et al., 2011; Ye et al., 2012). Previously performed clinical studies on the prognostic impact of *TCF21* expression in ccRCC tissue revealed that *TCF21* expression levels significantly correlated with Fuhrman Nuclear Grade and cancer-specific survival of ccRCC patients (Ye et al., 2012). *TCF21* methylation levels in urine samples were significantly correlated with tumor size, Fuhrman grade and clinical stage (Xin et al., 2016). However, no studies have functionally addressed the tumor suppressor activity of *TCF21* in renal cancer cells. Therefore, the aim of this study was to explore the functional potential of *TCF21* expression in the tumorigenesis of ccRCC *in vitro*.

## METHODS

### Cancer cell lines

We used the human ccRCC 786-O cell line (ATCC CRL-1932). 786-O cells are reported to manifest high methylation- and low expression of *TCF21* (Costa et al., 2011). Cells were cultured in Gibco RPMI Medium 1640 (1X) + GlutaMAX ™-I (Invitrogen), supplemented with 10% fetal calf serum (Invitrogen), penicillin (50 IU/ml) and streptomycin sulfate (50 µg/ml) (Invitrogen).

### Vector construction and transfection

The coding sequence of *TCF21* (including HA-tag) was cloned out of a pCS2+-TCF21 construct (kindly provided by Prof. Dr. Plass, Division of Epigenomics and Cancer Risk Factors, German Cancer Research Center (DKFZ), Heidelberg, Germany), amplified and recloned into a pBABE-puro vector. Plasmid DNAs were sequence-confirmed. Twenty-five micrograms of pBABE-TCF21-HA or pBABE-puro vector alone were transfected into cells of the 786-O cell line using electroporation. Electroporation was performed in a 4 mm gap cuvette (Bio-Rad Laboratories, Hercules, CA, USA, #165-2088) using a Gene Pulser (Bio-Rad, München, Germany) with electric parameters 24kV with 1000 uF capacitance; a single exponential decay pulse was applied. Selection medium containing puromycin was added to the cells after 48 hours recovery, and colonies grew after two weeks of culture. Eight colonies were selected for functional assays: four from pBABE-puro mock transfected 786-O cells (N1F4, B5F1, N1G4 and B6D10) and four expressing HA-tagged exogenous *TCF21* (2B12, 5D2, 9D12, 9H9). Unless the clones are specifically named, data from "pBABE-mock" or "pBABE-TCF21" contain pooled data from all four clones.

**Western blotting**

Cells were lysed on ice in RIPA buffer and normalized to 40μg of protein per sample. Lysates were loaded and fractionated by SDS-PAGE (14% gel) under protein-reducing conditions and immunoblotted on PVDF membranes. β-actin was used as loading control. After blotting, the PVDF membranes were blocked in 5% dried skim milk in TBS with 0.5% Tween. Primary antibodies used were monoclonal mouse anti-HA (supernatant from hybridoma clone 12CA5) at a dilution of 1:3, and anti-actin (mouse anti-β-actin AC-15, Sigma A5441, 1:15000). ECL reagent (Amersham Biosciences) was used for detection with ImageQuant LAS 4000 (GE Healthcare).

**Proliferation assay**

A total of 2 x $10^4$ 786-O pBABE-mock cells (4 different clones), 786-O pBABE-TCF21 cells (4 different clones) and 786-O cells treated with 3 μM decitabine (5-aza-2' deoxycytidine) were plated in 6-well plates in two separate experiments (786-O cells treated with decitabine were plated once) in triplicates in selection medium and were counted after 2, 4 and 5 days. Medium containing decitabine was replaced every 24 hours to avoid drug hydrolysis and inactivation. Cells were counted in duplicate with the BioRad TC20 Automated Cell Counter (Hercules, CA) and averaged.

**Colony formation assay**

A total of 200 786-O pBABE mock cells (4 different clones) and 786-O pBABE-TCF21 cells (4 different clones) were plated in 6-well plates on five different occasions in triplicates in selection medium until 786-O pBABE-mock cells formed sufficiently large colonies (> 50 cells per colony, 10-14 days). Cells were then washed with PBS and fixed and stained using a mixture of 6.0% glutaraldehyde and 0.5% crystal violet for 30 minutes at room temperature, before being washed in water. Wells were individually photographed and analyzed by the Colony Counter plug-in for Image J software. Numbers of colonies and colony area were calculated in Image J.

**Migration assays**

Boyden chambers (Transwell Permeable Supports; Cole-Parmer; BergmanLabora AB) were used to evaluate the migratory capacity of 786-O pBABE-mock cells (N1G4 and B6D10 clones) and 786-O pBABE-TCF21 cells (9D12 and 5D2 clones). A total of 3 x $10^4$ cells were seeded in the upper section of a Boyden chamber containing serum-free medium. The lower section, separated from the upper one by a membrane with 8 μM pores, contained medium with 10% serum. Cells were grown at 37°C for 16h, fixed in methanol and stained with DAPI (1:2000). Unmigrated cells on top of the membrane were removed with a cotton tip. The number of migrated cells on the bottom of the membrane was evaluated by counting

cells in 10 different views per membrane using microscopy at 10x magnification. The experiments were performed in duplicate and were repeated two times (N1G4/B6D10 versus 9D12/5D2 and N1G4 versus 5D2).
For the real-time migration assay, in each experiment a modified Boyden-chamber setup was used, with 10% serum in the lower well as chemoattractant. Migration was recorded in real-time at 5 min intervals over 24 hours using the xCELLigence Real-Time Cell Analysis system (Acea Biosciences), which quantifies cell numbers in the lower compartment by electrical impedance as in [PMID 25174586].
Rate of migration was quantified by calculating a series of moving slopes over 12-interval periods and taking the maximum slope in each migration curve. Within each experiment 4 technical replicates per clone were recorded and the experiment was repeated on three separate days. Data were analyzed using a hierarchical linear mixed model using experimental day as random variable.

**Zebrafish injections**
An incross of *vhl*+/- zebrafish embryos (van Rooijen et al., 2009) carrying a transgene for GFP-labelled *cadherin-17* (kidney-specific) at the 1-2 cell stage were injected with 1-2 nL of mRNA (concentration 50 ng/µl) transcribed from the linearized pCS2+-TCF21 plasmid (SP6 mMessage mMachine kit, Ambion) in pure water with 0.05% Phenol Red using a nanoject2000 microinjector (World Precision Instruments). Pronephros volume (determined by GFP-fluorescence) was measured at 5.75 days post fertilization, and imaged with an LSM700 confocal microscope (Zeiss). All embryos were genotyped after imaging as previously described (van Rooijen et al., 2009) and only confirmed *vhl*-/- embryos were analyzed. All zebrafish experiments were approved by the Animal Care Committee of the University Medical Center Utrecht in the Netherlands.

**Quantitative RT-PCR**
Total RNA was extracted and purified using the RNeasy Mini Kit (QIAGEN, 74106). cDNA was synthesized from 1 µg of RNA by using the iScript cDNA Synthesis Kit (Bio-Rad, 170-8891) according to the supplier's protocol. A cDNA concentration of 5 ng/µl was used for the quantitative RT-PCRs; samples were run with iQ SYBR Green Supermix (Bio-Rad, 170-8880) and CFX96 Touch Real-Time PCR Detection System (Bio-Rad); 95°C for 3 min, followed by 40 cycles of 10s of 95°C, 10s of 50-65°C and 20s of 72°C, then 10s at 95°C followed by a melt of the product from 65°C to 95°C. Values were normalized to the housekeeping gene *GAPDH*. All experiments were performed in triplicate on two different dates, from independent mRNA harvests. Relative expression ratios of target genes were calculated using the comparative cycle threshold method. Primer sequences are provided in Supplemental Table 1.

**Fluorescence-activated cell sorting (FACS)**

We trypsinized cells from each clone and stained unfixed live cells with anti-E-cadherin (BD Biosciences, Cat # 563571) and anti-CD24 (BD Biosciences, Cat # 562789). 10,000 Events were acquired in a FACSCanto II flow cytometer (BD Biosciences). Representative samples were plotted as histograms; Median Fluorescence Intensity (MFI) of each channel was used for quantification. Statistical analysis was performed by 2-tail Student t-test. Differences were considered statistically significant at $p < 0.05$.

## RESULTS

**786-O ccRCC cells have methylated *TCF21***

We first asked whether *TCF21* could regulate ccRCC cell proliferation. To this end, we generated isogenic stable cell lines for *in vitro* comparison of cell proliferation in 786-O cells transfected with an empty pBABE vector ("pBABE-Mock" clones N1F4, B5F1, B6D10, N1G4) and 786-O cells stably expressing pBABE-TCF21 (clones 2B12, 5D2, 9D12, 9H9). *TCF21* mRNA expression is very low-to-undetectable in control 786-O cells by qPCR. Over-expression of *TCF21* was examined by qPCR (Figure 1A) and by western blot (Figure 1B). Treatment of 786-O cells with 3 μM of the demethylating agent decitabine (5-aza-2'-deoxycytidine) increased *TCF21* RNA levels (Figure 1C), indicating that the endogenous low level of *TCF21* is due to methylation of the promotor.

***TCF21* ectopic expression suppresses clonogenic cell proliferation**

To investigate whether *TCF21* expression results in a reduction of cell proliferation in the context of the ccRCC cell line 786-O, we performed standard growth curves on the four clones that were pBABE-mock transfected and compared them to standard growth curves from the four clones expressing *TCF21* after 2, 4 and 5 days. Although the difference in proliferation was not significant at any of the chosen time points, we observed a mild trend towards decreased proliferation in the pBABE-TCF21 clones (Figure 2A). In addition, treatment of 786-O cells with 3 μM of the demethylating agent decitabine resulted in a significant reduction of cell proliferation in comparison to 786-O cells transfected with an empty pBABE vector ($p<0.01$) (data not shown). We therefore suggest that *TCF21* expression moderately suppressed proliferation of this 786-O cancer cell line, and that the hypothesis that proliferation is suppressed by *TCF21* warranted further investigation.

We next assessed the ability of our clones to generate colonies from single cells in colony formation assays. This *in vitro* survival assay measures clonogenic potential and can be associated with tumorigeneity. No difference in the overall number of established colonies was observed between 786-O pBABE-mock and 786-O pBABE-TCF21 cells ($p>0.5$).

However, individual colonies of 786-O pBABE-mock cells were larger compared to *TCF21*-expressing cells (Figure 2B-C, $p<0.01$). These data are partly consistent with the proliferation data and support the idea that while *TCF21* overexpression does not seemingly affect cell survival (colony number), proliferation (colony size) is somewhat suppressed.

786-O cells are derived from a ccRCC which, like most ccRCCs, harbors biallelic somatic mutations of the von Hippel-Lindau (*VHL*) tumor suppressor gene (Gnarra et al., 1994). We have previously generated a zebrafish model with biallelic constitutive *vhl* mutations, and have reported the embryonic renal phenotype as exhibiting an alveolar hyperplastic morphology (van Rooijen et al., 2011). Given the apparent effect of *TCF21* on 786-O

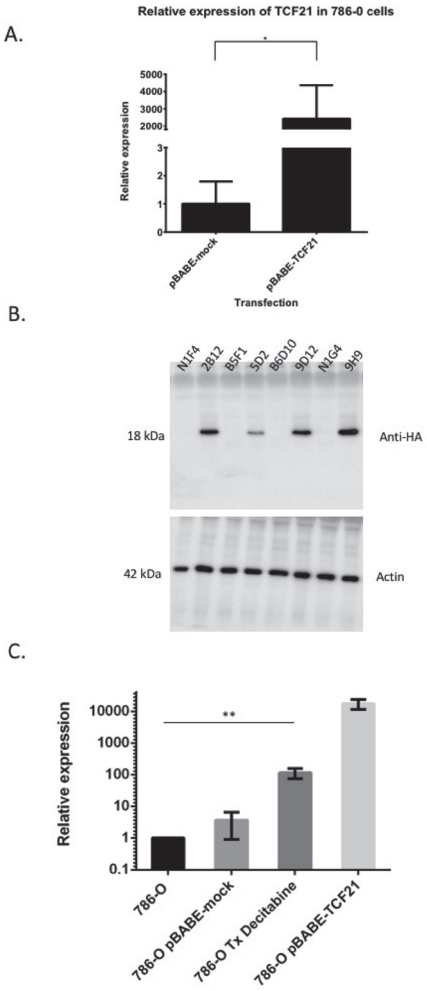


**Figure 1.** *TCF21* methylation and reconstitution. (A) *TCF21* mRNA expression levels as measured by qPCR normalized to the low endogenously detected levels in 786-O cells. N=2, performed in triplicate. (B) Western blots of eight clones of 786-O that were used for this study; four clones were mock-transfected with pBABE-puro (N1F4, B5F1, B6D10, N1G4) and four were transfected with HA-tagged pBABE-TCF21 (2B12, 5D2, 9D12, 9H9). Upper blot was immunostained with anti-HA to detect exogenous TCF21 (18 kDa), lower blot is loading control stained with anti-actin (42 kDa). N=2, representative result shown. (C) Treating 786-O cells with 3$\mu$M decitabine increases the expression of *TCF21* mRNA, as measured by qPCR. p=0.004, one-way ANOVA, n=1 in duplicate.

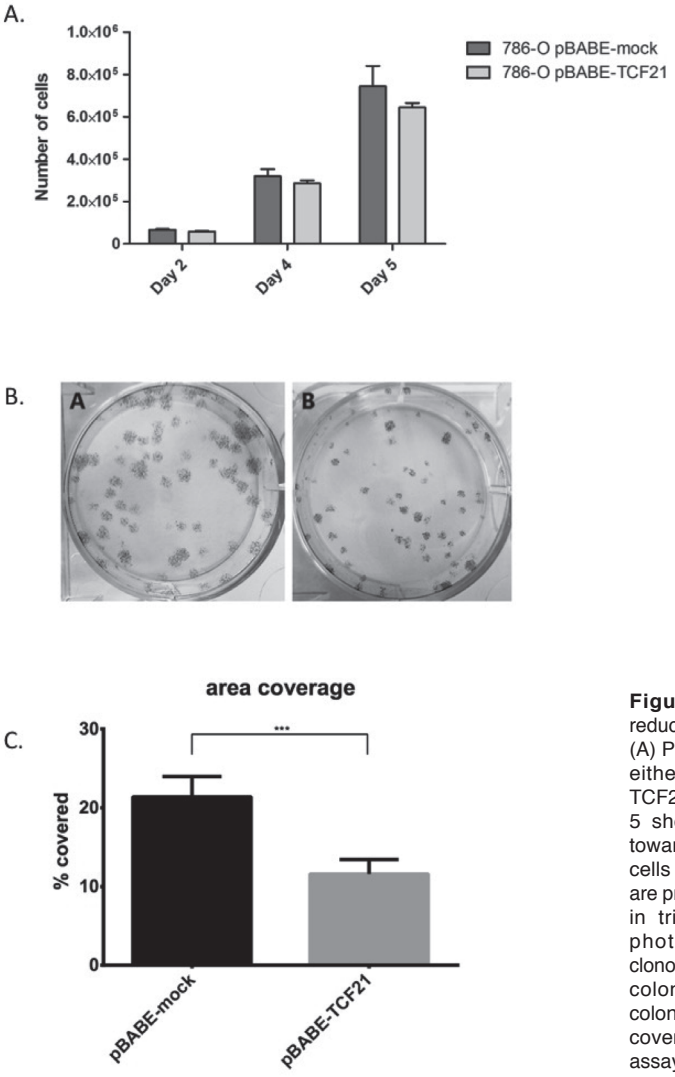


**Figure 2.** *TCF21* expression reduces clonogenic cell proliferation. (A) Pooled data from all four clones either pBABE-mock or pBABE-TCF21 for cell counts on Day 2, 4 or 5 showing an insignificant trend toward lower proliferation in 786-O cells overexpressing *TCF21*. Data are presented as mean ± SEM. N=2, in triplicate. (B) Representative photographs of wells from clonogenic assay. Left, pBABE-mock colonies; Right, pBABE-TCF21 colonies. (C) Quantification of area covered by colonies in clonogenic assays. N=5, in triplicate.



*vhl*-/- cells, we questioned whether injection of *TCF21* RNA into our *vhl*-/- zebrafish embryos would partially or completely rescue the pronephric phenotype. To that end, 17 *vhl*-/- zebrafish embryos were injected with human *TCF21* RNA (n=8), or mock-injected with dye only as a control (n=9) within an hour after fertilization, and imaged 4 days later, when the pronephros phenotype in *vhl*-/- is very clear, and imaged with z-stacks on a confocal microscope for 3D volume. All embryos were genotyped for confirmation after the experiment and only images of confirmed *vhl*-/- were analyzed. No differences were

observed in pronephros volumes between mock-injected or *TCF21* mRNA-injected (Supplemental Figure 1).

***TCF21* expression suppresses migration**

Because the effect of the colony formation assays could only be partially explained by the modest cell proliferation differences observed in Figure 2A, we hypothesized that the colony area differences (Figure 2C) might as well be attributed to altered cell migration. Initial analysis of migration using the chemotaxis-based Boyden chamber assay on two pBABE-mock clones (N1G4 and B6D10) and two pBABE-TCF21 clones (5D2 and 9D12), showed a trend towards inhibition of migration in *TCF21*-expressing cells (analysis repeated for N1G4 and 5D2 clones). 59% fewer of the *TCF21*-expressing cells migrated on average (Figure 3A and 3B). To verify these findings, we subsequently serum-starved all four pBABE-mock and four pBABE-TCF21 clones for 24 hours and then exposed them to either empty medium or 10% FCS for each clone in triplicate and measured impedance changes for 24 hours using an xCELLigence system. To calculate migration, we took the maximum linear slope over a moving average of 10 time-points for each clone, in triplicate. We observed a decrease in cell migration as represented by impedance measurements in the isogenic clones expressing *TCF21* ($p=0.0495$, $n=3$, Figure 3C). Taken together, these data indicate that ccRCC cells become less likely to migrate upon reconstitution of *TCF21* expression.

**No differential expression of selected epithelial or mesenchymal markers by *TCF21* in 786-O cells**

Epithelial-to-mesenchymal transition (EMT) is a reversible process by which fully differentiated cells lose their epithelial features and acquire a migratory mesenchymal phenotype, with concomitant increased expression of mesenchymal-associated proteins and decreased expression of epithelial markers. EMT is known to contribute to the metastasis of RCC (Mikami et al., 2014), although the underlying cellular and molecular mechanisms have not been clarified yet. The inhibition of migration in ccRCC cells by re-expression of *TCF21* (Figure 3) suggests that *TCF21* might function in the renal epithelium by consolidating epithelial characteristics, or alternatively, in repressing mesenchymal characteristics. We investigated mesenchymal and epithelial marker expression in the eight 786-O clones expressing pBABE-mock versus pBABE-TCF21 by qPCR. No changes were observed in mRNA levels of the mesenchymal markers vimentin (*VIM*) and snail (*SNAI1*), but we did observe significant upregulation of epithelial marker E-cadherin (*CDH1*) in the clones expressing ectopic *TCF21* (Figure 4A). These data could suggest that cells with hypermethylated *TCF21* promotors are more predisposed to EMT, thereby potentially contributing to the tumor suppressor function of *TCF21* in renal tumors.

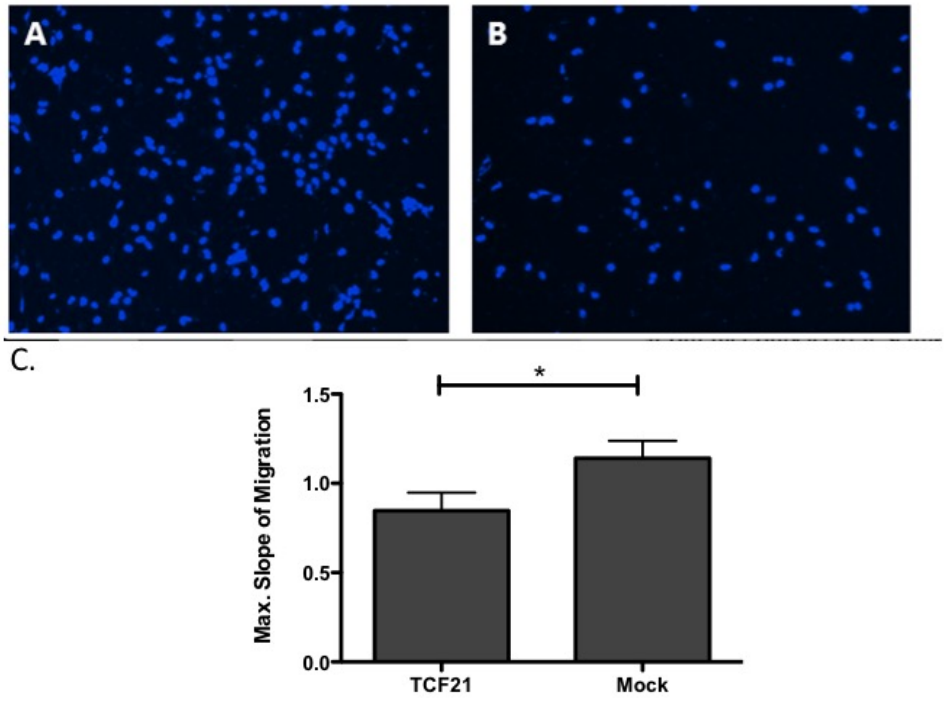


**Figure 3.** *TCF21* expression reduces migration of cells *in vitro*. Representative photos of DAPI (blue)-stained nuclei after migration through a Boyden chamber of pBABE-mock transfected (A) or pBABE-TCF21 transfected (B) clones. (C) The rate of change in impedance of cells across a transwell membrane in an XCelligence system indicates that clones expressing *TCF21* migrate significantly slower than pBABE-mock transfected cells (p =0.0495, n=3).



In a melanoma cell line (C8161), re-expression of *TCF21* was described to activate expression of the metastatic suppressor *KISS1* and consequently inhibit motility of the cells (Arab et al., 2011; Zhang et al., 2012). We investigated *KISS1* expression levels in 786-O clones expressing pBABE-mock and clones expressing pBABE-TCF21; expression levels were undetectably low in both untransfected as well as transfected 786-O cells, while being robustly expressed in control human placenta (average Cq value 21,4).

As consistent up-regulation of genes involved in the Sonic hedgehog signaling pathway and Akt cell proliferation pathway has been reported in both CCSKs as well as ccRCCs (Cutcliffe et al., 2005; Dormoy et al., 2009; Guo et al., 2015), we investigated expression of a few genes involved in these pathways (*EGFR, SMO, CCND1*) in pBABE-mock and pBABE-TCF21 cells; no significant difference in expression was observed (Figure 4A).

Lastly, to test the functional relevance of increased *CDH1* expression, we performed fluorescence-activated cell sorting (FACS) of extracellular epithelial differentialtion markers

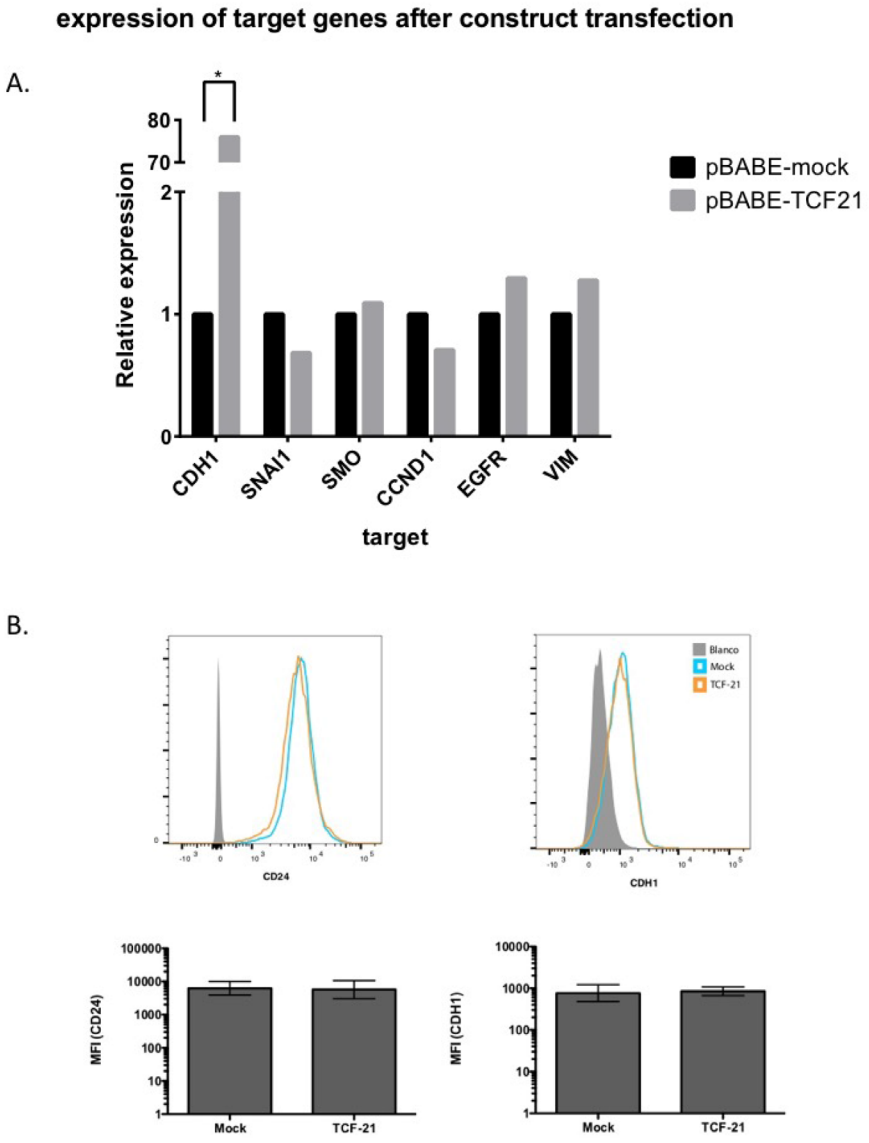


**Figure 4:** *TCF21* expression does not regulate selected epithelial or mesenchymal markers. (A) The isogenic clones (pBABE-mock and pBABE-TCF21) were grown to subconfluency and mRNA was extracted for qPCR. Expression levels of E-Cadherin (*CDH1*), Snail (*SNAI1*), Smoothened (*SMO*), Cyclin D1 (*CCND1*), Epidermal Growth Factor Receptor (*EGFR*), and Vimentin (*VIM*) were normalized to *GAPDH* housekeeping gene and the pBABE-mock clones pooled. N=2, in triplicate. (B) FACS analyses of the eight isogenic clones indicates no difference in the functional expression of E-cadherin (CDH1) or glycoprotein CD24 in clones expressing pBABE-TCF21 (TCF-21) vs mock transfected clones (mock). The grey histograms are unstained controls., Below the histograms are the quantification of the Mean Fluorescence Intensity (MFI) for the four clones with pBABE-TCF21 ('TCF21") vs pBABE-Mock ("Mock"). They are no significant differences observed.

CD24 and CDH1. Each 786-O clone expressing either pBABE-mock or pBABE-TCF21 was stained by directly conjugated fluorescence antibodies for the endogenous extracellular epitope of E-cadherin or CD24 and sorted on the strength of the fluorescent signal and side scatter. In contrast to the qPCR data, we observed no differential E-cadherin or CD24 protein expression in the pBABE-TCF21 clones collectively than in the pBABE-mock clones (Figure 4B).

## DISCUSSION

In the present study, functional experiments demonstrate that reconstitution of *TCF21* expression in 786-O cells results in decreased clonogenic proliferation and suppressed migration *in vitro*. These data support a tumor suppressor function for *TCF21* in the context of ccRCC, in accordance with several studies which have demonstrated that *TCF21* acts as a tumor suppressor gene in different tumor types. For example, re-expression of *TCF21* reduced cell growth and colony formation in lung cancer cells *in vitro* and *in vivo* (Smith et al., 2006), reduced cell proliferation, promoted apoptosis and suppressed cell invasion and migration in colorectal cancer *in vitro* (Dai et al., 2016) and reduced cell proliferation and epithelial-mesenchymal transition in breast cancer cells *in vitro* (Wang et al., 2015). In addition, down-regulation of *TCF21* through hypermethylation has been reported to be associated with poor outcome in patients with ccRCC and metastatic melanoma (Ye et al., 2012).

As reported before, and confirmed in the current study, expression of *TCF21* is (at least partly) repressed by methylation in 786-O cells. This *TCF21* hypermethylation has also been demonstrated in other clear cell renal cell carcinoma (ccRCC) cell lines and human ccRCC tissue samples (Costa et al., 2011; Xin et al., 2016; Ye et al., 2012). Likewise, in other human cancer types, such as gastric cancer, colorectal cancer, melanoma, head and neck cancer and non-small cell lung carcinoma, promoter hypermethylation is described to be the predominant mechanism for *TCF21* downregulation (Arab et al., 2011; Dai et al., 2016; Smith et al., 2006; Yang et al., 2015).

To increase metastatic and invasive capacities, cancer cells often show loss of epithelial and gain of mesenchymal characteristics, which permit invasion along the basement membrane, establishing an opportunity for metastasis (Birchmeier et al., 1996; Thiery, 2002). *TCF21* is known to be involved in mesenchymal-to-epithelial transition (MET) (Acharya et al., 2012; Quaggin et al., 1999; Smith et al., 2006; Wang et al., 2015). Although we did not detect decreased expression of mesenchymal markers in our 786-O cells transfected with *TCF21*, our data support a positive association of *TCF21* expression and increased mRNA expression of the epithelial marker E-cadherin (*CDH1*), which was markedly up-regulated in *TCF21*-expressing 786-O cells. However, we were unable to functionally validate the

expression of surface expressed E-Cadherin, or other epithelial differentiation marker CD24 in FACS analyses. Inactivation of *CDH1* is described to be prominently associated with tumor invasiveness, metastatic dissemination, and poor patient prognosis; the significance of *CDH1* for metastatic potential has been shown in a variety of *in vitro* and *in vivo* models (Frixen et al., 1991; Onder et al., 2008; von Burstin et al., 2009). Therefore, increase of *CDH1* expression might be a possible reason for decreased migration of *TCF21*-expressing 786-O cells in the current study, although we did not detect changes in the extracellular epitope for E-Cadherin. Although re-expression of *TCF21* in melanoma cells and Caki-1 ccRCC cells has been described to activate expression of the metastatic suppressor *KISS1* (Arab et al., 2011; Zhang et al., 2012*)*, in the current study *KISS1* expression does not seem to be involved in the suppressed migration of 786-O cells transfected with *TCF21*. Further studies are warranted to consolidate these data.

Recently, we reported that CCSKs bearing the *BCOR* internal tandem duplication showed hypermethylation of *TCF21*, while CCSKs bearing the translocation t(10;17)(q22;p13) showed significantly lower methylation levels of the *TCF21* promoter, suggesting that, alternatively, internal tandem duplication of *BCOR* (working as an epigenetic modifier) may be directly or indirectly responsible for *TCF21* hypermethylation in CCSKs (Gooskens et al., 2016). To functionally validate the tumorigenic role of *TCF21* hypermethylation in CCSKs, CCSK models urgently need to be developed. Due to the rarity of CCSK and because pediatric renal tumors are often histologically diagnosed after surgery, it is a challenge to develop such research tools as cell lines or other CCSK models. If we are able to develop efficient and physiologically relevant models through additional studies and could generate similar results in CCSK cells as in ccRCC cells, then treatment with demethylating agents might be an option for these patients. The demethylating agent decitabine used in the current study resulted in a strong reduction of cell proliferation.

## CONCLUSIONS

In summary, our study revealed that restoration of *TCF21* expression in 786-O ccRCC cells results in decreased clonogenic proliferation and migration, suggesting that *TCF21* may constitute a potential therapeutic target for ccRCC tumors. CCSK models need to be developed to fully determine the influence of reconstitution of *TCF21* expression in CCSK cells.

**Acknowledgements**

The authors wish to thank Glenn van de Hoek for his technical support. We thank the zebrafish caretaker team at the Hubrecht Institute as well.

**Funding**
This work was supported by the EU FP7 programme EURenOmics (grant number 305608), the Dutch Kidney Foundation (KOUNCIL, CP11.18), the Pediatric Oncology Center Society for Research (KOCR) and the DaDa foundation.

# REFERENCES


1. Acharya, A., Baek, S.T., Huang, G., Eskiocak, B., Goetsch, S., Sung, C.Y., Banfi, S., Sauer, M.F., Olsen, G.S., Duffield, J.S., Olson, E.N., Tallquist, M.D., 2012. The bHLH transcription factor Tcf21 is required for lineage-specific EMT of cardiac fibroblast progenitors. Development 139, 2139-2149.
2. Arab, K., Smith, L.T., Gast, A., Weichenhan, D., Huang, J.P., Claus, R., Hielscher, T., Espinosa, A.V., Ringel, M.D., Morrison, C.D., Schadendorf, D., Kumar, R., Plass, C., 2011. Epigenetic deregulation of TCF21 inhibits metastasis suppressor KISS1 in metastatic melanoma. Carcinogenesis 32, 1467-1473.
3. Argani, P., Perlman, E.J., Breslow, N.E., Browning, N.G., Green, D.M., D'Angio, G.J., Beckwith, J.B., 2000. Clear cell sarcoma of the kidney: a review of 351 cases from the National Wilms Tumor Study Group Pathology Center. Am J Surg Pathol 24, 4-18.
4. Astolfi, A., Melchionda, F., Perotti, D., Fois, M., Indio, V., Urbini, M., Genovese, C.G., Collini, P., Salfi, N., Nantron, M., D'Angelo, P., Spreafico, F., Pession, A., 2015. Whole transcriptome sequencing identifies BCOR internal tandem duplication as a common feature of clear cell sarcoma of the kidney. Oncotarget 6, 40934-40939.
5. Birchmeier, C., Birchmeier, W., Brand-Saberi, B., 1996. Epithelial-mesenchymal transitions in cancer progression. Acta Anat (Basel) 156, 217-226.
6. Costa, V.L., Henrique, R., Danielsen, S.A., Eknaes, M., Patricio, P., Morais, A., Oliveira, J., Lothe, R.A., Teixeira, M.R., Lind, G.E., Jeronimo, C., 2011. TCF21 and PCDH17 methylation: An innovative panel of biomarkers for a simultaneous detection of urological cancers. Epigenetics 6, 1120-1130.
7. Cui, S., Schwartz, L., Quaggin, S.E., 2003. Pod1 is required in stromal cells for glomerulogenesis. Dev Dyn 226, 512-522.
8. Cutcliffe, C., Kersey, D., Huang, C.C., Zeng, Y., Walterhouse, D., Perlman, E.J., Renal Tumor Committee of the Children's Oncology, G., 2005. Clear cell sarcoma of the kidney: up-regulation of neural markers with activation of the sonic hedgehog and Akt pathways. Clin Cancer Res 11, 7986-7994.
9. Dai, Y., Duan, H., Duan, C., Zhou, R., He, Y., Tu, Q., Shen, L., 2016. Down-regulation of TCF21 by hypermethylation induces cell proliferation, migration and invasion in colorectal cancer. Biochem Biophys Res Commun 469, 430-436.
10. Dormoy, V., Danilin, S., Lindner, V., Thomas, L., Rothhut, S., Coquard, C., Helwig, J.J., Jacqmin, D., Lang, H., Massfelder, T., 2009. The sonic hedgehog signaling pathway is reactivated in human renal cell carcinoma and plays orchestral role in tumor growth. Mol Cancer 8, 123.
11. Frixen, U.H., Behrens, J., Sachs, M., Eberle, G., Voss, B., Warda, A., Lochner, D., Birchmeier, W., 1991. E-cadherin-mediated cell-cell adhesion prevents invasiveness of human carcinoma cells. J Cell Biol 113, 173-185.
12. Furtwangler, R., Gooskens, S.L., van Tinteren, H., de Kraker, J., Schleiermacher, G., Bergeron, C., de Camargo, B., Acha, T., Godzinski, J., Sandstedt, B., Leuschner, I., Vujanic, G.M., Pieters, R., Graf, N., van den Heuvel-Eibrink, M.M., 2013. Clear cell sarcomas of the kidney registered on International Society of Pediatric Oncology (SIOP) 93-01 and SIOP 2001 protocols: a report of the SIOP Renal Tumour Study Group. Eur J Cancer 49, 3497-3506.
13. Gnarra, J.R., Tory, K., Weng, Y., Schmidt, L., Wei, M.H., Li, H., Latif, F., Liu, S., Chen, F., Duh, F.M., et al., 1994. Mutations of the VHL tumour suppressor gene in renal carcinoma. Nat Genet 7, 85-90.
14. Gooskens, S.L., Furtwangler, R., Vujanic, G.M., Dome, J.S., Graf, N., van den Heuvel-Eibrink, M.M., 2012. Clear cell sarcoma of the kidney: a review. Eur J Cancer 48, 2219-2226. Gooskens, S.L., Gadd, S., Guidry Auvil, J.M., Gerhard, D.S., Khan, J., Patidar, R., Meerzaman, D., Chen, Q.R., Hsu, C.H., Yan, C., Nguyen, C., Hu, Y., Mullighan, C.G., Ma, J., Jennings, L.J., de Krijger, R.R., van den Heuvel-Eibrink, M.M., Smith, M.A., Ross, N., Gastier-Foster, J.M., Perlman, E.J., 2015. TCF21 hypermethylation in genetically quiescent clear cell sarcoma of the kidney. Oncotarget 6, 15828-15841.
15. Gooskens, S.L., Gadd, S., van den Heuvel-Eibrink, M.M., Perlman, E.J., 2016. BCOR internal tandem duplications in clear cell sarcoma of the kidney. Genes Chromosomes Cancer 55, 549-550.
16. Guo, H., German, P., Bai, S., Barnes, S., Guo, W., Qi, X., Lou, H., Liang, J., Jonasch, E., Mills, G.B., Ding, Z., 2015. The PI3K/AKT Pathway and Renal Cell Carcinoma. J Genet Genomics 42, 343-353.
17. Hidai, H., Bardales, R., Goodwin, R., Quertermous, T., Quertermous, E.E., 1998. Cloning of capsulin, a basic helix-loop-helix factor expressed in progenitor cells of the pericardium and the coronary arteries. Mech Dev 73, 33-43.
18. Karlsson, J., Lilljebjorn, H., Holmquist Mengelbier, L., Valind, A., Rissler, M., Ora, I., Fioretos, T., Gisselsson, D., 2015. Activation of human telomerase reverse transcriptase through gene fusion in clear cell sarcoma of the kidney. Cancer Lett 357, 498-501.
19. Lu, J., Richardson, J.A., Olson, E.N., 1998. Capsulin: a novel bHLH transcription factor expressed in epicardial progenitors and mesenchyme of visceral organs. Mech Dev 73, 23-32. Mikami, S., Oya, M., Mizuno, R., Kosaka, T., Katsube, K., Okada, Y., 2014. Invasion and metastasis of renal cell carcinoma. Med Mol Morphol 47, 63-67.
20. Mullen, E.A., Geller, J.I., Gratias, E., Perlman, E.J., Ehrlich, P.F., Khanna, G., Naranjo, A., Fernandez, C.V., Gow, K., Ferrer, F., Hamilton, T., Glick, R., Kandel, J., Barnhart, D., He, Y., Dasgupta, R., Hoffer, F., Servaes, A., Gastier-Foster, J.M., Hill, D.A., Huff, V., Grundy, P.E., Dome, J.S., 2014. Comprehensive update of pediatric renal tumor epidemiology: analysis of the first 4000 patients on children's oncology group (COG) renal tumor classification and biology protocol AREN03B2. Pediatr

Blood Cancer 61, 1.
21. Onder, T.T., Gupta, P.B., Mani, S.A., Yang, J., Lander, E.S., Weinberg, R.A., 2008. Loss of E-cadherin promotes metastasis via multiple downstream transcriptional pathways. Cancer Res 68, 3645-3654.
22. Plotkin, M., Mudunuri, V., 2008. Pod1 induces myofibroblast differentiation in mesenchymal progenitor cells from mouse kidney. J Cell Biochem 103, 675-690.
23. Quaggin, S.E., Schwartz, L., Cui, S., Igarashi, P., Deimling, J., Post, M., Rossant, J., 1999. The basic-helix-loop-helix protein pod1 is critically important for kidney and lung organogenesis. Development 126, 5771-5783.
24. Quaggin, S.E., Vanden Heuvel, G.B., Igarashi, P., 1998. Pod-1, a mesoderm-specific basic-helix-loop-helix protein expressed in mesenchymal and glomerular epithelial cells in the developing kidney. Mech Dev 71, 37-48.
25. Roy, A., Kumar, V., Zorman, B., Fang, E., Haines, K.M., Doddapaneni, H., Hampton, O.A., White, S., Bavle, A.A., Patel, N.R., Eldin, K.W., John Hicks, M., Rakheja, D., Leavey, P.J., Skapek, S.X., Amatruda, J.F., Nuchtern, J.G., Chintagumpala, M.M., Wheeler, D.A., Plon, S.E., Sumazin, P., Parsons, D.W., 2015. Recurrent internal tandem duplications of BCOR in clear cell sarcoma of the kidney. Nat Commun 6, 8891.
26. Smith, L.T., Lin, M., Brena, R.M., Lang, J.C., Schuller, D.E., Otterson, G.A., Morrison, C.D., Smiraglia, D.J., Plass, C., 2006. Epigenetic regulation of the tumor suppressor gene TCF21 on 6q23-q24 in lung and head and neck cancer. Proc Natl Acad Sci U S A 103, 982-987.
27. Thiery, J.P., 2002. Epithelial-mesenchymal transitions in tumour progression. Nat Rev Cancer 2, 442-454.
28. Ueno-Yokohata, H., Okita, H., Nakasato, K., Akimoto, S., Hata, J., Koshinaga, T., Fukuzawa, M., Kiyokawa, N., 2015. Consistent in-frame internal tandem duplications of BCOR characterize clear cell sarcoma of the kidney. Nat Genet 47, 861-863.
29. van Rooijen, E., Santhakumar, K., Logister, I., Voest, E., Schulte-Merker, S., Giles, R., van Eeden, F., 2011. A zebrafish model for VHL and hypoxia signaling. Methods Cell Biol 105, 163-190.
30. van Rooijen, E., Voest, E.E., Logister, I., Korving, J., Schwerte, T., Schulte-Merker, S., Giles, R.H., van Eeden, F.J., 2009. Zebrafish mutants in the von Hippel-Lindau tumor suppressor display a hypoxic response and recapitulate key aspects of Chuvash polycythemia. Blood 113, 6449-6460.
31. von Burstin, J., Eser, S., Paul, M.C., Seidler, B., Brandl, M., Messer, M., von Werder, A., Schmidt, A., Mages, J., Pagel, P., Schnieke, A., Schmid, R.M., Schneider, G., Saur, D., 2009. E-cadherin regulates metastasis of pancreatic cancer in vivo and is suppressed by a SNAIL/HDAC1/HDAC2 repressor complex. Gastroenterology 137, 361-371, 371 e361-365. Wang, J., Gao, X., Wang, M., Zhang, J., 2015. Clinicopathological significance and biological role of TCF21 mRNA in breast cancer. Tumour Biol 36, 8679-8683.
32. Xin, J., Xu, R., Lin, S., Xin, M., Cai, W., Zhou, J., Fu, C., Zhen, G., Lai, J., Li, Y., Zhang, P., 2016. Clinical potential of TCF21 methylation in the diagnosis of renal cell carcinoma. Oncol Lett 12, 1265-1270.
33. Yang, Z., Li, D.M., Xie, Q., Dai, D.Q., 2015. Protein expression and promoter methylation of the candidate biomarker TCF21 in gastric cancer. J Cancer Res Clin Oncol 141, 211-220.
34. Ye, Y.W., Jiang, Z.M., Li, W.H., Li, Z.S., Han, Y.H., Sun, L., Wang, Y., Xie, J., Liu, Y.C., Zhao, J., Tang, A.F., Li, X.X., Guan, Z.C., Gui, Y.T., Cai, Z.M., 2012. Down-regulation of TCF21 is associated with poor survival in clear cell renal cell carcinoma. Neoplasma 59, 599-605.
35. Zhang, H., Guo, Y., Shang, C., Song, Y., Wu, B., 2012. miR-21 downregulated TCF21 to inhibit KISS1 in renal cancer. Urology 80, 1298-1302 e1291.

# SUPPLEMENTAL

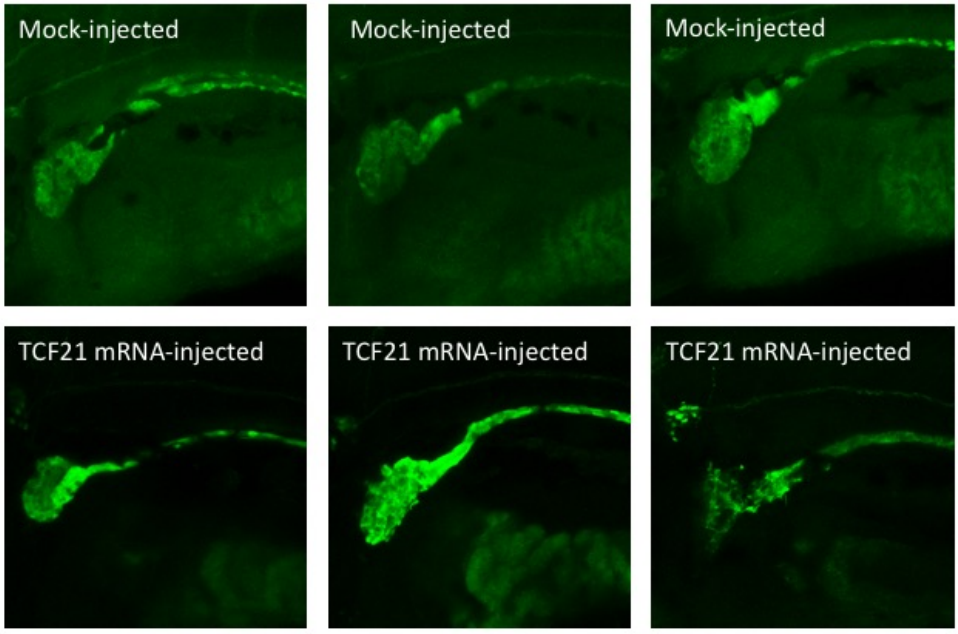


**Supplemental Figure 1.** Confocal images of the trunk of *vhl*-/- zebrafish embryos (5 days post fertilization, anterior is to the left in all images) in a background with green fluorescent pronephros (Tg-*cdh17*:GFP). Upper panels, three mock-injected embryos, and lower panels, three embryos injected with human TCF21 mRNA. N=3, 17 animals imaged total. All embryos scored were genotype confirmed.

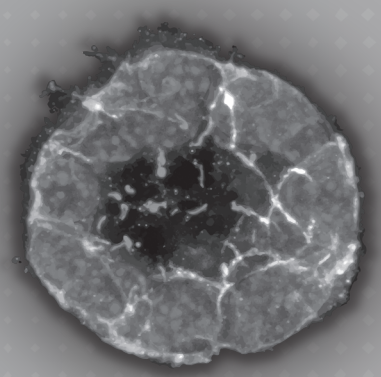

# CHAPTER 10

# General Discussion

In this thesis I have investigated the interactions between tumor suppressor proteins that are involved in ciliary biology, especially the tumor suppressor protein VHL, and their importance in tumorigenesis, especially in the kidney. The main question I initially tried to answer in this work was whether or not cancer could be considered a ciliopathy. To this end, I investigated the ciliary function of several tumor suppressor genes, or genes which were involved in ciliary function as well as processes such as proliferation, apoptosis or the cell cycle. A number of tumor suppressor proteins, as well as proteins which play a role in the cell cycle, mitosis, DNA regulation and repair, cell cycle arrest and apoptosis are all found at the cilium or near the centrosome during the $G_0$ phase of the cell cycle [1-4]. Perhaps proteins like these are found at or around the primary cilium because it is positioned near the nucleus during periods of ciliation and is linked with the cell cycle because the basal body acts as the mother centriole during cell division, making it a convenient organizing center and timing mechanism for the action of these proteins. It is tempting therefore to speculate that the cilium is a tumor protective organelle and that certain types of cancer might actually be ciliopathies. However it is probably not accurate to think of the primary cilium or cancer in this way. Some of the genes found mutated in certain cancers, like *VHL,* also have ciliary functions, but it is currently not possible to differentiate between the ciliary function and possible tumorigenesis involvement of a protein. It is generally not feasible to determine if the tumor-related function of a protein is dependent on its ciliary function, although there are some exceptions. For example, the p19 short isoform of pVHL partially retains the tumor suppressor function of the long isoform (p30) but does not have the same ciliary role [5]. However, for most ciliary proteins, isoforms with the same separation of function are not available, making research difficult. A ciliopathy is a disease which arises primarily because of a defect in ciliation [3]. While it is true that some cancers, similar to ccRCC, display loss of ciliation, it would still not be appropriate to refer to them as ciliopathies. Indeed, it is probably generally inappropriate to think of the ciliary function and the tumor suppressor function of these proteins as separate, as they are simply separate simultaneous outcomes of the same underlying biological processes. It is certainly true that not all cancers are characterized by malfunctioning cilia, which would not be true if the cilium was a universal tumor suppressor. Indeed, in some cancer types, such as medulloblastoma, cilia can actually play a cancer-promoting role (see Chapter 2).

**pVHL function, HIF and renal cancer biology**

Therefore, I instead focused mostly on the function of the tumor suppressor protein pVHL. As discussed elsewhere in this thesis (Chapters 2, 3, 4, 5), pVHL is capable of binding microtubules and modulating their stability, but the canonical function of pVHL is to regulate the cell's response to hypoxia. In the absence of functional pVHL, downstream HIF signaling causes an increase in glycolytic metabolism, cell survival and angiogenesis,

contributing to a pre-cancerous environment that potentiates the development of further mutations which lead to tumorigenesis (see chapter 2). The underlying genetic mechanisms of ccRCC development are interesting in that *VHL* must be mutated, but the mutation of *VHL* is not sufficient for tumor formation alone [6]. After the mutation of *VHL*, one or more genes must also be mutated in order for transformation from a tumor to a cancer to take place. The identity of this gene/genes and timing or sequence of their mutation is the subject of significant debate [7]. However, before this happens, the tubular cells which eventually develop into the tumor lose their cilia and form into disorganized cysts. Without pVHL to stabilize microtubules, mutant cells develop ciliation deficiencies, as discussed in Chapter 2 The loss of pVHL and subsequent loss of cilia thereby contributes to the cystic environment which precedes ccRCC development, creating a climate that promotes disorganized growth [8]. The lack of cilia contributes to the general disorganization of the tissue and to the out-of-phase division of the cells which also produces the cystic phenotype. A certain subset of these cysts may become atypical cysts, which then develop further into solid tumors or tumors with a cystic component [9]. However, in patients with Von Hippel-Lindau (VHL) syndrome, who possess a germline mutation in one allele of *VHL,* a large number of renal cells will develop a second mutation in the other *VHL* allele, but only a small subsection of renal cells possessing biallelic *VHL* mutation will develop cysts and an even smaller subsection of these cystic cells will eventually develop into tumors [8, 10]. These observations in VHL patients and data from mouse models would suggest that *VHL* mutation alone is not sufficient for the growth of neoplasms, like cysts, because only a small subsection of mutant cells become cystic. However, the zebrafish model used throughout this thesis only possesses a *vhl* mutation and the pronephros of these animals reliably display enlarged cells that are histologically similar to human ccRCC cells at an early age, although they do not develop into cysts [11]. The exact mechanisms behind these observations remain unclear. Indeed, although cyst formation is believed to be important for ccRCC development and has been shown in patients with VHL disease and animal models, it has still not been demonstrated to be a precursor of sporadic ccRCC. Although it may lead to cyst formation, it would appear that *VHL* depletion alone does not lead to the formation of cancerous growths, but it does seem to potentiate renal cells to further mutation which eventually does lead to cancer.



As mentioned above, loss of cilia also contributes to renal cyst development. This has been shown in genetic diseases which involve cystic kidneys such as polycystic kidney disease [12], and many ciliopathies involve renal cysts as part of their symptoms including Bardet-Biedl syndrome, Meckel-Gruber syndrome, oro-facio-digital syndrome 1, Joubert syndrome, and others [13]. However, in these diseases, renal cysts do not usually develop into neoplasms. Because not all *VHL*-null renal cells develop cysts, and renal cysts do not

always lead to tumor growth, Guinot *et al* generated two mouse models to study the extent to which the primary cilium acts as a tumor suppressor in renal tissue [14]. These mouse models were generated with renal epithelium specific mutations in either *Kif3a/Trp53* or *Kif3a/Vhl/Trp53*. *Kif3a* encodes a kinesin family member protein required for ciliation while *Trp53* encodes the murine homologue of the human *TP53* gene, an extremely important tumor suppressor protein discussed in Chapter 6 and 2 and extensively reviewed elsewhere [15]. Previously, *Trp53/Vhl* renal epithelium specific double-mutant mice had been shown to develop not only cysts but also tumors, albeit at a low incidence and after a long period of latency, unlike mice with only *Vhl* renal epithelium-specific mutations which only develop occasional cysts and never develop renal masses. *Vhl/Kif3a/Trp53* triple mutant mice displayed a higher incidence of atypical cysts and small solid tumors, but these tumors lacked the pathological characteristics typically attributed to ccRCC. Notably, an increased proportion of the cysts that were found in these animals that also displayed increased proliferation compared with control animals. Kidney tissue typically displays slow cell turnover [16] and it has been shown that renal cyst formation requires cellular turnover after loss of the primary cilia [17]. The authors suggest that a low rate of replication explains why there are many histologically normal mutant tubules, even after a long time period. The authors conclude that the loss of primary cilium via *Kif3a* ablation and *Trp53* does not immediately lead to ccRCC development but instead potentiates tumor development by increasing proliferation and promoting the growth of atypical cysts which can then develop further mutations which, in the cyst-based theory of ccRCC development, should lead to eventually to the development of a ccRCC tumor. Our own data agrees with this conclusion. As we discuss in Chapter 6, lack of functional p53 probably does not directly contribute to tumorigenesis in ccRCC, which has a much lower incidence of *TP53* mutations compared with many other tumor types. Instead, *Trp53* mutation probably sensitizes mutant renal cells to further mutations. As the authors note, their results show that loss of ciliation does not contribute to the oncogenic transformation of cells but it does contribute to proliferation which, along with the accompanying *Trp53* mutation, creates a larger pool of proliferating precursor cells. The loss of ciliation does not cause an increase in proliferation on its own, as covered in Chapter 2. However, because *VHL* mutant cells also upregulate proliferative signals, lack of primary cilia removes a crucial checkpoint in the process of duplication, allowing these cells, which are normally ciliated, to progress through the cell cycle without having to build and then disassemble the cilium. The results of this experiment provides support for the hypothesis that the primary cilium acts as a tumor suppressor organelle in the kidney, as well as the hypothesis that ccRCC first develops as a cystic disease and progresses to a tumor after more mutations are acquired. However, the identities of the driver mutations which cause ccRCC tumorigenesis remain unknown. Santhakumar *et al.* developed a transgenic zebrafish model which could be used to investigate the

identities of these genes . This zebrafish expresses EGFP with prolyl hydroxylase 3 (PHD3), and important protein upstream of of pVHL. In response to hypoxia, PHD3 is upregulated leading to strong transgene expression in hypoxic cells of these zebrafish. Unlike human patients with VHL syndrome who possess heterozygous *VHL* mutations, heterozygous *vhl* mutant zebrafish do not develop cancer at an increased rate when compared with control animals. However, when the *vhl* heterozygote zebrafish were treated with dimethylbenzanthracene (DMBA), a carcinogen, they developed liver and intestinal tumors which displayed transgene expression, suggesting that a subset of tumor cells had a mutation in the second allele of *vhl.* By isolating cells expressing EGFP and performing single cell sequencing on them, this zebrafish model could be used to identify candidate genes which might be important for tumorigenesis along with *VHL*.

After *VHL* mutation, the action of pVHL as a negative regulator of the hypoxia response pathway is lost, leading to tumor-promoting and tumor-protective phenotypes, although not excessive proliferation. It is in this environment of genetic instability, stimulated angiogenesis and glycolysis, another mutation arises which leads to tumor promotion [18] (Figure 1). Thus, an obvious question is whether *VHL* mutations are completely necessary for ccRCC development, or if they simply make further tumor-driving mutations significantly more likely. Indeed, in a certain subsection of later stage tumors, HIF2 is upregulated while HIF1 is lost via gene deletion/mutation [19-21]. This leads to the hypothesis that HIF1 hyperactivation following the loss of functional pVHL may be in fact dispensable for cancer development and that HIF1 functions solely in a tumor protective role while HIF2 activity is the driving force behind tumorigenesis. However, studies have shown that tumors do not develop in the kidneys of mice that have a deletion of either HIF gene in a mouse with a renal tubule specific *vhlh* deletion [22]. In addition, studies of the genetics of human ccRCCs taken from patients have near-universally found *VHL* mutations and deep sequencing has shown that these mutations are truncal and therefore must be present for further mutation [23]. Because ccRCCs without genetic disruption of *VHL* are rare and HIF1 activity seems to be required for tumor growth, it is unlikely that either is dispensable for the initial growth of kidney tumors, even though *VHL* mutation is not sufficient for tumorigenesis and HIF1 appears to lose its importance to the tumor over time. Thus, it is likely that ccRCC develops as a transition between the cystic, pre-cancerous state induced by constitutive HIF1 activation while HIF2 activity and then proceeds to drive the development of the tumor in this environment.

Much debate remains about the identity of the gene (or genes) which comprise the second hit in ccRCC. Multiple groups have sequenced the exomes of a number of ccRCC tumors taken from patients in an effort to understand the genetic evolution of ccRCC [23, 24].

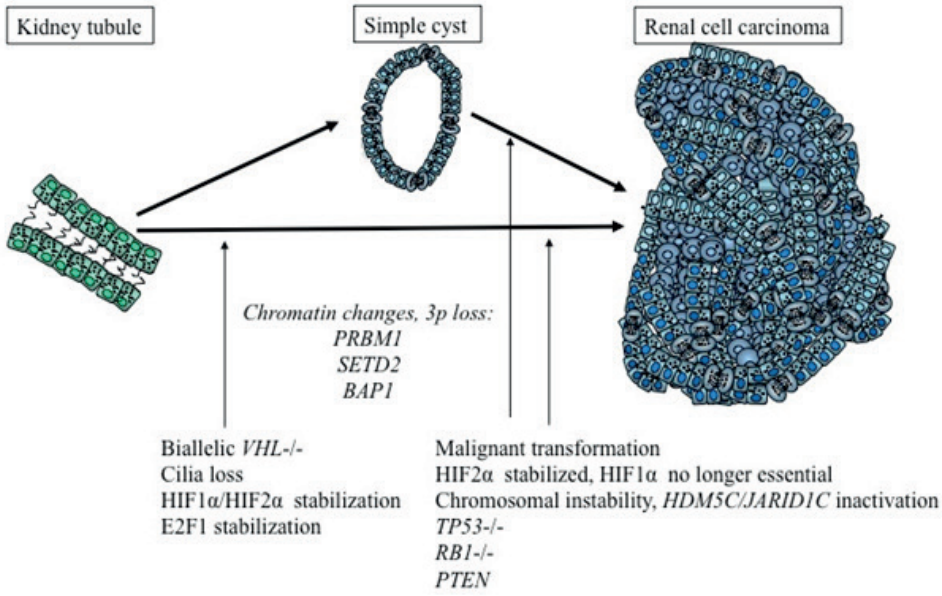


**Figure 1.** Figure reproduced from [7]. Schematic representation of the development of ccRCC from a healthy tubule cell. Initially, biallelic loss of VHL leads to the loss of cilia and hyperstablization of HIF. This can lead to cysts and also contributes to the development of further mutations. In patients with VHL disease, cyst formation precedes the development of tumors, but this step may not be necessary for tumorigenesis in sporadic cases of ccRCC. In later stages, HIF2 signaling becomes more important than HIF1 signaling and further mutations are gained which contribute to malignancy.

These tumors show a considerable amount of intra-tumor heterogeneity in terms of genetic background. Different pieces of the same tumor may develop from the same initial mutation with different subsequent hits. After the initial *VHL* mutation, a number of further mutations are seen. Based on the work of this group and others, we can see that a large number of genes can serve as second hits but certain patterns emerge. For example, a subset of genes which encode for histone modifying proteins are frequently found mutated in ccRCC. Although it is not known exactly what role these histone modifiers play in the development of ccRCC tumors, they are mutated in a significant portion of ccRCC in many different studies making them strong candidates to be the second hit required for tumorigenesis. Intriguingly, three of these genes, the methyltransferases *SETD2* and *PBRM1* as well as the deubiquitinylase *BAP1*, are located very close to *VHL* on chromosome 3p and are frequently lost along with it during loss-of-heterozygosity events. As mentioned elsewhere in this thesis (Chapters 1 and 2), *Bap1* heterozygote mice with a renal-tubule specific *Vhl* mutation develop tumors very similar to human ccRCC [25] while post-natal conditional *Vhl* mutation alone does not lead to tumorigenesis in mice [6] and mice with

germline deletion of *Vhl* do not survive [26]. This raises the possibility that the exceptional ubiquity of *VHL* mutations in ccRCC compared with known causal mutations in other tumors comes about partially because of its placement in the genome. Disruptions in the *VHL* gene potentiate the development of further mutations which work in concert with *VHL* mutations to produce ccRCC tumors. Although it is still unknown what role histone modification plays in the etiology of ccRCC, it is clear that modification of the genome contributes in some way to tumorigenesis. Much work remains to be done to identify which genes are affected by these modifications.

We have identified and studied one gene found hypermethylated in ccRCC and a rare pediatric renal caner, clear cell sarcoma (Chapter 8). This gene, *TCF21*, has been shown to be involved in the differentiation of cells in the kidney and lung, amongst others. Although the transcription factor produced from this gene is responsible for antagonizing the growth and migration of epithelial cells, mouse models of *Tcf21* deletion actually show a growth deficiency in the same cells. Although we could not identify an effect of hypermethylated TCF21 in our zebrafish *vhl*-/- model, the possibility remains that the hypermethylation of this gene contributes to tumor growth after *VHL* is lost. Because the zebrafish model is a model of HIF activation rather than a tumor model, it is possible that we simply do not have a proper model to examine the effect of TCF21. Indeed, we did see that hypermethylation of TCF21 is present in the 786-0 *VHL*-/- RCC cell line, and that reconstitution of TCF21 expression significantly affects the proliferation and migration behavior of our ccRCC tumor cell lines, indicating that the hypermethylation of *TCF21* and genes like it may be involved in the transition of VHL deficient tissues into tumors. Future research in this area should focus on the functional consequences of the hypermethylation of genes such as *TCF21* and how this contributes to tumor growth. One strategy might be to focus on the targets of the methyltransferases which are most often mutated. Although the targets of these methyltransferases would be hypo instead of hypermethylated, it is still clear that histone methylation plays a significant role in the development of ccRCC. A pattern of activity may emerge which would help to explain the role of DNA and histone modifications in ccRCC development.



**Treatment of ccRCC**

ccRCC is characterized in part by its extreme resistance to cytotoxic therapy and its high rate of acquired resistance to other treatments. Although therapy for ccRCC has improved in recent years, most treatments still target peripheral symptoms and aspects of tumor biology and treatments which can effectively cause tumor cell death are still not available. As we describe in Chapter 6, these cells express high levels of pro-survival proteins such as Survivin which directly blocks the activity of caspase proteins required for the process

of apoptosis. We showed that *VHL*-deficient cells and zebrafish express high levels of p53, an extremely important tumor suppressor protein, due in part to a subsequent change in the localization of programmed cell death 5 (PDCD5) which we showed was an interaction partner of pVHL (Chapter 6). Interestingly, PDCD5 is also sometimes found in the primary cilium (unpublished oberservations) raising the possibility of this protein also having a ciliary role, much like pVHL. Usually, high levels of p53 would lead to increases in cell cycle arrest and apoptosis, but instead, *vhl* mutant zebrafish, ccRCC tumor lines and *VHL* siRNA depleted wild-type cell lines

all display decreased apoptotic signaling, even after irradiation. Although other pro-survival genes are usually mutated in mature ccRCC, the activity of survivin and other genes upregulated downstream of HIF are sufficient to significantly reduce apoptosis. *TP53* (the gene encoding p53) is mutated in the majority of human cancers, but interestingly it is not frequently mutated in ccRCC. Thus, the activity of hyperstablized HIF helps mutant cells to survive apoptotic signaling and eventually develop further mutations that lead to the development of a tumor. In addition, this resistance to cell death, even when exposed to damaging environmental factors, means that tumors harboring VHL mutations are extremely difficult to treat effectively. Current treatments, such as tyrosine kinase inhibitors, mostly target the excessive angiogenesis which accompanies the growth of ccRCC tumors as we discus in Chapter 4. Tumors require blood-vessel access in order to grow, and malignancy is partially defined by the ability of the tumor to recruit blood vessel ingrowth. ccRCC tumors are highly vascularized, even more so than other tumors because of the upregulated pro-angiogenic signaling downstream of HIF and many of the growth and development mechanisms of ccRCC arise from pathways which govern angiogenesis and the growth and migration of blood vessels (see Chapters 4, 5). If a therapy could effectively curb the excessive angiogenesis of the tumor, it would reduce the tumor burden on the organ and slow the development of malignancy. The currently available drugs for ccRCC attempt to take advantage of this strategy by targeting signaling pathways involved in angiogenesis, especially the VEGF pathway and the mTOR pathway, as discussed in Chapter 4. The current accepted treatment regimen for ccRCC is a successive program of serial monotherapies with a new treatment being prescribed after the first medication has lost effectiveness [27]. In addition to the therapeutic strategies covered in the conclusion of Chapter 4, a number of other promising treatments have emerged. Treatments that are being tested include wider spectrum inhibitors that target multiple pathways, such as lenvantinib which inhibits the activity of both the VEGF pathway and to a lesser extent the fibroblast growth factor (FGF) and platelet derived growth factor (PDGF) pathway and has shown promising results in

ccRCC [28]. The FGF pathway is another growth factor pathway with similar downstream effects to VEGF signaling such as increased angiogenesis. Unlike VEGFR tyrosine kinase inhibitors, there is evidence that combination therapy combining lenvatinib with everolimus gives better results than everolimus alone and can improve outcomes even in patients who already display resistance to VEGFR TKI therapy, although more study is needed since very few patients were used in the phase II trial that was used to acquire FDA approval [28]. Cabozantinib is another inhibitor of multiple tyrosine kinases including the MET pathway and VEGFR pathway that has shown promising results in recent phase III trials as a second line therapy [29]. In addition to tyrosine kinase inhibitors, another treatment strategy under investigation is inhibition of the programmed cell death (PD-1) pathway. Tumor cells often express PD-1 ligand 1 and 2, which interacts with PD-1 on cytotoxic t-cells, consequently suppressing the activity of these antitumor immune cells. These inhibitors, such as nivolumab, block the action of either PD-1 or PD-1 ligands to re-activate the immune system. There is evidence that these treatments may be highly effective and combination therapy that uses both PD-1 inhibition and VEGFR inhibition is being tested as a first-line response to ccRCC in place of VEGF inhibition alone. However, these treatments carry the risk of significant toxicity and further optimization is needed [30]. Future work in this area may make use of models, such as the ones we introduce in chapter 4, to optimize combination therapies that may avoid the risk of resistance inherent in the current treatment strategies. In addition, treatments such as PD-1 inhibition may actually be able to cause tumor cell death and long-term tumor-free survival rather than only preventing tumor progression, leading to a new era in the treatment of ccRCC.

**Tumor suppressor genes and cilia**

Research into the biology of the primary cilium is still in its relative infancy. The primary cilium was long considered to be largely unimportant, even though it was first described over a century ago. It was only after more research into intraflagellar transport, the process by which proteins and other cargo are moved from place to place along the axoneme, that the primary cilium began to be recognized as a vital cellular organelle. It was then discovered that many well-known and well-studied proteins had a ciliary function or localization which had never been shown before. Thus, data is greatly needed in the field of ciliary research simply about which genes and proteins are involved in the cilium. A number of screen experiments have now been performed to attempt to identify and categorize ciliary genes and their protein products. One of the largest screens performed to date was partially automated and was based on the same IMCD3 cells used in many of the chapters of this thesis. These cells were transfected with a library of siRNA targeting all known coding genes and then imaged with a computer with specialized software which was able to determine the presence of cilia per cell and therefore quantify ciliation and cell numbers. Any siRNA

which caused a ciliation defect but did not significantly alter the number of cells would then be a prime candidate for further functional validation [31]. In addition to the results of this siRNA screen, a number of *in silico* analyses and other screens were performed and the results were combined as part of the consortium Syscilia into the Syscilia gold standard, a manually curated list of genes with at least 2 types of evidence linking them to the primary cilium. Our work in the Syscilia consortium was to functionally validate the results of other labs, such as *in silico* analysis and the siRNA screen mentioned above [32, 33]. To this end, we selected a number of putative ciliary genes which encoded proteins with functions similar to VHL and the other genes we worked on in our lab in terms of tumor suppression, cell cycle or DNA regulation or oncogene activity. We showed that these genes are in fact important for ciliation, proving the power of this type of wide-spectrum investigation. The genes which I cover in this thesis are *HUWE1, ANAPC4, FAM110A* and *STARD3NL*, which are described in Chapter 7. These genes were all initially found in screens for proteins and genes which were involved in ciliogenesis. HUWE1 is an E3 ubiquitin ligase, like pVHL, that is known to play a role in apoptotic signaling. Interestingly, HUWE1 has been shown to ubiquitinylate, and therefore promote the degredation of, both the pro-apoptotic protein p53 and the pro-survival protein Mcl1. HUWE1 is a very large protein with a significant number of interaction partners and its function is far from well understood. STARD3NL is a protein of mostly unknown function which is believed to function in cholesterol metabolism. FAM110A has an almost entirely unknown function. The exact function of ANAPC4 is unclear, although it is part of a well-studied protein complex. In Chapter7, I go into greater detail about the known functions of the protein products of these genes and show that they are important for ciliation, but we have not done a large amount of functional research. For example, we still only have a vague idea as to how these proteins contribute to ciliation. Future research should continue to elucidate the cellular function of these proteins and how loss of these genes leads to ciliary dysfunction.

PTEN is an important tumor suppressor protein that is frequently mutated in cancer. PTEN antagonizes PI3K signaling which leads downstream to inhibition of the AKT pathway. Activation of AKT leads to inhibition of apoptosis, and AKT signaling is also frequently upregulated in cancer. PTEN is also sometimes mutated in ccRCC, but interestingly complete loss of PTEN is rare. In Chapter 5 we show that loss of VHL causes an upregulation of mir132/212, a miR family which is known to target PTEN. miRs are small non-coding RNA which target mRNA transcripts and suppress their translation. A number of miRs have been previously described upregulated in hypoxia and pseudohypoxia, but not miR 132/212, which was already known to target PTEN in vascular smooth muscle cells in order to contribute to angiogenesis [34]. Perhaps the relatively low frequency of bilateral *PTEN* mutations in ccRCC is due to the already depressed cellular levels of PTEN due to the

presence of this miR. However, there is a large amount of cross-talk between PTEN signaling and HIF signaling, so it is difficult to determine which part of their relationship is important for tumorigenesis and tumor biology. Intriguingly, it was recently shown that PTEN also contributes to ciliation by phosphorylating disheveled protein. This means that, much like pVHL, PTEN is also a tumor suppressor protein that plays a role in the cilium. In the future, treatments which target miRNA expression in ccRCC may allow PTEN to accumulate in tumor cells, restoring its tumor suppressor and pro-ciliogenesis functions.

## FUTURE PERSPECTIVES

The relatively recent discovery of genes found frequently mutated in ccRCC in addition to *VHL* represents a promising direction for future research. Genes such as *BAP1, PBRM1 and SETD2* have now been identified which appear to be important for ccRCC development, but their function, especially in the context of renal cells, is still unknown. It is therefore important to study the function of these genes and how their mutation leads to tumorigenesis. This is especially true because, despite years of intense work, an animal model of ccRCC that accurately recapitulates the human disease is still not available. The *Bap1* heterozygote, *Vhl* mutant mouse may finally provide researchers with a more accurate model but more work remains to be done to characterize the ccRCC-like tumors in these animals and elucidate the mechanisms which lead to their development. A better understanding of the function of these genes in the kidney may provide insight into the questions such as what differentiates a cyst from an atypical cyst, how does an atypical cyst progress into a ccRCC tumor, and why do *VHL* mutations appear to be required, despite not being sufficient for tumorigenesis or cyst development on their own.



The role of the primary cilium as a tumor suppressor or tumor promoting organelle is difficult to study for a number of reasons. As mentioned above, it is frequently not possible to isolate the ciliary function of a protein from its other functions. In many cases, these functions are inseparable because they are based on the same molecular action of the protein in question. Indeed, research which attempts to disassociate the ciliary function of a protein or gene from its other functions is likely misguided. The primary cilium is inexorably linked with a wide variety of cellular processes and it is not relevant to think of it as a completely self-contained organelle without connection to the rest of the cell. In the kidney, the tumor suppressor activity of the primary cilium has been fairly well established. In the cyst-dependant hypothesis of ccRCC development, loss of the primary cilium leading to cyst development is a crucial step and has been demonstrated in animal models. However, in other tumor types, the primary cilium plays a different role and can even promote

tumorigenesis as discussed in Chapter 2. The role of the primary cilium as a tumor suppressor, or even a tumor promoter, must therefore be evaluated on a case-by-case basis depending on the tumor type being studied.

**Concluding remarks**

The link between the primary cilium and tumorigenesis remains unclear, but it is true that cilia play a role in certain subtypes of cancer. Proteins which are important for ciliogenesis, maintenance of the cilium, ciliary signaling or other ciliary functions, as well as proteins which are found at or around the cilium have been shown to be involved in cancer biology. This is especially true of ccRCC, which is associated with ciliary loss due to the loss of pVHL, which plays a role in microtubule dynamics, and other downstream signaling effects. The biology of ccRCC is complex and involves many different important cell signaling pathways. This also makes treating ccRCC difficult. Although much more work remains to be done, it may be possible to target these aspects of ccRCC, *VHL* and ciliary biology in the future in order to better treat patients.

# REFERENCES


1. Johnson, C.A. and S.J. Collis, *Ciliogenesis and the DNA damage response: a stressful relationship.* Cilia, 2016. **5**: p. 19.
2. Yuan, S. and Z. Sun, *Expanding horizons: ciliary proteins reach beyond cilia.* Annu Rev Genet, 2013. **47**: p. 353-76.
3. Waters, A.M. and P.L. Beales, *Ciliopathies: an expanding disease spectrum.* Pediatr Nephrol, 2011. **26**(7): p. 1039-56.
4. Chavali, P.L., M. Putz, and F. Gergely, *Small organelle, big responsibility: the role of centrosomes in development and disease.* Philos Trans R Soc Lond B Biol Sci, 2014. **369**(1650).
5. Lolkema, M.P., et al., *Allele-specific regulation of primary cilia function by the von Hippel-Lindau tumor suppressor.* Eur J Hum Genet, 2008. **16**(1): p. 73-8.
6. Kleymenova, E., et al., *Susceptibility to vascular neoplasms but no increased susceptibility to renal carcinogenesis in Vhl knockout mice.* Carcinogenesis, 2004. **25**(3): p. 309-15.
7. Klasson, T.D. and R.H. Giles, *Molecular Genetics of Renal Cancer.* eLS. John Wiley & Sons, Ltd: Chichester., 2016.
8. Montani, M., et al., *VHL-gene deletion in single renal tubular epithelial cells and renal tubular cysts: further evidence for a cyst-dependent progression pathway of clear cell renal carcinoma in von Hippel-Lindau disease.* Am J Surg Pathol, 2010. **34**(6): p. 806-15.
9. Choyke, P.L., et al., *The natural history of renal lesions in von Hippel-Lindau disease: a serial CT study in 28 patients.* AJR Am J Roentgenol, 1992. **159**(6): p. 1229-34.
10. Mandriota, S.J., et al., *HIF activation identifies early lesions in VHL kidneys: evidence for site-specific tumor suppressor function in the nephron.* Cancer Cell, 2002. **1**(5): p. 459-68.
11. van Rooijen, E., et al., *A zebrafish model for VHL and hypoxia signaling.* Methods Cell Biol, 2011. **105**: p. 163-90.
12. Lee, S.H. and S. Somlo, *Cyst growth, polycystins, and primary cilia in autosomal dominant polycystic kidney disease.* Kidney Res Clin Pract, 2014. **33**(2): p. 73-8.
13. Arts, H.H. and N.V. Knoers, *Current insights into renal ciliopathies: what can genetics teach us?* Pediatr Nephrol, 2013. **28**(6): p. 863-74.
14. Guinot, A., et al., *Combined deletion of Vhl, Trp53 and Kif3a causes cystic and neoplastic renal lesions.* J Pathol, 2016. **239**(3): p. 365-73.
15. Wasylishen, A.R. and G. Lozano, *Attenuating the p53 Pathway in Human Cancers: Many Means to the Same End.* Cold Spring Harb Perspect Med, 2016. **6**(8).
16. Rinkevich, Y., et al., *In vivo clonal analysis reveals lineage-restricted progenitor characteristics in mammalian kidney development, maintenance, and regeneration.* Cell Rep, 2014. **7**(4): p. 1270-83.
17. Piontek, K., et al., *A critical developmental switch defines the kinetics of kidney cyst formation after loss of Pkd1.* Nat Med, 2007. **13**(12): p. 1490-5.
18. Hanahan, D. and R.A. Weinberg, *Hallmarks of cancer: the next generation.* Cell, 2011. **144**(5): p. 646-74.
19. Shen, C., et al., *Genetic and functional studies implicate HIF1alpha as a 14q kidney cancer suppressor gene.* Cancer Discov, 2011. **1**(3): p. 222-35.
20. Raval, R.R., et al., *Contrasting properties of hypoxia-inducible factor 1 (HIF-1) and HIF-2 in von Hippel-Lindau-associated renal cell carcinoma.* Mol Cell Biol, 2005. **25**(13): p. 5675-86.
21. Biswas, S., et al., *Effects of HIF-1alpha and HIF2alpha on Growth and Metabolism of Clear-Cell Renal Cell Carcinoma 786-0 Xenografts.* J Oncol, 2010. **2010**: p. 757908.
22. Schonenberger, D., et al., *Formation of Renal Cysts and Tumors in Vhl/Trp53-Deficient Mice Requires HIF1alpha and HIF2alpha.* Cancer Res, 2016. **76**(7): p. 2025-36.
23. Gerlinger, M., et al., *Genomic architecture and evolution of clear cell renal cell carcinomas defined by multiregion sequencing.* Nat Genet, 2014. **46**(3): p. 225-33.
24. Sato, Y., et al., *Integrated molecular analysis of clear-cell renal cell carcinoma.* Nat Genet, 2013. **45**(8): p. 860-7.
25. Wang, S.S., et al., *Bap1 is essential for kidney function and cooperates with Vhl in renal tumorigenesis.* Proc Natl Acad Sci U S A, 2014. **111**(46): p. 16538-43.
26. Gnarra, J.R., et al., *Defective placental vasculogenesis causes embryonic lethality in VHL-deficient mice.* Proc Natl Acad Sci U S A, 1997. **94**(17): p. 9102-7.
27. Greef, B. and T. Eisen, *Medical treatment of renal cancer: new horizons.* Br J Cancer, 2016. **115**(5): p. 505-16.
28. Motzer, R.J., et al., *Lenvatinib, everolimus, and the combination in patients with metastatic renal cell carcinoma: a randomised, phase 2, open-label, multicentre trial.* Lancet Oncol, 2015. **16**(15): p. 1473-82.
29. Choueiri, T.K., et al., *Cabozantinib versus everolimus in advanced renal cell carcinoma (METEOR): final results from a randomised, open-label, phase 3 trial.* Lancet Oncol, 2016. **17**(7): p. 917-27.
30. Albiges, L., et al., *Efficacy of targeted therapies after PD-1/PD-L1 blockade in metastatic renal cell carcinoma.* Eur J Cancer, 2015. **51**(17): p. 2580-6.
31. Wheway, G., et al., *An siRNA-based functional genomics screen for the identification of regulators of ciliogenesis and ciliopathy genes.* Nat Cell Biol, 2015. **17**(8): p. 1074-87.
32. Boldt, K., et al., *An organelle-specific protein landscape identifies novel diseases and molecular mechanisms.* Nat Commun, 2016. **7**: p. 11491.
33. van Dam, T.J., et al., *The SYSCILIA gold standard (SCGSv1) of known ciliary components and its applications within a systems biology consortium.* Cilia, 2013. **2**(1): p. 7.
34. Anand, S., et al., *MicroRNA-132-mediated loss of p120RasGAP activates the endothelium to facilitate pathological angiogenesis.* Nat Med, 2010. **16**(8): p. 909-14.

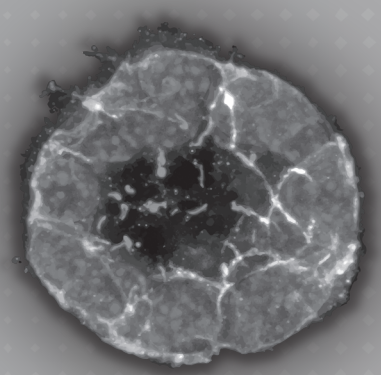

# APPENDICES

Summary in English
Summary in Dutch
Acknowledgements
List of publications
Curriculum Vitae

## ENGLISH SUMMARY

Cancer affects a large number of people the world over. Cancer is a class of extremely complex diseases that arise from malfunctions in otherwise vital cellular processes, especially those that govern aspects of cellular functions like proliferation, apoptosis or the cell cycle. These processes are delicately balanced in healthy cells and are tightly regulated by a wide array of interconnected cellular signaling pathways. When these processes or their regulators are dysfunctional, tumorigenesis can occur.

The primary cilium is a cellular organelle that can be found projecting from the cell surface of the majority of human cells. This organelle has many functions in cell signaling, including playing a role in the development, pattering and growth of cells and tissues. Dysfunction of the cilium can lead to disease. In addition, a number of proteins important for the function of the cilium are also known to be involved in tumorigenesis. One such protein is the von Hippel-Lindau tumor suppressor protein (pVHL). Mutations in the *VHL* gene that encodes pVHL lead to ciliogenesis defects and are universally found in kidney cancer tumors.

The central topic of this book is an investigation of the function of tumor suppressor proteins that are involved in ciliary biology and the connection between their ciliary role and tumorigenesis. I especially focus on pVHL and its central role in kidney cancer.

In **Chapter 1** I provide an overview of both pVHL and the primary cilium. I review the structure and function of the primary cilium and introduce the ciliopathies, a class of diseases that arise from ciliary dysfunction. This chapter also contains an overview of the many functions of pVHL, including its ciliary functions, and how dysfunctional pVHL contributes to the development of kidney tumors. Finally, I discuss the connection between the cilium and cancer and introduce the models used in this thesis.

**Chapter 2** covers the role of the cilium and ciliary proteins in cancer in more depth. The primary cilium plays a central role in development. Thus, this chapter focuses on the role of ciliary proteins in hereditary tumor predisposition syndromes, many of which display symptoms early in life. Special attention is paid to syndromes in which known classical tumor suppressor genes are mutated, including von Hippel-Lindau disease, which arises from inherited mutations in *VHL*.

**Chapter 3** contains a detailed review of the etiology of von Hippel-Lindau disease. The genetic background of the disease, its effects, and some treatment options are covered.

The primary animal model used in this book is a zebrafish model of von Hippel-Lindau disease. This zebrafish model has the same genetic background as human patients and faithfully reproduces many of the aspects of the human disease. In **Chapter 4,** we used this model and an *in vitro* cellular model to test the efficacy of a combination therapy in reducing pathophysiological angiogenesis that is inherent in von Hippel-Lindau disease. This approach shows the value of these models to test novel therapies and presents a promising new treatment approach.

**Chapter 5** again revisits the pathophysiological angiogenesis that accompanies dysfunctional pVHL signaling. In this chapter we show that a family of miRNA, important regulators of protein transcription, is excessively produced after the loss of pVHL function. The function of this miRNA contributes to excessive angiogenesis and reduces levels of important anti-proliferation proteins, including the important anti-tumor protein Phosphatase and Tensin Homologue (PTEN), which may contribute to tumor formation in kidney cancer.

In **Chapter 6** we show that VHL signaling affects the p53 pathway, a vital tumor suppressor signaling pathway, surprisingly leading to an upregulation of anti-survival signaling. However, due to the induction of other pro-survival pathways, *VHL*-deficient cells and organisms still survive, which may explain why p53 signaling is only rarely disrupted in *VHL*-related cancer and why these cancers are difficult to treat.

During the work that went into this book, I investigated the function of a number of candidate genes in order to find out more about their role in the cilium and the cell. The ciliary function of many genes has not yet been described. In **Chapter 7** we present four novel regulators of ciliogenesis which were originally identified in screens: *HUWE1, STARD3NL, ANAPC4* and *FAM110A*. We used a 3D cellular model to show that these genes are required for proper ciliation and examined their function.



Another novel ciliary protein is described in **Chapter 8:** *DCDC2*. We show that mutations in this gene cause a renal hepatic ciliopathy in human patients and that depletion of this gene also causes a ciliopathy phenotype in zebrafish. Functional testing showed that loss of *DCDC2* causes excessive signaling in the Wnt pathway, an important developmental signaling pathway. Inhibiting Wnt signaling rescued the ciliopathy symptoms, presenting an interesting opportunity for treatment, and shedding light on the role of Wnt signaling in ciliogenesis which is still incompletely understood.

In addition to VHL, a number of other genes are frequently found disrupted in kidney cancer. One such class of genes is a group of genes that control histone methylation, a

system of gene regulation. However, the targets of these histone methylating genes are still largely unidentified. In **Chapter 9** we identify one gene which is methylated in some subsets of kidney cancer: *TCF21*. We showed that *TCF21* methylation is responsible for increased colony size and migration in a kidney cancer cell line, suggesting a tumor suppressor role for *TCF21*.

Finally, in **Chapter 10** I present an in-depth discussion of the topics contained in this book. Specifically, I discuss the connection between ciliary genes and cancer, as well as how pVHL deficiency leads to kidney cancer and how its ciliary role plays a part in tumorigenesis. In addition, I discuss the complex genetics of kidney cancer and treatment modalities and provide future perspectives on research in this field.

A

## NEDERLANDSE SAMENVATTING

Kanker heeft invloed op een groot aantal mensen over de hele wereld. Kanker is een klasse van zeer complexe ziekten die voortkomen uit defecten in celprocessen die van levensbelang zijn in een gezonde situatie, met name de processen die bijvoorbeeld proliferatie, apoptose of celcyclus regelen. Deze processen verkeren in een delicaat evenwicht in gezonde cellen en zijn strak gereguleerd door een breed scala aan onderling verbonden cellulaire signaaltransductie trajecten binnen de cel. Wanneer deze processen of hun regulatoren disfunctioneel zijn, kunnen tumoren ontstaan.

Het primaire cilium is een celorganel dat uitsteekt van het celoppervlak van de meeste menselijke cellen. Dit organel heeft vele functies in celsignaaltransductie, inclusief een rol in de ontwikkeling, patroonvorming en groei van cellen en weefsels. Dysfunctie van het cilium kan leiden tot ziekte. Daarnaast is bekend dat een aantal eiwitten die belangrijk zijn voor het functioneren van het cilium, ook betrokken zijn bij het ontstaan van tumoren. Één van die eiwittenis het von Hippel-Lindau tumorsuppressor eiwit (pVHL). Mutaties in het VHL-gen dat codeert voor pVHLn eiwit leiden tot ciliogenese defecten en zijn in alle gevallen te vinden in nierkanker tumoren.

Het centrale onderwerp van dit boek is een onderzoek van de functie van tumorsuppressor eiwitten die betrokken zijn bij de biologie van cilia, en de verbinding tussen hun rol in cilia en hun rol bij het ontstaan van tumoren. Ik leg de nadruk vooral op pVHL en zijn centrale rol in nierkanker.

In hoofdstuk 1 geef ik een overzicht van zowel pVHL als het primaire cilium. Ik bekijk de structuur en functie van het primaire cilium en introducer de ciliopathies, een klasse van ziekten die veroorzaak worden door ciliaire dysfunctie. Dit hoofdstuk bevat ook een overzicht van de vele functies van pVHL, inclusief zijn functies in cilia, en hoe dysfunctionele pVHL bijdraagt aan de ontwikkeling van nier tumoren. Tot slot bespreek ik de relatie tussen het cilium en kanker en introduceer ik de modellen die in dit proefschrift gebruikt worden.

Hoofdstuk 2 behandelt de rol van het cilium en ciliaire eiwitten in kanker in meer diepte. Het primaire cilium speelt een centrale rol in ontwikkeling. Daarom richt dit hoofdstuk zich op de rol van ciliaire eiwitten in erfelijke tumor predispositie syndromen, waarvan vele vroeg in het leven symptomen geven. Speciale aandacht wordt besteed aan syndromen waarin bekende klassieke tumorsuppressor genen gemuteerd zijn, waaronder de ziekte van von Hippel-Lindau, die ontstaat doorerfelijke mutaties in *VHL*.

Hoofdstuk 3 bevat een gedetailleerd overzicht van de etiologie van de ziekte van von Hippel-Lindau. De genetische achtergrond van de ziekte, de gevolgen ervan, en sommige behandelingsopties worden behandeld.

Het primaire diermodel dat in dit boek gebruikt wordt is een zebravismodel van de von Hippel-Lindau ziekte. Dit zebravismodel heeft dezelfde genetische achtergrond als menselijke patiënten en weergeeft op betrouwbare wijze veel van de aspecten van de ziekte bij de mens weer. In hoofdstuk 4 hebben we dit model en een *in vitro* cellulair model gebruikt voor het testen van de werkzaamheid van een combinatietherapie om de pathofysiologische angiogenese, inherent aan de ziekte van von Hippel-Lindau, te verminderen. Deze aanpak laat de waarde van deze modellen voor het testen van nieuwe therapieën zien, en biedt een nieuwe benadering van de behandeling.

Hoofdstuk 5 beschrijft opnieuw de pathofysiologische angiogenese die een gevolg is van de disfunctionele signaaltransductie van pVHL. In dit hoofdstuk laten we zien dat een specifieke miRNA familie, welke belangrijke regulatoren van eiwit transcriptie zijn, overdreven veel geproduceerd wordt na het verlies van de functie van pVHL. Deze miRNA draagt bij aan de buitensporige angiogenese en verminderde hoeveelheden van belangrijke anti-proliferatie eiwitten, inclusief het belangrijke anti-tumor eiwit phosphaste and tensin homologue (PTEN), wat zou kunnen hebben bijdragen aan de vorming van tumoren in nierkanker.

In hoofdstuk 6 laten we zien dat VHL-signaaltransductie invloed heeft op het onmisbare tumor onderdrukkende p53-signaaltransductie traject, wat verrassend genoeg tot een verhoogde anti-overleving signaaltransductie leidt. Echter, als gevolg van de inductie van andere pro-overleving signaaltransductie signalen, overleven *VHL*-deficiënte cellen en organismen wel, wat kan verklaren waarom p53-signaaltransductie slechts zelden wordt verstoord in VHL-gerelateerde kanker en waarom deze kankers zo moeilijk te behandelen zijn.

Tijdens het werk dat in dit boek wordt beschreven, heb ik de functie van een aantal kandidaat-genen onderzocht om meer over hun rol in het cilium en de cel te ontdekken. Van deze kandidaatgenen is de functie in het cilium nog niet beschreven. In hoofdstuk 7 introduceren wij vier nieuwe regelaars van ciliogenesis die oorspronkelijk zijn geïdentificeerd in screens van actieve stoffen: *HUWE1*, *STARD3NL*, *ANAPC4* en *FAM110A*. We hebben gebruik gemaakt van een cellulair 3D- model om aan te tonen dat deze genen nodig zijn voor een goed ontwikkelt en werkend cilium en om hun functie te onderzoeken.

Een ander nieuw ciliair eiwit wordt beschreven in hoofdstuk 8: *DCDC2*. We laten zien dat mutaties in dit gen in menselijke patiënten een renale en hepatische ciliopathie veroorzaken, en dat uitschakeling van dit gen in de zebravis leidt tot een ciliopathie fenotype. Uit functionele testen bleek dat verlies van *DCDC2* voor overmatige Wnt-signaaltranductie zorgt, een signaaltransductie traject belangrijk voor normale ontwikkeling. De symptomen van het ciliopathie fenotype konden gered worden door het remmen van Wnt-signaaltransductie. Dit laat ons een interessante kans voor behandeling zien, én het werpt een licht op de rol van Wnt-signaaltransductie in ciliogenese, welke nog steeds niet volledig begrepen wordt.

Naast VHL, zijn er een aantal andere genen die vaak gemuteerd blijken te zijn in nierkanker. Een zo een voorbeeld is een groep genen die histon methylering reguleert, een bekend genregulatie systeem. De genen waarop deze histon methylatie regulerende genen hun functie uitoefenen zijn echter nog grotendeels onbekend. In hoofdstuk 9 identificeren we een gen dat in sommige deelverzamelingen van nierkanker gemethyleerd is: *TCF21*. We toonden aan dat methylering van *TCF21* verantwoordelijk is voor verhoogde kolonie grootte en migratie in een nierkanker cellijn, wat een tumorsuppressor rol voor TCF21 suggereert.

Tenslotte presenteer ik in hoofdstuk 10 een diepgaande discussie over de onderwerpen die in dit boek omschreven zijn. Ik behandel met de name de relatie tussen ciliaire genen en kanker, en hoe pVHL deficiëntie tot nierkanker leidt en hoe de ciliaire rol van pVHL een rol heeft in het ontstaan van tumoren. Daarnaast bespreek ik de ingewikkelde genetica van nierkanker en behandelingsmethoden, en bied ik perspectieven voor toekomstig onderzoek op dit gebied.

A

## ACKNOWLEDGEMENTS

It would be totally impossible for me to appropriately thank everyone who supported me during my thesis. I have been ridiculously lucky to have so many wonderful friends and helpful colleagues, on whom I have relied time and time again. I can't possibly mention everyone's name (especially because I'm kind of forgetful) so rest assured that if your name isn't here I still appreciate everything you've done for me, no matter how small. Thanks so much!

First, of course, I have to thank **Rachel.** In this small space, there's no way I could possibly encompass all the ways you've helped me over my time in your lab. Endlessly helpful, wildly patient, exceptionally kind and funny, I couldn't have asked for a better supervisor. I consider myself privileged to have gotten my PhD in your lab, and one day I hope to be half the scientist you are. All the best to you and your family!

Next I would like to thank **Alyson Macinnes,** who took a chance on a guy with no science experience who was working at a fashion company, based almost entirely on a phone conversation and a shared alma mater. Without that, I wouldn't be where I am now. Thanks for being welcoming and helpful, even when it was very clear that I had no idea what I was doing. Thanks also to **Paul,** who was a great first supervisor for a mostly lost guy from another country. Serious in the lab, and a lot of fun outside of it. Thanks for your patience and help!

Special thanks to **Gisela.** With the amount of basic questions I asked you over the course of my thesis (especially at the beginning), you must have felt like you had yet another masters student! Thanks for always helping me with everything even though you were always already so busy. Thanks for being an excellent colleague and a nice person. Good luck with everything, not that you need it!

Thanks to my Paranymphs! **Ed**. What can I say? We've known each other for 20 years and we're basically family. You came out to visit me so many times and if I was home, you always found time to hang out with me in the US if you could. There's nobody I'd rather have standing with me at my defense. Thanks for everything through all these years, and here's to the next 20. **Alex,** my friend! I owe you a lot. If you hadn't invited me to live with you, I'd probably still be stuck out in the wilderness. It was living here and doing things with you and everyone else (that you frequently organized for the benefit of everyone!) that really made my time in the Netherlands fun. You always had time to help me out or listen to me, even when nobody else was there, and I appreciate it immensely. Good luck with your own PhD! I still believe in your professional sky diving career too!

Next I want to thank all my colleagues and lab-mates. Thanks to my supervisors, prof. dr. **Marianne Verhaar** and prof. dr. **Nine Knoers** for their thoughtful input. Thanks to my students **Lars, Michelle** and **Rianne** for their hard work and dedication. I'm lucky to have had such amazing, productive students who somehow always managed to do what was needed even when my instructions were really vague. I wish you all the best in the future!

**Glenn**, you were always fun to hang out with, work with or go to conferences with, even if you don't believe I speak Spanish. Good luck with the fish and the rest of your thesis and may you always be able to find somebody to cook your dinner. Maybe one day I'll actually pay you those beers I supposedly owe you. **Nayia**, or should I say Nadja? Always a fun person to share a drink or sit through a boring conference with. You're already back in Cyprus living it up, but all the best anyway! **Marijn,** my Kanye West buddy! A really nice person and a great colleague. Best wishes to you and your family! Thanks also to **Glen** (my fellow American!) and **Kirsten** and everyone else at the stratenum for the good times and not being upset whenever I showed up and started working there even though nobody knew who I was.

I owe a lot of thanks to all the people I've shared a lab with, including **Petra de Bree, Petra de Graaf, Chris, Merle, Maarten, Dries, Zhiyong, Alain, Krista, Khatera, Ka Man, Miriam, Veronica, Sebastiaan, Marlies, Gemma, Joost, Jaap, Diana, Merle, Janine, Frederieke, Arianne, Henry** and everyone else in Nephrology and Experimental cardiology. Thanks for all of your help, as well as all the events, borrels and fun times. Best wishes to all of you! **Hendrik,** my fellow night shift member and a good friend, even though I betrayed the pub quiz team and joined the enemy. Thanks for always being there to talk to, have a beer with, answer my questions, and do all the stats. I couldn't have asked for a better partner to invade all the Hubrecht events with. I'm pretty sure you'll be running this place in a few years. Good luck with everything! **Judith,** my old roomie, fellow New York enthusiast, basketball friend and co-champion of table football. Thanks for being a good friend even though I moved out of the office and somehow always managed to miss your parties. As an expat I'll always appreciate the thanksgivings we (mostly you) organized. Good luck making science a better place! **Ollie** I'll always remember that one Monday morning meeting where we couldn't stop laughing. Thanks for always being kind to me even when I forgot to replace the western blot buffers. **Dimitri** thanks for helping to keep the fun level of the lab up, and all the best in your new career. Thanks to you **Bas,** I will always know the meaning of the phrase "heb je snoepjes?". You were a good colleague. Thanks also for the barbeques! Your trampoline is safe now. Thanks to all of my collaborators and anyone who I worked with or who helped me with the technical aspects of a protocol.

Thank you to the secretarial staff at nephrology and hypertension. A big thank you to the animal caretakers at the Hubrect, especially **Rob** who is not only excellent at his job but also a great person and friend. He throws a good barbeque too! Thanks for all your help over the years.

There isn't enough space in this whole book for me to properly thank all of my wonderful friends. Each of you deserves your own essay, but at the risk of going on forever (or worse, forgetting someone) I'm going to have to keep it short and mostly general. That said, I want to emphasize as much as I can how important you all are to me, and how happy you made me. If I was tired (always) or stressed out (frequently) I knew I just had to hang on until the next time I we spent together and I could pick myself up again. None of this work exists without you, because I honestly wouldn't have made it. The meals and drinks and movies together, trips to the zoo, music festivals, trips to Belgium, or whatever else was going on, always gave me life. Thanks to everyone who invited me into their home (or didn't kick me out when I showed up uninvited), or to a concert, or to watch sports or go to any kind of activity no matter how small. You don't know how much it meant to me, but it meant a lot! Thank you, thank you, thank you!

Thanks to my American friends, in New York and elsewhere, who always made me feel like I was home. Even though I only saw most of you every 6 months (at best!), every time we got together felt like I had been there the whole time. Thanks for always including me in all the online activities and inviting me to things even if you knew I couldn't go. I always felt connected to home and that meant a lot to me. Special thanks go to **Joe, Ray, Jeremy, Dan, Justin,** and **Mike Dolmatch**, all of whom went out of their way to come to a small town halfway around the world to visit me. It was great getting to explore and show off the place I live with you! I want to give an extra extra special thanks to my great friend **George.** Weirdly enough, despite the fact that we lived 3600 miles away, there isn't anybody that I talked with more than you over the course of my 5 years in Europe. Thanks for always being there for me, no matter how stupid my jokes were or how much I complained about work. Without you I probably wouldn't have gotten through this. Sorry I'm again moving to the wrong timezone, but you know I'll always find time to talk to you! I'm sure you're overjoyed.

Special thanks to my good friend **Sharif.** From late night intellectual discussions to house parties, from whole pig BBQs to whiskey Thursdays, we had a lot of great times! You were one of my first really good friends in Utrecht, and still one the best. Thanks for adopting me even though I was a member of the great unwashed hordes of America. Good luck with your PhD and try not to let the crazy food and people of my native land get to you. Shout

out as well to the rest of the **IBB crew,** who graciously tolerated my presence despite the fact that I was the jerk making everyone speak English.

I was lucky enough to be adopted at the **Hubrecht** after I showed up enough for people to stop asking who I was and why I was there (I said I was there for my fish, but I mostly came for the borrels) and the wonderful people I met and spent time with improved my life immensely. After we moved to the new building I really enjoyed getting to be with them and my other friends from the **UMC** and **PMC** more often. There are more people I want to thank than I can possibly list, so I'm going to cop out and do mostly groups. Sorry! If you don't see your name here I probably still think you're great.

Shout outs to, but not in any way limited to: **the Pub Quiz team** for always being the highlight of my Wednesdays. Thanks to my **climbing buddies**, especially everybody who convinced me to get into it in the first place. Thanks to the **van Rheenen group** for generally being awesome as well as letting me crash your office a bunch of times when I was bored on the 5th floor. Thanks to **Jessica** for being a good room mate and a good friend. Thanks to **Annabel** for always organizing fun activities and bringing me along. Thanks to **Javi** for being my friend since back in the language class days. Thanks to **Anna** for all the coffee breaks, all the other times we spent together and always listening to me gripe. Thanks to **Mauro** for talking with me about the NFL and always being a gracious host. Thanks also to **PJ**, **Maartje** and **Luca** for hosting me at their houses many times, even some times when I wasn't invited. Thanks to **Adi** for chatting about playing music with me even though I haven't played in ages. Thanks to **Ajit** for being a great guy and the godfather of borrels. Thanks to all **the students** for generally being really fun and letting me crash your parties. Thanks to all of the **usual suspects** at the BBQs and Friday borrels who made every week fun. Thanks to **so many other people who I couldn't find a way to include here without just making a huge list of names** (sorry!) and to anyone who I forgot. You're all amazing!

Lastly and most importantly, I want to thank **Mom, Dad, Emily** and all the rest of my wonderful family. No matter what, I could always count on you. Your support and faith in me has always lifted me up and given me strength. I could always count on being spoiled around any of you, and being able to relax no matter what. When I had shoulder surgery, my family came from two different countries just to be with me. I'm incredibly lucky to have had that kind of support. You never got down on me even when things were hard. You never got mad at me even when I disappeared for ages. You always supported my choices and believed in me, even though I originally told everybody I was just going for 6 months. Thank you so much. I love you!

## LIST OF PUBLICATIONS

*Shared first authorships marked with an **

**Klasson TD,** Giles RH. "Molecular Genetics of Renal Cancer". eLS Reviews, 2016.

Frantzen C, **Klasson TD**, Links TP, Giles RH. "Von Hippel-Lindau Disease" *GeneReviews* at GeneTests: NIH Medical Genetics Information Resource. Copyright, University of Washington, Seattle, 1997-2010. Updated 2015. Available at http://www.ncbi.nlm.nih.gov/books/NBK1463/

**Klasson TD***, Essers PB*, Pereboom TC, Mans DA, Nicastro M, Boldt K, Giles RH, Macinnes A. "The von Hippel-Lindau tumor suppressor regulates programmed cell death 5 mediated degradation of Mdm2. *Oncogene*. 2015 Feb 5;34(6):771-9."

Schueler M, Braun DA, Chandrasekar G, Gee HY, **Klasson TD**, Halbritter J, Bieder A, Porath JD, Airik R, Zhou W, LoTurco JJ, Che A, Otto EA, Böckenhauer D, Sebire NJ, Honzik T, Harris PC, Koon SJ, Gunay-Aygun M, Saunier S, Zerres K, Bruechle NO, Drenth JP, Pelletier L, Tapia-Páez I, Lifton RP, Giles RH, Kere J, Hildebrandt F. "DCDC2 mutations cause a renal-hepatic ciliopathy by disrupting Wnt signaling." The American Journal of Human Genetics. 2015 Jan 8;96(1):81-92. doi: 10.1016/j.ajhg.2014.12.002. Epub 2014 Dec 31.

Slaats GG, Ghosh AK, Falke LL, Le Corre S, Shaltiel IA, van de Hoek G, **Klasson TD**, Stokman MF, Logister I, Verhaar MC, Goldschmeding R, Nguyen TQ, Drummond IA, Hildebrandt F, Giles RH. "Nephronophthisis-associated CEP164 regulates cell cycle progression, apoptosis and epithelial-to-mesenchymal transition." PLoS Genetics. 2014 Oct 23;10(10):e1004594. doi: 10.1371/journal.pgen.1004594. eCollection 2014.

**Klasson TD,** Giles RH. **"**The role of the cilium in hereditary tumor predisposition syndromes" *Journal of Pediatric Genetics* (2014)3:129-140. https://www.ncbi.nlm.nih.gov/pmc/articles/PMC5020991/

Pereboom TC, Bondt A, Pallaki P, **Klasson TD**, Goos YJ, Essers PB, Groot Koerkamp MJ, Gazda HT, Holstege FC, Costa LD, MacInnes AW. "Translation of branched-chain aminotransferase-1 transcripts is impaired in cells haploinsufficient for ribosomal protein genes." Experimental Hematology. 2014 May;42(5):394-403.e4. doi: 10.1016/j.exphem.2013.12.010. Epub 2014 Jan 23.

**In publication**

**Klasson TD,** Brandt M, van Rooijen E, Verhulst D, Groenewegen G, Cheng C, Giles RH. "Pre-clinical models to validate combination therapy approaches to reduce pathophysiological angiogenesis". Submitted to Disease Models and Mechanisms.

**Klasson TD***, Lei ZY*, Brandt M, van de Hoek G, Logister I, Cheng KL, Sluijter JP, Giles RH."Inhibition of miRNA-132/212 Suppresses VHL-Regulated Pathophysiological Angiogenesis"

SL Gooskens*, **TD Klasson***, I Logister, R. Pieters, EJ Perlman, RH Giles, MM van den Heuvel-Eibrink. **"**The tumorigenic role of *TCF21* hypermethylation in renal tumors."

**Klasson TD***, Slaats GG*, Chen Z, Noordegraaf S, Custers L, Logister I, Johnson CA, Knoers NV, Devuyst O, Giles RH. "Validation of novel regulators of renal ciliogenesis: HUWE1, FAM110A, STARD3NL and ANAPC4."

## CURRICULUM VITAE

Timothy Daniel Klasson was born on June 28th, 1989, in New York City. As a child he lived in Manhattan until moving to the superior borough of Brooklyn, where his family still lives. Tim attended Packer Collegiate Institute in Brooklyn, New York, where he graduated in 2007. From there he attended Wesleyan University in Middletown, Connecticut. There, Tim received degrees in molecular biology and biochemistry and biology, graduating in 2011. Tim moved to the Netherlands in 2012 in order to pursue an internship in the lab of Alyson Macinnes at the Hubrecht Institute in Utrecht. In 2012 he began his PhD under the supervision of Dr. Rachel Giles, Prof. Dr. Marianne Verhaar and Prof. Dr. Nine Knoers at the Department of Nephrology and Hypertension at the University Medical Center, Utrecht. The results of his PhD are presented in this thesis.